VAPOR-LIQUID EQUILIBRIA AND GROUP CONTRIBUTION

THEORIES FOR BINARY SYSTEMS OF

ALCOHOLS AND HYDROCARBONS

By

SHUEN-CHENG HWANG

Bachelor of Science in Engineering
Taiwan Cheng Kung University
Tainan, Taiwan
Republic of China
1967

Master of Science
Oklahoma State University
Stillwater, Oklahoma
1972

Submitted to the Faculty of the Graduate College
of the Oklahoma State University
in partial fulfillment of the requirements
for the Degree of
DOCTOR OF PHILOSOPHY
December, 1975

VAPOR-LIQUID EQUILIBRIA AND GROUP CONTRIBUTION

THEORIES FOR BINARY SYSTEMS OF

ALCOHOLS AND HYDROCARBONS

Thesis Approved:

Robert H. Robinson, Jr.
Thesis Adviser

John H. Erbar

Billy L. Crynes

Cyril M. Dunitz

N. N. Durham
Dean of the Graduate College

PREFACE

An apparatus was designed and constructed for measuring solution vapor pressure over the entire composition range at 25°C for the nine binary systems of alcohols (methanol, ethanol and n-propanol) with n-hexane, cyclohexane and benzene. Two methods were adopted for the calculation of vapor-lqiuid equilibrium data from experimental vapor pressure-liquid composition data. Results of the calculation are discussed and compared with literature data.

The excess Gibbs free energies from this study and the heat of mixing data from the literature were used to test the applicability of group contribution theories for representing the excess thermodynamic properties and vapor-liquid equilibria.

Finally, I am much indebted to my wife, Lois, my parents, brothers and sisters for their constant encouragement and support during my graduate studies.

TABLE OF CONTENTS

LIST OF TABLES

ix

LIST OF FIGURES

xi

xiv

NOMENCLATURE

Major Symbols

English Letters

A, B	– Van Laar constants in Equations II-1 and II-2
A', B', C', ...	– Redlich-Kister constants in Equation II-8
a_o, a_1	– Constants in Equation V-4
G^E	– Excess Gibbs free energy
ΔG^M	– Gibbs free energy of mixing
H^E	– Excess enthalpy
ΔH^M	– Enthalpy of mixing
k	– Boltzmann's constant
N^i	– Number of molecules of component i
N_{uv}	– Number of contact between segments u and v
N_{uv}^{oi}	– Number of contact between segments u and v in pure component i liquid
n_i	– Moles of component i
n_T	– Total number of moles in a mixture
n_v	– Number of groups of type v
P	– System pressure
P*	– Pure component vapor pressure
q	– Pure component area parameter
R	– Universal gas law constant

English Letters (Continued)

R_i − Size term for component i defined by Equation II-38

r_a, r_p − Number of segments of an alcohol or paraffin molecule

r_1, r_2 − Volume parameter for components 1, 2

S^E − Excess entropy

S_i − Number of size group in molecule i

T − Absolute temperature

u_{ij} − UNIQUAC binary interaction parameter

v − Molar volume

X_k − Group fraction defined by Equation II-41

X_v − Variable defined by Equation II-27

x − Liquid phase mole fraction

y − Vapor phase mole fraction

z − Coordination number

z_v − Number of contact points of group v

Greek Letters

α − A sepcific value of x_1

β − Second virial coefficient

Γ_k − Group activity coefficient of group k

Γ_k^* − Standard-State group activity coefficient of group k

γ − Activity coefficient

δ − Spacing between adjacent values of x_1

θ_i − Area fraction defined by Equation II-35

Λ – Wilson parameter defined by Equation II-4

λ – Wilson energy parameter

ν_i^* – Fugacity coefficient of pure i at pressure P_i^*

ν_{ki} – Number of interaction functional groups of kind k in molecule i

Σ – Summation sign

τ – Parameter defined by Equation II-33

Φ_i – Segment fraction defined by Equation II-34

ϕ – Fugacity coefficient

Ω'_{uv} – Exchange energy between segments u and v

Subscripts

a   – Alcohol

H   – Hydroxyl hydrogen segment

I   – Hydrocarbon segments in alcolho molecules

i, j   – Components i, j

ij   – Denotes interaction between components i and j

k, 1   – Groups k, 1

k1   – Denotes interaction between groups k and 1

mix   – Mixture property

O   – Hydroxyl oxygen segment

P   – Benzene, cyclohexane or n-hexane

S   – Hydrocarbon segments in benzene, cyclohexane, or n-hexane

u, v   – Types of group

uv   – Denotes interaction between groups u and v

1, 2	– Components 1, 2
12	– Denotes interaction between components 1 and 2

Superscripts

E	– Excess thermodynamic property
G	– Group-interaction contribution
i	– Component i
L	– Liquid phase
M	– Thermodynamic mixing property
o	– Ideal solution property
oi	– Pure component i
S	– Size contribution
V	– Vapor phase
*	– Standard-state property

Miscellaneous

ASOG	– Analytical solutions of groups method
calc'd	– Calculated value
exp	– Exponential operator for e
expt'l	– Experimental value
ℓn	– Natural logarithm
QLT	– Quasi-lattice theroy
UNIQUAC	– Universal quasi-chemical equation
∂	– Partial operator
$\int$	– Integral sign

CHAPTER I

INTRODUCTION

The phase equilibria and excess thermodynamic properties of nine

binary systems were investigated both experimentally and theoretically.

There were three major objectives in this study.

The first objective was to obtain systematic phase equilibrium

data in binary systems of alcohols with hydrocarbons. An apparatus

for measuring isothermal vapor-lqiuid equilibrium data was designed,

constructed and calibrated. Vapor pressures over the entire liquid

composition range of selected binary systems were measured at $25^{\circ}C$.

The following systems were studied:

(1)   methanol-benzene (MeOH-BZ)

(2)   ethanol-benzene (EtOH-BZ)

(3)   n-propanol-benzene (nPrOH-BZ)

(4)   methanol-cyclohexane (MeOH-CC6)

(5)   ethanol-cyclohexane (EtOH-CC6)

(6)   n-propanol-cyclohexane (nPrOH-CC6)

(7)   methanol-n-hexane (MeOH-nC6)

(8)   ethanol-n-hexane (EtOH-nC6)

(9)   n-propanol-n-hexane (nPrOH-nC6)

Note that these systems are binary mixtures of alcohols with aliphatic,

alicyclic and aromatic hydrocarbons that contain six carbon atoms.

These binary systems are highly non-ideal mixtures of polar and

1

non-polar components. The heat of mixing data of these systems at 25°C are available in the literature.

The second objective was to investigate techniques for vapor-liquid equilibrium data reduction. Barker's and Mixon's indirect methods were used. Results of the calculations are discussed.

The third objective was to test the applicability of group contribution theories to excess thermodynamic properties and vapor-liquid equilibrium predictions. The quasi-lattice theory, the universal quasi-chemical equation, and the analytical solutions of groups method were evaluated. Predicted values were compared with experimental data.

The procedures used to accomplish these objectives and the results of this study are presented in the following chapters.

CHAPTER II

LITERATURE REVIEW

The literature review pertinent to the present study is divided into four distinct sections: 1) experimental apparatus which have been used to measure isothermal vapor-liquid equilibrium data, 2) vapor-liquid equilibrium and heat of mixing data for the systems studied, 3) methods of vapor-liquid equilibrium data reduction, and 4) group contribution theories.

Experimental Apparatus

Numerous experimental apparatus have been developed to measure isothermal vapor-liquid equilibrium (VLE) data. The most common method employs a recirculating still which involves measurements of the following thermodynamic properties: temperature, vapor pressure, liquid composition and vapor composition (P-x-y). However, Van Ness and coworkers (35,57,58) indicate that if the thermodynamic properties of the vapor phase are known a priori, then VLE data can be determined from just the experimental vapor pressure-liquid composition (P-x) data without vapor-phase analysis.

The total pressure method has recently been used by several investigators (22,42). The static method of measuring vapor pressures over the entire liquid composition range is much faster and often more accurate than the recirculation method.

The apparatus described by Gibbs and Van Ness (22) consists a glass test cell, temperature bath, piston-injector, degassing component, vapor pressure measurement and vacuum system. The pure components are degassed by either distillation or vacuum sublimation. The degassed liquids are then transferred into two separate piston-injectors where they are stored under positive pressure. For each experimental run, the pure liquids are metered volumetrically into the test cell. The compositions in the cell are calculated from the accurately measured volumes injected. Two titration runs made with the pure liquids added in the reverse order are required to cover the entire composition range for a binary mixture. The vapor pressures are measured with a fused quartz precision pressure gauge.

The apparatus described by Reynolds (42) employs isothermal pressure measurement in twelve cells with varying composition to obtain VLE data. The twelve equilibrium cells made from glass or metal are connected to a manifold. The cells are loaded and degassed individually. The liquid compositions are accurately determined by weight. An advantage of Reynolds' design is that the liquid is never transferred out of the cell.

The apparatus used in the present study is similar to that described by Gibbs and Van Ness (22). However, the methods of vapor pressure measurement and the liquid measuring and injecting differ from those of Gibbs and Van Ness.

Experimental Data

Due to recent developments in solution theories, more isothermal VLE data in binary systems are needed for testing proposed theories.

One major objective of this study is to obtain more systematic VLE data at 25°C for highly non-ideal binary systems containing alcohols with hydrocarbons.

Chemical Abstracts from January, 1907 to March, 1974 and compilations of VLE data by Chu, Wang, Levy and Paul (15), and by Hala, Pick, Fried and Vilim (25) were used to locate published isothermal VLE data for the systems studied. Chemical Abstracts from January, 1907 to March, 1974 were also used to locate the heat of mixing data.

Available isothermal VLE and heat of mixing data at 25°C are summarized in Table I. Several investigators report experimental VLE or heat of mixing data for these systems at other temperatures. However, only the data which will be referred to later in this study are summarized in Table I.

Vapor-Liquid Equilibrium Data Reduction

Methods for VLE data reduction have been discussed recently by Van Ness and coworkers (1,2,13,56). In this section, the procedure necessary for the indirect reduction of VLE data to obtain vapor compositions and excess Gibbs free energies is discussed.

Barker's Method

The indirect method proposed by Barker (5) involves the use of a model for calculation of liquid phase activity coefficients or excess Gibbs free energies. Parameters for each activity coefficient or excess Gibbs free energy model are empirical constants. They must be evaluated by statistical method to give the best fit to the

TABLE I

SUMMARY OF AVAILABLE PHASE EQUILIBRIUM AND HEAT OF MIXING DATA

System	VLE Data		Heat of Mixing Data	
	Temperature, $^\circ$C	Reference No.	Temperature, $^\circ$C	Reference No.
Methanol–Benzene	25(1 point), 35 45(1 point), 55	48	25 25,35,45	23,60 10,37
Ethanol–Benzene	25 45 55	51 11 29	25 25,35,45	23,30 10,37
n–Propanol–Benzene	40 45	34 12	25,35,45	10,37
Methanol–Cyclohexane	25 25,40,50	33 14*	25	33
Ethanol–Cyclohexane	25 5,20,35,50,60	61 46	25	23,49,59 60
n–Propanol–Cyclohexane	55,65	52	25	59,60
Methanol–n–Hexane	45	21	25,30,33.7,40, 45,50	45
Ethanol–n–Hexane	25 35,45,55 55	51 31 29	25 25,35,45 30,45	30 9 44

TABLE I (Continued)

	VLE Data		Heat of Mixing Data	
System	Temperature, ^{o}C	Reference No.	Temperature, ^{o}C	Reference No.
n-Propanol-n-Hexane	45	10	25,35,45	9

* No vapor pressures available.

experimental P-x data. Three existing activity coefficient models which were used in this study are described below.

The equations proposed by Van Laar (54) include two empirical constants, A and B, for each binary system. They are:

$$\ln \gamma_1^L = \frac{Ax_2^2}{(Ax_1/B + x_2)^2} \tag{II-1}$$

and

$$\ln \gamma_2^L = \frac{Bx_1^2}{(Bx_2/A + x_1)^2} \tag{II-2}$$

The Van Laar equations are widely used in applied work because they are simpler than many other equations which have been proposed.

Wilson (63) derived an expression for excess Gibbs free energy based on molecular considerations. The generalized equation is

$$G^E/RT = -\sum_{i=1}^{n} \left[x_i \ln \left(\sum_{j=1}^{n} x_j \Lambda_{ij} \right) \right] \tag{II-3}$$

where

$$\Lambda_{ij} \equiv v_j/v_i \exp \left[(\lambda_{ii} - \lambda_{ij})/RT \right] \tag{II-4}$$

The Wilson's parameter λ_{ij} represent the strength of interaction between molecules i and j. The energy differences $(\lambda_{ii} - \lambda_{ij})$ are temperature-dependent but in many cases they can be treated as constant over small temperature range without introducing serious error.

The activity coefficient may be derived from Equation II-3. The result is

$$\ln \gamma_k^L = -\ln \left[\sum_{j=1}^{n} x_j \Lambda_{kj} \right] + 1 - \sum_{i=1}^{n} \frac{x_i \Lambda_{ik}}{\sum_{j=i}^{n} x_i \Lambda_{ij}} \qquad \text{(II-5)}$$

For binary mixtures, Equation II-5 reduces to

$$\ln \gamma_1^L = -\ln(x_1 + \Lambda_{12} x_2) + x_2 \left[\frac{\Lambda_{12}}{x_1 + \Lambda_{12} x_2} \right.$$

$$\qquad \text{(II-6)}$$

$$\left. - \frac{\Lambda_{21}}{\Lambda_{21} x_1 + x_2} \right]$$

$$\ln \gamma_2^L = -\ln(x_2 + \Lambda_{21} x_1) - x_1 \left[\frac{\Lambda_{12}}{x_1 + \Lambda_{12} x_2} \right.$$

$$\qquad \text{(II-7)}$$

$$\left. - \frac{\Lambda_{21}}{\Lambda_{21} x_1 + x_2} \right]$$

The third model used in this study is Redlich-Kister equation which relates the Gibbs free energy to liquid composition by a series expansion:

$$G^E/RT = x_1 x_2 \left[A' + B' (x_1 - x_2) + C' (x_1 - x_2)^2 \right.$$

$$\qquad \text{(II-8)}$$

$$\left. + D' (x_1 - x_2)^3 + \cdots \right]$$

where A', B', C', D', $\cdots$ are temperature-dependent parameters.

The activity coefficients derived from Equation II-8 are given by

$$\ln \gamma_1^L = a^{(1)} x_2^2 + b^{(1)} x_2^3 + c^{(1)} x_2^4 + d^{(1)} x_2^5 + \cdots \quad \text{(II-9)}$$

$$\ln \gamma_2^L = a^{(2)} x_1^2 + b^{(2)} x_1^3 + c^{(2)} x_1^4 + d^{(2)} x_1^5 + \cdots \quad \text{(II-10)}$$

where

$$a^{(1)} = A' + 3B' + 5C' + 7D' + \cdots$$

$$a^{(2)} = A' - 3B' + 5C' - 7D' + \cdots$$

$$b^{(1)} = -4 \, (B' + 4C' + 9D' + \cdots)$$

$$b^{(2)} = 4 \, (B' - 4C' + 9D' - \cdots)$$

$$c^{(1)} = 12 \, (C' + 5D' + \cdots)$$

$$c^{(2)} = 12 \, (C' - 5D' + \cdots)$$

$$d^{(1)} = -32 \, (D' + \cdots)$$

$$d^{(2)} = 32 \, (D' - \cdots)$$

$$\cdots$$

The number of parameters required to accurately represent the experimental P-x data depends on the molecular complexity of the mixture, on the accuracy of the experimental data, and on the number of available experimental data points. Redlich-Kister equations with up to nine parameters were used in this study.

Mixon's Method

The indirect method of Barker requires the assumption of a particular activity coefficient or excess Gibbs free energy model and the evaluation of its parameters by statistic methods. This deficiency of Barker's method has been avoided by Mixon, Gumowski and Carpenter (36). They present another indirect method in which the _a priori_ assumption of a particular activity coefficient model is not required. Basically,

Mixon's method involves an iterative numerical calculation of activity coefficients.

The excess Gibbs free energy of mixing is related to the activity coefficients by the following thermodynamic relationships

$$G^E = RT \sum_{i=1}^{n} x_i \ln (\gamma_i^L) \qquad \text{(II-11)}$$

and

$$RT \ln (\gamma_i^L) = \left[\frac{\partial (n_T G^E)}{\partial n_i}\right]_{T, P, n_j \neq n_i} = \bar{G}_i^E \qquad \text{(II-12)}$$

where $\bar{G}_i^E$ is the partial molal excess Gibbs free energy for component i.

For binary mixture, the equations for the partial molal excess Gibbs free energies developed by Dodge (19) are

$$\bar{G}_1^E = G^E + (\partial G^E/\partial x_1)_{T, P} - x_1 (\partial G^E/\partial x_1)_{T, P} \qquad \text{(II-13)}$$

and

$$\bar{G}_2^E = G^E - x_1 (\partial G^E/\partial x_1)_{T, P} \qquad \text{(II-14)}$$

Substitution of Equation II-13 and II-14 into Equation II-12 gives

$$RT \ln \gamma_1^L = G^E + (\partial G^E/\partial x_1)_{T, P} - x_1 (\partial G^E/\partial x_1)_{T, P} \qquad \text{(II-15)}$$

and

$$RT \ln \gamma_2^L = G^E - x_1 (\partial G^E/\partial x_1)_{T, P} \qquad \text{(II-16)}$$

If equally spaced values of x_1 are used, the finite difference representation for the partial derivatives in Equation II-15 and II-16 can be written as

$$\left(\partial G^E/\partial x_1\right)_{x_1=\alpha} = \frac{G^E_{\alpha+\delta} - G^E_{\alpha-\delta}}{2\delta} \qquad (II-17)$$

where

α = value of x_1 for which $\partial G^E/\partial x_1$ is evaluated

δ = spacing between adjacent values of x_1.

Expression for the vapor pressure in terms of the excess Gibbs free energy and its composition derivatives can be written as

$$P = x_1 \, P_1^* \, \exp\left\{\frac{1}{RT}\left[G^E_\alpha + \frac{G^E_{\alpha+\delta} - G^E_{\alpha-\delta}}{2\delta} - x_1\left(\frac{G^E_{\alpha+\delta} - G^E_{\alpha-\delta}}{2\delta}\right)\right]\right\}$$
$$+ x_2 \, P_2^* \, \exp\left\{\frac{1}{RT}\left[G^E_\alpha - x_1\left(\frac{G^E_{\alpha+\delta} - G^E_{\alpha-\delta}}{2\delta}\right)\right]\right\} \qquad (II-18)$$

With the initially assumed values of G^E (may be all equal to zero) at each values of x_1, the vapor pressures can be calculated by Equation II-18 and compared with experimental values. A combination of Newton's method with block relaxation technique may be used to improve the values of G^E. The iterative procedure is repeated until the difference between the calculated and experimental vapor pressures is within a desired tolerance. The vapor compositions under the assumption of an ideal vapor phase can be computed by the following equation

$$y_i = \frac{\gamma_i^L \, x_i \, P_i^*}{P} \, , \quad i = 1, 2 \qquad (II-19)$$

If the liquid-phase is assumed to be incompressibile and the vapor-phase non-idealities are significant, Equation II-18 should be replaced by

$$P = \sum_{i=1}^{2} \frac{\gamma_i^L \, x_i \, P_i^* \, \nu_i^* \, \exp \left[\frac{\nu_i^L \, (P - P_i^*)}{RT} \right]}{\phi_i^V} \qquad \text{(II-20)}$$

where

$$\exp \left[\frac{\nu_i^L \, (P - P_i^*)}{RT} \right] = \text{Poynting correction factor for the pure component fugacity at a pressure } P \text{ other than } P_i^*.$$

To correct the incompressible liquid phase and non-ideal vapor phase, values of y_i calculated by Equation II-19 are used to estimate vapor phase fugacity coefficients by the virial equation truncated after the second virial coefficient. The equations for calculation of vapor phase fugacity coefficients are

$$\ln \phi_1^V = (2/v) \, (y_2 \, \beta_{12} + y_1 \, \beta_{11}) - \ln \, (Pv/RT) \qquad \text{(II-21)}$$

$$\ln \phi_2^V = (2/v) \, (y_1 \, \beta_{12} + y_2 \, \beta_{22}) - \ln \, (Pv/RT) \qquad \text{(II-22)}$$

where

β_{11} and β_{22} = pure component second virial coefficients

β_{12} = second interaction virial coefficient for components 1 and 2.

The correlation proposed by O'Connell and Prausnitz (38) for calculation of second virial coefficients was used in this study.

The fugacity coefficient of pure component i at system temperature and pure component vapor pressure, P_i^*, can be calculated by simplifying Equation II-21 or II-22:

$$\ln \nu_i^* = (2/v_i) \ (\beta_{ii}) - \ln \ (P_i^* \ v_i/RT), \ i = 1, \ 2 \qquad (II-23)$$

The fugacity coefficients calculated from Equations II-21, II-22 and II-23 are used with Poynting correction factors to calculate the vapor pressure by Equation II-20. Again, the combination of Newton's method with block relaxation technique is used to improve the values of G^E. After the pressure calculations converge, vapor compositions are calculated by the following equation:

$$y_i = \frac{\gamma_i^L \ x_i \ P_i^* \ \nu_i^* \ \exp \left[\dfrac{v_i^L \ (P - P_i^*)}{RT} \right]}{\phi_i^v \ P} \qquad i = 1, \ 2 \qquad (II-24)$$

Mixon's method for computing vapor compositions from experimental P-x data has one disadvantage. Since equally spaced values of x_1 are used, the corresponding values of vapor pressure are required to perform the calculation. Mixon suggests that smoothed vapor pressures can be obtained by a least square polynomial fit to the experimental P-x data. However, for some mixtures, no reasonable polynomial will result in a good fit of experimental P-x data. In order to take full advantage of Mixon's method, smoothed vapor pressures at equally spaced values of x_1 were obtained by graphical methods instead of fitting the experimental P-x data to a polynomial.

Group Contribution Theories

Numerous group contribution theories have been developed for predicting phase equilibrium and excess thermodynamic properties of solutions. This section makes no pretense of encompassing all previous contributions. The group contribution theories selected for this study are quasi-lattice theory, universal quasi-chemical equation, and analytical solutions of groups method. In this section, the procedures and equations necessary for predicting VLE data and excess thermodynamic properties are discussed.

Quasi-Lattice Theory

The generalized quasi-lattice theory described by Barker (4,6) is used in the present study. This theory is based on a quasi-lattice model which considers each molecule i in solution to be composed of a number, r_i, of segments arranged on z-coordinated lattice sites. Each type of segment v possesses a number, z_v, of contact points which have specific interactions with adjacent segments.

The quasi-lattice theory requires a knowledge of the type and number of contact points of each segment on each molecule and the exchange energies for all possible interactions of these segments. In the present study, the type and number of contact points are specified in the manner of Goats, et al. (23,24). For example, each n-hexane, cyclohexane or benzene molecule is considered to have only hydrocarbon-type segment, S. For paraffin segments, there are three contact points on each methyl group and two on each methylene group. The benzene is considered to have twelve contact points. The alcohols

are considered to contain three types of sites -- hydroxyl hydrogen segment, H, hydroxyl oxygen segment, O, and paraffin-type segments, I. The H segments are considered to have one contact point, O segments two, and paraffin-type segments are specified as they are for the n-paraffinic hydrocarbons.

The excess enthalpy of the solution expressed in terms of the numbers of contacts, N_{uv}, between segments of types u and v is given by

$$H^E = - \sum_u \sum_{v>u} (\sum_i N_{uv}^{oi} - N_{uv}) \, \Omega'_{uv} \qquad \text{(II-25)}$$

where the exchange energies Ω'_{uv} are considered to be adjustable parameters, and the superscript oi denotes the assembly of N^i molecules of pure liquid i.

For the present study of binary mixtures containing alcohol with benzene, cyclohexane or n-hexane, the general equations for calculating the excess thermodynamic properties have been given by Barker (4,9) as following:

$$X_H (X_H + X_O \, e^{-\Omega'_{OH}/kT} + X_I \, e^{-\Omega'_{HI}/kT} + X_S \, e^{-\Omega'_{HS}/kT}) =$$

$$\frac{x_a}{2} \, n_H^a \, z_H$$

$$X_O (X_H \, e^{-\Omega'_{OH}/kT} + X_O + X_I \, e^{-\Omega'_{OI}/kT} + X_S \, e^{-\Omega'_{OS}/kT}) =$$

$$\frac{x_a}{2} \, n_O^a \, z_O$$

$$X_I \left(X_H \, e^{-\Omega'_{HI}/kT} + X_0 \, e^{-\Omega'_{OI}/kT} + X_I + X_S \, e^{-\Omega'_{IS}/kT} \right) =$$

$$\frac{x_a}{2} \, n_I^a \, z_I$$

$$X_S \left(X_H \, e^{-\Omega'_{HS}/kT} + X_0 \, e^{-\Omega'_{OS}/kT} + X_I \, e^{-\Omega'_{IS}/kT} + X_S \right) =$$

$$\frac{x_p}{2} \, n_S^P \, z_S \tag{II-26}$$

where

x_a = mole fraction alcohol

x_p = mole fraction of benzene, cyclohexane or n-hexane,

and

X = new variable defined as

$$N_{uu} = N X_u^2 \tag{II-27a}$$

$$N_{uv} = 2 N X_u X_v \, \exp \left(-\Omega'_{uv}/kT \right) \tag{II-27b}$$

Combining Equations II-25, II-26 and II-27, the excess enthalpy of
the binary solution becomes

$$H^E = -2RT \left[\left(X_H X_0 - x_a X_H^1 X_0^1 \right) \left(-\Omega'_{OH}/RT \right) \exp \left(-\Omega'_{OH}/RT \right) \right.$$

$$+ \left(X_H X_I - x_a X_H^1 X_I^1 \right) \left(-\Omega'_{HI}/RT \right) \exp \left(-\Omega'_{HI}/RT \right)$$

$$+ \left(X_0 X_I - x_a X_0^1 X_I^1 \right) \left(-\Omega'_{OI}/RT \right) \exp \left(-\Omega'_{OI}/RT \right)$$

$$+ X_H X_S \left(-\Omega'_{HS}/RT \right) \exp \left(-\Omega'_{HS}/RT \right)$$

$$+ X_0 \, X_S \, (-\Omega'_{OS}/RT) \, \exp \, (-\Omega'_{OS}/RT)$$

$$+ X_I \, X_S \, (-\Omega'_{IS}/RT) \, \exp \, (-\Omega'_{IS}/RT) \tag{II-28}$$

where X^1's are evaluated by solving Equation II-26 for the special case of $x_a = 1.0$.

The equation for calculating excess Gibbs free energy is given by Barker (4) as follows:

$$G^E = x_a \, RT \, \{ n_H \, z_H \, \ln \, (X_H/x_a X_H^1) + n_0 \, z_0 \, \ln \, (X_0/x_a \, X_0^1)$$

$$+ \, n_I \, z_I \, \ln(X_I/x_a \, X_I^1)$$

$$+ \, r_a \, (\tfrac{z}{2} - 1) \, \ln \, [(x_a \, r_a + x_p \, r_p)/r_a]\}$$

$$+ \, x_p \, RT \, \{ n_S \, z_S \, \ln \, (X_S/x_p \, X_S^1)$$

$$+ \, r_p \, (\tfrac{z}{2} - 1) \, \ln \, [(x_a \, r_a + x_p \, r_p)/r_p]\} \tag{II-29}$$

A non-linear regression technique was employed to fit experimental heat of mixing data by Equation II-28. The energy parameters and the variables, X's, thus obtained were used in Equation II-29 for calculating excess Gibbs free energy.

Universal Quasi-Chemical Equation

A semi-theoretical equation for the excess Gibbs free energy of partly or completely miscible systems was developed by Abrams and Prausnitz (3). For predicting binary system excess Gibbs free energy, the universal quasi-chemical (UNIQUAC) equation requires only two

adjustable binary energy parameters and two pure-component structure parameters (a size parameter, r, and surface parameter, q).

The excess Gibbs free energy for binary systems can be expressed in terms of the parameters as following:

$$G^E = G^E(\text{combinatorial}) + G^E(\text{residual}) \qquad \text{(II-30)}$$

where

$$G^E(\text{combinatorial}) = RT \left[x_1 \ln \frac{\Phi_1}{x_1} + x_2 \ln \frac{\Phi_2}{x_2} \right.$$

$$\left. + \frac{z}{2} \left(q_1 x_1 \ln \frac{\theta_1}{\Phi_1} + q_2 x_2 \ln \frac{\theta_2}{\Phi_2} \right) \right] \qquad \text{(II-31)}$$

and

$$G^E(\text{residual}) = -RT \left[q_1 x_1 \ln (\theta_1 + \theta_2 \tau_{21}) \right.$$

$$\left. + q_2 x_2 \ln (\theta_2 + \theta_1 \tau_{12}) \right] \qquad \text{(II-32)}$$

where

$$\tau_{21} \equiv \exp \left[- \left(\frac{u_{21} - u_{11}}{RT} \right) \right] \qquad \text{(II-33a)}$$

$$\tau_{12} \equiv \exp \left[- \left(\frac{u_{12} - u_{22}}{RT} \right) \right] \qquad \text{(II-33b)}$$

In Equation II-31, the average segment fraction, Φ_i, is defined as

$$\Phi_i = \frac{x_i r_i}{x_1 r_1 + x_2 r_2} \qquad \text{(II-34)}$$

and the average area fraction, θ_i, is defined as

$$\theta_i = \frac{x_i q_i}{x_1 q_1 + x_2 q_2} \qquad \text{(II-35)}$$

In Equation II-33, the adjustable binary energy parameters $(u_{21} - u_{11})$ and $(u_{12} - u_{22})$ given in Abrams' paper (3) were obtained from experimental phase equilibrium data by a fitting technique.

Equations II-30 through II-32 give the excess Gibbs free energy for a binary mixture. With the G^E-x data, the vapor-liquid equilibrium data can be predicted by Mixon's method described in previous section.

Analytical Solutions of Groups Method

The analytical solutions of groups (ASOG) approach was developed by Derr and Deal (18) based on previous work on group contribution theories by Deal, et al. (41,64).

The ASOG method correlates the interaction of functional groups. For the binary systems studied in present work, the functional groups include methylene ($-CH_2-$), hydroxyl ($-OH$), and benzene (C_6H_5-) groups. The methyl (CH_3-) group is considered equivalent to methylene group.

The activity coefficient of a component i in solution is treated as a sum of two terms,

$$\ln \gamma_i = \ln \gamma_i^S + \ln \gamma_i^G \tag{II-36}$$

where γ_i^S is the size contribution term to the activity coefficient and is expressed in terms of size term, R_i, as

$$\ln \gamma_i^S = 1 - R_i + \ln R_i \tag{II-37}$$

where

$$R_i = \frac{S_i}{S_1 \, x_1 + S_2 \, x_2} \tag{II-38}$$

where S_i is the number of size groups in molecule i.

In Equation II-36, the group-interaction contribution term, γ_i^G, to the activity coefficient is treated as the difference between group contributions. These contributions are summed over all interaction groups comprising the solution of interest. Thus:

$$\ln \gamma_i^G = \sum_k \nu_{ki} \ln \Gamma_k - \sum_k \nu_{ki} \ln \Gamma_k^* \qquad \text{(II-39)}$$

where ν_{ki} is the number of interaction functional groups of kind k in molecule i, and Γ is the group activity coefficient calculated from Wilson Equation as:

$$\ln \Gamma_k = - \ln \sum_1 X_1 A_{k1} + [1 - \sum_1 \frac{X_1 A_{1k}}{\sum_m X_m A_{1m}}] \qquad \text{(II-40)}$$

where A_{k1} is the interaction parameter for each functional group in the mixture, and X_k is the group fraction defined as

$$X_k = \frac{\sum_i x_i \nu_{ki}}{\sum_k \sum_i x_i \nu_{ki}} \qquad \text{(II-41)}$$

The standard-state group activity coefficient, Γ_k^*, is also determined by Equations II-40 and II-41 for each separate pure component.

The activity coefficients calculated by the ASOG method are used to calculate excess Gibbs free energy by the following equation:

$$G^E = RT \sum_i x_i \ln (\gamma_i) \qquad \text{(II-42)}$$

The activity coefficients are also used, together with an equation of state and vapor non-ideality corrections, to calculate the vapor pressures and vapor compositions for binary mixtures.

CHAPTER III

EXPERIMENTAL APPARATUS AND MATERIALS

The apparatus used in this study was designed so that it could be used to measure the binary mixture vapor pressures over the entire liquid composition range at constant temperature. The major components of the apparatus and their arrangement are shown in Figure 1.

The apparatus contains five major components. All the components, except vacuum system and degassing assembly, are inside a constant temperature air bath. A constant temperature liquid bath may be raised to immerse the equilibrium cell during a run and lowered to expose the cell.

The details of the major components and the materials used in this study are discussed in the following sections.

Vacuum System

The important construction features of the vacuum system are shown in Figure 2. (Letters used in this section refer to Figure 2.) The vacuum is achieved by combination of a Precision VacTorr mechanical pump (model D-25) (A), and a Bendix oil diffusion pump (B). All the vacuum lines are 1/2-inch-OD copper tubing. A glass cold trap (F) immersed in liquid nitrogen is used to trap condensable materials before they reach the vacuum pump, eliminating the chance of corrosion and damage to the
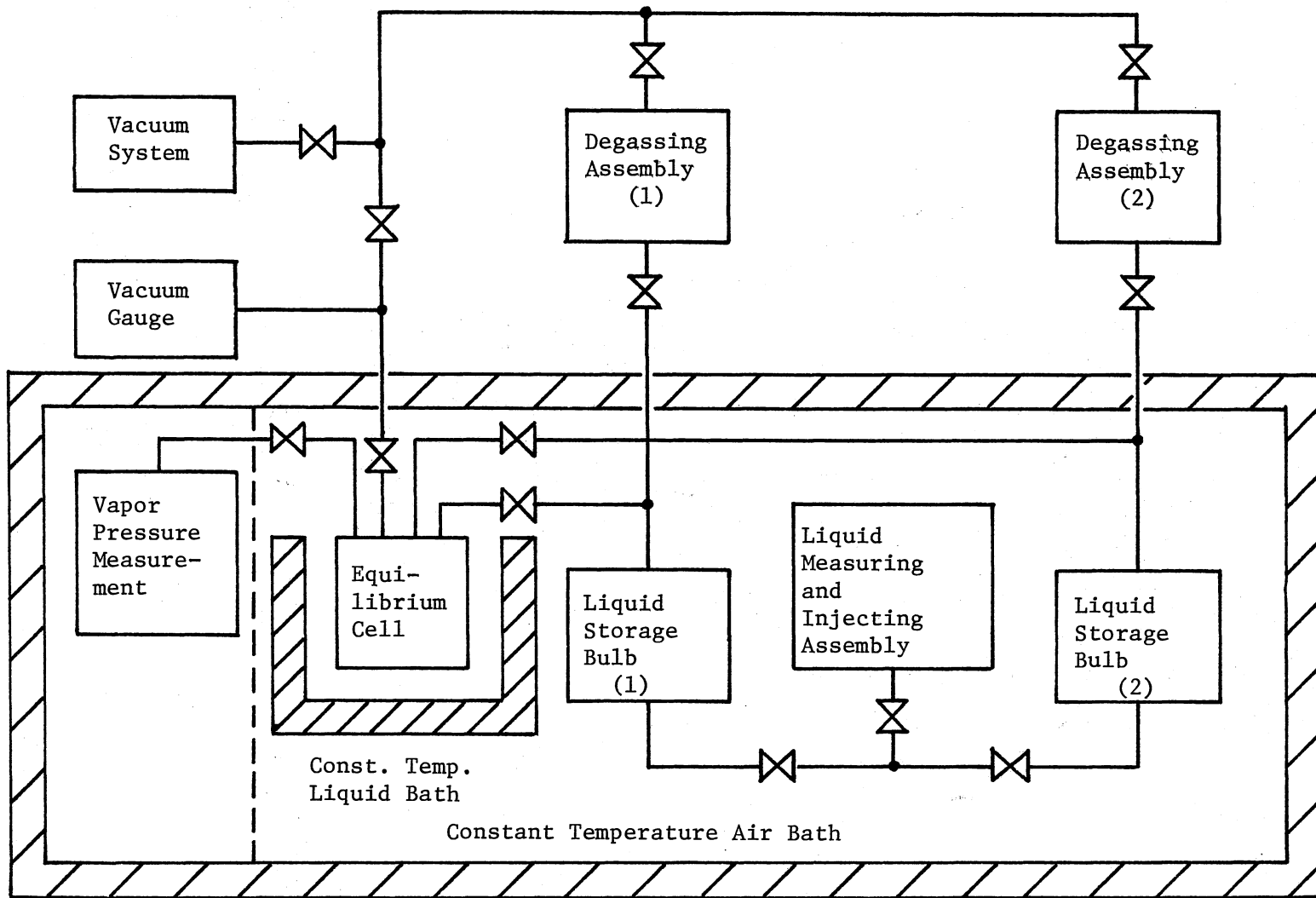
Figure 1.   Schematic Diagram of Apparatus
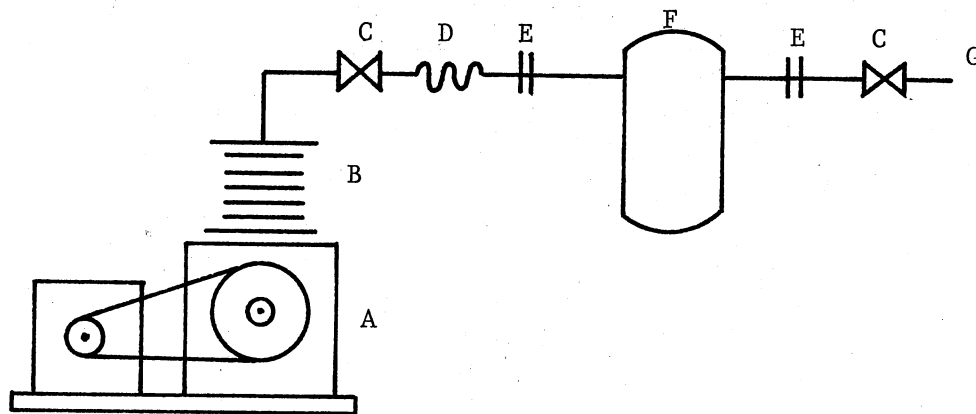
A. Mechanical Pump

B. Diffusion Pump

C. High Vacuum Shutoff Valves

D. Cajon Flexible Bellows Tubing

E. Ultra-Torr Unions

F. Glass Cold Trap

G. Connection to Degassing Assembly

Figure 2. Vacuum System

vacuum pump. The cold trap is connected to the vacuum lines by hand-
tightened Cajon ultra-torr unions (E). A Cajon stainless-steel flexible
bellows tubing (D) is used between the glass and metal joint to prevent
the breakage of glass during installing or removing the cold trap. All
valves (C) used in the vacuum system are 1/2-inch Circle Seal high
vacuum brass shutoff valves.

The pressure in the vacuum system is measured with a thermocouple/
ionization vacuum gauge (Precision Scientific Company, Cat. No. 10479).

Degassing Assembly

The degassing assembly is shown in Figure 3. (Letters used in this
section refer to Figure 3.). The design of the degassing bulb is based
on that of Gibbs and Van Ness (22). The condensation chamber (F) is a
6-inch-diameter glass cylinder with a 3-inch-diameter concentric cold
finger (E). All valves (D) in this degassing assembly are 0-4 mm high
vacuum teflon needle valves (Manufactured by West Glass Inc.). The
200-ml liquid sample bulb (G) is connected to the condensation chamber
by a 18/9 glass joint (H) with O-ring seal. A Swagelok reducing union
(I) (from 1/4-inch to 1/8-inch) connects the degassing assembly to
liquid storage bulb. A 1/2-inch hand-tightened Cajon ultra-torr union
(C), followed by a Cajon stainless-steel flexible bellows tubing (B),
connects the degassing assembly to vacuum system.

Chain clamps cushioned with asbetos belting hold the condensation
chamber in a vertical orientation. A Flexaframe multi-clutch connec-
tor holds the clamp to a Flexaframe rod which is mounted on the top of
the constant temperature air bath by a Flexaframe foot. A shield
constructed from 1/4-inch Plexiglas is used to protect the investigator
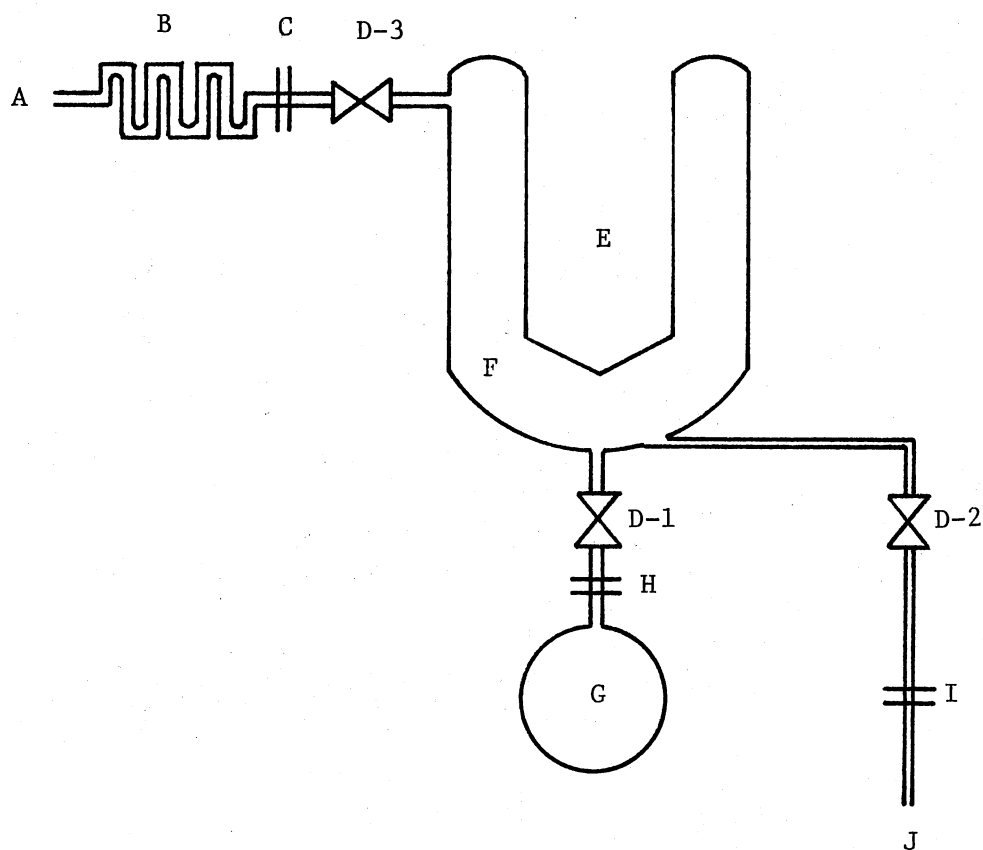
A. Connection to Vacuum System

B. Cajon Flexible Bellows Tubing

C. Ultra-Torr Union

D. High Vacuum Teflon Needle Valves

E. Cold Finger

F. Condensation Chamber

G. Liquid Sample Bulb

H. Glass Joint with O-Ring Seal

I. Swagelok Reducing Union

J. Connection to Liquid Storage Bulb

Figure 3. Degassing Assembly

from the danger of implosion of the degassing bulb. Also each degass-
ing bulb is wrapped with electrical tape, leaving a vertical slot for
viewing inside the bulb.

Liquid Storage, Measuring and Injecting Assembly

Figure 4 shows the schematic drawing of the liquid storage bulbs
and the measuring and injecting assembly. (Letters used in this section
refer to Figure 4.) Each storage bulb (C) has a capacity of 200 ml.
The measuring bulb set (D) is a set of glass bulb jointed by 5-cm-long,
1-mm-ID capillaries. A hash mark is made at the middle of each capil-
lary. The volume of each glass bulb was calibrated with distilled
water. Two measuring bulb sets have been used in this study. Results
of their calibrations are described later.

A Ruska model 2426 hand-operated pump (F) was used for transferring
mercury from the reservior (E) to the measuring bulb set (D). The
connection lines among the liquid storage bulb, degassing assembly,
and equilibrium cell are 1/8-inch-OD copper tubing. Those among the
liquid storage bulb, measuring bulb set, and Ruska pump are 1/8-inch-OD
stainless-steel tubing. All of the valves (G) are 1/8-inch Circle
Seal high vacuum stainless-steel shutoff valves.

Equilibrium Cell and Vapor Pressure Measurement

The equilibrium cell is shown in Figure 5. (Letters used in this
section refer to Figure 5.) The 4-inch-square brass cell lid (D) is
fastened to the ceiling of the constant temperature air bath by a
support frame. The test cell (E) is a stock end piece of 2-inch-ID
Corning industrial glass pipe with a capacity of about 150 ml.
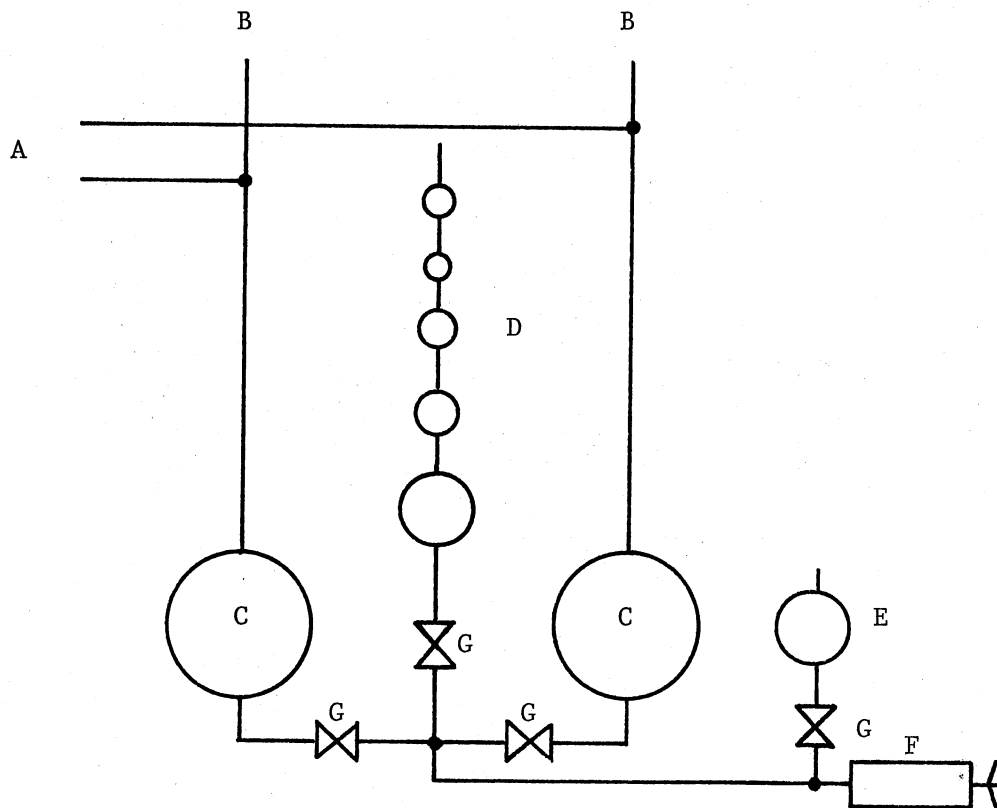
A.   Connection to Equilibrium Cell

B.   Connection to Degassing Assembly

C.   Liquid Storage Bulb

D.   Measuring Bulb Set

E.   Mercury Reservoir

F.   Ruska Pump

G.   High Vacuum Shutoff Valves

Figure 4.   Liquid Storage Bulb and Measuring and Injecting
           Assembly
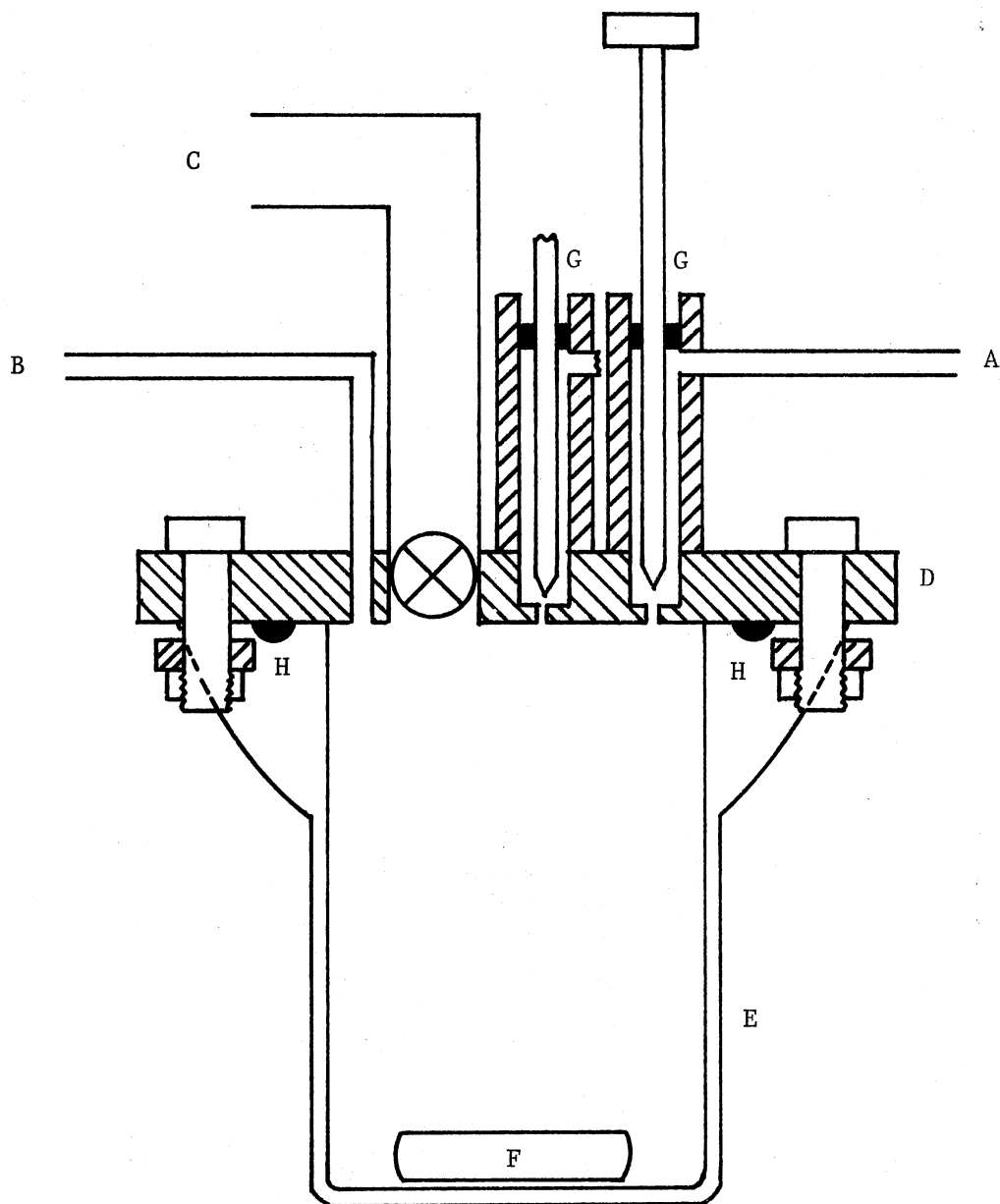
A. Connection to Liquid Storage Bulb
B. Connection to Mercury-in-Glass Manometer
C. Vacuum Connection
D. Cell Cover
E. Glass Cup
F. Teflon-Coated Magnetic Spanbar
G. Needle Valves
H. O-Ring

Figure 5. Equilibrium Cell

A brass ring with four bolts compresses an O-ring (H) against the well-polished cell lid to provide a vacuum seal. A teflon-coated magnetic spinbar (F) rests in the bottom of the cell. Stirring inside the equilibrium cell and the constant temperature liquid bath is actuated by an air-driven magnetic stirrer beneath the liquid bath. The construction of the custom-machined needle valves (G) is similar to that of Gibbs and Van Ness (22).

Vapor pressures inside the equilibrium cell are measured by a mercury-in-glass manometer. The manometer is in a separate constant temperature air bath made from 3/4-inch plywood. The temperature in the air bath is kept 3 to 5°C higher than that in the equilibrium cell to avoid condensation of liquid in the connection lines of manometer. The pressure difference between the two arms of the manometer was measured with a Caertner cathetometer (model M908).

<center>Constant Temperature Baths</center>

The constant temperature baths include a liquid bath and two air baths. The constant temperature liquid bath is a 5-1/2 inch-diameter glass water bath. The water bath is set on a scissor jack. It can be easily raised to immerse the equilibrium cell during a run and lowered to expose the cell. Temperature inside the water bath is controlled by a Haake constant temperature circulator (model FP). Water at 5-10°C is provided to the built-in colling coil of the circulator by a commercial water chiller. The controller regulates the bath temperature within $\pm$ 0.005°C during a run. Temperature of the water bath is measured by a mercury-in-glass thermometer with divisions of 0.01°C. The mercury thermometer was calibrated at 25°C with a platinum

resistance thermometer. The uncertainty in temperature measurement is $\pm$ 0.01°C.

The constant temperature air bath, which contains most of the major components as shown in Figure 1, is a 1/2-inch plywood box with dimensions of 51 inches by 21-1/2 inches by 30 inches. It is mounted on a frame constructed from slotted angle iron. The temperature in the air bath is controlled by a precision proportional temperature controller (Bayley Instrument Company, model 116). Heat is provided by a 250-watt strip heater which is connected to the temperature controller. The cooling coil is constructed of approximately two feet of 1/4-inch-OD copper tubing. Cooling water at 5-10°C is also provided by the commercial water chiller. The heater and the cooling coil are inside a small housing. The air is circulated with a "squirrel cage" blower. Air passes through the heater and the cooling coil and is drawn into the blower. The temperature in the air bath is at 26.0 $\pm$ 0.2°C. The higher temperature in the air bath prevented condensation of liquid in the connection lines between the equilibrium cell and pressure.

The constant temperature air bath for the vapor pressure measuring assembly is constructed from 3/4-inch plywood. Preheated compressed air passes through the air bath, which maintains a temperature of 28-30°C. The higher temperature around the manometer avoids condensation of liquid in the connection lines and manometer.

Materials

The organic chemicals used in this investigation are summarized in Table II with the manufacturers' specified minimum purities. All

TABLE II

ORGANIC CHEMCIALS USED IN THIS INVESTIGATION

Compound	Manufacturer	Specified Minimum Purity	Most Probable Impurity
Methanol	Fisher Scientific Co.	99.9 mole %	---
Ethanol	U. S. Industrial Chemical Company	Reagent Quality 200 Proof	---
n-Propanol	Fisher Scientific Co.	Certified Grade Boiling Range-- 96.9-97.3°C	---
Benzene	Phillips Petro. Co.	99.91 mole %	Toluene
Cyclohexane	Phillips Petro. Co.	99.94 mole %	2,4-Dimethylpentane and 2,2-Dimethylpentane
n-Hexane	Phillips Petro. Co.	99.99 mole %	Methyl cyclopentane

chemicals were used as received without further purification. The
physical properties of the organic chemicals used in this investiga-
tion are listed in Table III.

TABLE III

PURE COMPONENT PHYSICAL PROPERTIES

Compound	Molecular[***] Weight MW	Critical Properties[***]			Acentric[***] Factor ω or ω_H	Dipole[**] Moment μ (Debye)	Association[**] Constant η	Density[*] ρ, 25°C (gm/cc)
		T_c (K)	P_c (atm)	V_c (cc/mole)				
Methanol	32.04	513.2	78.5	118.0	0.105	1.66	1.21	0.7865
Ethanol	46.07	516.3	63.0	167.0	0.152	1.69	1.00	0.7851
n-Propanol	60.09	536.7	51.0	218.2	0.201	1.68	0.57	0.7999
Benzene	78.11	562.1	48.6	260.1	0.211	0.0	0.0	0.8737
Cyclohexane	84.16	553.2	40.0	308.0	0.209	0.0	0.0	0.7739
n-Hexane	86.17	507.3	29.9	368.0	0.298	0.0	0.0	0.6548

*   From Timmermans, J. (ed.) "Physico-Chemical Constants of Pure Organic Components," Vol. 2, Elsevier Publishing Co., N. Y., (1965).

**   O'Connell, J. P. and J. M. Prausnitz, I&EC Process Design and Development, 6, (2), 245(April, 1967).

*** From Reid, R. C. and T. K. Sherwood, "The Properties of Gases and Liquids," 2nd ed., McGraw-Hill Book Company, New York, N. Y. (1966).

CHAPTER IV

EXPERIMENTAL PROCEDURE

The experimental procedure for obtaining binary mixture vapor
pressure data is described in this chapter. This description includes
evacuation of the system, leak testing, degassing the sample, and an
experimental run to obtain total vapor pressure-liquid composition
data.

Evacuation of the System and Leak Testing

At the beginning of each experimental run, all the apparatus where
the degassed sample must exist is evacuated. This includes the equi-
librium cell, degassing bulbs, liquid storage bulbs, and the connecting
lines. The accuracy of vapor pressure measurement depends sensitively
on the elimination of all air from the apparatus and liquid samples.
The method for obtaining a completely degassed liquid sample will be
discussed in the next section.

Since a leak-tight system was imperative, the apparatus (especially
the equilibrium cell, mercury manometer, and connecting lines) had to
be tested for leaks before and between each experimental run. After
the pressure in the pumping system was less than five microns, the
shutoff valve next to the vacuum pump was closed. The entire apparatus
was allowed to sit for 24 hours. If the pressure in the whole appa-
ratus did not rise over 0.10 mmHg, leaks were considered negligible.

Vacuum leak sealant (manufactured by Bendix Corporation) was applied

to seal the leaks. Similar leak testing was performed on the equilibrium

cell. When the vacuum condition was achieved, the equilibrium cell was

isolated from the vacuum system. After the cell had been sitting un-

disturbed overnight, if the pressure change in the cell was not detec-

table by the mercury manometer, the vacuum system was considered

satisfactory, since an actual experimental run requires only 8-10 hours.

Degassing the Sample

This section describes the procedure which was used to obtain a

completely degassed liquid sample. Two commonly used techniques for

degassing pure components are vacuum sublimation (8,28), and boiling-

condensation method (16,17,27). The vacuum sublimation technique was

used in this study.

After the degassing bulb F was evacuated, (Letters used in this

section refer to Figure 3.) the liquid sample bulb G was filled with

pure component and was connected to the degassing bulb. The needle

valve D-1 was then opened to allow the air in the space between the

valve D-1 and the liquid surface to be evacuated. Then the cold

finger E was filled with liquid nitrogen. The rate of vaporization

of the liquid was regulated by the needle valve D-1 so that the mole-

cules of the desired liquid were collected on the surface of the cold

finger while the uncondensable gas molecules passed into the vacuum

system through valve D-3. When degassing a liquid sample with a high

freezing point (such as benzene or cyclohexane), heat must be supplied

to the liquid in the sample bulb G to prevent the liquid from freezing

due to vaporization. After the liquid had been frozen onto the cold

finger E, the valve D-3 was closed and the sublimate was allowed to thaw. Once thawed, the liquid was drawn back into the sample blub. The procedure for evacuation, freezing, and thawing was repeated until the liquid sample was completely degassed. Experience has shown that two or three cycles are required. After all the liquid sample was frozen onto the cold finger, the valves D-1 and D-3 were closed. The sublimate was allowed to thaw in the condensation chamber F, and was then transferred through valve D-2 into the liquid storage bulb. During the transfer of sample, either the degassing bulb was warmed up or the storage bulb was cooled off in order to obtain a pressure difference so that the sample could be easily transferred. After the sample was transferred, a positive pressure was applied to the storage bulb to insure that the liquid filled all available space in the storage bulb, needle valves, and connecting lines. The positive pressure in the storage bulb also prevented the atmospheric air from redissolving in the degassed sample.

<div align="center">Vapor Pressure Measurement</div>

After two pure components were completely degassed and transferred into the storage bulbs, the equilibrium cell was evacuated and leak-tested. The constant temperature water bath was raised to submerge the cell. After the cell reached the water bath temperature and the liquids in the storage bulbs were equilibrated with air bath temperature, about 25 ml of the first component was metered into the cell. The injecting procedure was as follows: With the valve between the measuring bulb and storage bulb opened, the mercury level in the measuring bulb was adjusted to the desired hash mark by the Ruska pump. Upon opening the needle valve on top of the equilibrium cell, the

mercury pushed the liquid sample into the cell. After the mercury level in the measuring bulb dropped to the correct hash mark, the needle valve was closed.

From a known difference between the mercury levels in the measuring bulb, the volume of liquid that has been transferred into the cell was calculated. The vapor pressure in the cell was checked every 5-10 minutes. When the pressure inside the cell was stable (usually 10-20 minutes), the pure component vapor pressure was recorded and compared with literature values if they were available. An additional 25 ml of the same component was then metered into the cell. After equilibrium was established, the vapor pressure was again recorded and compared with the previous result. The completeness of degassing could be partially checked by comparing these two vapor pressure measurements. If the pure component is not completely degassed, the second vapor pressure measurement should be higher than the first since more air had been injected into the cell. If the pressure difference was within experimental error ($\pm$ 0.2 mmHg), the liquid was considered to be thoroughly degassed.

If complete degassing of the first component was achieved, a small amount of the second component was metered into the cell to form a dilute solution. After the mixture reached the thermal and phase equilibrium (usually 20-30 minutes), the total vapor pressure of the binary mixture was recorded. The injection process was repeated until about 60 ml of the second component was added.

After the final vapor pressure was recorded, the constant temperature water bath was lowered. The equilibrium cell was dismounted

from the cell lid. After the cell has been emptied, cleaned, and

dried, it was remounted, evacuated, and leak-tested. If the equilib-

rium cell was found to be leak-proof, a second run, similar to the

first, was made with the order of component addition reversed. Thus

the total vapor pressure data over the entire composition range for

a binary mixture were obtained with two titration runs.

During each experimental run, a sufficient composition range

was covered such that the vapor pressure curves of the two titration

runs overlapped over an interval of composition range. If the pure

components are thoroughly degassed, the two vapor pressure curves will

coincide with each other. This is another method used to check the

completeness of degassing.

CHAPTER V

EXPERIMENTAL RESULTS

In the first part of this chapter, the results of pure component
density measurement and apparatus calibration are presented. In the
second part, the results of binary mixture vapor pressure data are
presented.

Pure Component Densities

Since the total composition of the binary mixture in the equilib-
rium cell was calculated from the accurately measured volumes of pure
components injected, the pure component density at the air bath tem-
perature had to be known. Pure component densities at $26^{\circ}C$ are very
scarce in the literature. A good approximation can be made by either
linearly interpolating or extrapolating from data for other tempera-
tures. However, the pycnometer apparatus described by Dullien (20)
provides an easy and accurate way to obtain density data. The de-
tailed procedure of measuring the density data with a pycnometer is
given elsewhere (43). The results of the density measurements are
shown in Table IV. Densities interpolated from literature values
are also shown in the table.

The density data obtained from this study are within the ranges
of literature values, except the n-hexane value, which is slightly
lower.

TABLE IV

PURE COMPONENT DENSITIES AT 26°C

Compound	Densities, ρ (gm/cc)	
	This Work	Literature Values (*)
Methanol	0.7857	0.7856--0.7858
Ethanol	0.7842	0.7842--0.7844
N-Propanol	0.7989	0.7989--0.7991
Benzene	0.8727	0.8725--0.8727
Cyclohexane	0.7729	0.7728--0.7731
N-Hexane	0.6537	0.6539--0.6542

* Linear interpolation between 25°C and 30°C from Timmermans, J. (ed.) "Physico-Chemical Constants of Pure Organic Components," Vol. 2, Elsevier Publishing Co., N. Y., 1965. (53)

Calibration of Measuring Bulbs

Two measuring bulb sets were designed in this study. The first measuring bulb set consists of five glass bulbs with volumes of approximately 3, 1, 2, 4, and 20 ml. The first (top) bulb serves as a mercury reservoir to avoid mercury spills. The five bulbs are joined in series by 5-cm-long, 1-mm-ID glass capillaries. A hash mark is made at the middle of each capillary. A strip of graph sheet with divisions of 1 mm is taped to the back of each capillary so that the mercury level in the capillary can be read.

The second measuring bulb set is the same as the first except that the 1-ml glass bulb is replaced by a 12-cm-long, 0.125-in-ID Trubore precision glass tubing. A hash mark is also made at the low end of the glass tubing to serve as a reference point.

The volume of each bulb was calibrated with distilled water. Eight volume measurements were made. The average volume (v_i) and the standard deviation (σ_{vi}) of each individual measuring bulb are given in Table V. The volume of the precision glass tubing is treated as a linear function of the height with the following relation:

$$v = 0.22650 - 0.083666\ h \qquad\qquad (V\text{-}1)$$

where

v (in cc) = volume of the tubing from the hash mark ($h=0$)

to a height of h (in cm).

TABLE V

VOLUMES OF INDIVIDUAL MEASURING BULBS

	Bulb No.	Volume v_i, (cc)	Standard Deviation σ_{vi}, (cc)
Set 1	1	0.8315	0.0040
	2	1.6565	0.0066
	3	3.4593	0.0041
	4	19.0713	0.0042
Set 2	1	--	0.0024
	2	1.6460	0.0026
	3	4.2593	0.0017
	4	23.3736	0.0035

Corrections to Pressure Measurements

In this study, the vapor pressures are expressed in terms of the height of mercury at standard conditions. Since the vapor pressures are measured with mercury manometer at the conditions different from standard, they have to be corrected. Two corrections were considered. The first one is the temperature correction as shown in the following equations:

$$h^{(0)} = \frac{\rho^{(t)}}{\rho^{(0)}} h^{(t)} \qquad\qquad (V-2)$$

where

$h^{(t)}$ = reading of manometer at $t^\circ C$ (mm).

(for this study, t is at 28-30°C)

$\rho^{(t)}$ = density of mercury at $t^\circ C$ (gm/cc).

$h^{(0)}$ = reading of manometer at $0^\circ C$ (mm).

$\rho^{(0)}$ = density of mercury at $0^\circ C$ (gm/cc).

= 13.5951 gm/cc..

The second correction is due to gravitational acceleration difference. The local gravitational acceleration is calculated by Helmert's equation (62). The results is shown in the following equation:

$$h^{(s)} = \frac{g}{g^{(s)}} h^{(0)} \qquad\qquad (V-3)$$

where

$h^{(s)}$ = reading of manometer at standard condition (mm).

$g^{(s)}$ = standard gravitational acceleration (cm/sec^2).

= 980.665 cm/sec^2.

g = local gravitational acceleration (cm/sec^2).

= 979.746 cm/sec^2.

The levels in the legs of the manometer are measured with a cathetometer. Since the linear expansion coefficient of the cathetometer scale is very small (0.000011/degree C), the error in the scale due to thermal expansion or contraction is small enough to be neglected.

Presentation of Experimental Data

The vapor pressures over the entire composition range for the binary mixtures of alcohols (methanol, ethanol and n-propanol) with benzene, cyclohexane and n-hexane at 25°C were obtained in the study. Experimental results are given in Tables VI through XIV. The total mole fraction is calculated directly from known volumes of pure components injected. The liquid mole fraction is calculated by a simple iterative scheme. The detailed discussion is given in Appendix A.

Graphical presentations of the experimental results are shown in Figures 6 through 14. Plotted with the experimental vapor pressure-liquid composition data are smoothed vapor pressure curves and vapor composition curves calculated by Mixon's method. Methods of data reduction are discussed in the following chapter.

TABLE VI

EXPERIMENTAL VAPOR PRESSURE DATA AT 25°C FOR THE SYSTEM
METHANOL(1)-BENZENE(2)

Total Mole Fraction z_1	Liquid Mole Fraction x_1	Vapor Pressure P, mmHg
0.0000	0.0000	95.12
0.0108	0.0103	129.08
0.0350	0.0340	157.56
0.0608	0.0597	168.29
0.0884	0.0874	173.66
0.1188	0.1178	176.35
0.1503	0.1494	177.81
0.2017	0.2009	179.30
0.2477	0.2471	180.34
0.2890	0.2885	180.84
0.3766	0.3763	181.95
0.4453	0.4452	182.44
0.5004	0.5004	183.00
0.5053	0.5053	182.97
0.5608	0.5608	183.05
0.6190	0.6191	182.52
0.6565	0.6566	182.41
0.6988	0.6990	181.72
0.7467	0.7470	179.99
0.8017	0.8020	177.55
0.8467	0.8471	173.73
0.8970	0.8974	166.33
0.9180	0.9184	161.70
0.9402	0.9405	155.44
0.9632	0.9635	147.89
0.9771	0.9772	141.24
0.9898	0.9899	133.93
1.0000	1.0000	127.17

TABLE VII

EXPERIMENTAL VAPOR PRESSURE DATA AT 25°C FOR THE SYSTEM
ETHANOL(1)-BENZENE(2)

Total Mole Fraction z_1	Liquid Mole Fraction x_1	Vapor Pressure P, mmHg
0.0000	0.0000	95.11
0.0068	0.0067	101.88
0.0153	0.0151	107.60
0.0298	0.0295	113.12
0.0539	0.0534	117.19
0.0876	0.0872	119.93
0.1453	0.1450	122.46
0.1965	0.1963	123.31
0.2419	0.2418	123.39
0.2830	0.2830	123.39
0.3701	0.3702	122.89
0.4385	0.4387	122.51
0.4935	0.4937	122.17
0.5299	0.5301	121.11
0.5387	0.5389	121.37
0.5725	0.5728	120.13
0.5896	0.5898	120.28
0.6224	0.6228	118.97
0.6819	0.6824	115.99
0.7326	0.7331	112.76
0.7913	0.7919	108.20
0.8602	0.8608	99.94
0.8902	0.8907	94.42
0.9222	0.9227	87.08
0.9563	0.9566	78.29
0.9759	0.9761	70.52
0.9900	0.9901	63.95
1.0000	1.0000	58.81

TABLE VIII

EXPERIMENTAL VAPOR PRESSURE DATA AT $25^{\circ}C$ FOR THE SYSTEM
N-PROPANOL(1)-BENZENE(2)

Total Mole Fraction z_1	Liquid Mole Fraction x_1	Vapor Pressure P, mmHg
0.0000	0.0000	95.09
0.0104	0.0104	97.07
0.0247	0.0247	97.26
0.0421	0.0421	97.78
0.0635	0.0635	97.75
0.0890	0.0890	97.17
0.1174	0.1174	97.11
0.1661	0.1663	96.76
0.2100	0.2102	96.01
0.2500	0.2503	95.38
0.2865	0.2868	94.68
0.3650	0.3653	92.90
0.4279	0.4282	91.36
0.4794	0.4798	89.85
0.5248	0.5252	87.93
0.5373	0.5377	87.71
0.5632	0.5637	86.67
0.5836	0.5839	85.23
0.6076	0.6082	84.18
0.6596	0.6602	81.47
0.7213	0.7220	77.73
0.7956	0.7964	71.62
0.8286	0.8294	67.59
0.8645	0.8653	61.60
0.9032	0.9040	54.32
0.9273	0.9279	47.89
0.9529	0.9534	39.87
0.9750	0.9753	31.78
0.9878	0.9880	26.62
0.9949	0.9950	23.71
1.0000	1.0000	20.95

TABLE IX

EXPERIMENTAL VAPOR PRESSURE DATA AT 25°C FOR THE SYSTEM
METHANOL(1)-CYCLOHEXANE(2)

Total Mole Fraction z_1	Liquid Mole Fraction x_1	Vapor Pressure P, mmHg
0.0000	0.0000	97.63
0.0113	0.0097	183.05
0.0226	0.0207	199.44
0.0496	0.0476	208.95
0.0874	0.0856	212.63
0.1269	0.1253	213.72
0.1912		213.87
0.2473		213.86
0.2963		213.86
0.3395		213.85
0.3780	Two-Liquid Phase	213.75
0.4581		213.70
0.5025		213.66
0.5200		213.62
0.5549		213.66
0.5694		213.62
0.5997		213.65
0.6526		213.65
0.7156		213.65
0.7919		213.60
0.8264	0.8282	213.60
0.8635	0.8656	212.85
0.9039	0.9062	209.79
0.9274	0.9297	204.49
0.9505	0.9527	193.81
0.9749	0.9766	171.80
0.9898	0.9907	149.09
1.0000	1.0000	127.24

TABLE X

EXPERIMENTAL VAPOR PRESSURE DATA AT 25°C FOR THE SYSTEM
ETHANOL(1)-CYCLOHEXANE(2)

Total Mole Fraction z_1	Liquid Mole Fraction x_1	Vapor Pressure P, mmHg
0.0000	0.0000	97.60
0.0286	0.0281	130.91
0.0556	0.0551	134.96
0.0823	0.0817	136.75
0.1312	0.1308	138.84
0.1752	0.1749	139.43
0.2334	0.2332	139.53
0.2839	0.2838	139.53
0.3440	0.3440	139.43
0.4166	0.4167	139.38
0.4830	0.4831	139.32
0.5358	0.5360	139.03
0.5565	0.5567	139.04
0.5789	0.5791	138.63
0.6146	0.6148	138.09
0.6448	0.6450	137.99
0.6547	0.6550	137.94
0.6930	0.6933	137.05
0.7359	0.7363	135.36
0.7845	0.7850	132.38
0.8317	0.8323	128.08
0.8670	0.8676	121.50
0.8943	0.8949	114.88
0.9233	0.9239	106.04
0.9438	0.9442	98.19
0.9651	0.9655	87.31
0.9765	0.9768	79.71
0.9881	0.9883	70.56
1.0000	1.0000	59.03

TABLE XI

EXPERIMENTAL VAPOR PRESSURE DATA AT 25°C FOR THE SYSTEM
N-PROPANOL(1)-CYCLOHEXANE(2)

Total Mole Fraction z_1	Liquid Mole Fraction x_1	Vapor Pressure P, mmHg
0.0000	0.0000	97.85
0.0099	0.0098	104.67
0.0205	0.0204	105.81
0.0506	0.0504	107.00
0.0820	0.0819	107.16
0.1127	0.1127	107.12
0.1624	0.1625	106.83
0.2071	0.2073	106.62
0.2475	0.2477	106.39
0.2844	0.2847	105.91
0.3179	0.3183	105.41
0.3905	0.3909	104.45
0.4492	0.4498	103.35
0.4493	0.4498	103.50
0.4979	0.4984	102.31
0.5013	0.5020	101.99
0.5385	0.5390	101.13
0.5467	0.5476	101.02
0.5730	0.5734	99.78
0.6015	0.6026	99.62
0.6682	0.6695	96.53
0.7511	0.7528	90.80
0.7898	0.7915	86.46
0.8323	0.8341	79.95
0.8792	0.8809	69.81
0.9323	0.9336	55.41
0.9615	0.9624	42.95
0.9852	0.9856	30.33
1.0000	1.0000	20.97

TABLE XII

EXPERIMENTAL VAPOR PRESSURE DATA AT 25°C FOR THE SYSTEM
METHANOL(1)-N-HEXANE(2)

Total Mole Fraction z_1	Liquid Mole Fraction x_1	Vapor Pressure P, mmHg
0.0000	0.0000	151.76
0.0052	0.0040	205.66
0.0117	0.0099	230.53
0.0207	0.0185	243.02
0.0373	0.0349	253.85
0.0603	0.0580	259.81
0.0942	0.0922	263.63
0.1324	0.1306	264.22
0.1762	0.1747	265.47
0.2179	0.2167	265.88
0.2569		265.85
0.3145		265.85
0.3644		265.85
0.4077		265.85
0.4955	Two-Liquid Phase	265.85
0.5115		265.86
0.5556		265.79
0.5607		265.83
0.6080		265.86
0.6711		265.86
0.7254		265.86
0.7891		265.86
0.8169	0.8199	265.88
0.8467	0.8500	264.95
0.8785	0.8822	263.79
0.9127	0.9166	259.54
0.9322	0.9362	252.92
0.9505	0.9543	241.08
0.9666	0.9700	223.30
0.9788	0.9815	203.72
0.9872	0.9893	183.15
0.9948	0.9957	149.10
1.0000	1.0000	127.00

TABLE XIII

EXPERIMENTAL VAPOR PRESSURE DATA AT 25°C FOR THE SYSTEM
ETHANOL(1)-N-HEXANE(2)

Total Mole Fraction z_1	Liquid Mole Fraction x_1	Vapor Pressure P, mmHg
0.0000	0.0000	151.95
0.0260	0.0257	183.26
0.0507	0.0503	185.70
0.0973	0.0970	188.92
0.1400	0.1397	189.92
0.1971	0.1970	190.22
0.2470	0.2470	190.26
0.3068	0.3069	190.26
0.3580	0.3581	189.97
0.4210	0.4213	189.87
0.4405	0.4407	190.21
0.4727	0.4732	188.97
0.5161	0.5164	188.97
0.5179	0.5184	188.47
0.5529	0.5532	188.82
0.6284	0.6292	187.13
0.6665	0.6675	185.65
0.7095	0.7107	183.51
0.7585	0.7599	179.53
0.7959	0.7974	175.11
0.8369	0.8386	168.00
0.8822	0.8839	156.17
0.9063	0.9079	145.89
0.9311	0.9326	132.28
0.9574	0.9586	112.79
0.9854	0.9859	82.29
1.0000	1.0000	59.03

TABLE XIV

EXPERIMENTAL VAPOR PRESSURE DATA AT 25°C FOR THE SYSTEM
N-PROPANOL(1)-N-HEXANE(2)

0.0000	0.0000	151.66
0.0065	0.0065	157.49
0.0246	0.0245	159.35
0.0527	0.0526	159.79
0.1048	0.1048	159.45
0.1511	0.1513	158.63
0.1939	0.1942	157.95
0.2323	0.2327	157.25
0.3159	0.3164	155.73
0.3831	0.3837	154.54
0.4384	0.4390	153.07
0.4847	0.4853	151.77
0.5090	0.5102	150.65
0.5239	0.5245	150.13
0.5473	0.5487	149.66
0.5693	0.5699	148.09
0.5917	0.5934	147.68
0.6439	0.6460	144.89
0.7064	0.7089	139.63
0.7822	0.7850	130.53
0.8162	0.8191	124.12
0.8534	0.8564	114.93
0.8940	0.8969	101.91
0.9385	0.9408	80.65
0.9623	0.9641	63.26
0.9863	0.9871	38.91
1.0000	1.0000	20.95
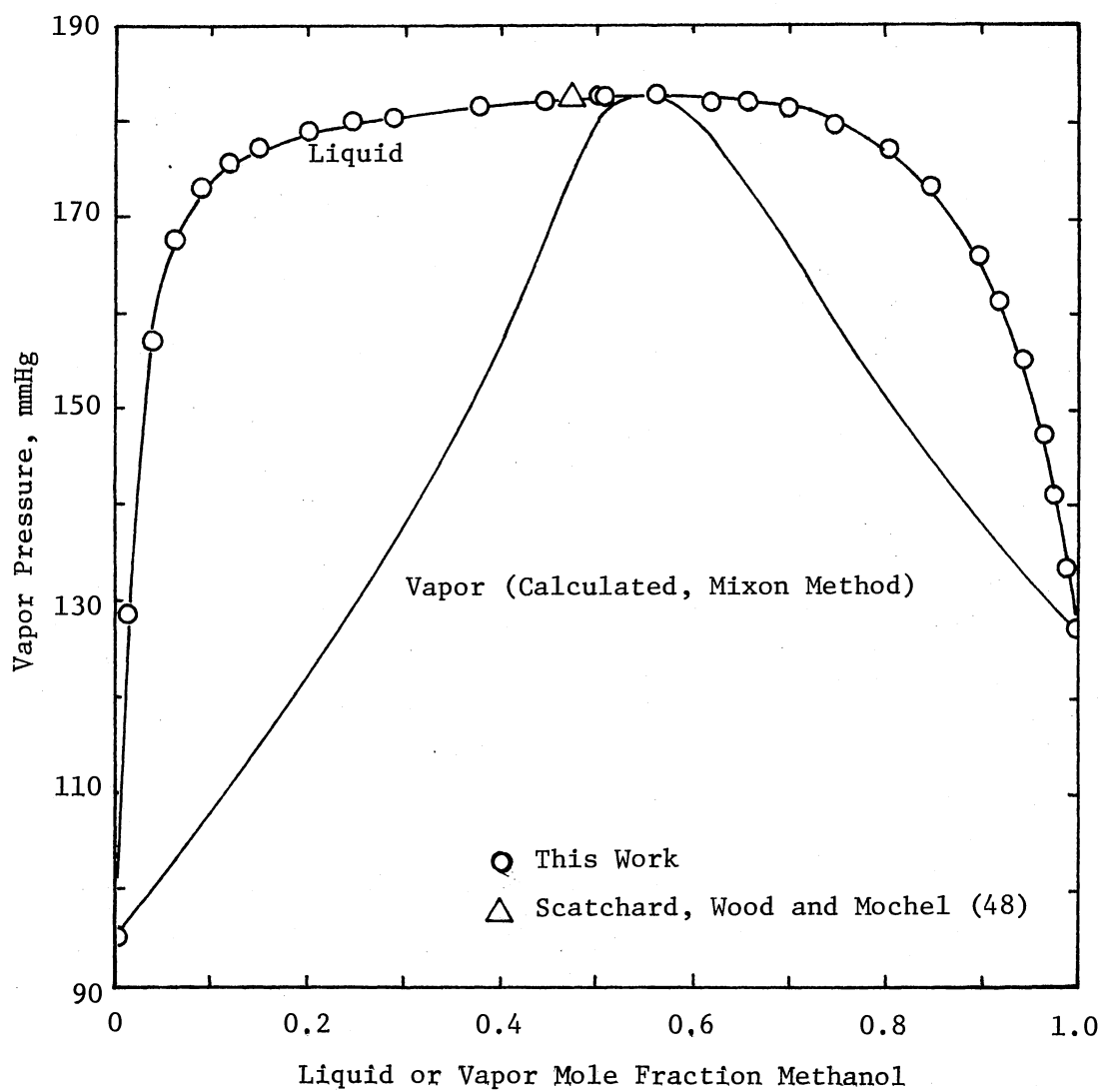
Figure 6. Vapor Pressure at 25°C for the System
Methanol(1)-Benzene(2)
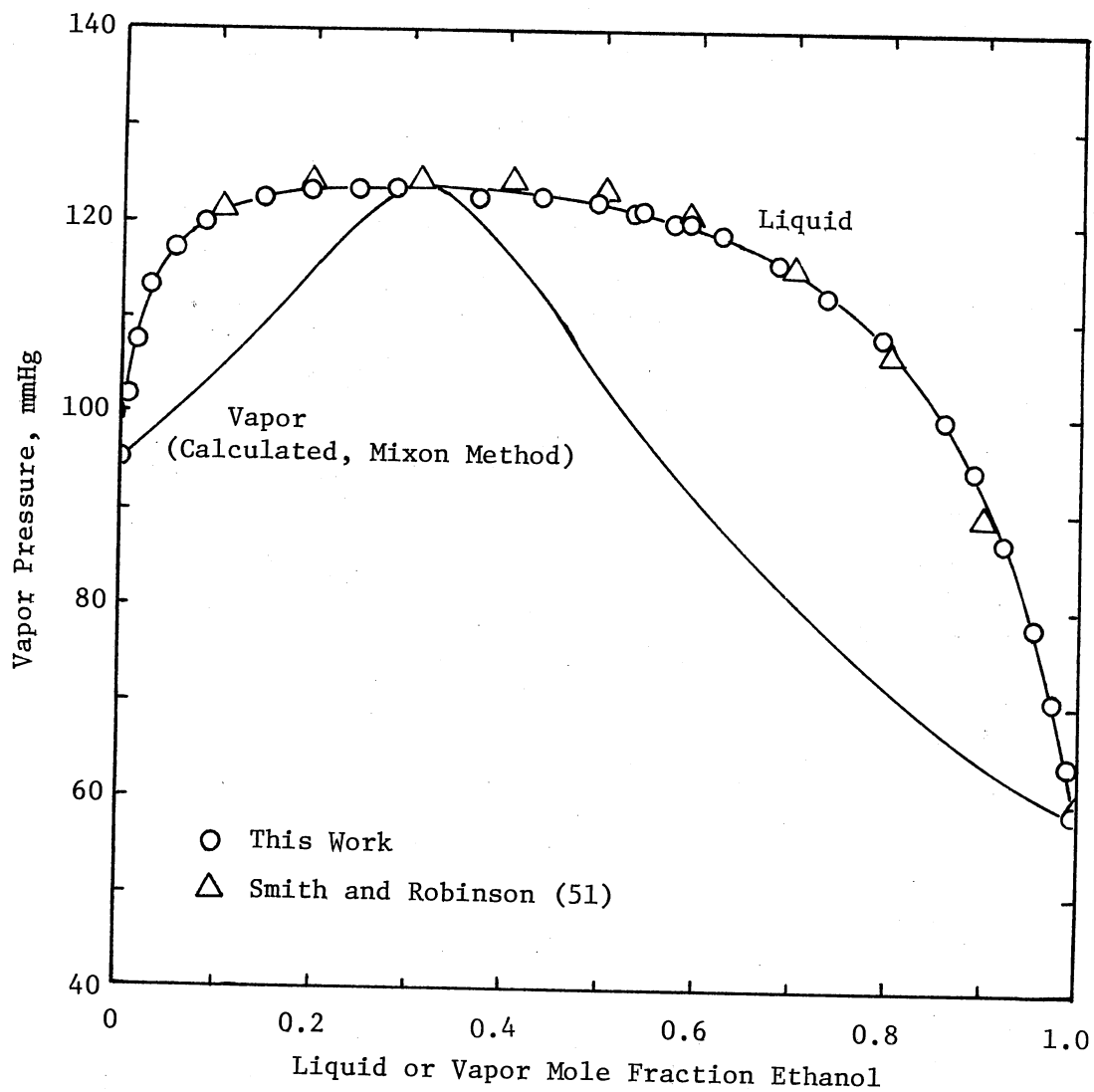
Figure 7. Vapor Pressure at 25°C for the System
Ethanol(1)-Benzene(2)
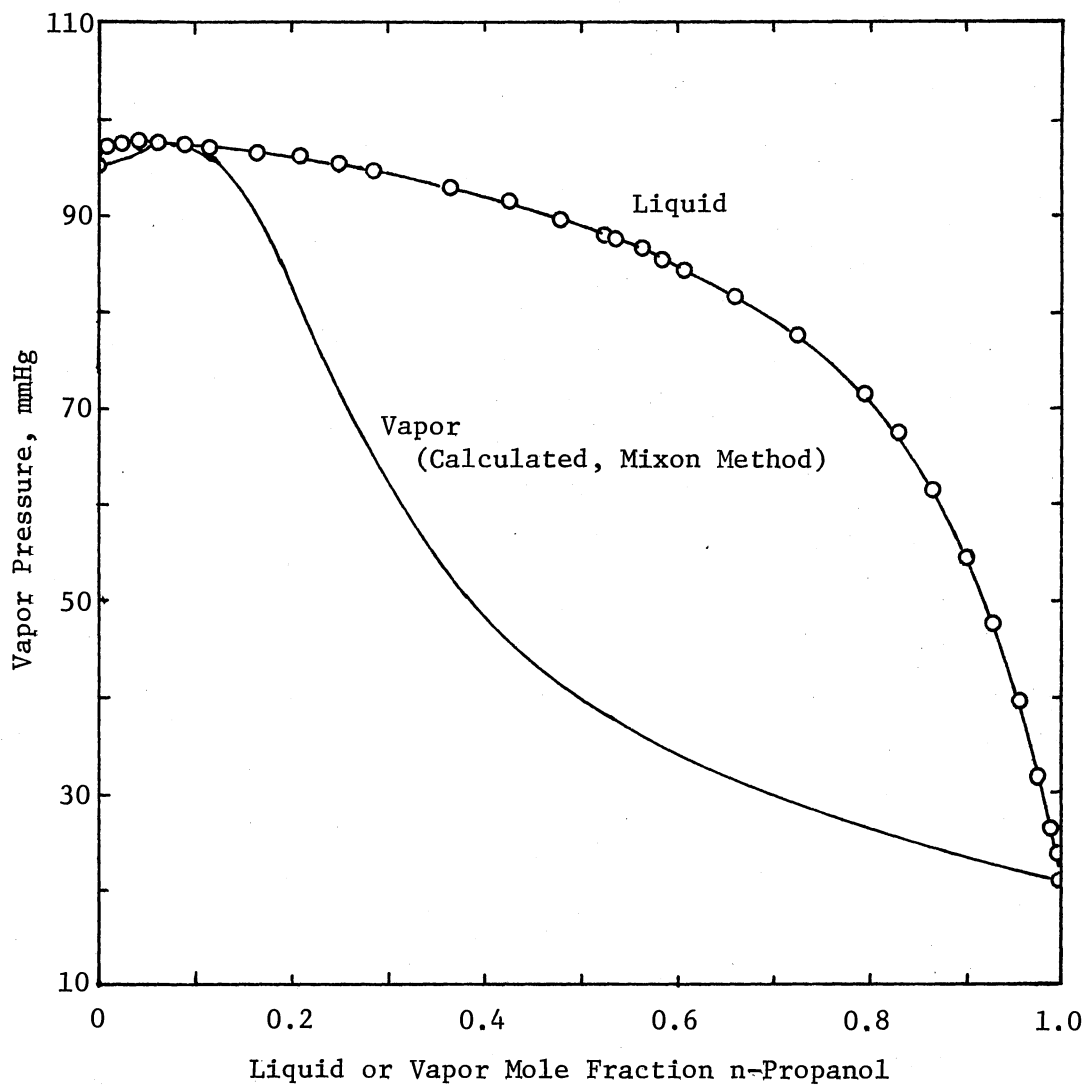
Figure 8. Vapor Pressure at $25^{\circ}C$ for the System
n-Propanol(1)-Benzene(2)
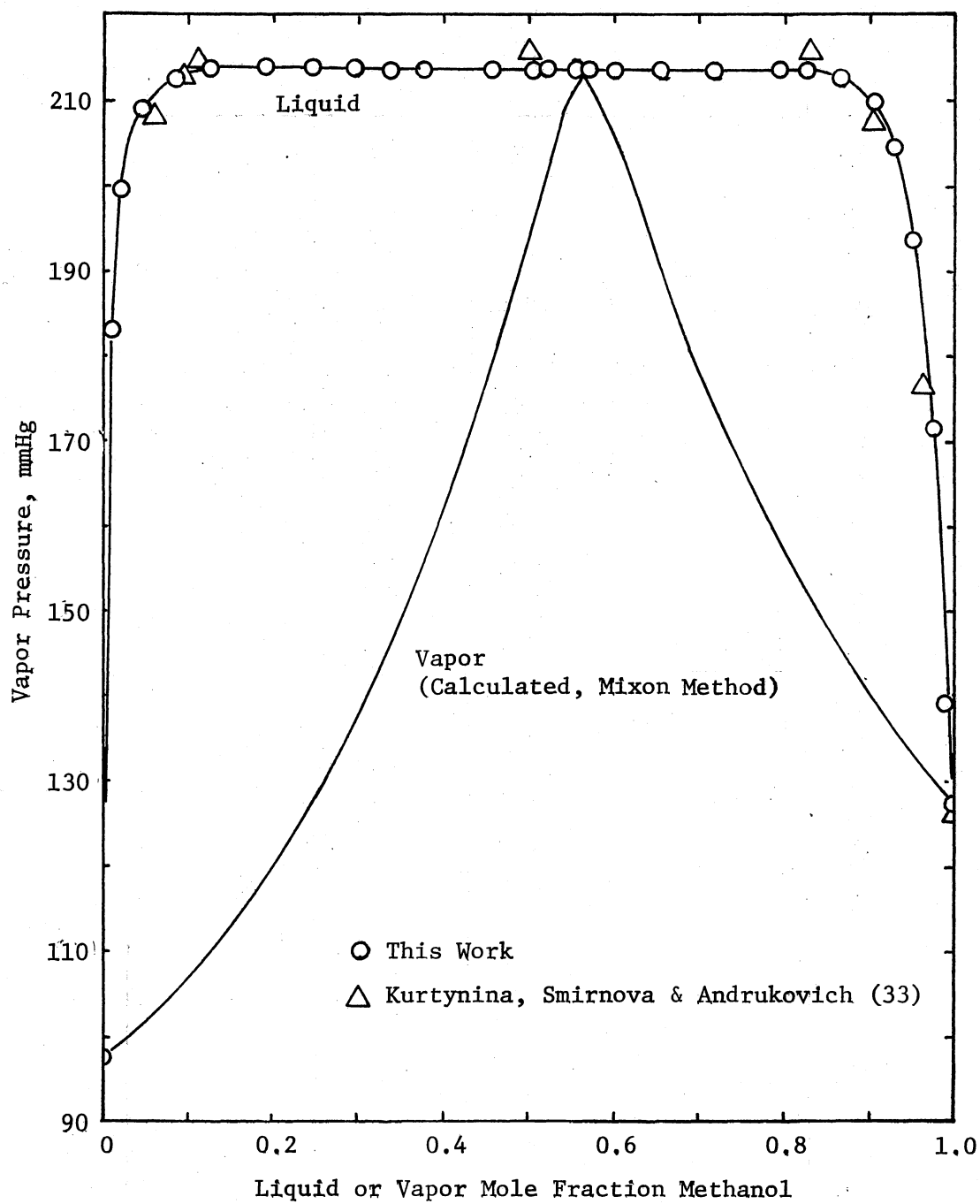
Figure 9. Vapor Pressure at 25°C for the System
Methanol(1)-Cyclohexane(2)
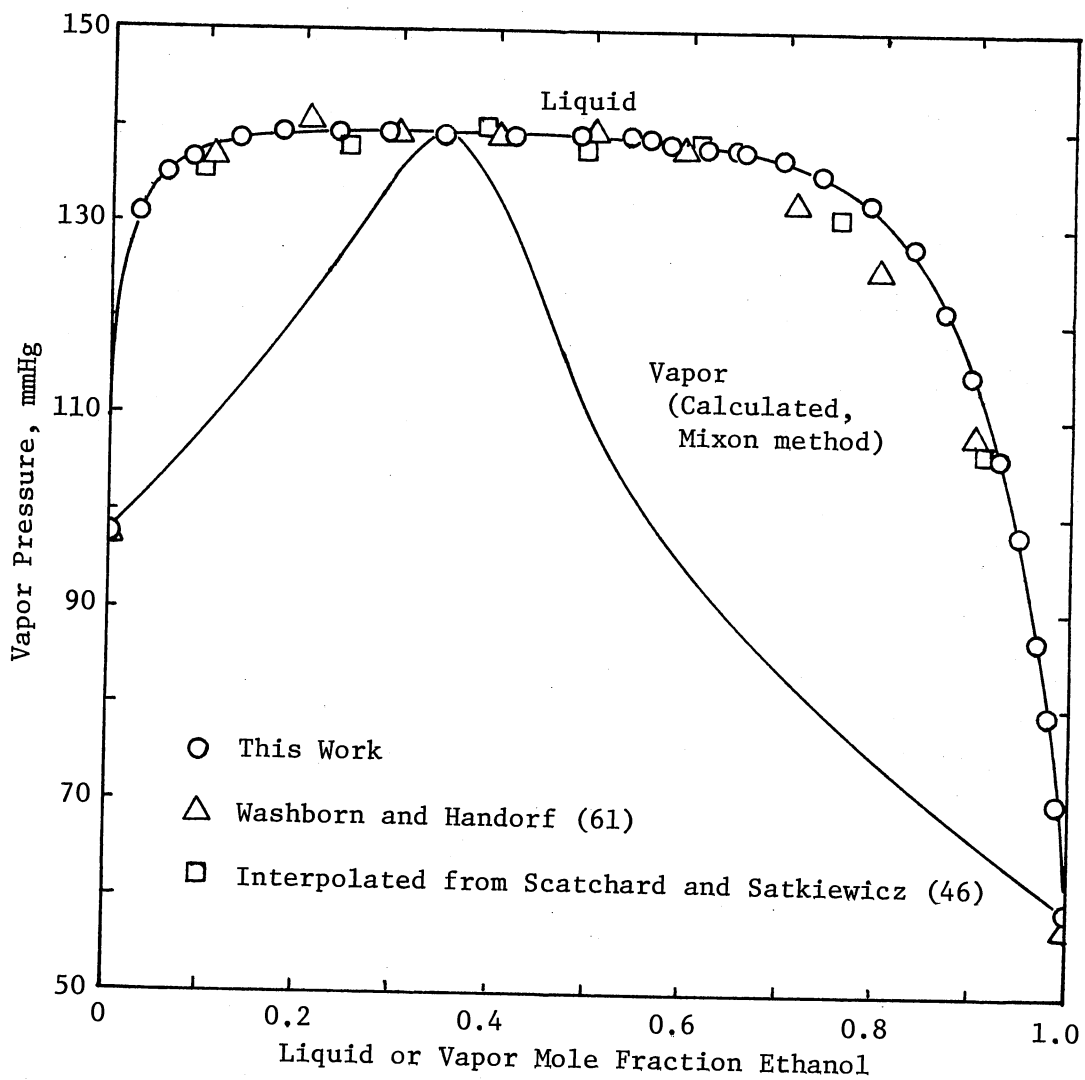
Figure 10. Vapor Pressure at 25°C for the System
Ethanol(1)-Cyclohexane(2)
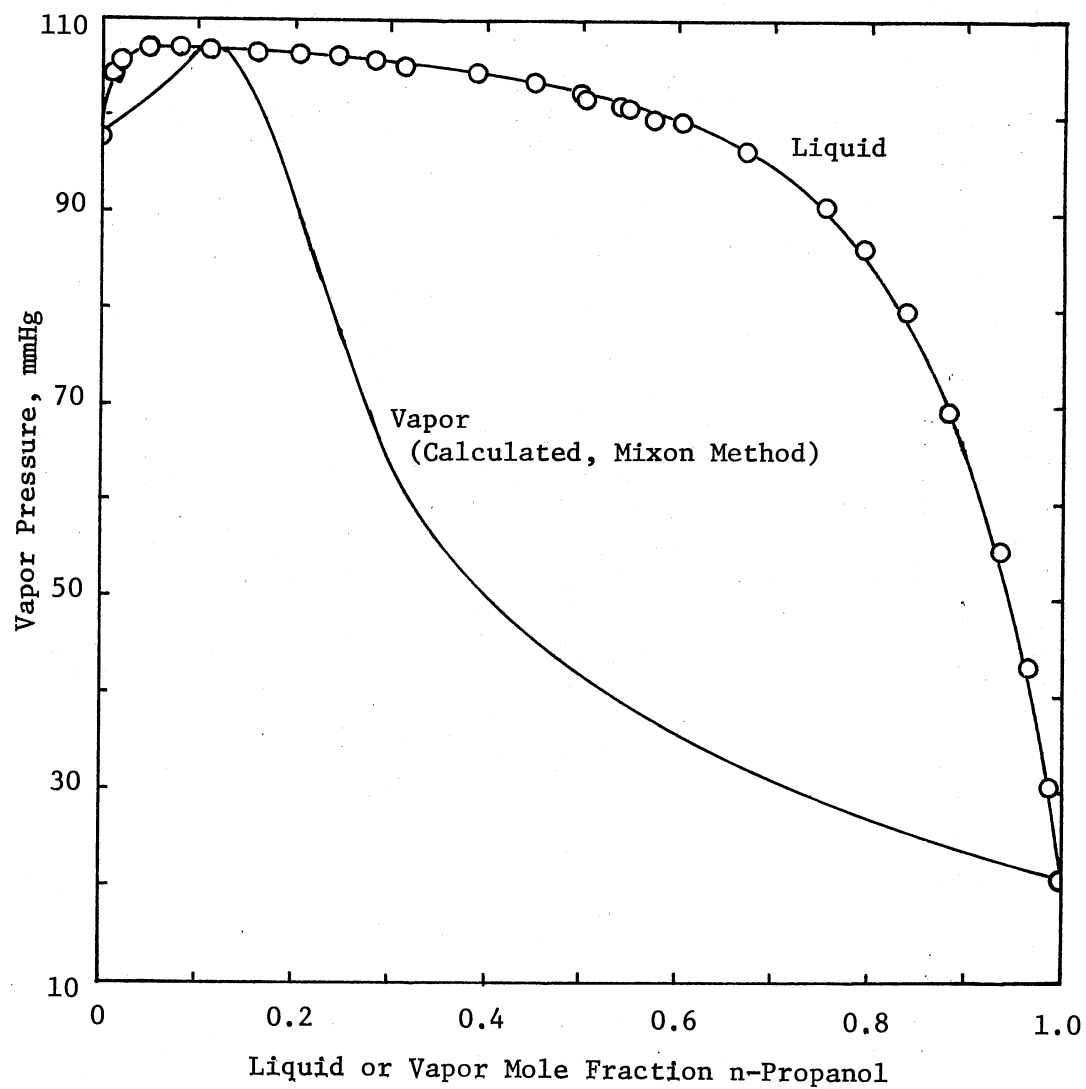
Figure 11. Vapor Pressure at 25°C for the System
n-Propanol(1)-Cyclohexane(2)
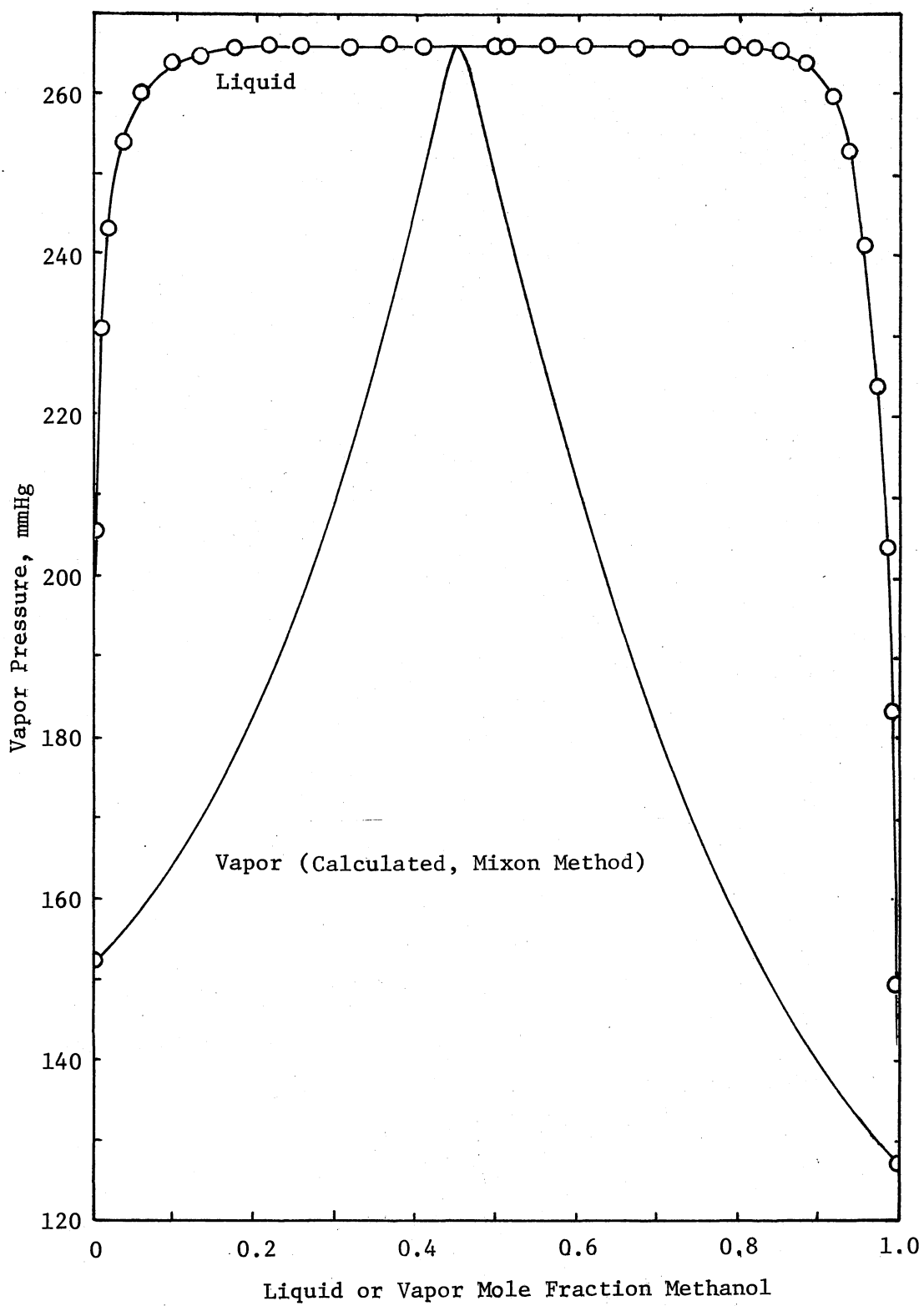
Figure 12. Vapor Pressure at 25°C for the System
Methanol(1)-n-Hexane(2)
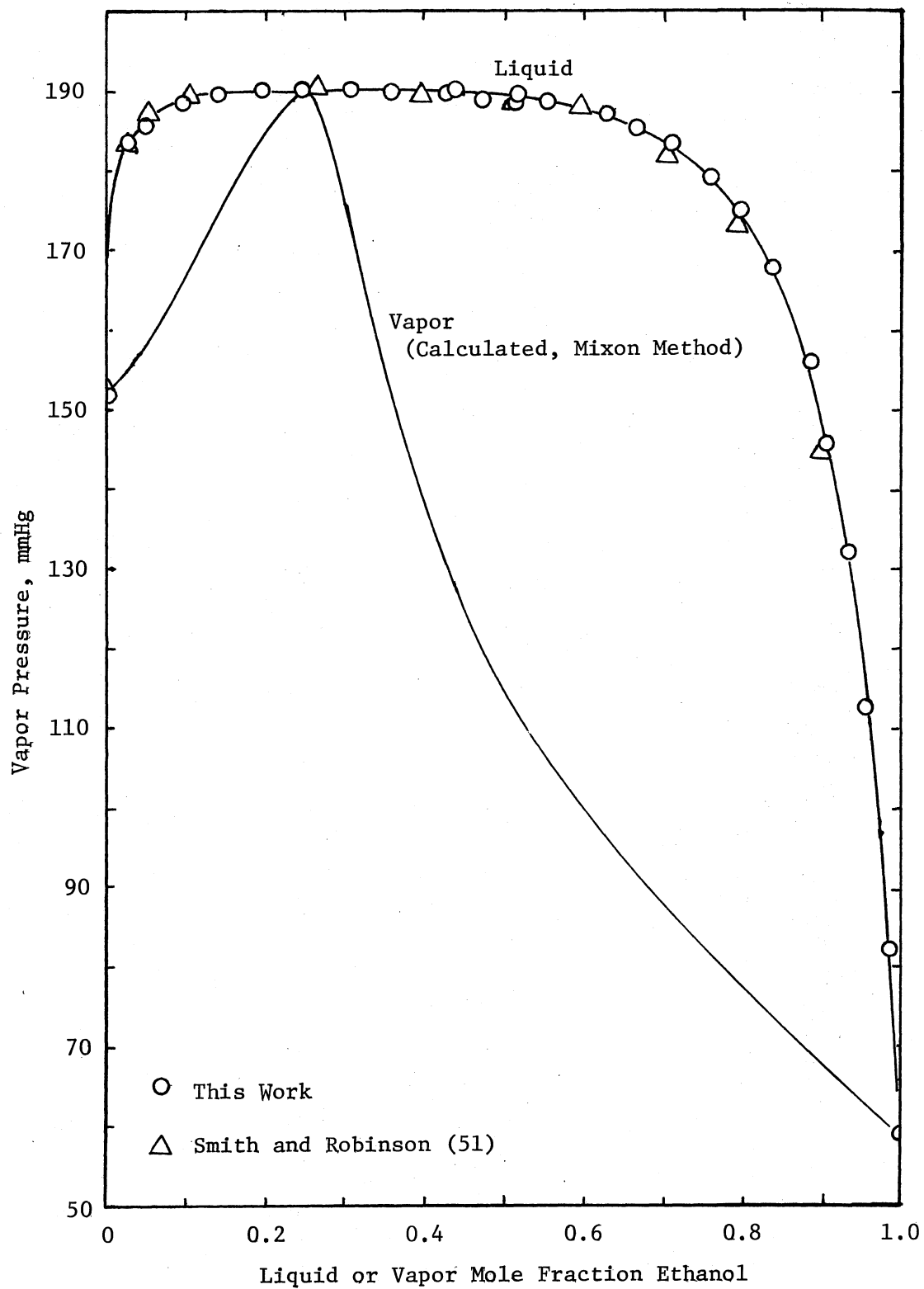
Figure 13. Vapor Pressure at 25°C for the System
Ethanol(1)-n-Hexane(2)
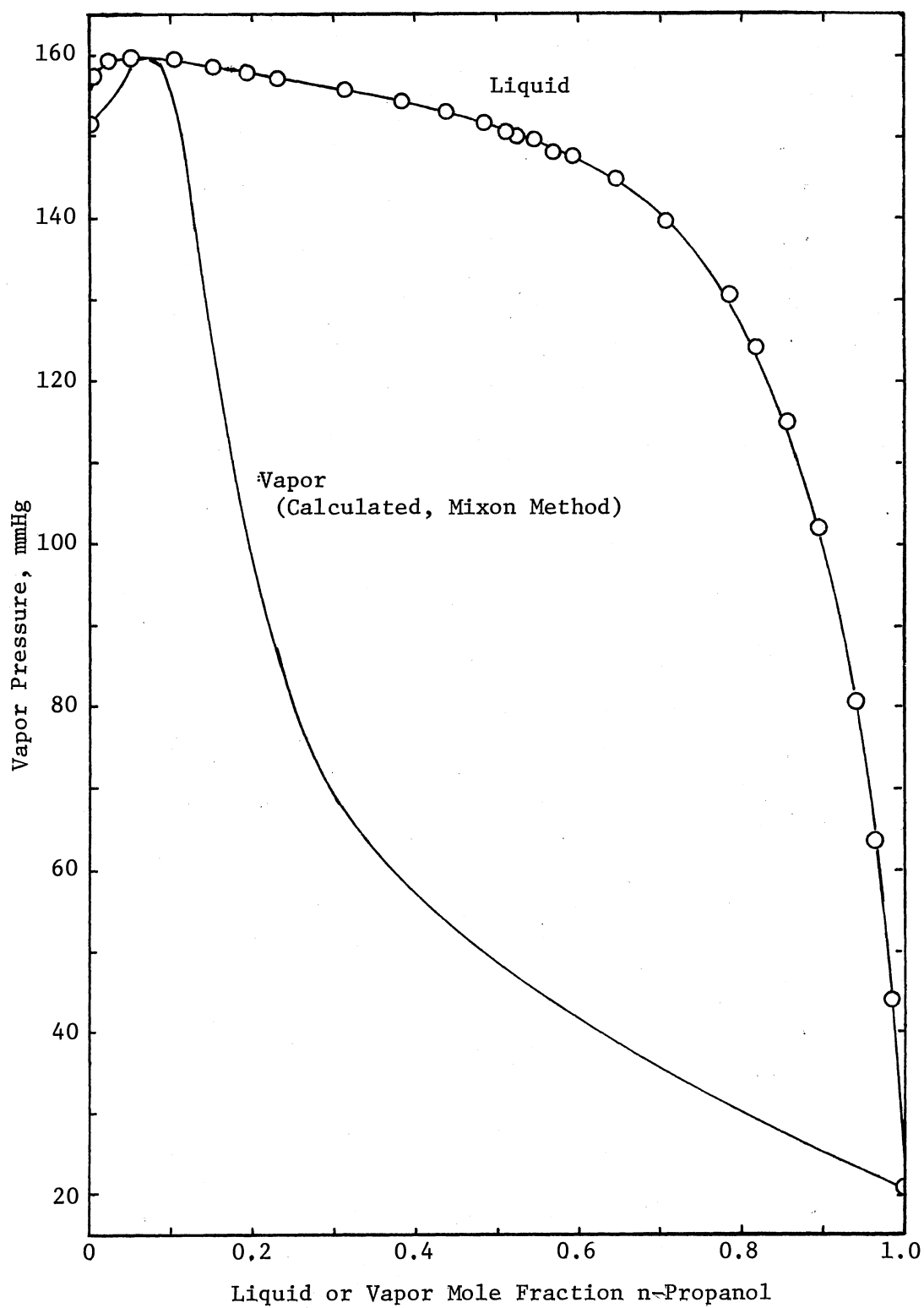
Figure 14. Vapor Pressure at 25°C for the System
n-Propanol(1)-n-Hexane(2)

CHAPTER VI

DISCUSSION OF EXPERIMENTAL RESULTS

In the previous chapter, the experimental data from this study have been tabulated and illustrated. In this chapter, discussions of the experimental results are presented.

First, the uncertainties in the experimental data are discussed. These include the mole fraction calculation and vapor pressure measurement. Next, methods for data reduction are described. Then, the excess thermodynamic properties for each system are evaluated. Finally, comparisons of the experimental results from this study with literature values are made.

Error Analysis

Any experimentally measured quantity is subject to error; hence, the result which is calculated based on experimental evidence is also limited in accuracy. The experimental error can be classified into three catagories: systematic, operator, and random errors. Since a complete discussion of the maximum error is impossible, only the error which is inherent in the apparatus design and dependent on the particular component being studied will be discussed.

Mole Fraction Calculation

One systematic error in liquid composition results from the measurements of injected volumes and pure component densities. A detailed discussion is presented in Appendix B. The magnitude of the error varies from point to point. Calculations (Appendix B) show that the maximum error among the systems studied is 0.00064 mole fraction unit.

Another possible error in liquid composition is due to the compressibility of the liquids in the storage bulbs. The correct densities for composition calculation should be the densities of the pure components at the temperature and pressure in the storage bulbs. However, as is discussed in Appendix B, the error associated with the use of the liquid densities at atmospheric pressure is negligible.

The total uncertainty in liquid composition calculation was estimated to be $\pm$ 0.0008 mole fraction unit.

Pressure Measurement

The most significant error in vapor pressure measurement is undoubtedly due to incomplete degassing of pure component. No general rule is available for testing the completeness of degassing. The methods used in this study have been discussed in Chapter IV. In this section, the error in vapor pressure measurement due to pressure-measurement apparatus and temperature effect will be discussed.

The corrections to the pressure measurements have been discussed in the previous chapter. The pressure difference in the manometer is measured by a cathetometer with divisions of 0.05 mm. Thus, the pressure reading will be within $\pm$ 0.10 mmHg.

Since vapor pressure is a function of temperature, error in temperature will translate into error in vapor pressure. The absolute accuracy of the temperature measurement is believed to be $\pm$ 0.01°C. The error in vapor pressure resulting from the error in temperature depends on the substance. In this study, for pure components at 25°C, an error of 0.01°C results error in vapor pressure of less than 0.10 mmHg.

The total error in vapor pressure resulting from the apparatus design and temperature effect is given in Table XV

The pure component vapor pressures were measured prior to taking data for each binary mixture. The results are given in Table XVI along with literature values. The effect of temperature on pure component vapor pressure is calculated using Antoine constants.

Based on the results given in the last column of Table XVI, the vapor pressure measurements are estimated to have imprecision of no more than $\pm$ 0.20 mmHg as shown in Table XV.

Data Reduction

Two indirect methods for reducing the experimental vapor-liquid equilibrium data were employed. In the first method, Barker's method, an activity coefficient model was used to fit the experimental vapor pressure-liquid composition data. In the second method, Mixon's method, an iterative numerical calculation of activity coefficient was used to fit the experimental vapor pressure at equally spaced intervals of liquid composition.

TABLE XV

CONTRIBUTIONS TO TOTAL ERROR IN VAPOR
PRESSURE

Source	Error in Vapor Pressure, mmHg
Resolution of Vapor Pressure Measuring Apparatus	± 0.10
Temperature Effect	± 0.10
Total Possible Error	± 0.20

TABLE XVI

PURE COMPONENT VAPOR PRESSURES AT $25^{\circ}C$

Compound	Literature Values P,mmHg	Temperature Effect $\Delta P(mmHg)/0.01^{\circ}C$	This Work P,mmHg		
			P_i	P_i,avg	$P_i - P_i$,avg
Methanol	125.40--127.18	0.066	127.17	127.14	0.03
			127.24		0.10
			127.00		-0.14
Ethanol	58.90-- 59.80	0.034	58.81	58.96	-0.15
			59.03		0.07
			59.03		0.07
n-Propanol	20.44-- 20.90	0.014	20.95	20.96	-0.01
			20.97		0.01
			20.95		-0.01
Benzene	95.03-- 95.25	0.044	95.12	95.11	0.01
			95.11		0.00
			95.09		0.02
Cyclohexane	97.41-- 98.25	0.044	97.63	97.69	-0.06
			97.60		-0.09
			97.85		0.16
n-Hexane	151.05--152.85	0.066	151.76	151.79	-0.03
			151.95		0.16
			151.66		-0.13
				Within	+0.20

67

Barker's Method

Three different activity coefficient models were used to express the liquid composition dependence of activity coefficient. From the assumed model, vapor pressures for the binary mixture can be calculated. The non-linear regression computer program by R. M. Baer at Chevron Research Corporation (32) and the VLE calculation program by V. C. Smith (50) were modified in this study for evaluating the parameters in each model in order to achieve the best fit to the experimental vapor pressures.

With the Redlich-Kister model, equations with up to nine parameters were investigated in this study. Table XVII gives the values of the root mean square deviation (RMSD) in vapor pressure for each analytical model and each system. The maximum error and the value of liquid mole fraction alcohol where the maximum error occurrs are also tabulated.

Table XVII shows that the maximum error for each system occurs at either low or high alcohol concentration. This inadequacy at low or high concentrations is felt to be a fault of the activity coefficient models. Since these three models are incapable of predicting partial miscibilities in the liquid mixtures such as methanol-cyclohexane and methanol-n-hexane, large deviations are to be expected for these two systems. A typical plot of deviation between calculated and experimental vapor pressures for the system ethanol-n-hexane is shown in Figure 15. Qualitatively, the Van Laar and the 2-parameter Redlich-Kister models give similar results.

Effects of the number of the Redlich-Kister parameters on the RMSD in vapor pressure are shown in Figures 16 through 18. Results with

TABLE XVII

COMPARISON OF FIT TO EXPERIMENTAL VAPOR PRESSURE DATA FOR EACH ANALYTICAL MODEL

Model	MeOH–BZ	EtOH–BZ	nPrOH–BZ	MeOH–CC6	EtOH–CC6	nPrOH–CC6	MeOH–nC6	EtOH–nC6	nPrOH–nC6
Van Laar									
RMSD (a)	6.7870	3.0292	1.4233	21.097	5.2182	2.8953	27.310	6.7222	5.2021
Max (b)	−15.961	−7.0198	2.3349	−59.402	−17.471	−5.7323	−63.479	−19.094	−9.0391
x_1 (c)	0.0103	0.0295	0.6602	0.0097	0.0281	0.0204	0.0185	0.0257	0.9641
Wilson									
RMSD	1.9047	1.6001	0.7241	1.6072	0.9449	1.1226	4.2462	1.6636	1.7443
Max	−3.8573	−3.2266	−1.4682	−3.5957	−3.1150	−3.7740	−10.835	−4.6790	−4.2460
x_1	0.9635	0.0151	0.0104	0.9062	0.0281	0.0098	0.0040	0.0257	0.0065
RK–2 (d)									
RMSD	7.9928	3.3203	1.4522	21.815	5.3967	3.1248	27.327	6.7817	5.3098
Max	−21.032	−8.4566	2.3535	−63.466	−18.568	−6.0188	−62.219	−19.625	−8.7334
x_1	0.0340	0.0295	0.6602	0.0097	0.0281	0.0204	0.0099	0.0257	0.9641
RK–3 (e)									
RMSD	3.2142	1.4510	0.5138	10.859	2.3141	1.6354	11.606	2.7607	1.7540
Max	−11.370	−3.8283	−1.3941	−40.200	−9.3843	−4.8598	−34.862	−11.759	−4.6796
x_1	0.0103	0.0151	0.0104	0.0097	0.0281	0.0098	0.0090	0.0257	0.0065
RK–4 (f)									
RMSD	2.1051	0.9711	0.3605	8.7213	1.5841	1.1670	10.975	2.1684	1.5620
Max	−7.7476	−2.2660	−1.2489	−30.675	−5.5162	−4.0504	−31.185	−7.9333	−4.4101
x_1	0.0103	0.0151	0.0104	0.0097	0.0281	0.0098	0.0040	0.0257	0.0065

(a) Root mean square deviation, mmHg
(b) Maximum error of $(P_{cal} - P_{exp})$, mmHg
(c) The value of x_1 at which the maximum error occurs

(d) Redlich–Kister model with 2 parameters
(e) Redlich–Kister model with 3 parameters
(f) Redlich–Kister model with 4 parameters

TABLE XVII (Continued)

Model	MeOH-BZ	EtOH-BZ	nPrOH-BZ	MeOH-CC6	EtOH-CC6	nPrOH-CC6	MeOH-nC6	EtOH-nC6	nPrOH-nC6
RK-5 (g)									
RMSD	1.5691	0.4560	0.3621	8.6373	1.1116	0.7761	7.2047	1.2110	0.9301
Max	-6.3440	-1.0909	-1.2564	-38.879	-4.5636	-3.0444	-26.957	-4.9370	-3.6959
x_1	0.0103	0.0151	0.0104	0.0097	0.0281	0.0098	0.0040	0.0257	0.0065
RK-6 (h)									
RMSD	1.5250	0.4486	0.3512	6.2803	0.8651	0.7705	7.0595	1.0589	0.8843
Max	-6.4310	1.0327	-1.2291	-26.639	-3.2018	-3.0557	-25.96	-3.7473	-3.5472
x_1	0.0103	0.0534	0.0104	0.0097	0.0281	0.0098	0.0040	0.0257	0.0065
RK-7 (i)									
RMSD	1.6702	0.4287	0.3550	7.1955	0.7998	0.7644	8.3200	1.2648	0.9166
Max	-6.8939	0.9824	-1.1696	-33.251	-2.6121	-3.0932	-28.298	-5.7256	-3.7293
x_1	0.0103	0.0534	0.0104	0.0097	0.0281	0.0098	0.0040	0.0257	0.0065
RK-8 (j)									
RMSD	1.4462	0.6239	0.3470	5.7073	0.8457	0.7642	8.6187	1.0980	0.9285
Max	-5.9532	-1.9883	-1.1951	-25.101	-3.7772	-3.1162	-29.559	-4.5788	-3.7107
x_1	0.0103	0.0151	0.0104	0.0097	0.0281	0.0098	0.0040	0.0257	0.0065
RK-9 (k)									
RMSD	1.5624	0.4709	0.3676	5.6350	0.7740	0.7995	7.8420	1.0528	0.9292
Max	-6.3144	1.0559	-1.1091	-24.564	-2.6810	-3.2164	-29.729	-4.7604	-3.7593
x_1	0.0103	0.0872	0.0104	0.0097	0.0281	0.0098	0.0040	0.0257	0.0065

(g) Redlich-Kister model with 5 parameters   (j) Redlich-Kister model with 8 parameters
(h) Redlich-Kister model with 6 parameters   (k) Redlich-Kister model with 9 parameters
(i) Redlich-Kister model with 7 parameters
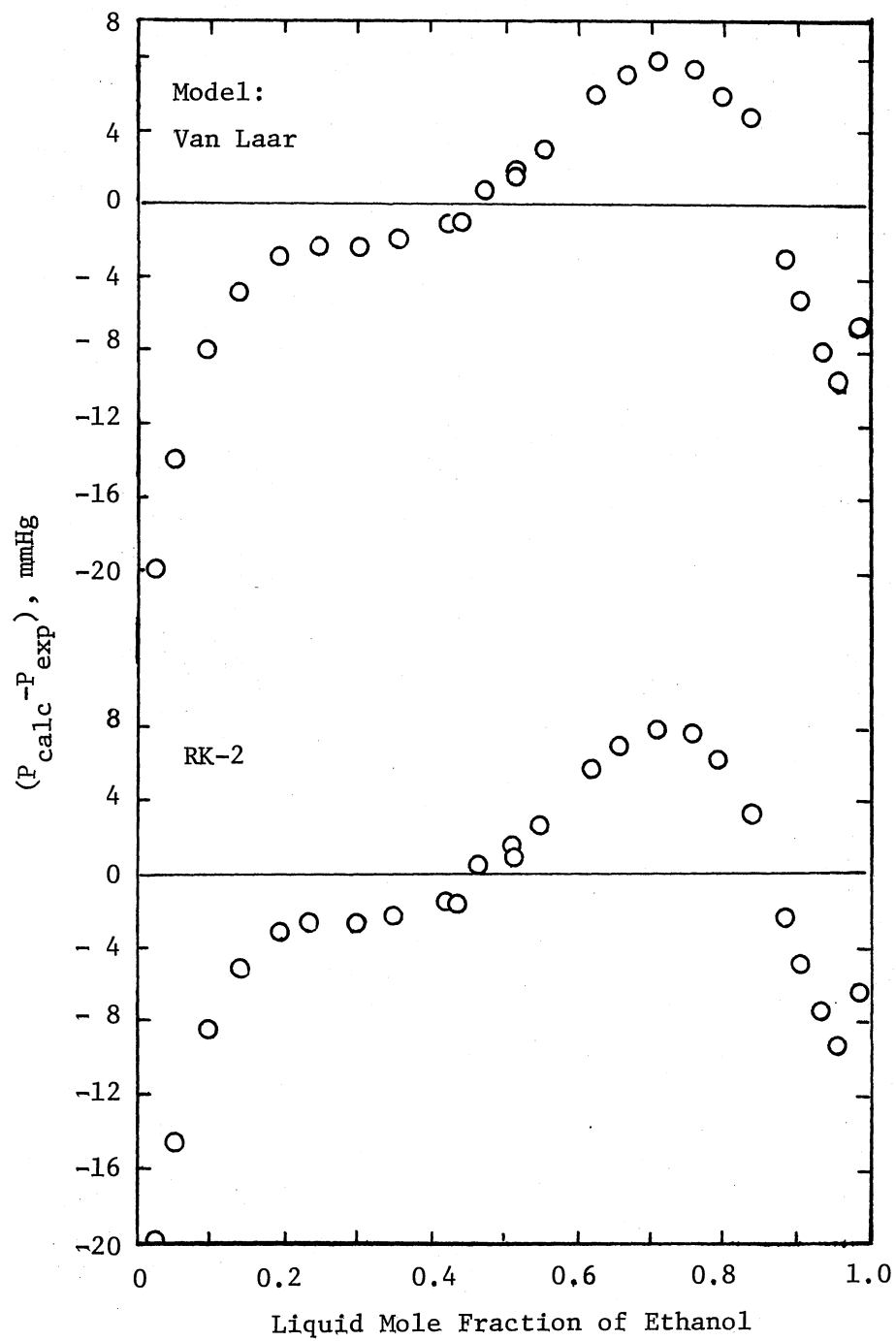
Figure 15. Deviation in Vapor Pressure at
25°C for the System Ethanol
(1)-n-Hexane(2)
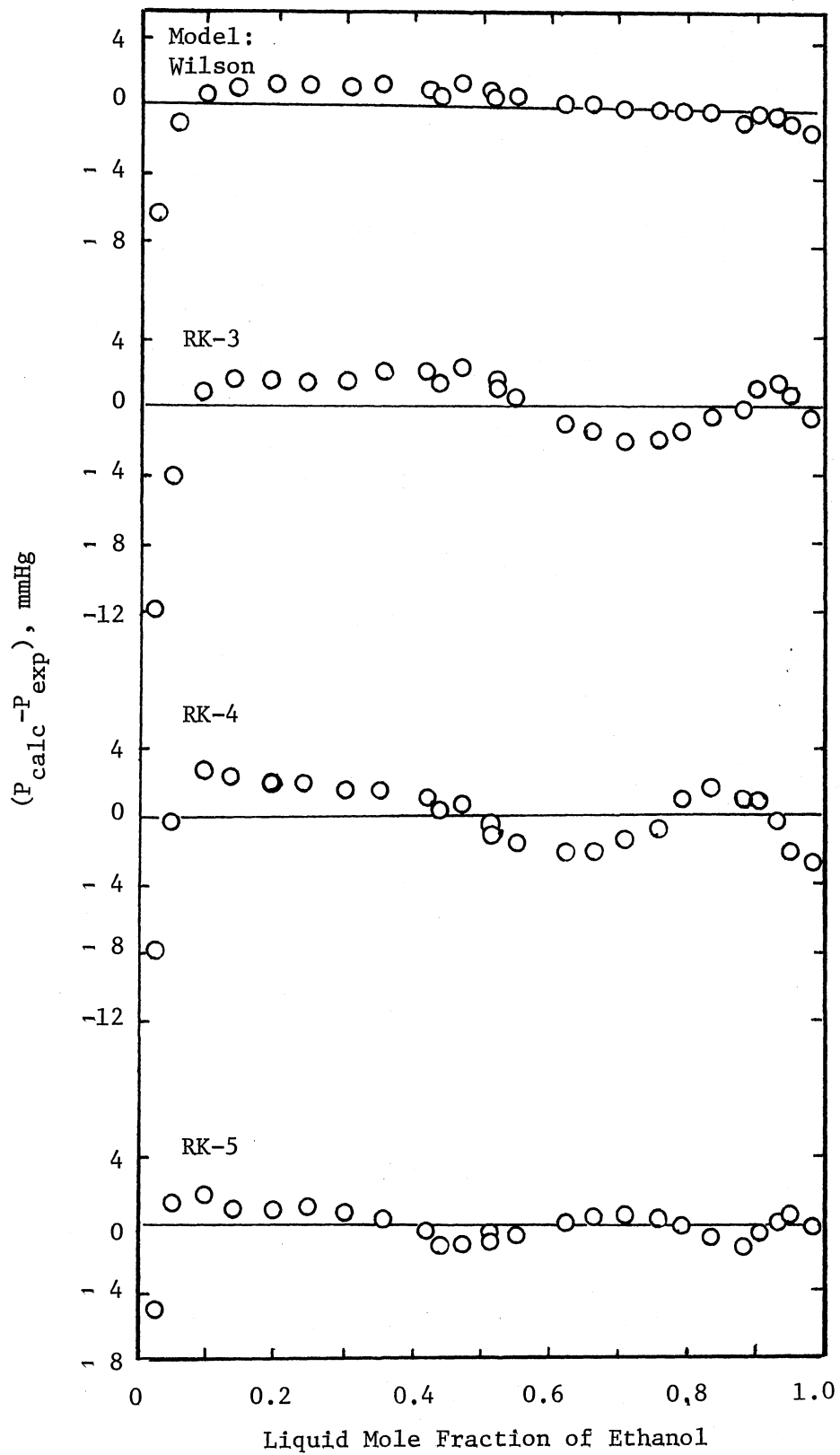
Figure 15. (Continued)
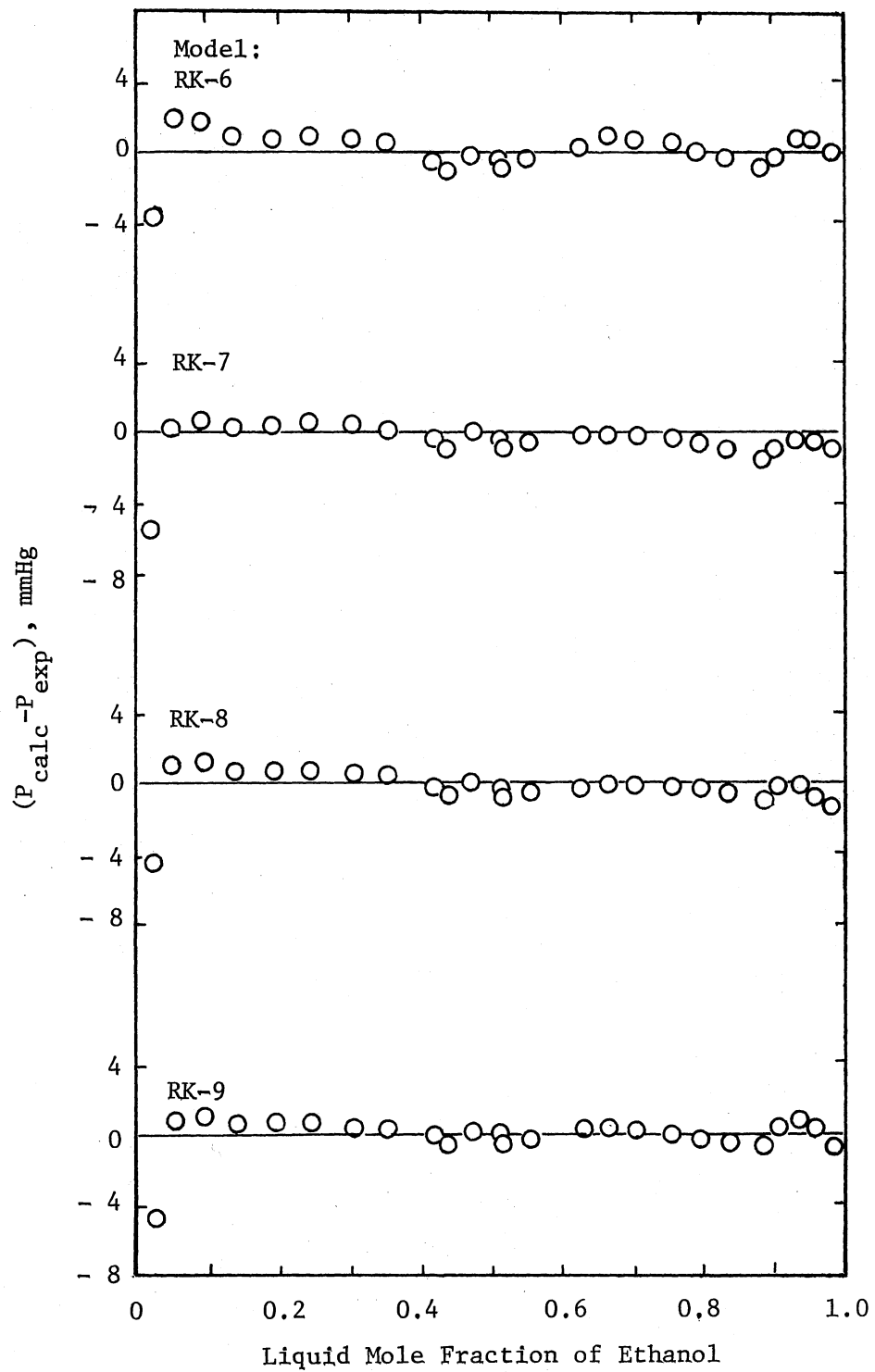
Figure 15. (Continued)
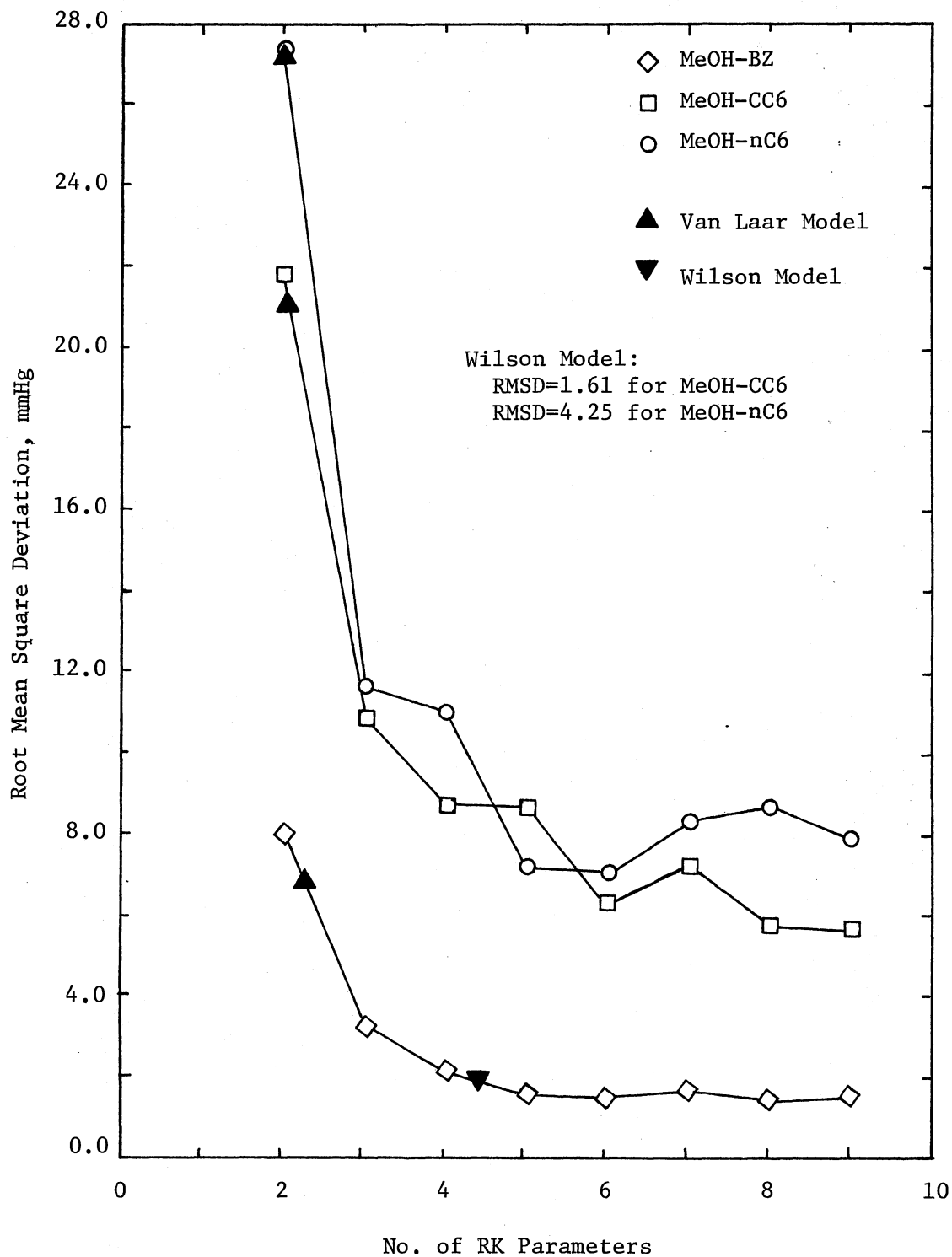
Figure 16. Root Mean Square Deviation of Vapor Pressure
by the Redlich-Kister Model for the
Systems Containing Methanol
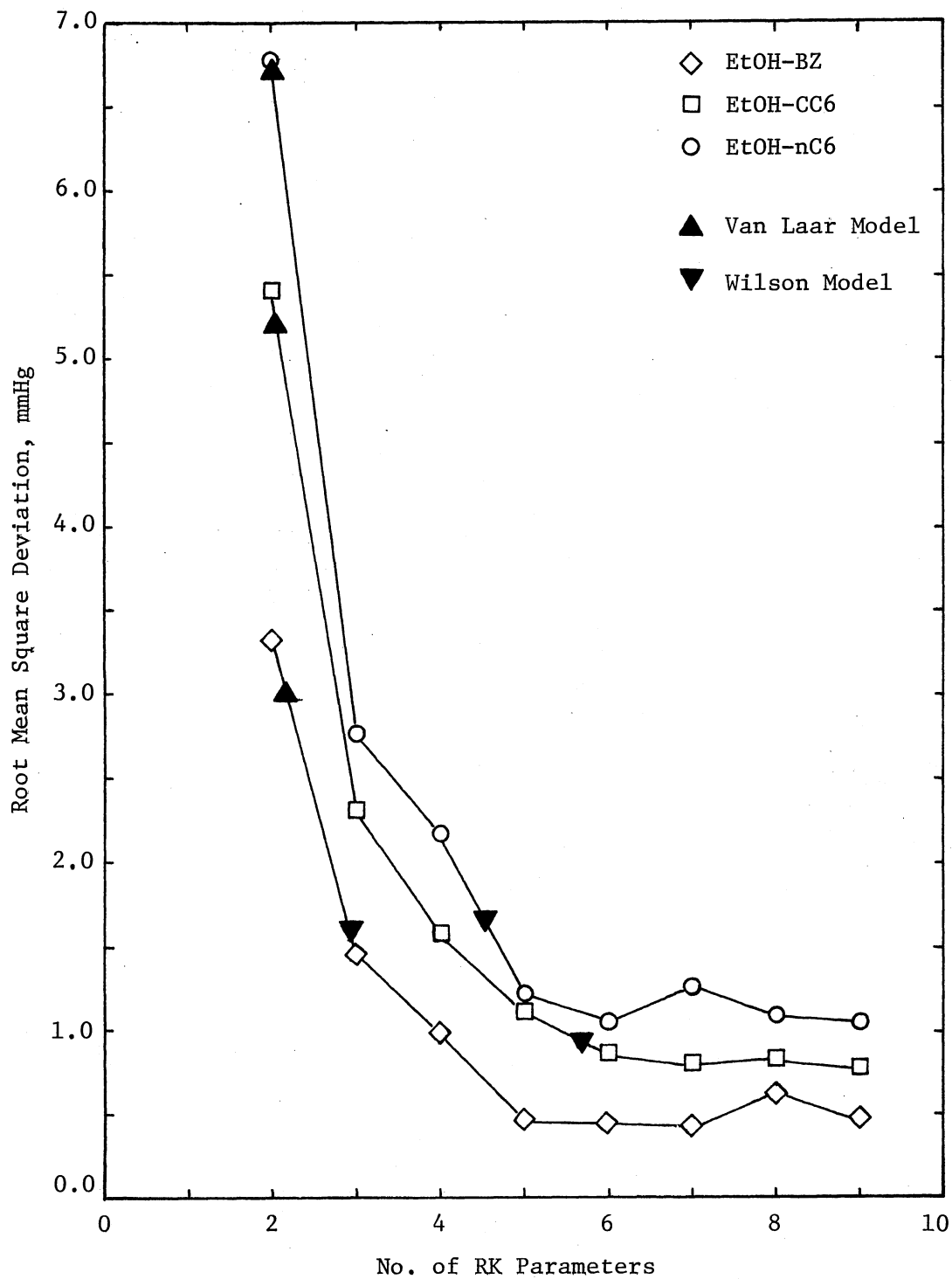
Figure 17. Root Mean Square Deviation of Vapor Pressure
by the Redlich-Kister Model for the
Systems Containing Ethanol
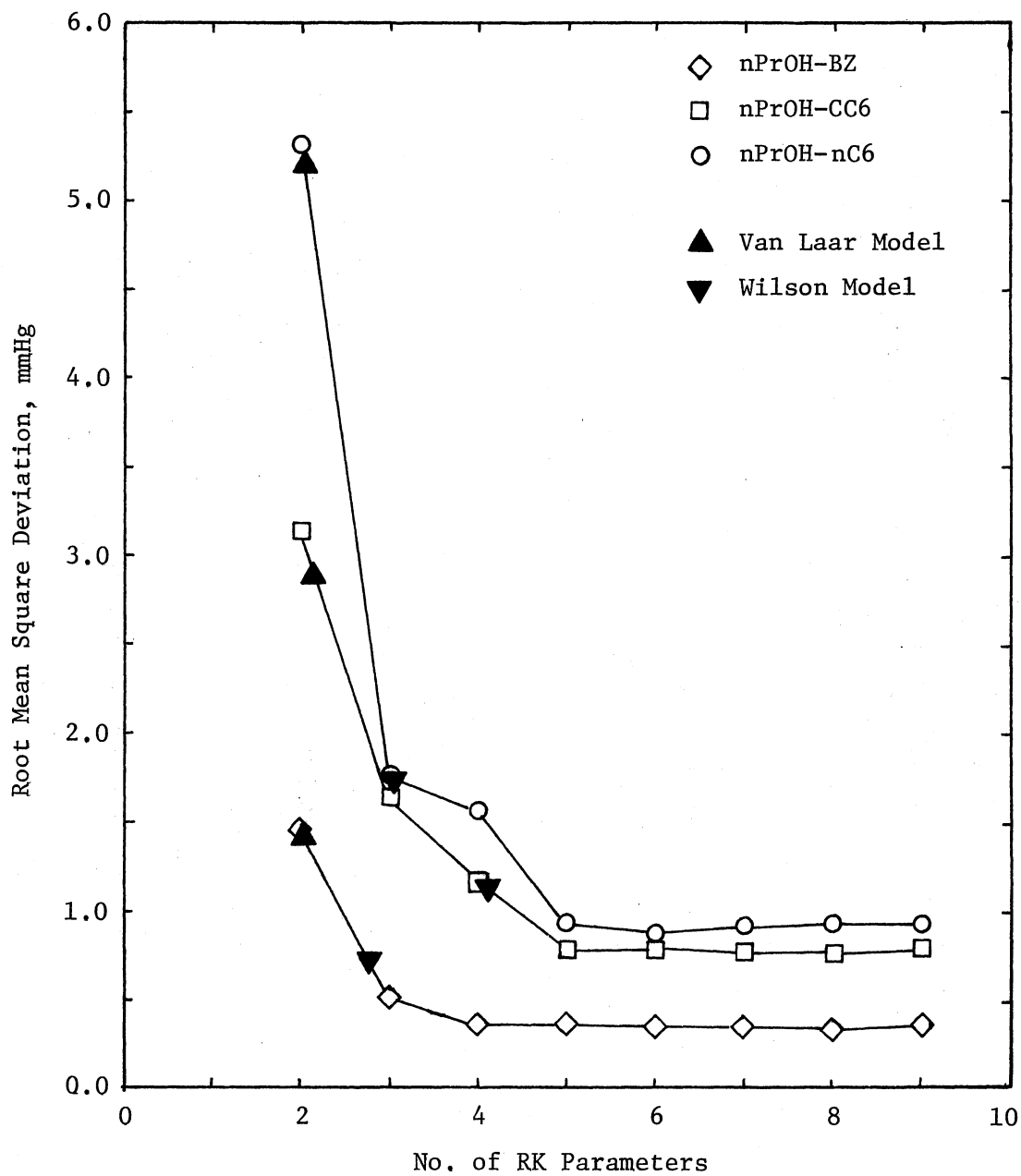
Figure 18. Root Mean Square Deviation of Vapor Pressure
by the Redlich-Kister Model for Systems
Containing n-Propanol

Van Laar and the Wilson models are also shown in the figures. In general, the Van Laar model gives better results than the 2-parameter Redlich-Kister model. A comparison between the Redlich-Kister and the Wilson models indicates that the Redlich-Kister model will require at least three (and even up to seven) parameters in order to obtain results comparable to the Wilson model. This substantiates that, as mentioned by Orye and Prausnitz (39), the Wilson model appears to be the best 2-parameter equation in representing the experimental vapor pressure data. As indicated by Harris and Prausnitz (26), significant improvement can be obtained by using 3-parameter instead of 2-parameter Redlich-Kister model. This is due to the factor that the additional even-powered correction term (the third parameter C') is symmetric in x and tends to sharpen (when C' is a negative value) or flatten (when C' is a positive value) the G^E curve to obtain a better representation of the excess Gibbs free energy of a binary mixture. However, no significant changes in RMSD are observed when five or more parameters are used.

The accuracy of representing the experimental P-x data is mainly related to the difference in the molecular sizes of the two components in the binary system. For example, in the binary systems of alcohols with benzene, only two parameters are required for the n-propanol-benzene system to obtain a RMSD of 1.50 mmHg, while three parameters are required for the ethanol-benzene system and six parameters are required for the methanol-benzene system. At $25^{\circ}C$, the ratio of molar volumes (benzene-to-alcohol) in the system containing methanol is 2.19 and is 1.52 in the system containing ethanol, while it is only 1.19 in

the system containing n-propanol. The effect of molecular size on

the representation of experimental vapor pressures is shown clearly in

Table XVII and in Figures 16 through 18.

Mixon's Method

The computer program for vapor-liquid equilibrium calculation with

Mixon's method was written by Smith (50). Mixon's method requires

values of vapor pressures at equally spaced intervals of x_1. In order

to fully take the main advantage of Mixon's method (which is to avoid

using a model to fit the P-x data), smoothed vapor pressure data were

obtained by graphical methods instead of fitting the P-x data by a

polynomial. The experimental P-x data points were plotted on a large

graph sheet and were smoothed with a French curve. The values of vapor

pressure at liquid mole fraction intervals of 0.05 were then read from

the graph.

The program for VLE calculation with Mixon's method failed to

converge for the systems which are highly non-ideal. The following

procedure was adopted in this study for vapor-liquid calculation using

Mixon's method. First, the values of G^E predicted by the 9-parameter

Redlich-Kister model were used. Starting at one end point (x_1=0) with

increasing mole fraction of component 1, the program was allowed to

execute until the vapor pressure iteration did converge up to or near

azeotrope point. Then the procedure was repeated in reverse order,

i.e., starting at the other end point (x_2=0) with increasing mole

fraction of component 2. Next, a combination of the best fit of G^E-x_1

data from the two separate runs was read in as new initial input. The

process was repeated until the program did converge over the entire range of liquid composition.

The initial tolerance set on convergence was 0.10 mmHg which is far less than the root mean square deviation of the best fit model for each system. Results of Mixon's method are summarized in Tables XVIII through XXVI. The vapor compositions at 25°C calculated by Mixon's method are shown graphically in Figures 19 through 27. The activity coefficients are shown in Figures 28 through 36.

The azeotrope point for each system is listed in Table XXVII. For the ethanol-cyclohexane system, the azeotrope occurs at an ethanol mole fraction of 0.340; whereas smoothing of the experimental y-x data of Washburn and Handrof (61) gives a value of 0.336. Azeotrope compositions for the ethanol-benzene and ethanol-n-hexane systems have been reported by Smith and Robinson (51). Agreement between the two sets of data is particularly good. The differences between these azeotropes are 0.001 mole fraction for ethanol-benzene and 0.004 for ethanol-n-hexane.

For the two partially miscible systems, the solubility data were estimated as 0.120 and 0.830 mole fraction of methanol for methanol-cyclohexane, and 0.210 and 0.810 mole fraction of methanol for methanol-n-hexane. The solubility data for the methanol-n-hexane system have been reported by Savini and coworkers (45), reporting values of 0.270 and 0.791 mole fraction of methanol. The solubility data for the methanol-cyclohexane system, reported by Kurthnine and coworkers (33), are 0.112 and 0.830 mole fraction of methanol.

Since Mixon's method involves an iterative numerical calculation of excess Gibbs free energies, the effect of excess Gibbs free energy

TABLE XVIII

VAPOR-LIQUID EQUILIBRIUM DATA AT 25°C FOR THE SYSTEM METHANOL(1)-BENZENE(2)
BY MIXON'S METHOD

Liquid Mole Fraction x_1	Smoothed Vapor Pressure P,mmHg	Vapor Mole Fraction y_1	Excess Gibbs Free Energy G^E, cal/g-mole	Activity Coefficients Comp 1	Comp 2
0.0500	165.00	0.4379	81.93	11.3447	1.0179
0.1000	174.90	0.4756	142.84	6.5358	1.0611
0.1500	177.75	0.4871	189.64	4.5349	1.1161
0.2000	179.25	0.4940	225.90	3.4795	1.1793
0.2500	180.30	0.4996	253.74	2.8322	1.2511
0.3000	181.00	0.5039	274.30	2.3895	1.3339
0.3500	181.50	0.5079	288.28	2.0704	1.4287
0.4000	182.00	0.5138	296.28	1.8380	1.5337
0.4500	182.50	0.5206	299.01	1.6601	1.6535
0.5000	182.90	0.5322	296.52	1.5304	1.7780
0.5500	183.00	0.5472	290.12	1.4322	1.9140
0.6000	182.70	0.5636	279.34	1.3503	2.0716
0.6500	182.20	0.5793	264.76	1.2776	2.2749
0.7000	181.30	0.5927	245.15	1.2078	2.5569
0.7500	180.00	0.6069	220.33	1.1461	2.9400
0.8000	177.50	0.6271	189.34	1.0950	3.4377
0.8500	173.30	0.6574	152.55	1.0550	4.1103
0.9000	165.40	0.7090	108.77	1.0255	4.9988
0.9500	152.00	0.8000	58.71	1.0073	6.3173

TABLE XIX

VAPOR-LIQUID EQUILIBRIUM DATA AT 25°C FOR THE SYSTEM ETHANOL(1)-BENZENE(2)
BY MIXON'S METHOD

Liquid Mole Fraction x_1	Smoothed Vapor Pressure P, mmHg	Vapor Mole Fraction y_1	Excess Gibbs Free Energy G^E, cal/g-mole	Activity Coefficients Comp 1	Comp 2
0.0500	116.40	0.2095	71.51	8.2639	1.0160
0.1000	120.40	0.2486	124.18	5.0754	1.0538
0.1500	122.10	0.2699	164.64	3.7275	1.0994
0.2000	123.00	0.2833	196.51	2.9556	1.1545
0.2500	123.30	0.2933	220.33	2.4538	1.2173
0.3000	123.50	0.3103	238.04	2.1673	1.2744
0.3500	123.50	0.3268	251.79	1.9569	1.3396
0.4000	123.20	0.3355	260.50	1.7554	1.4300
0.4500	122.80	0.3449	263.93	1.5978	1.5320
0.5000	122.00	0.3568	262.99	1.4783	1.6436
0.5500	120.90	0.3692	257.65	1.3786	1.7754
0.6000	119.80	0.3801	248.00	1.2894	1.9449
0.6500	117.60	0.3978	233.30	1.2230	2.1198
0.7000	115.00	0.4186	215.41	1.1688	2.3350
0.7500	111.50	0.4437	192.31	1.1211	2.5996
0.8000	107.40	0.4736	165.59	1.0810	2.9621
0.8500	101.70	0.5137	132.59	1.0454	3.4570
0.9000	92.80	0.5829	94.73	1.0222	4.0592
0.9500	79.90	0.7031	50.89	1.0060	4.9776

TABLE XX

VAPOR-LIQUID EQUILIBRIUM DATA AT $25^{o}C$ FOR THE SYSTEM N-PROPANOL(1)-BENZENE(2)
BY MIXON'S METHOD

Liquid Mole Fraction x_1	Smoothed Vapor Pressure P,mmHg	Vapor Mole Fraction y_1	Excess Gibbs Free Energy G^E, cal/g-mole	Activity Coefficients Comp 1	Activity Coefficients Comp 2
0.0500	97.60	0.0627	59.24	5.8049	1.0128
0.1000	97.50	0.0895	103.44	4.1417	1.0368
0.1500	97.00	0.1104	141.30	3.3909	1.0673
0.2000	96.50	0.1201	171.93	2.7527	1.1158
0.2500	95.50	0.1299	194.80	2.3574	1.1648
0.3000	94.40	0.1402	213.69	2.0961	1.2191
0.3500	93.30	0.1476	226.91	1.8703	1.2867
0.4000	91.90	0.1563	235.85	1.7073	1.3592
0.4500	90.50	0.1642	240.41	1.5697	1.4461
0.5000	88.90	0.1721	240.71	1.4554	1.5485
0.5500	86.90	0.1815	236.74	1.3641	1.6628
0.6000	84.60	0.1920	228.98	1.2878	1.7984
0.6500	81.90	0.2038	216.95	1.2222	1.9614
0.7000	79.00	0.2168	200.96	1.1645	2.1712
0.7500	75.70	0.2315	180.04	1.1123	2.4508
0.8000	71.20	0.2525	154.15	1.0699	2.8027
0.8500	64.30	0.2884	122.99	1.0390	3.2131
0.9000	54.80	0.3504	87.27	1.0168	3.7535
0.9500	40.70	0.4908	45.62	1.0034	4.3769

TABLE XXI

VAPOR-LIQUID EQUILIBRIUM DATA AT $25^{\circ}C$ FOR THE SYSTEM METHANOL(1)-CYCLOHEXANE(2)
BY MIXON'S METHOD

Liquid Mole Fraction x_1	Smoothed Vapor Pressure P,mmHg	Vapor Mole Fraction y_1	Excess Gibbs Free Energy G^E, cal/g-mole	Activity Coefficients Comp 1	Activity Coefficients Comp 2
0.500	209.20	0.5419	95.10	17.8409	1.0175
0.1000	213.20	0.5503	169.69	9.2346	1.0738
0.8500	213.40	0.5620	216.39	1.1112	6.2812
0.9000	210.50	0.5714	157.86	1.0521	9.0949
0.9500	195.00	0.6290	88.60	1.0165	14.5986

TABLE XXII

VAPOR-LIQUID EQUILIBRIUM DATA AT $25^{\circ}C$ FOR THE SYSTEM ETHANOL(1)-CYCLOHEXANE(2)
BY MIXON'S METHOD

Liquid Mole Fraction x_1	Smoothed Vapor Pressure P,mmHg	Vapor Mole Fraction y_1	Excess Gibbs Free Energy G^E, cal/g-mole	Activity Coefficients Comp 1	Comp 2
0.0500	134.10	0.2917	87.33	13.2269	1.0194
0.1000	137.80	0.3180	151.84	7.4127	1.0642
0.1500	139.00	0.3284	202.32	5.1480	1.1192
0.2000	139.40	0.3333	242.25	3.9310	1.1840
0.2500	139.50	0.3345	273.41	3.1582	1.2611
0.3000	139.50	0.3366	296.64	2.6483	1.3470
0.3500	139.45	0.3442	313.46	2.3219	1.4339
0.4000	139.40	0.3516	325.19	2.0740	1.5350
0.4500	139.30	0.3543	331.29	1.8563	1.6663
0.5000	139.20	0.3562	331.59	1.6782	1.8252
0.5500	138.90	0.3585	326.32	1.5327	2.0179
0.6000	138.50	0.3621	315.30	1.4143	2.2493
0.6500	137.70	0.3676	298.83	1.3172	2.5332
0.7000	136.50	0.3737	276.55	1.2337	2.9037
0.7500	134.60	0.3834	248.12	1.1645	3.3814
0.8000	131.50	0.3979	213.40	1.1069	4.0334
0.8500	125.20	0.4259	171.51	1.0625	4.8871
0.9000	113.60	0.4828	122.99	1.0322	5.9936
0.9500	96.00	0.5896	67.30	1.0098	8.0510

TABLE XXIII

VAPOR-LIQUID EQUILIBRIUM DATA AT 25°C FOR THE SYSTEM N-PROPANOL(1)-CYCLOHEXANE(2) BY MIXON'S METHOD

Liquid Mole Fraction x_1	Smoothed Vapor Pressure P,mmHg	Vapor Mole Fraction y_1	Excess Gibbs Free Energy G^E, cal/g-mole	Activity Coefficients Comp 1	Comp 2
0.0500	107.00	0.1120	83.77	11.3691	1.0211
0.1000	107.10	0.1190	142.78	6.0430	1.0703
0.1500	106.80	0.1267	186.32	4.2781	1.1202
0.2000	106.60	0.1337	222.17	3.3811	1.1785
0.2500	106.20	0.1370	248.77	2.7625	1.2475
0.3000	105.50	0.1428	269.27	2.3843	1.3190
0.3500	104.80	0.1473	283.84	2.0941	1.4037
0.4000	104.10	0.1511	292.96	1.8666	1.5040
0.4500	103.20	0.1551	296.64	1.6884	1.6190
0.5000	102.10	0.1595	295.45	1.5468	1.7528
0.5500	100.90	0.1638	289.23	1.4275	1.9153
0.6000	99.40	0.1689	278.03	1.3291	2.1096
0.6500	97.50	0.1750	261.86	1.2466	2.3477
0.7000	94.90	0.1828	240.53	1.1777	2.6422
0.7500	91.00	0.1947	213.99	1.1227	2.9973
0.8000	85.10	0.2136	182.35	1.0803	3.4219
0.8500	76.30	0.2457	145.68	1.0491	3.9271
0.9000	65.00	0.2978	104.15	1.0242	4.6781
0.9500	48.50	0.4136	55.69	1.0061	5.8363

TABLE XXIV

VAPOR-LIQUID EQUILIBRIUM DATA AT 25°C FOR THE SYSTEM METHANOL(1)-N-HEXANE(2)
BY MIXON'S METHOD

Liquid Mole Fraction x_1	Smoothed Vapor Pressure P, mmHg	Vapor Mole Fraction y_1	Excess Gibbs Free Energy G^E, cal/g-mole	Activity Coefficients Comp 1	Comp 2
0.0500	258.20	0.4236	93.77	17.2416	1.0169
0.1000	263.70	0.4358	167.70	9.0618	1.0721
0.1500	265.20	0.4454	220.22	6.2107	1.1219
0.2000	265.50	0.4487	269.08	4.6135	1.2038
0.8500	265.30	0.4563	221.34	1.1236	6.2349
0.9000	262.40	0.4611	162.54	1.0604	9.1703
0.9500	245.10	0.5016	93.53	1.0209	15.8678

TABLE XXV

VAPOR-LIQUID EQUILIBRIUM DATA AT 25°C FOR THE SYSTEM ETHANOL(1)-N-HEXANE(2)
BY MIXON'S METHOD

Liquid Mole Fraction x_1	Smoothed Vapor Pressure P, mmHg	Vapor Mole Fraction y_1	Excess Gibbs Free Energy G^E, cal/g-mole	Activity Coefficients Comp 1	Comp 2
0.0500	185.80	0.2040	86.67	12.7924	1.0200
0.1000	188.80	0.2259	149.83	7.2037	1.0635
0.1500	190.00	0.2368	200.01	5.0673	1.1172
0.2000	190.20	0.2421	239.41	3.8904	1.1800
0.2500	190.25	0.2509	270.69	3.2273	1.2444
0.3000	190.25	0.2577	295.87	2.7621	1.3205
0.3500	190.20	0.2582	314.41	2.3714	1.4212
0.4000	190.10	0.2592	326.20	2.0813	1.5357
0.4500	189.80	0.2603	332.42	1.8568	1.6717
0.5000	189.40	0.2622	332.42	1.6788	1.8296
0.5500	188.70	0.2650	327.32	1.5374	2.0180
0.6000	187.80	0.2679	316.31	1.4178	2.2504
0.6500	186.40	0.2720	299.95	1.3192	2.5397
0.7000	184.10	0.2781	277.50	1.2368	2.9023
0.7500	180.40	0.2875	249.42	1.1694	3.3686
0.8000	174.60	0.3014	214.82	1.1127	3.9980
0.8500	165.40	0.3241	173.65	1.0669	4.8881
0.9000	149.00	0.3681	124.65	1.0318	6.1861
0.9500	119.30	0.4740	67.54	1.0088	8.2713

TABLE XXVI

VAPOR-LIQUID EQUILIBRIUM DATA AT 25°C FOR THE SYSTEM N-PROPANOL(1)-N-HEXANE(2)
BY MIXON'S METHOD

Liquid Mole Fraction x_1	Smoothed Vapor Pressure P,mmHg	Vapor Mole Fraction y_1	Excess Gibbs Free Energy G^E, cal/g-mole	Activity Coefficents	
				Comp 1	Comp 2
0.0500	159.70	0.0774	84.96	11.6990	1.0217
0.1000	159.30	0.0841	144.44	6.3389	1.0679
0.1500	158.60	0.0906	190.47	4.5374	1.1178
0.2000	157.80	0.0956	227.44	3.5733	1.1753
0.2500	157.00	0.0989	256.35	2.9401	1.2429
0.3000	156.00	0.1020	278.45	2.5113	1.3189
0.3500	155.00	0.1046	294.50	2.1939	1.4073
0.4000	153.90	0.1071	304.75	1.9515	1.5092
0.4500	152.50	0.1098	309.73	1.7626	1.6271
0.5000	150.80	0.1127	309.49	1.6111	1.7646
0.5500	149.10	0.1155	304.34	1.4842	1.9327
0.6000	146.90	0.1188	293.85	1.3788	2.1344
0.6500	144.10	0.1229	278.45	1.2915	2.3817
0.7000	140.40	0.1279	257.59	1.2169	2.6947
0.7500	135.50	0.1347	231.35	1.1546	3.0980
0.8000	128.00	0.1454	199.12	1.1040	3.6143
0.8500	116.70	0.1632	161.09	1.0642	4.3068
0.9000	100.90	0.1934	116.30	1.0313	5.3968
0.9500	74.10	0.2713	63.04	1.0083	7.1796
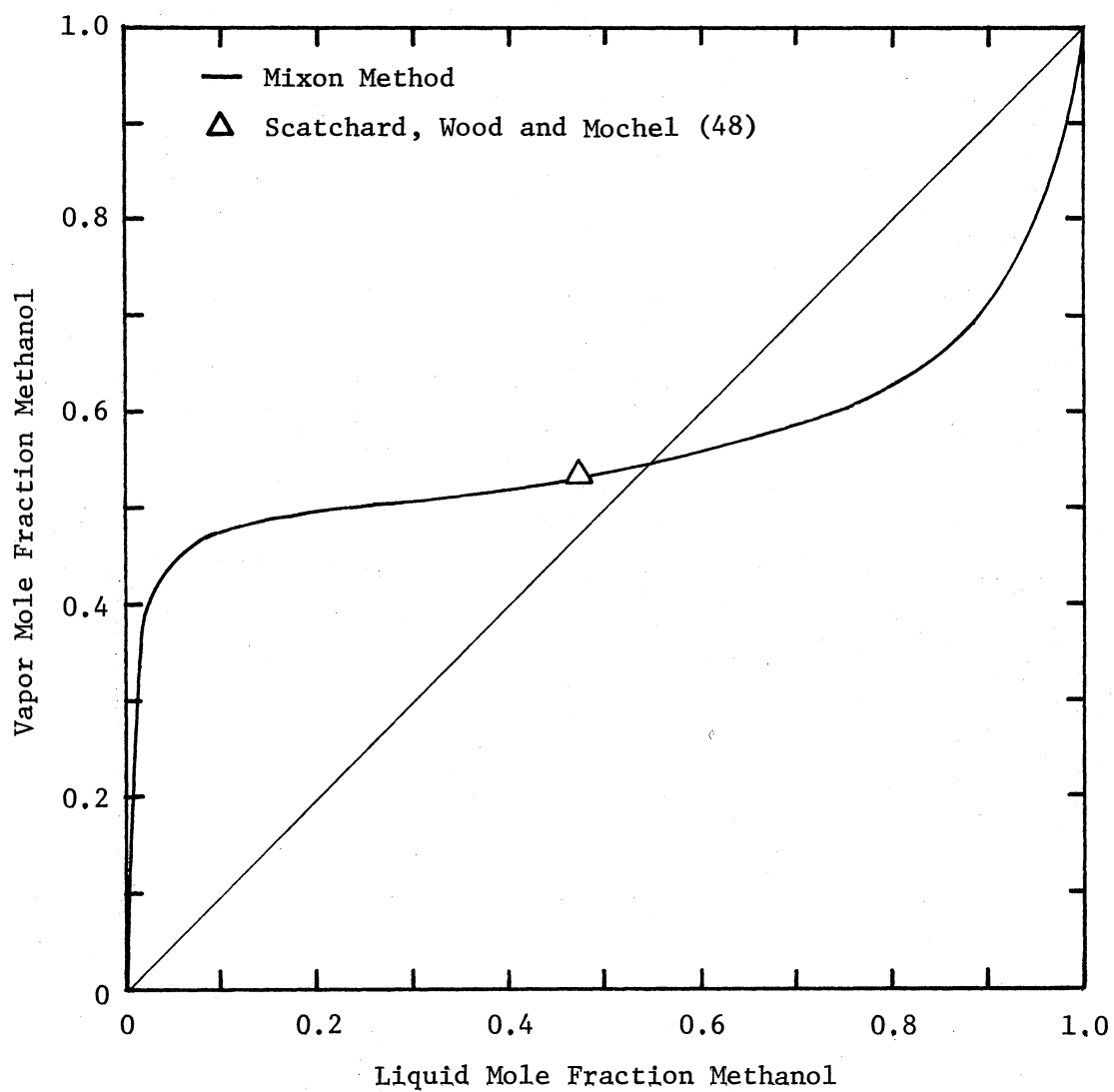
Figure 19. Vapor-Liquid Composition Data at 25°C for
the System Methanol(1)-Benzene(2)
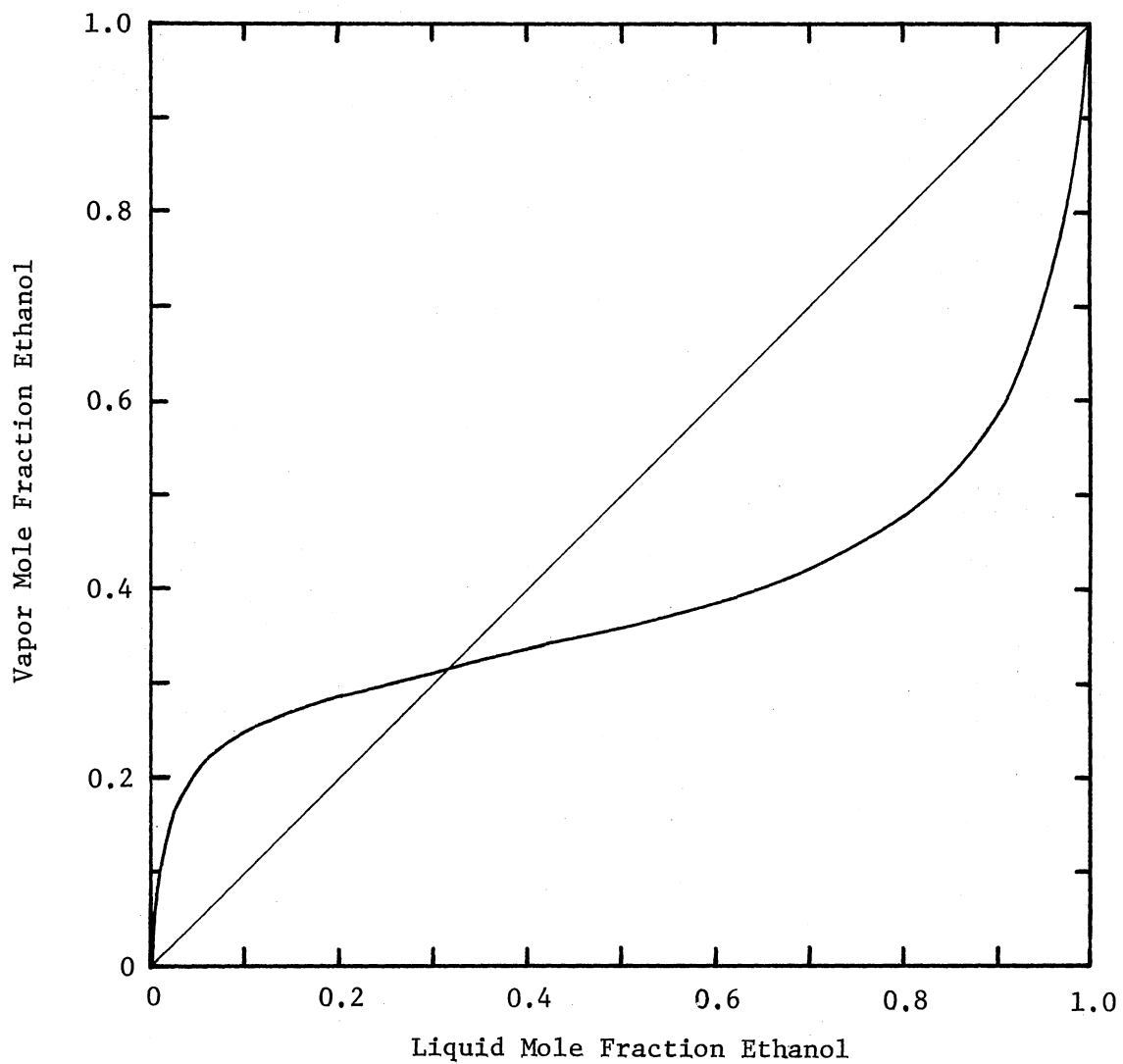
Figure 20. Vapor-Liquid Composition Data at 25°C for
the System Ethanol(1)-Benzene(2)
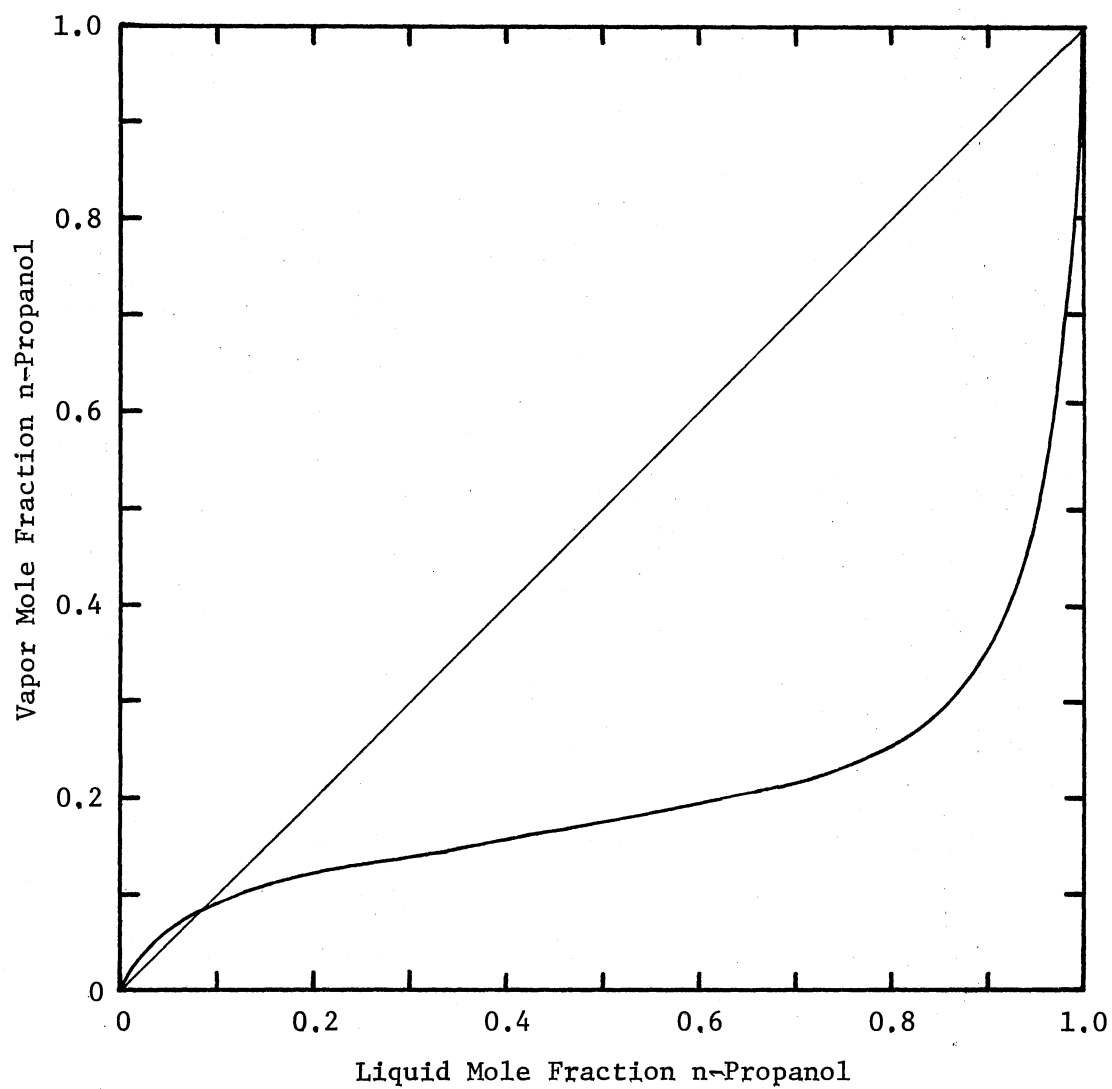
Figure 21.   Vapor-Liquid Composition Data at 25°C for
the System n-Propanol(1)-Benzene(2)
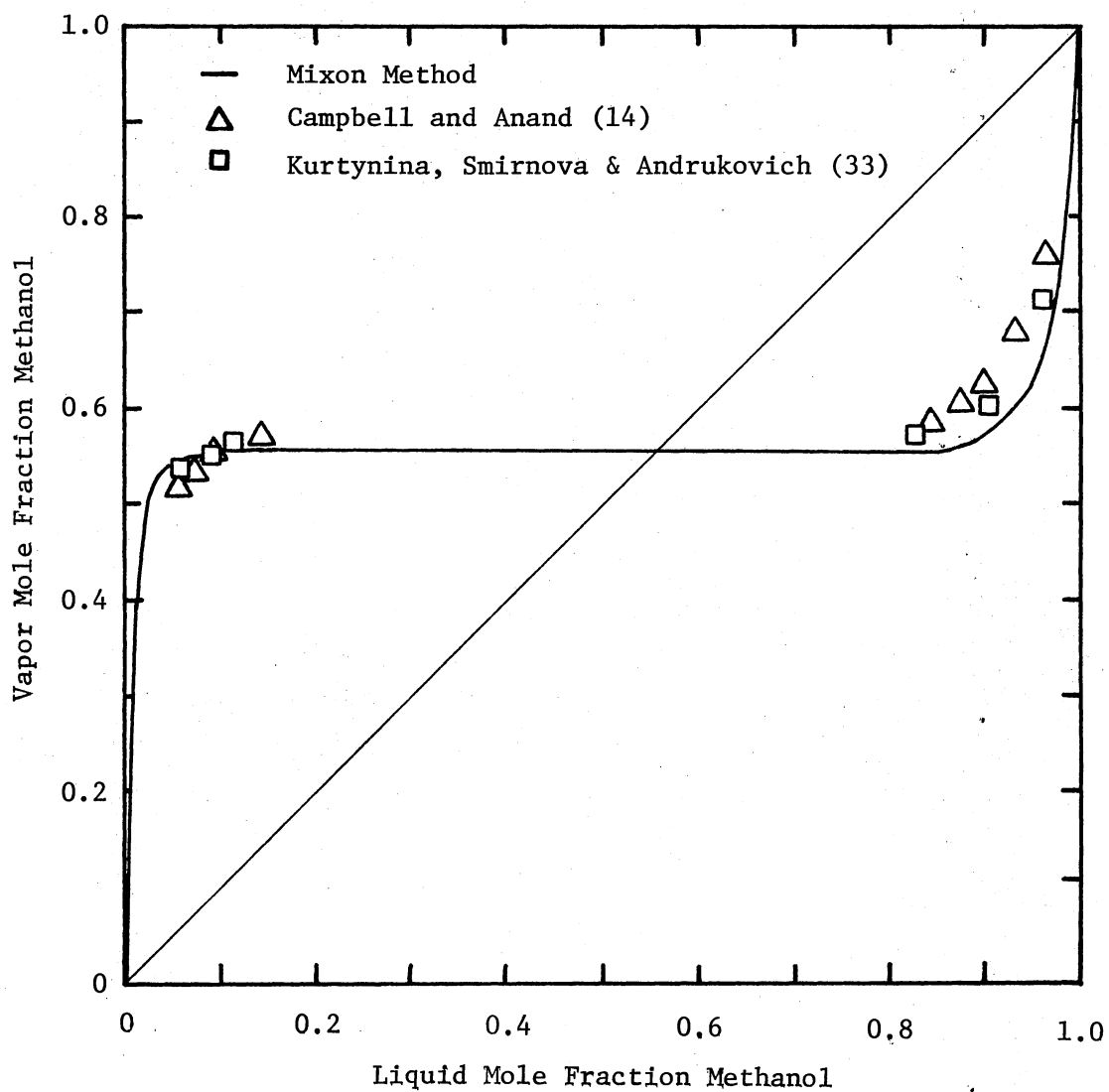
Figure 22. Vapor-Liquid Composition Data at 25°C for
the System Methanol(1)-Cyclohexane(2)
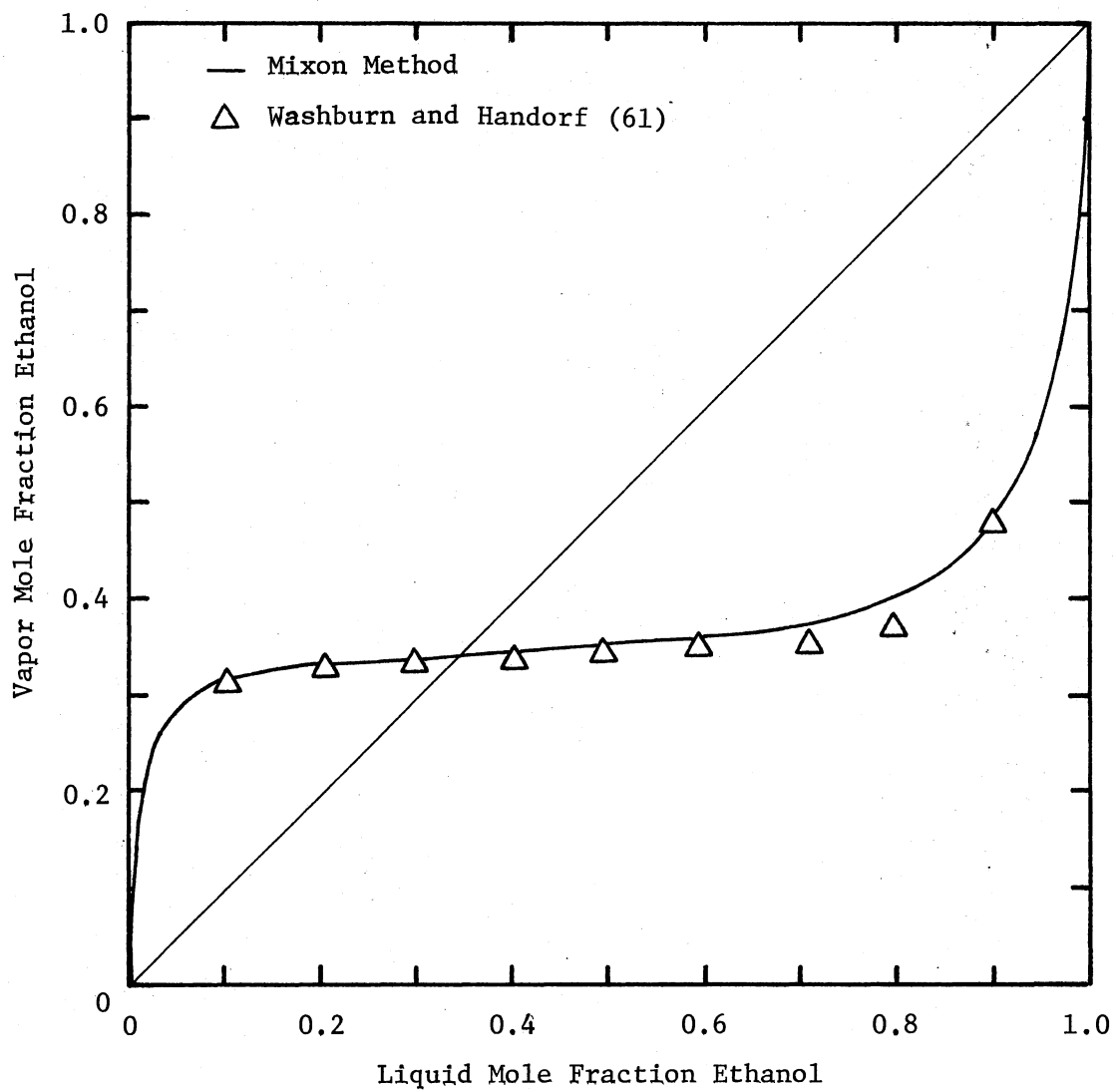
Figure 23.   Vapor-Liquid Composition Data at 25°C for
the System Ethanol(1)-Cyclohexane(2)
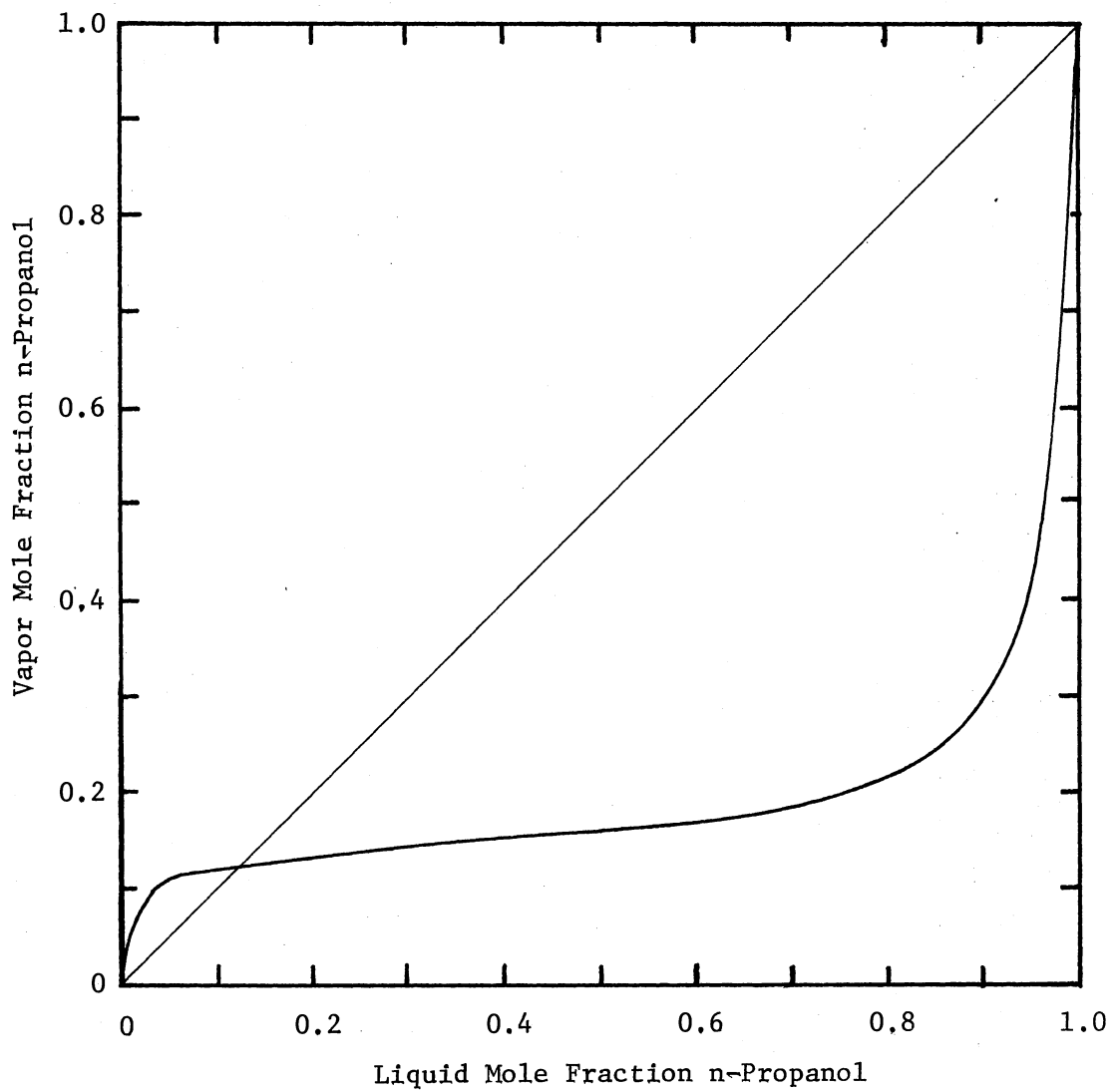
Figure 24. Vapor-Liquid Composition Data at 25°C for
the System n-Propanol(1)-Cyclohexane(2)
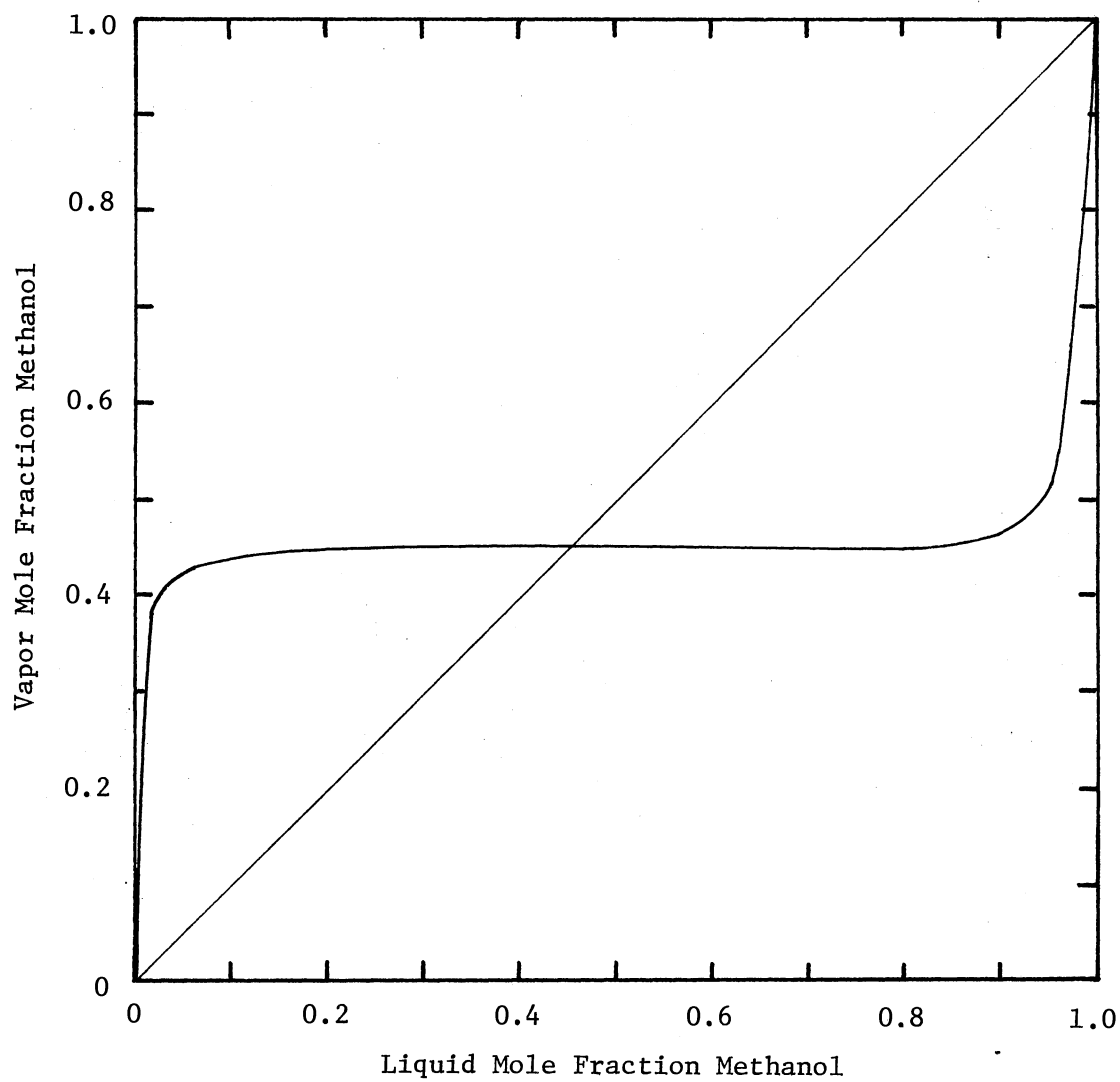
Figure 25.   Vapor-Liquid Composition Data at 25°C for the
System Methanol(1)-n-Hexane(2)
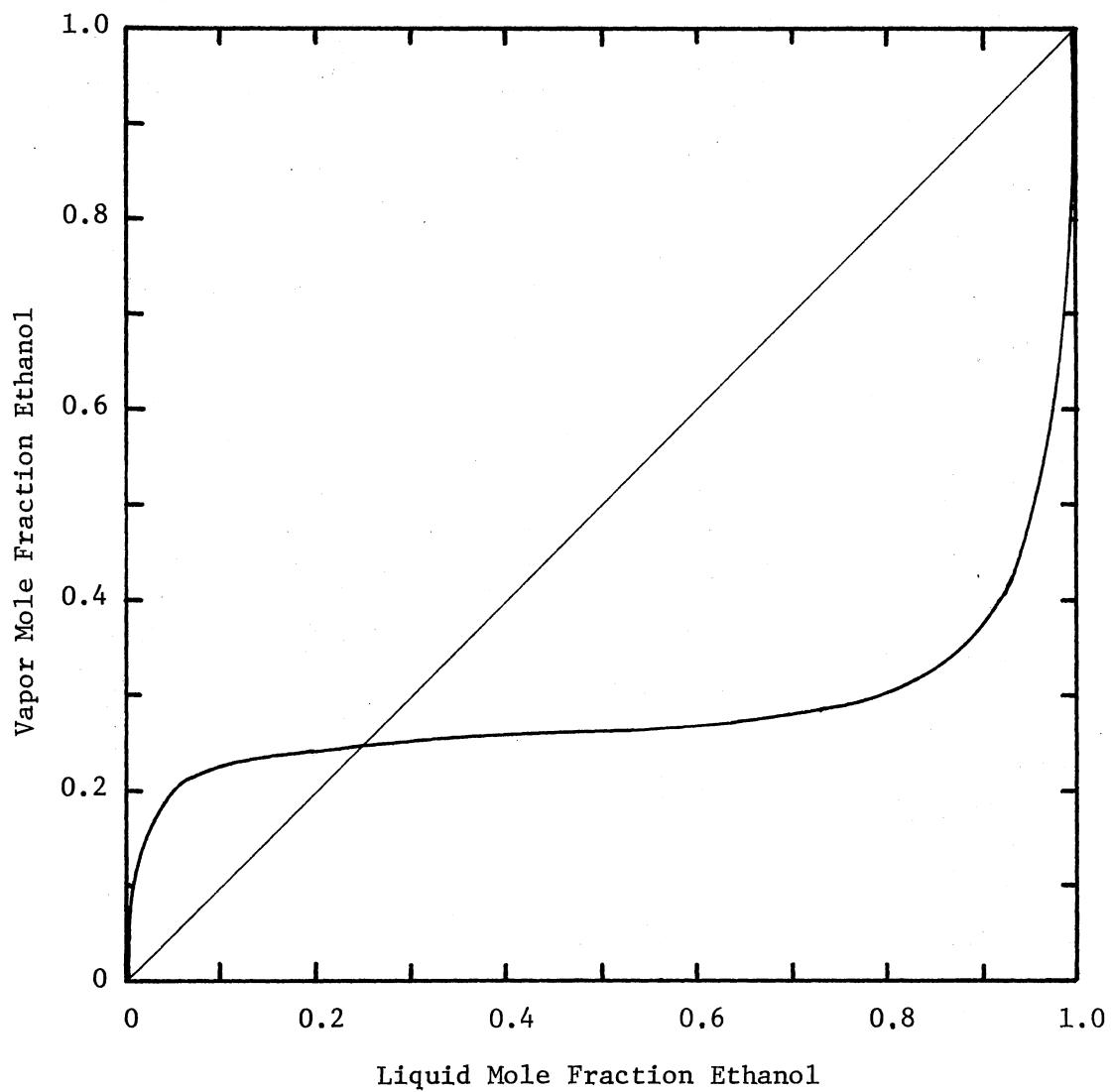
Figure 26. Vapor-Liquid Composition Data at 25°C for the
System Ethanol(1)-n-Hexane(2)
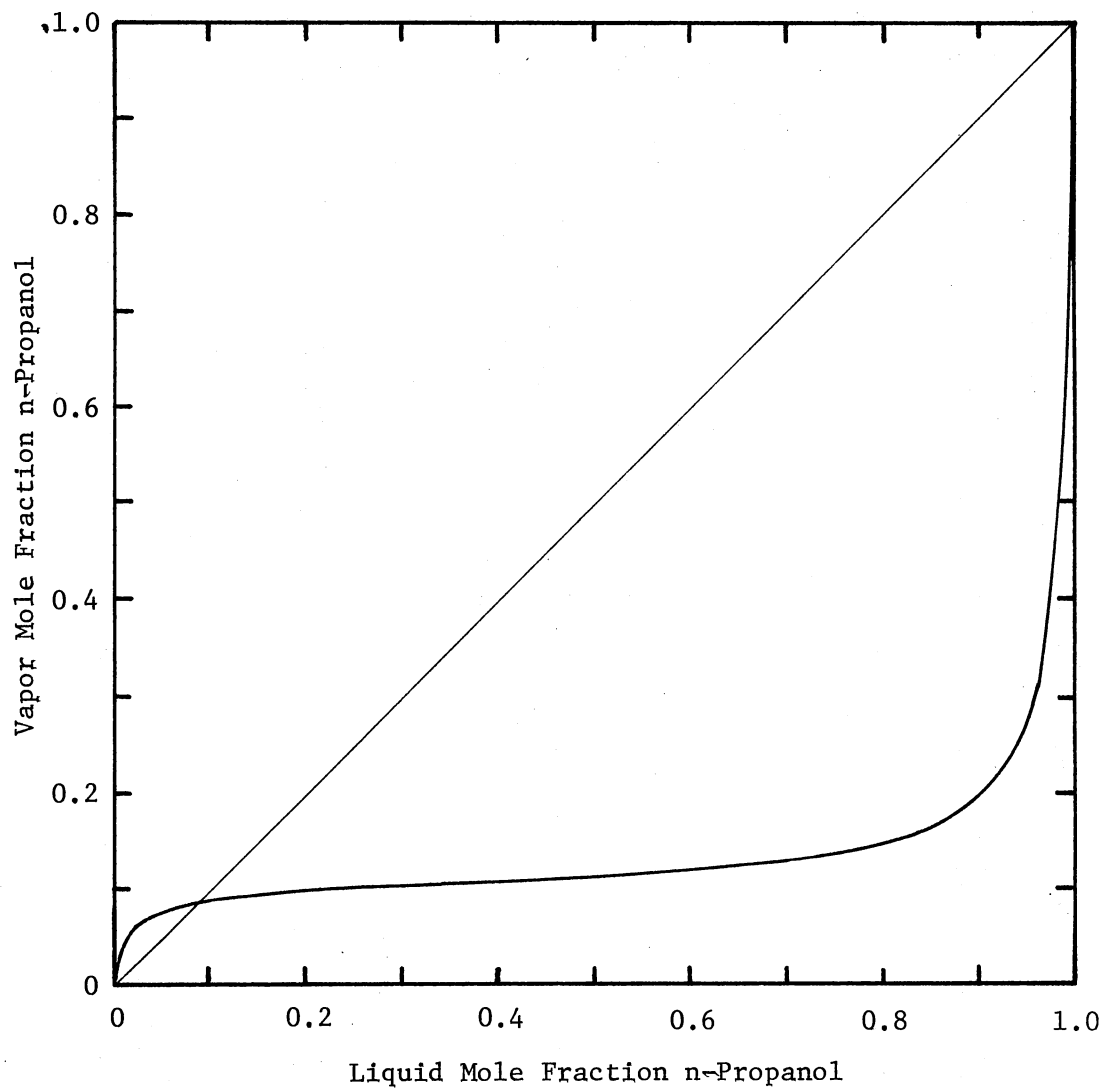
Figure 27. Vapor-Liquid Composition Data at 25°C for the
System n-Propanol(1)-n-Hexane(2)
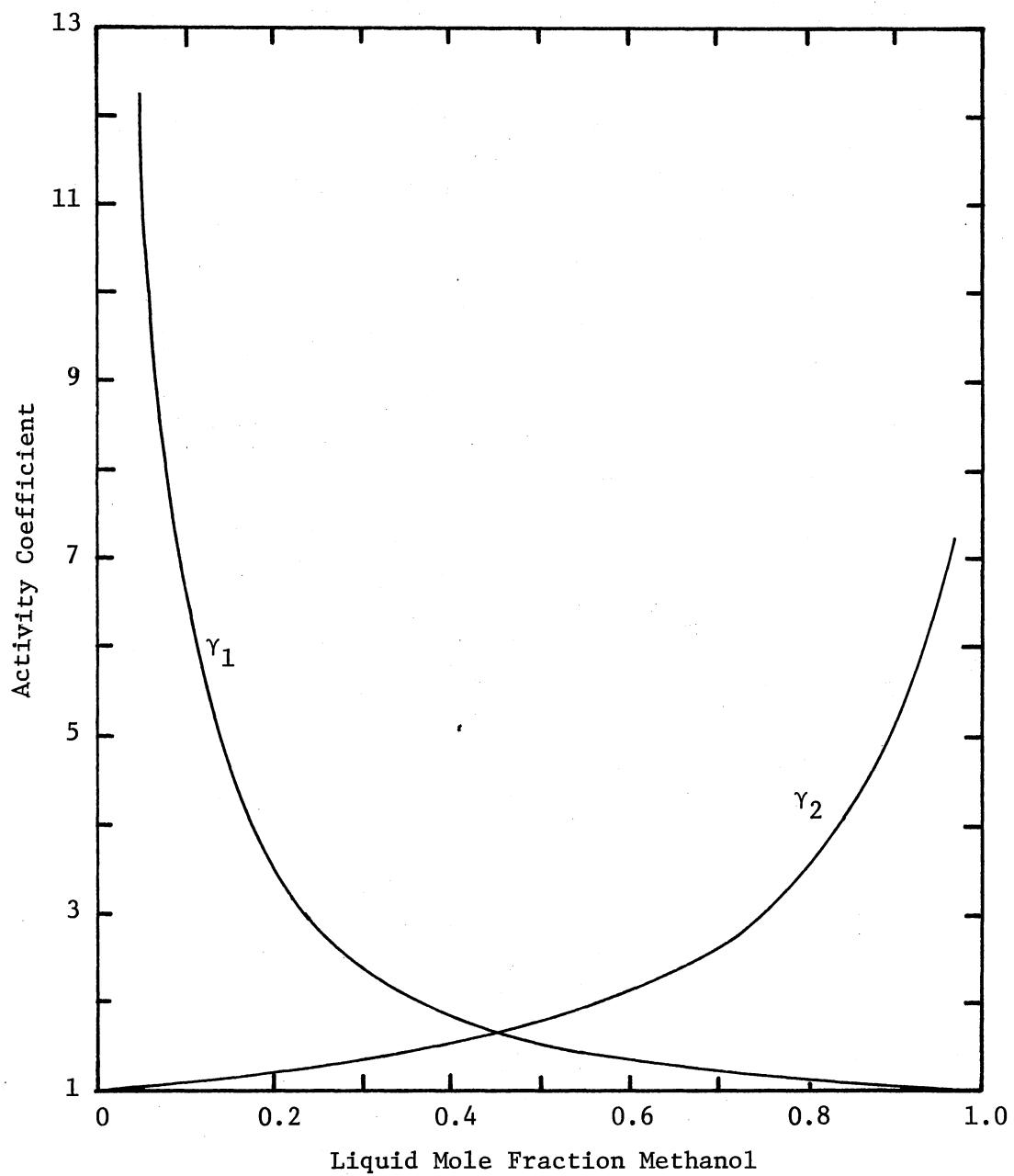
Figure 28. Activity Coefficients at 25°C for the
System Methanol(1)-Benzene(2)
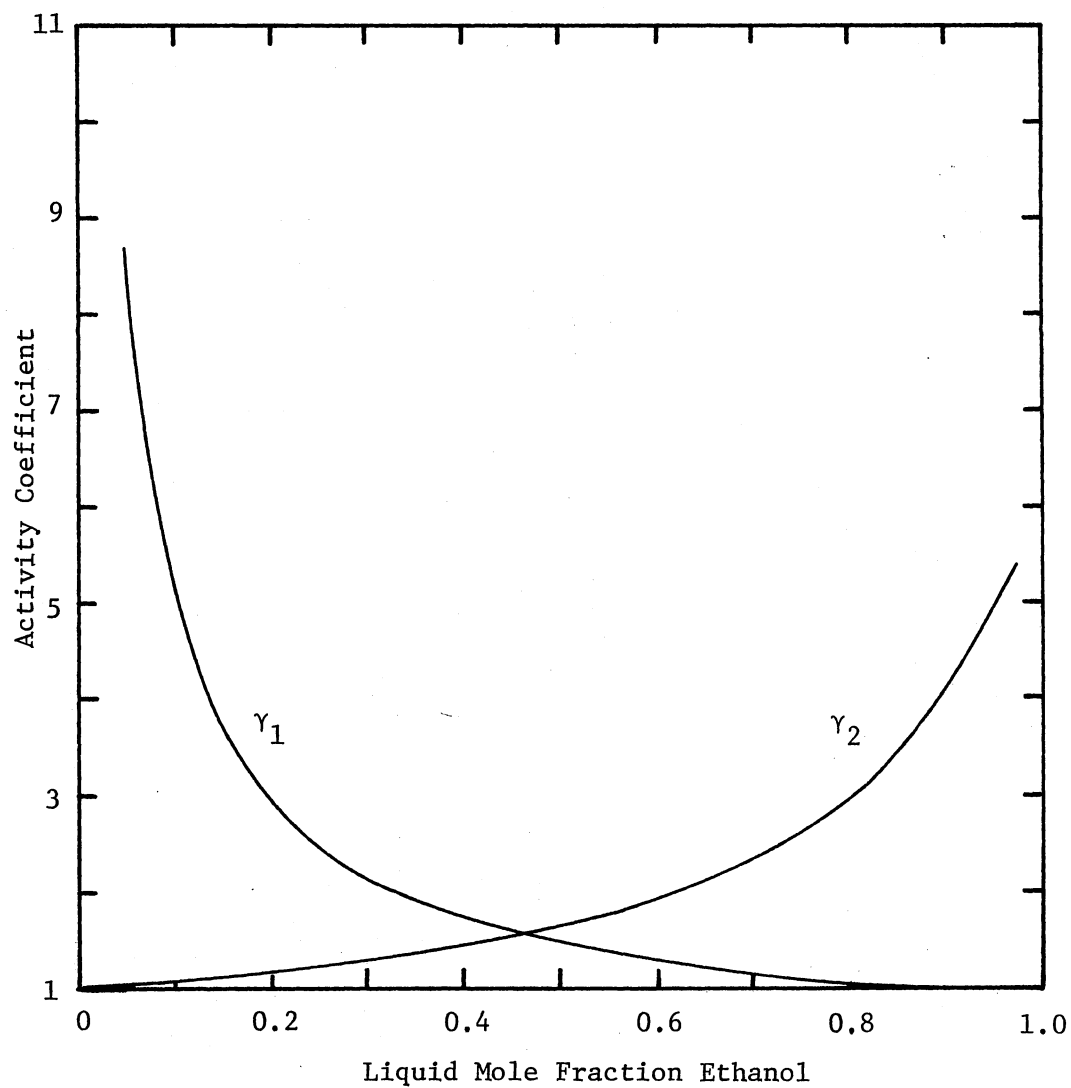
Figure 29.   Activity Coefficients at 25°C for the
System Ethanol(1)-Benzene(2)
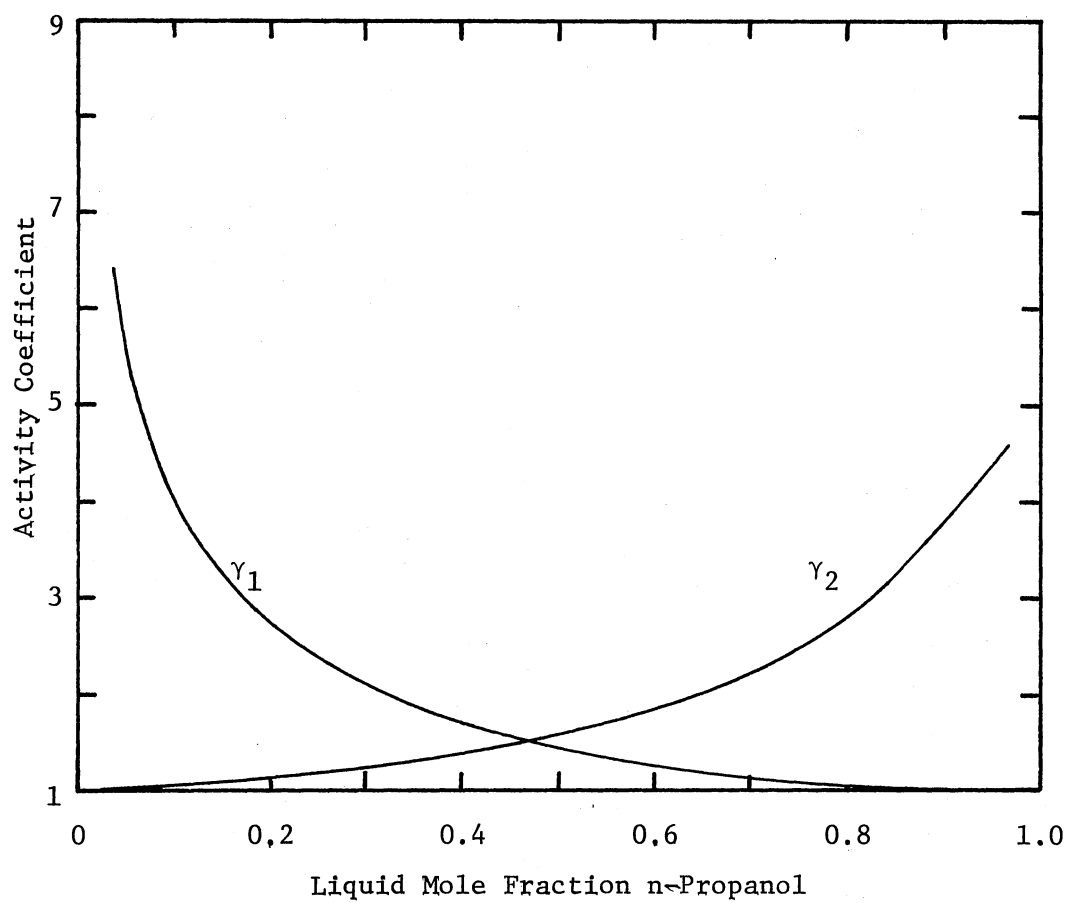
Figure 30. Activity Coefficients at 25°C for the
System n-Propanol(1)-Benzene(2)
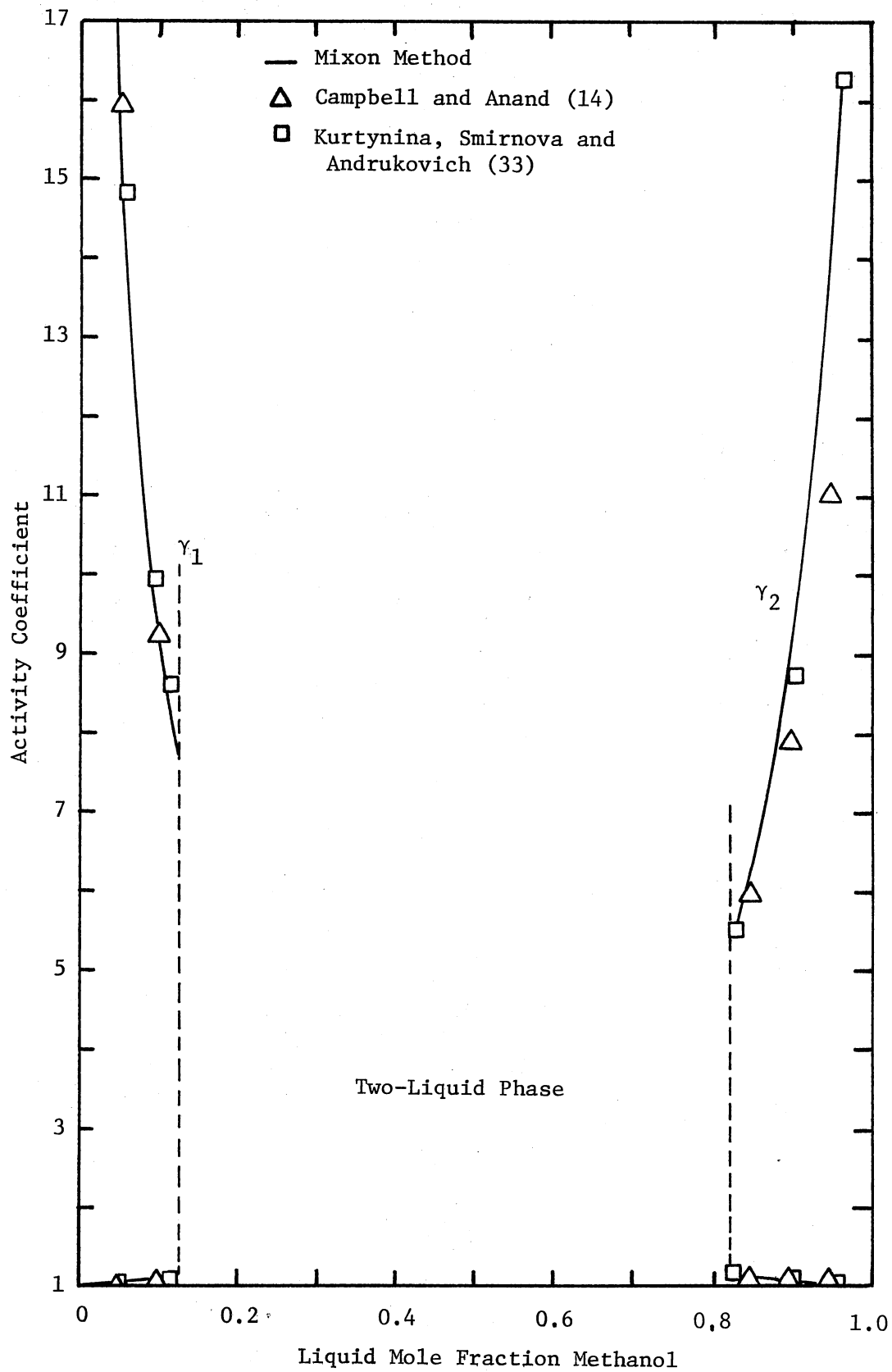
Figure 31. Activity Coefficients at 25°C for the
System Methanol(1)-Cyclohexane(2)
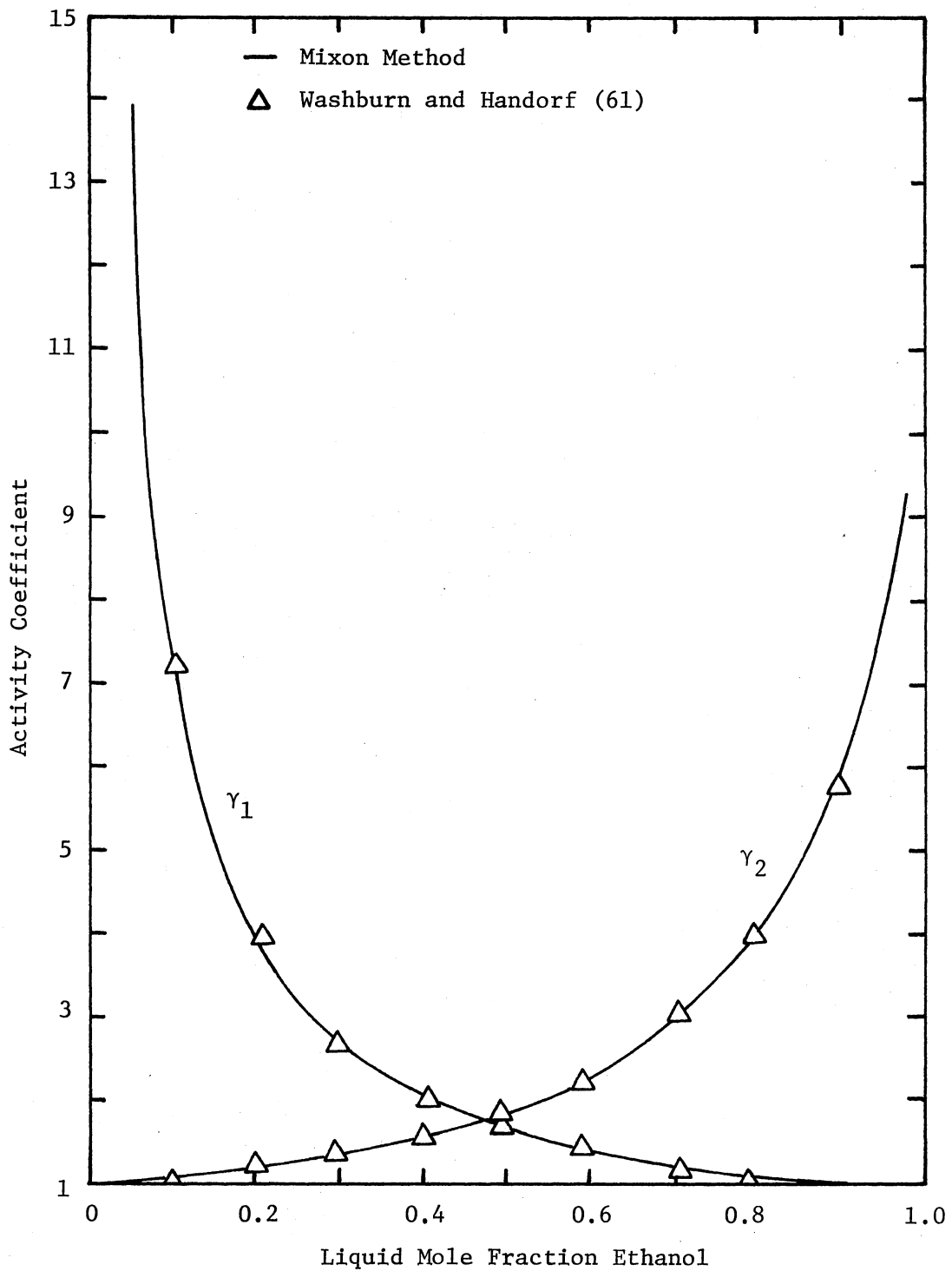
Figure 32. Activity Coefficients at $25^{\circ}C$ for
the System Ethanol(1)-
Cyclohexane(2)
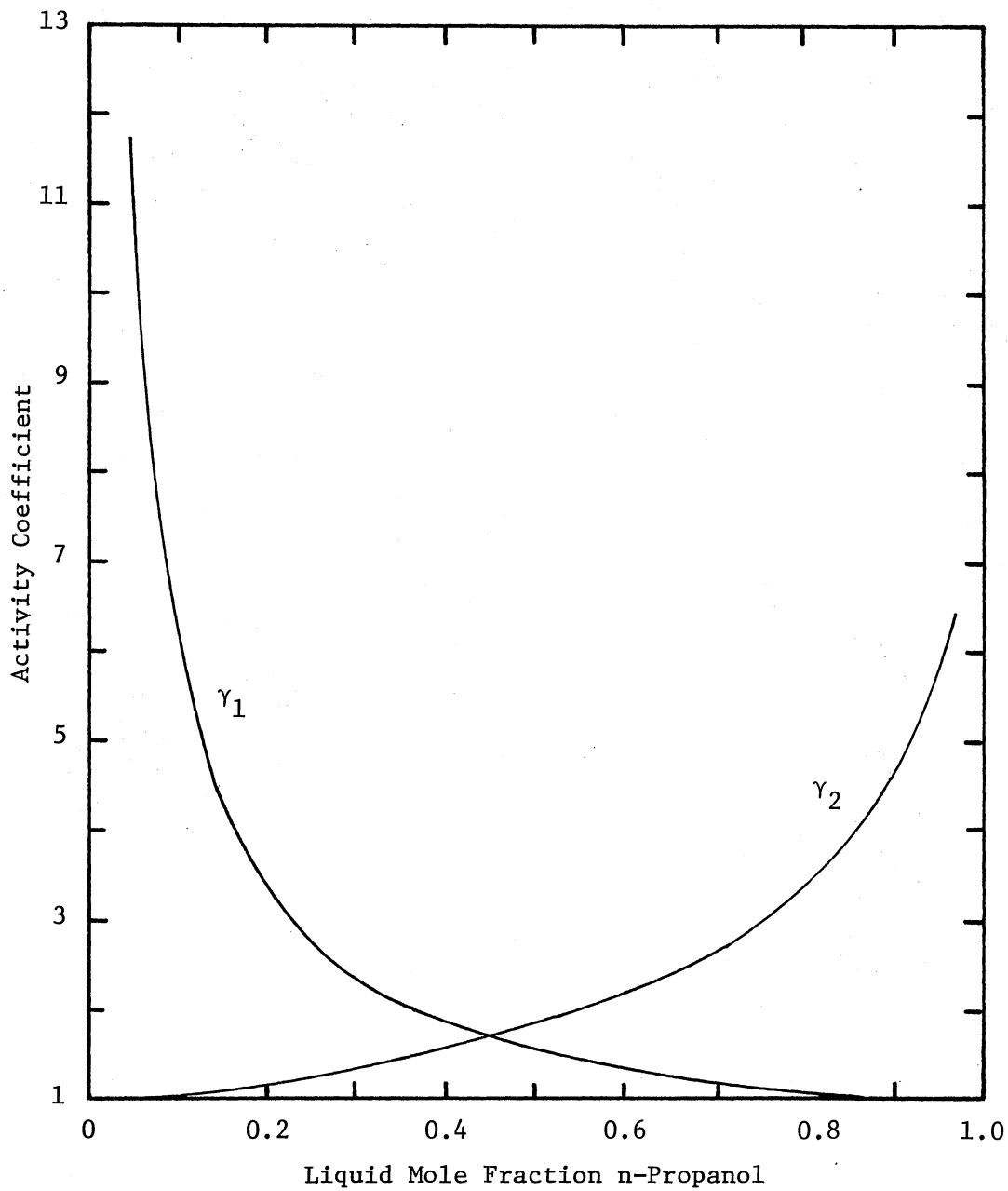
Figure 33. Activity Coefficients at $25^{\circ}C$ for the System n-Propanol(1)-Cyclohexane(2)
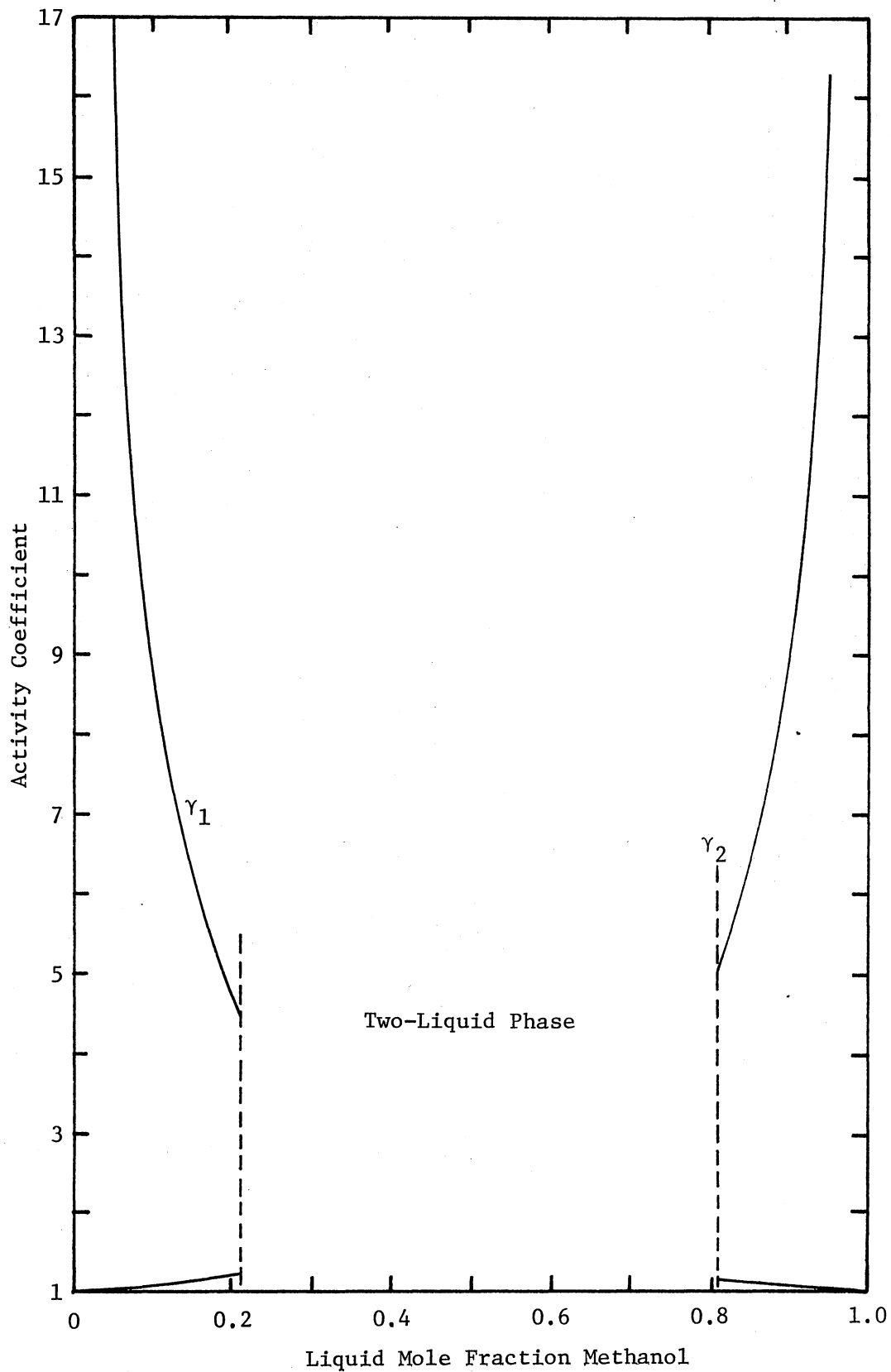
Figure 34. Activity Coefficients at $25^{\circ}C$ for the
System Methanol(1)-n-Hexane(2)
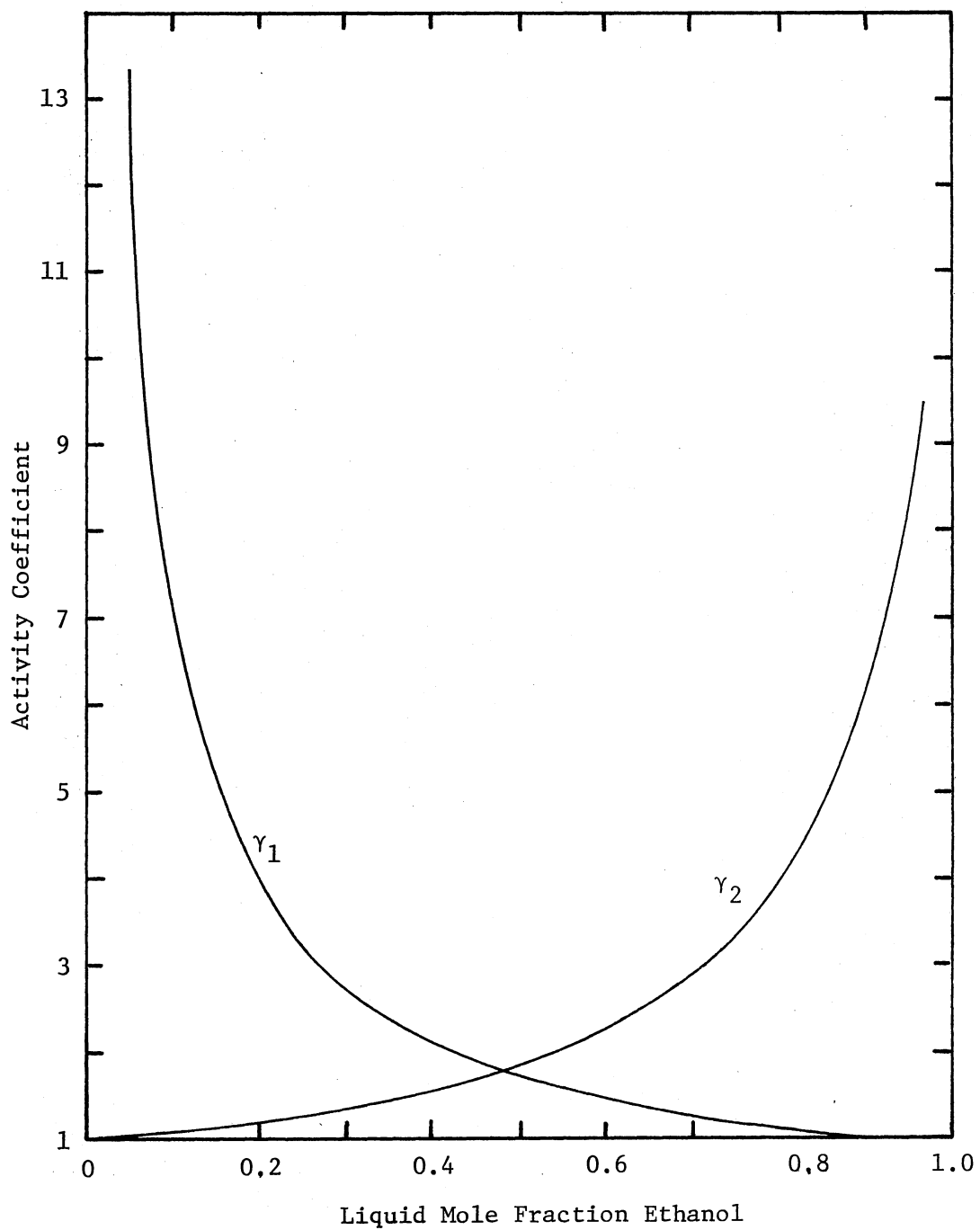
Figure 35. Activity Coefficients at $25^{\circ}C$ for the System Ethanol(1)-n-Hexane(2)
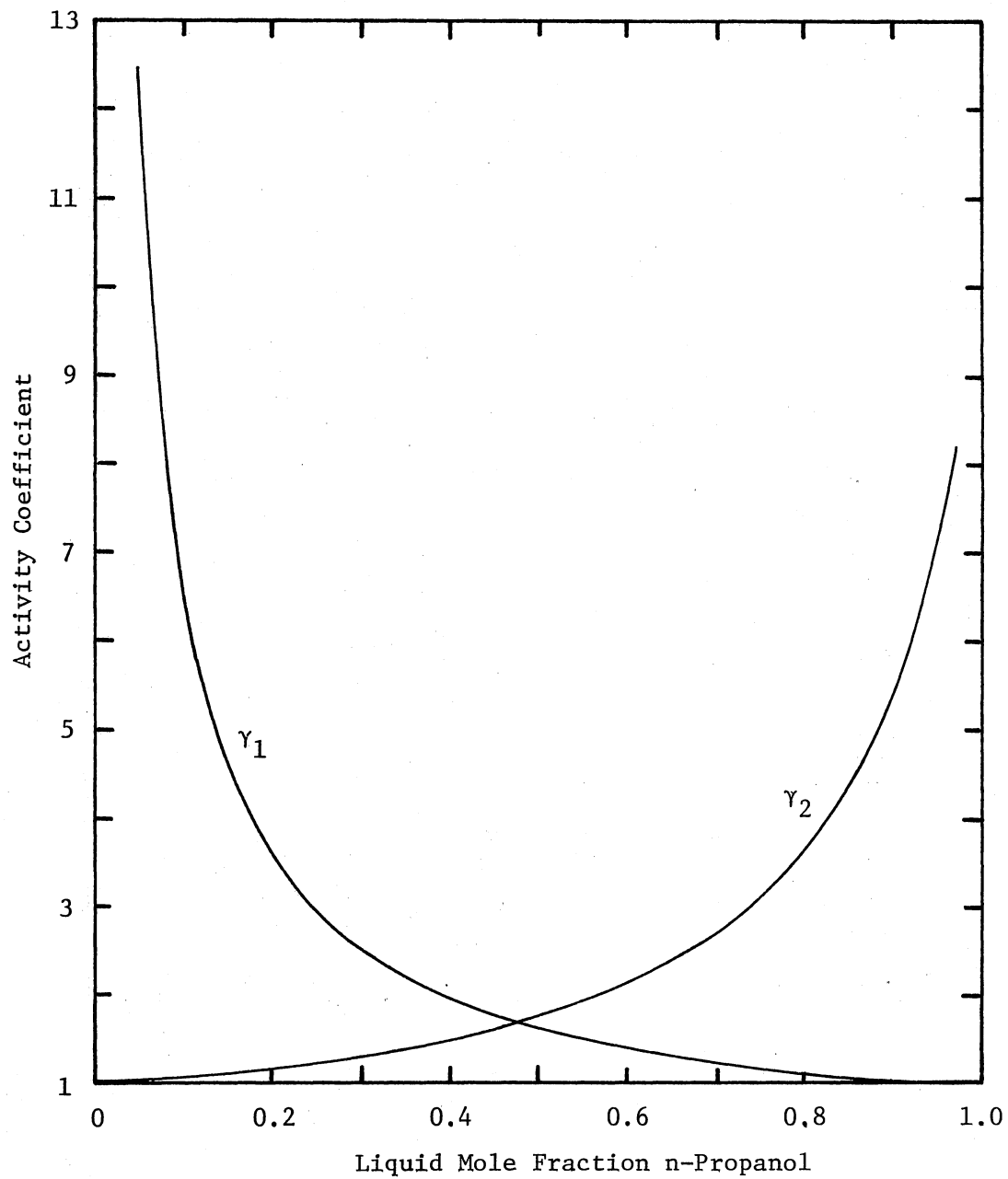
Figure 36. Activity Coefficients at $25^{\circ}C$ for the
System n-Propanol(1)-n-Hexane(2)

TABLE XXVII

AZEOTROPE COMPOSITION AT 25°C FOR EACH SYSTEM

System	Azeotrope Composition, Mole Fraction of Alcohol	
	This Work	Literature Value
Methanol-Benzene	0.539	NA[**]
Ethanol-Benzene	0.313	0.312 (51)
n-Propanol-Benzene	0.080	NA
Methanol-Cyclohexane	--[*]	--
Ethanol-Cyclohexane	0.340	0.336 (61)
n-Propanol-Cyclohexane	0.121	NA
Methanol-n-Hexane	--	--
Ethanol-n-Hexane	0.249	0.245 (51)
n-Propanol-n-Hexane	0.085	--

* No azetrope.
** Not available in literature.

on vapor pressure calculation was investigated. Results indicate that increase (or decrease) in the excess Gibbs free energy of 1% will result in an increase (or decrease) in the vapor pressure by a magnitude of 1 mmHg (by about 1% of vapor pressure).

Excess Thermodynamic Properties

The three excess thermodynamic properties--excess heat of mixing, excess Gibbs free energy and excess entropy--are related by the equation

$$G^E = H^E - TS^E \tag{VI-1}$$

If any two of these three excess properties are known, the third property can be calculated.

Values of the Gibbs free energy calculated by Mixon's method were combined with the heat of mixing data from the literature to calculate the temperature-excess entropy product, TS^E. Results of these calculations are presented in Tables XXVIII through XXXVI. This information is shown graphically in Figures 37 through 45.

These figures show that the typical properties of a mixture of a polar liquid with a non-polar liquid are:

1. Heat of mixing is positive with a miximum in a mixture dilute in the polar component, i.e., low concentration of alcohol.

2. Excess Gibbs free energy is positive and nearly symmetrical in composition.

3. The excess thermodynamic properties for the systems of alcohol-cyclohexane and alcohol-n-hexane are quite similar.

TABLE XXVIII

EXCESS THERMODYNAMIC PROPERTIES AT $25^{\circ}C$ FOR THE SYSTEM METHANOL(1)-BENZENE(2)

Liquid Mole Fraction x_1	Excess Gibbs Free Energy [*] G^E, cal/g-mole	Heat of Mixing [**] H^M, cal/g-mole	Excess Temperature-Entropy Product TS^E, cal/g-mole
0.10	142.8	136.0	-6.8
0.20	225.9	167.0	-58.9
0.30	274.3	171.5	-102.8
0.40	296.3	166.1	-130.2
0.50	296.5	148.6	-147.9
0.60	279.3	126.5	-152.8
0.70	245.2	100.0	-145.2
0.80	189.4	69.1	-120.3
0.90	108.8	35.8	-73.0

[*]   Calculated from P-x data by Mixon's method.

[**] Smoothed experimental data of Mrazek and Van Ness (37) and Vesely and Pick (60) and Brown, Fock and Smith (10).

TABLE XXIX

EXCESS THERMODYNAMIC PROPERTIES AT $25^{\circ}C$ FOR THE SYSTEM ETHANOL(1)-BENZENE(2)

Liquid Mole Fraction x_1	Excess Gibbs[*] Free Energy G^E, cal/g-mole	Heat of Mixing[**] H^M, cal/g-mole	Excess Temperature- Entropy Product TS^E, cal/g-mole
0.10	124.2	161.0	36.8
0.20	196.5	201.2	4.7
0.30	238.0	208.0	-30.0
0.40	260.5	204.0	-56.5
0.50	263.0	187.9	-75.1
0.60	248.0	153.0	-95.0
0.70	215.4	117.4	-98.0
0.80	165.6	80.0	-85.6
0.90	94.7	39.0	-55.4

*   Calculated from P-x data by Mixon's method.

**   Smoothed experimental data of Mrazek and Van Ness (37) and Brown, Fock and Smith (10).

TABLE XXX

EXCESS THERMODYNAMIC PROPERTIES AT $25^{\circ}C$ FOR THE SYSTEM N-PROPANOL(1)-BENZENE(2)

Liquid Mole Fraction x_1	Excess Gibbs Free Energy[*] G^E, cal/g-mole	Heat of Mixing[**] H^M, cal/g-mole	Excess Temperature-Entropy Product TS^E, cal/g-mole
0.10	103.4	174.0	70.6
0.20	171.9	229.8	57.9
0.30	213.7	248.4	34.7
0.40	235.9	245.9	10.0
0.50	240.7	224.5	-16.2
0.60	229.0	193.1	-35.9
0.70	201.0	150.5	-50.5
0.80	154.2	101.0	-53.2
0.90	87.3	51.6	-35.7

[*]   Calculated from P-x data by Mixon's method.

[**]   Smoothed experimental data of Mrazek and Van Ness (37) and Brown, Fock and Smith (10).

TABLE XXXI

EXCESS THERMODYNAMIC PROPERTIES AT $25^{\circ}C$ FOR THE SYSTEM METHANOL(1)-CYCLOHEXANE(2)

Liquid Mole Fraction x_1	Excess Gibbs Free Energy [*] G^E, cal/g-mole	Heat of Mixing [**] H^M, cal/g-mole	Excess Temperature-Entropy Product TS^E, cal/g-mole
0.05	95.1	65.0	-30.1
0.10	169.7	90.0	-79.0
0.85	216.4	115.0	-101.4
0.90	157.9	95.5	-62.4
0.95	88.6	63.1	-25.5

*   Calculated from P-x data by Mixon's method.

**   Smoothed experimental data of Kurtynina, Smirnova and Andrukovich (33).

TABLE XXXII

EXCESS THERMODYNAMIC PROPERTIES AT 25°C FOR THE SYSTEM ETHANOL(1)-CYCLOHEXANE(2)

Liquid Mole Fraction x_1	Excess Gibbs Free Energy[*] G^E, cal/g-mole	Heat of Mixing[**] H^M, cal/g-mole	Excess Temperature-Entropy Product TS^E, cal/g-mole
0.10	151.8	108.0	-43.8
0.20	242.3	141.5	-100.8
0.30	296.6	153.2	-143.4
0.40	325.2	156.7	-168.5
0.50	331.6	153.3	-178.3
0.60	315.3	142.5	-172.8
0.70	276.6	125.1	-151.5
0.80	213.4	99.8	-113.6
0.90	122.3	61.2	-61.1

[*]   Calculated from P-x data by Mixon's method.

[**]   Smoothed experimental data of Goates, Snow and James (23) and Vesely and Pick (60).

TABLE XXXIII

EXCESS THERMODYNAMIC PROPERTIES AT $25^{\circ}C$ FOR THE SYSTEM N-PROPANOL(1)-CYCLOHEXANE(2)

Liquid Mole Fraction x_1	Excess Gibbs Free Energy[*] G^E, cal/g-mole	Heat of Mixing[**] H^M, cal/g-mole	Excess Temperature-Entropy Product TS^E, cal/g-mole
0.10	142.8	97.3	−45.5
0.20	222.2	126.0	−96.2
0.30	269.3	140.1	−129.2
0.40	293.0	141.3	−151.7
0.50	295.5	134.0	−161.5
0.60	278.0	118.7	−159.3
0.70	240.5	94.9	−145.6
0.80	182.4	69.3	−113.1
0.90	104.2	38.0	−66.2

*   Calculated from P-x data by Mixon's method.

**   Smoothed experimental data of Vesely and Pick (60).

TABLE XXXIV

EXCESS THERMODYNAMIC PROPERTIES AT 25°C FOR THE SYSTEM METHANOL(1)-N-HEXANE(2)

Liquid Mole Fraction x_1	Excess Gibbs Free Energy G^E, cal/g-mole [*]	Heat of Mixing [**] H^M, cal/g-mole	Excess Temperature-Entropy Product TS^E, cal/g-mole
0.05	93.8	73.9	-19.9
0.10	167.7	92.5	-75.2
0.15	220.2	106.1	-114.1
0.20	269.1	115.7	-153.4
0.85	221.3	98.7	-122.6
0.90	162.5	77.9	-84.6
0.95	93.5	46.9	-46.6

[*]   Calculated from P-x data by Mixon's method.

[**]   Smoothed experimental data of Savini, Winterhalter and Van Ness (45).

115

TABLE XXXV

EXCESS THERMODYNAMIC PROPERTIES AT 25°C FOR THE SYSTEM ETHANOL(1)-N-HEXANE(2)

Liquid Mole Fraction x_1	Excess Gibbs* Free Energy G^E, cal/g-mole	Heat of Mixing** H^M, cal/g-mole	Excess Temperature- Entropy Product TS^E, cal/g-mole
0.10	149.8	101.5	-48.3
0.20	239.4	126.4	-113.0
0.30	295.8	136.4	-159.4
0.40	326.1	138.0	-188.1
0.50	332.4	133.0	-199.4
0.60	316.3	122.0	-194.3
0.70	277.5	106.0	-171.5
0.80	214.8	82.0	-132.8
0.90	124.7	48.0	-76.7

*   Calculated from P-x data by Mixon's method.

**   Smoothed experimental data of Jones and Lu (30) and Brown, Fock and Smith (9).

TABLE XXXVI

EXCESS THERMODYNAMIC PROPERTIES AT 25°C FOR THE SYSTEM N-PROPANOL(1)-N-HEXANE(2)

Liquid Mole Fraction x_1	Excess Gibbs[*] Free Energy G^E, cal/g-mole	Heat of Mixing[**] H^M, cal/g-mole	Excess Temperature- Entropy Product TS^E, cal/g-mole
0.10	144.4	97.0	-47.4
0.20	227.4	134.7	-92.7
0.30	278.5	145.4	-133.1
0.40	304.8	146.6	-158.2
0.50	309.5	137.5	-172.0
0.60	293.9	120.6	-173.3
0.70	257.6	99.5	-158.1
0.80	199.1	72.8	-126.3
0.90	116.3	40.0	-76.3

*   Calculated from P-x data by Mixon's method.

**   Smoothed experimental data of Brown, Fock and Smith (9).
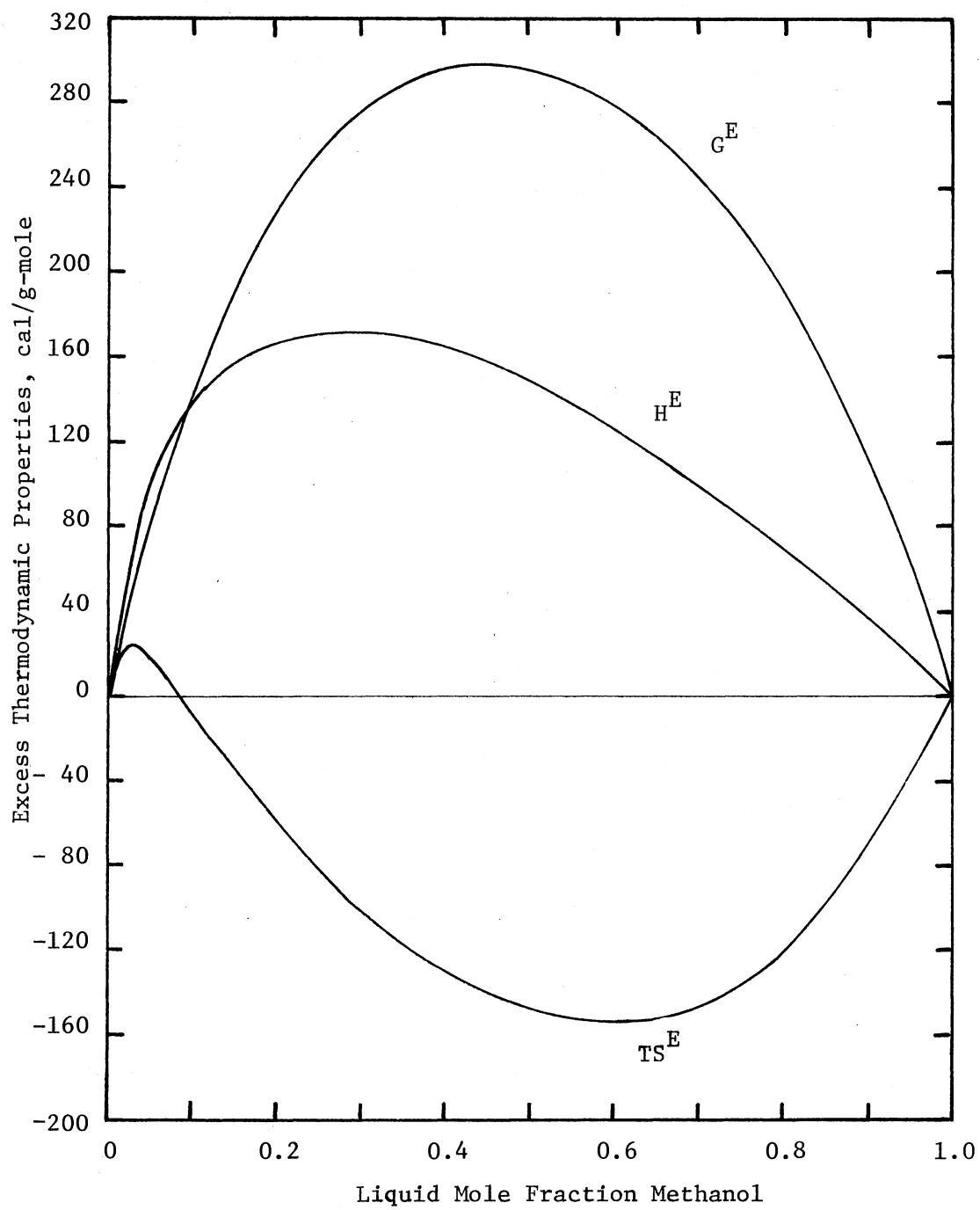
Figure 37. Excess Thermodynamic Properties at 25°C for
the System Methanol(1)-Benzene(2)
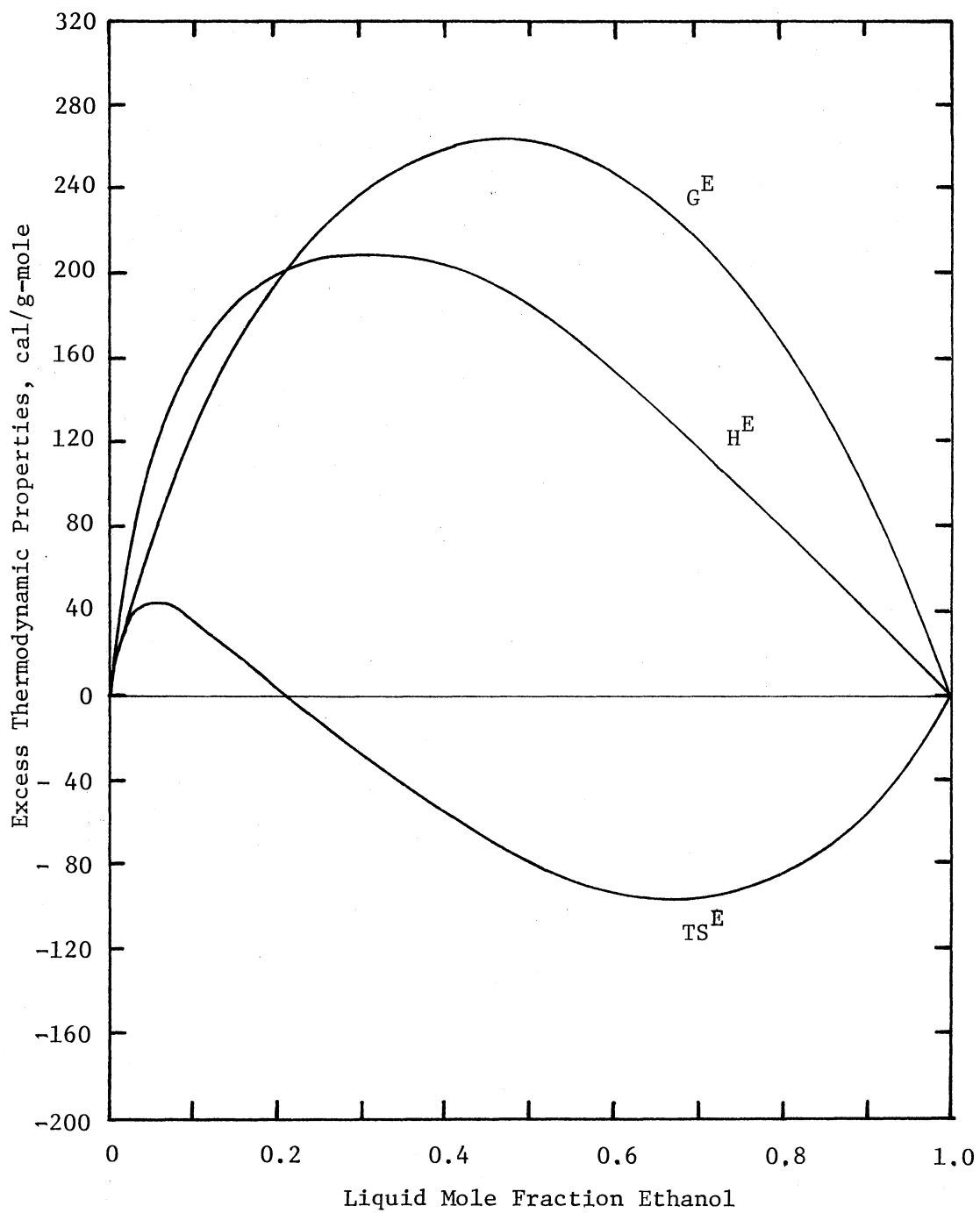
Figure 38. Excess Thermodynamic Properties at 25°C for
the System Ethanol(1)-Benzene(2)
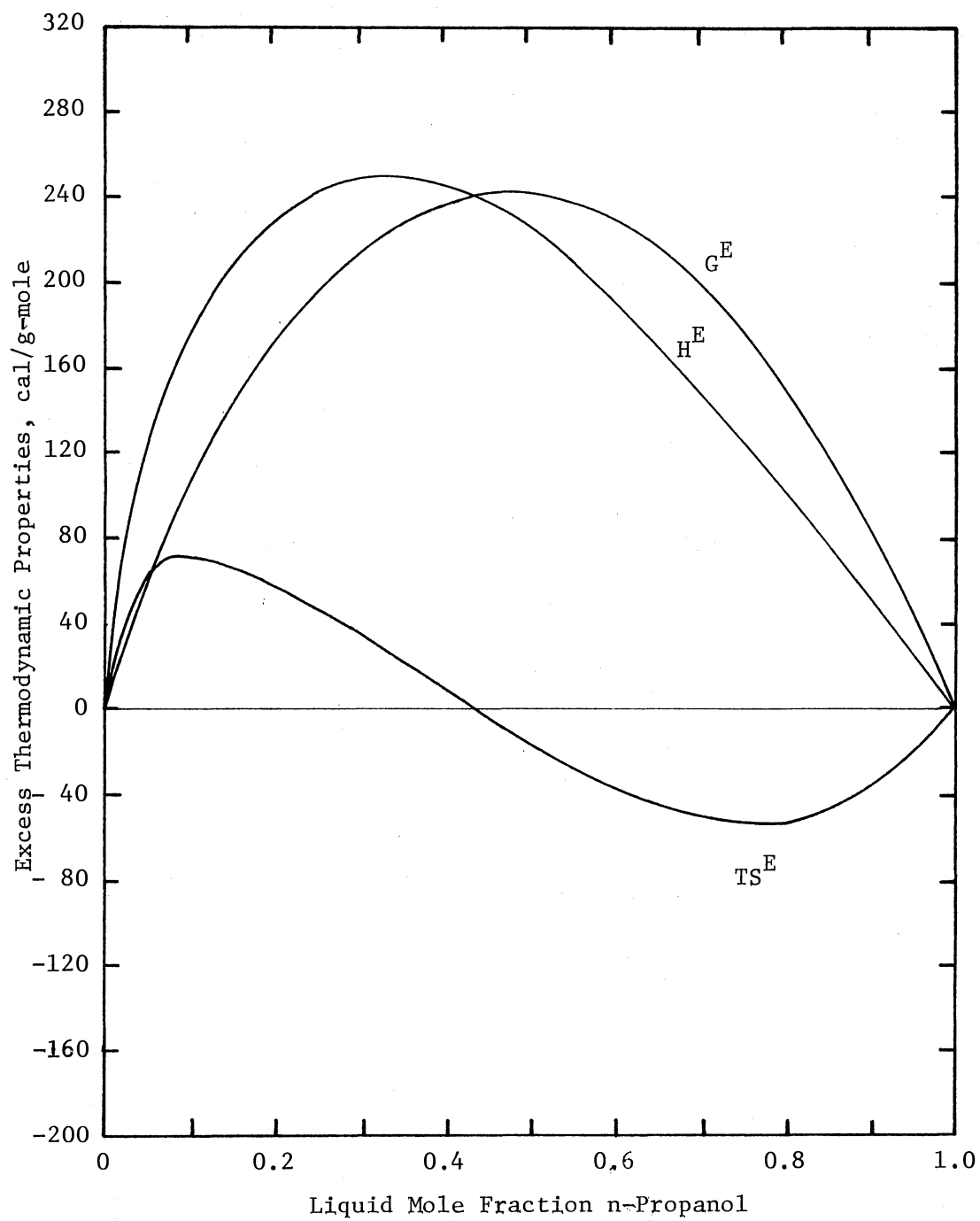
Figure 39. Excess Thermodynamic Properties at 25°C for the System n-Propanol(1)-Benzene(2)
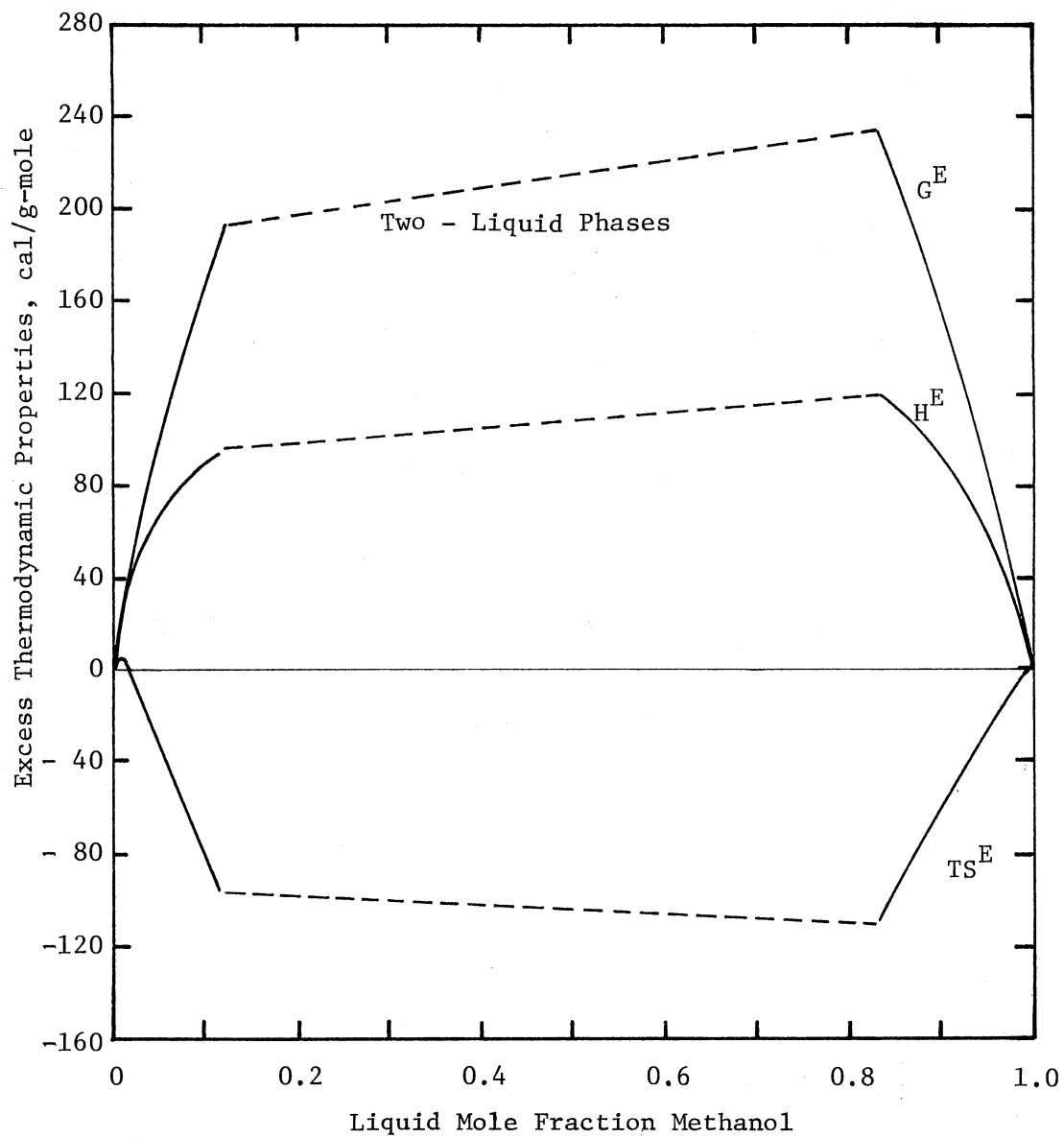
Figure 40. Excess Thermodynamic Properties at
25°C for the System Methanol(1)-
Cyclohexane(2)
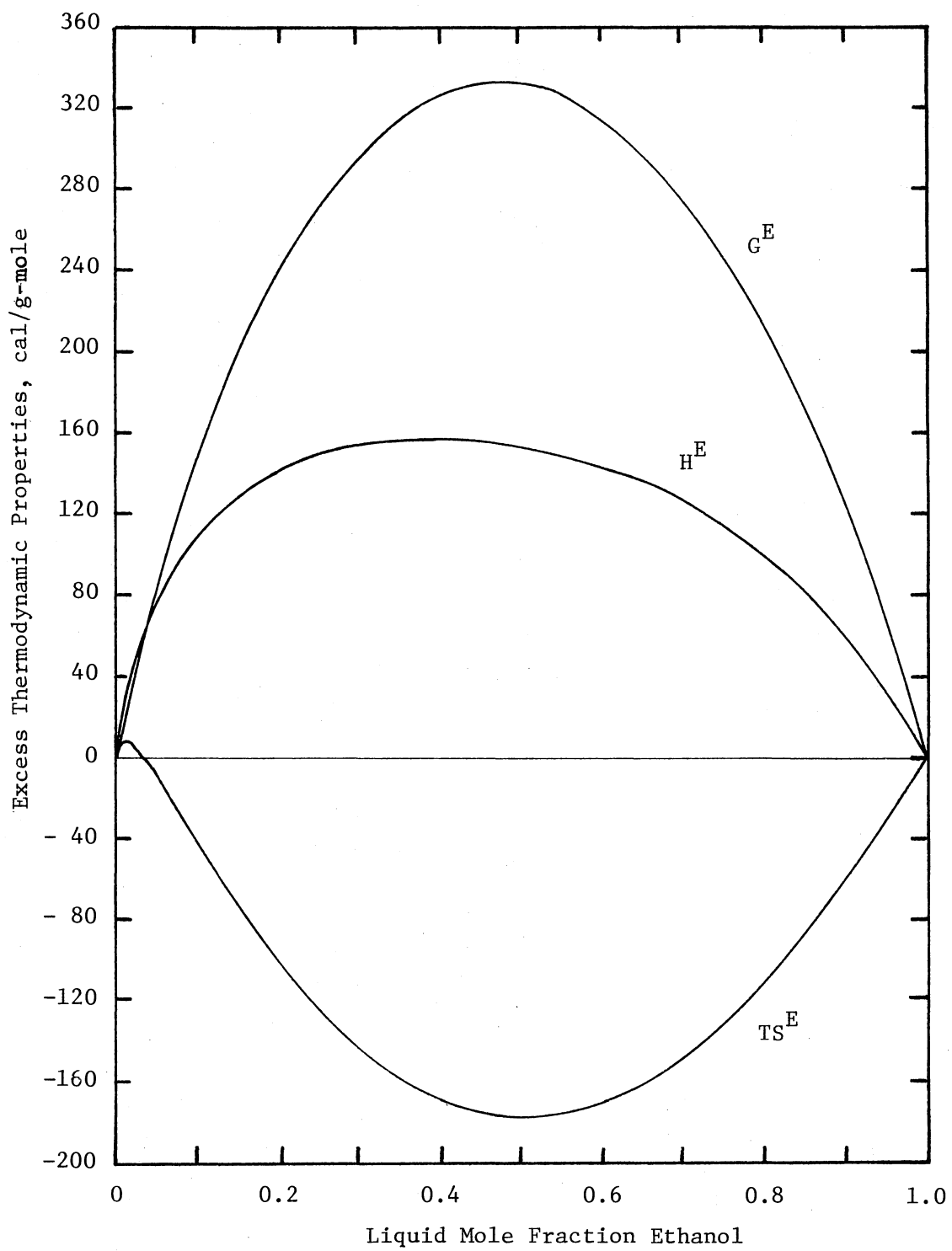
Figure 41. Excess Thermodynamic Properties
at 25°C for the System Ethanol
(1)-Cyclohexane(2)
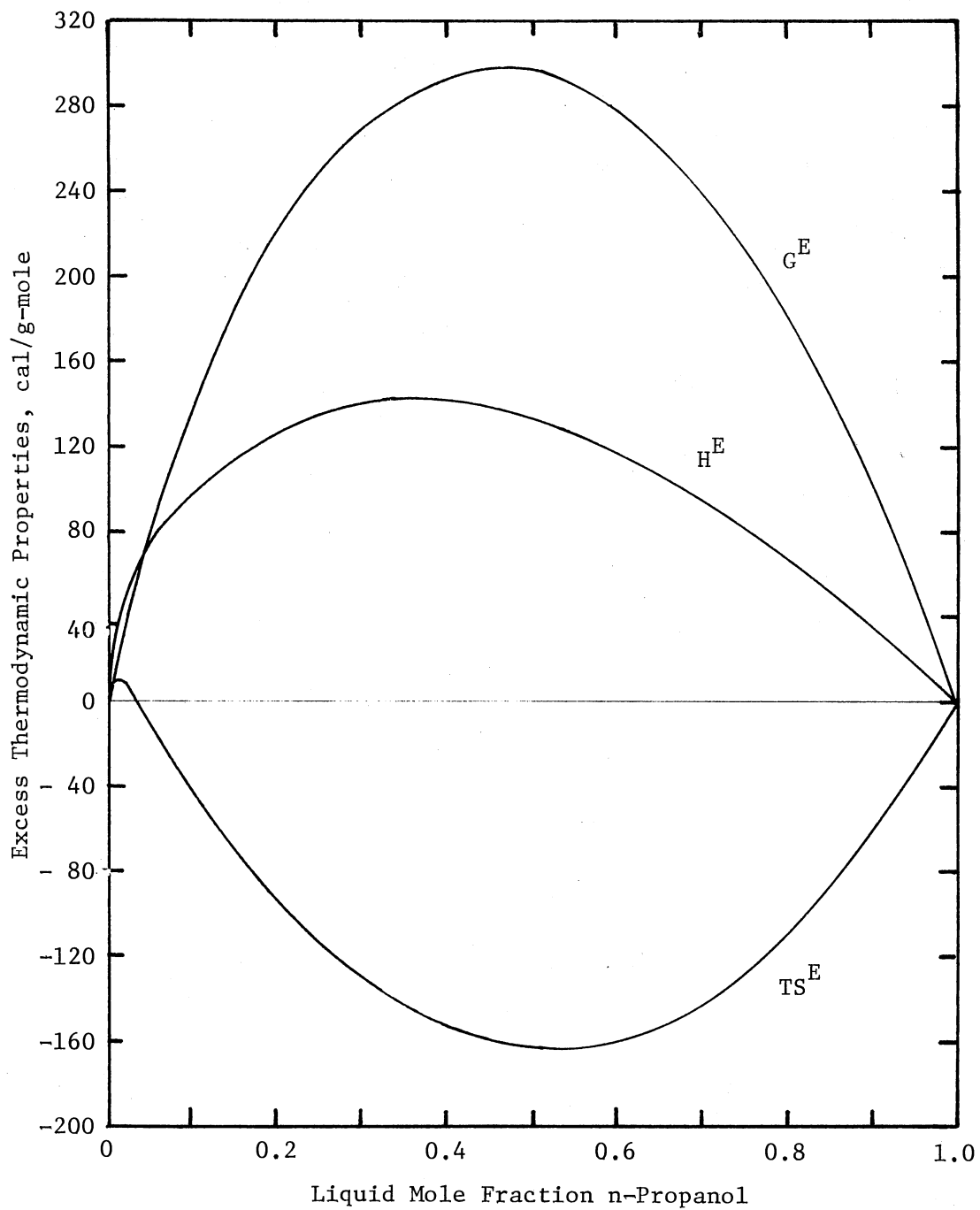
Figure 42. Excess Thermodynamic Properties at 25°C
for the System n-Propanol(1)-
Cyclohexane(2)
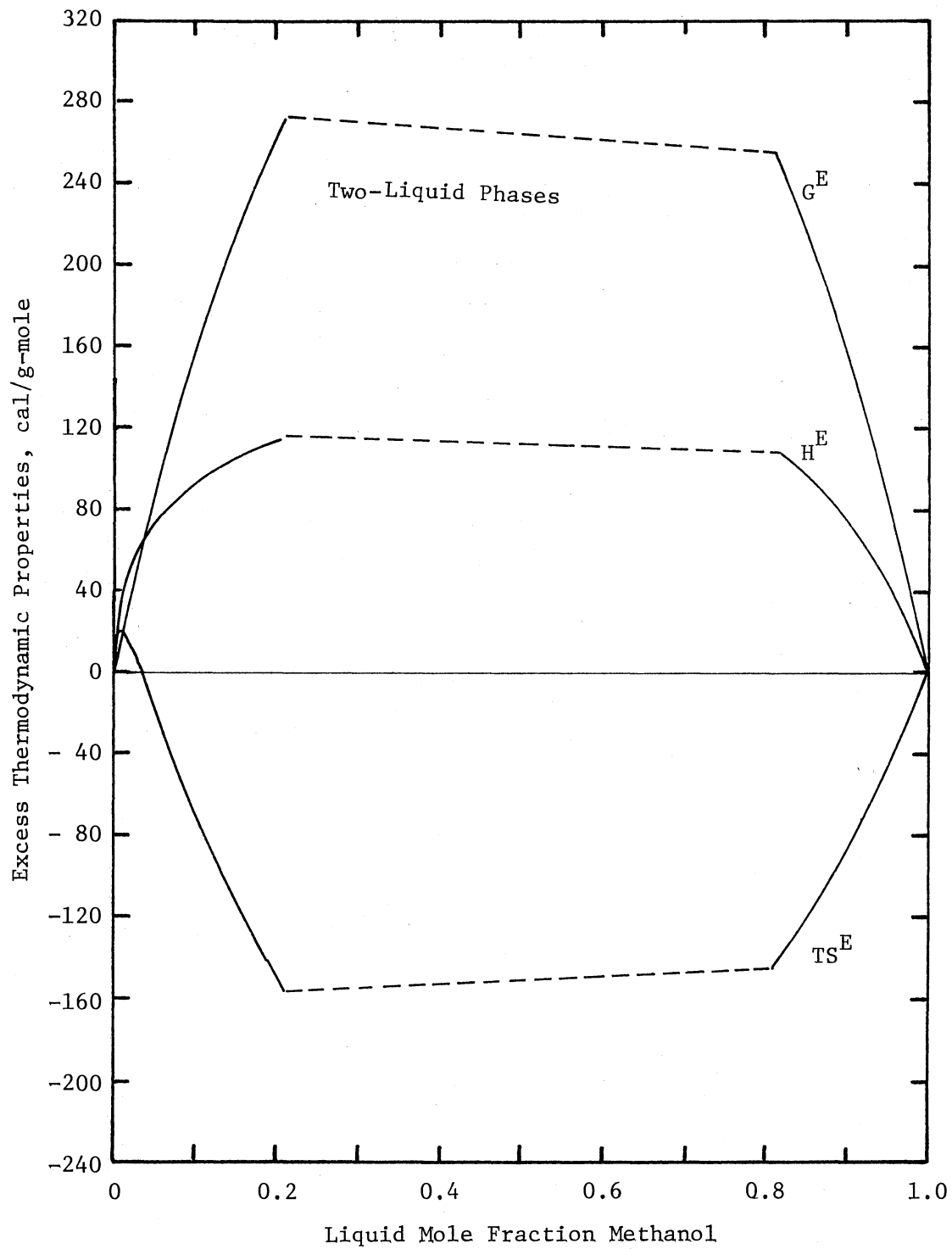
Figure 43. Excess Thermodynamic Properties at 25°C
for the System Methanol(1)-
n-Hexane(2)
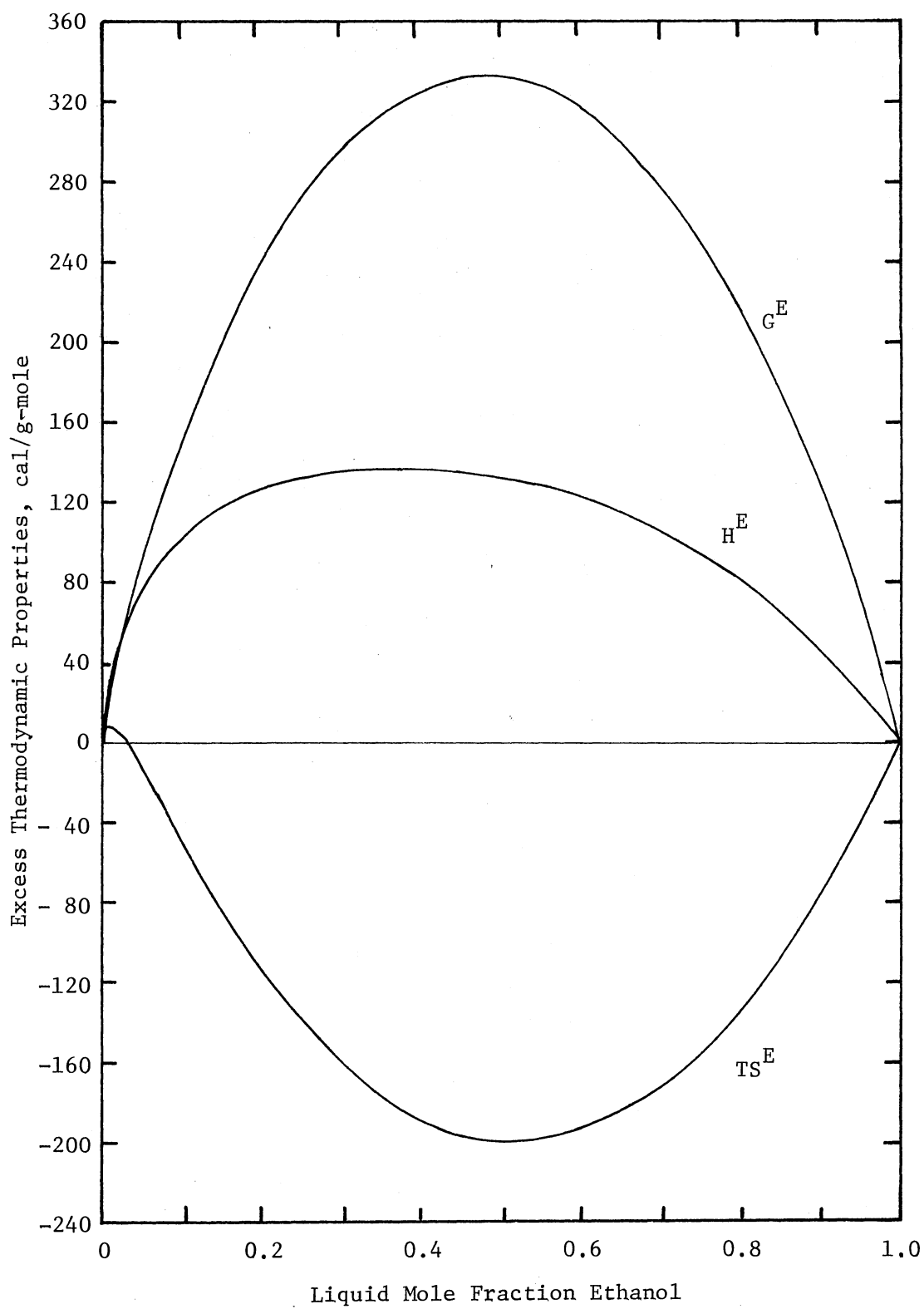
Figure 44. Excess Thermodynamic Properties at 25°C
for the System Ethanol(1)-n-Hexane(2)
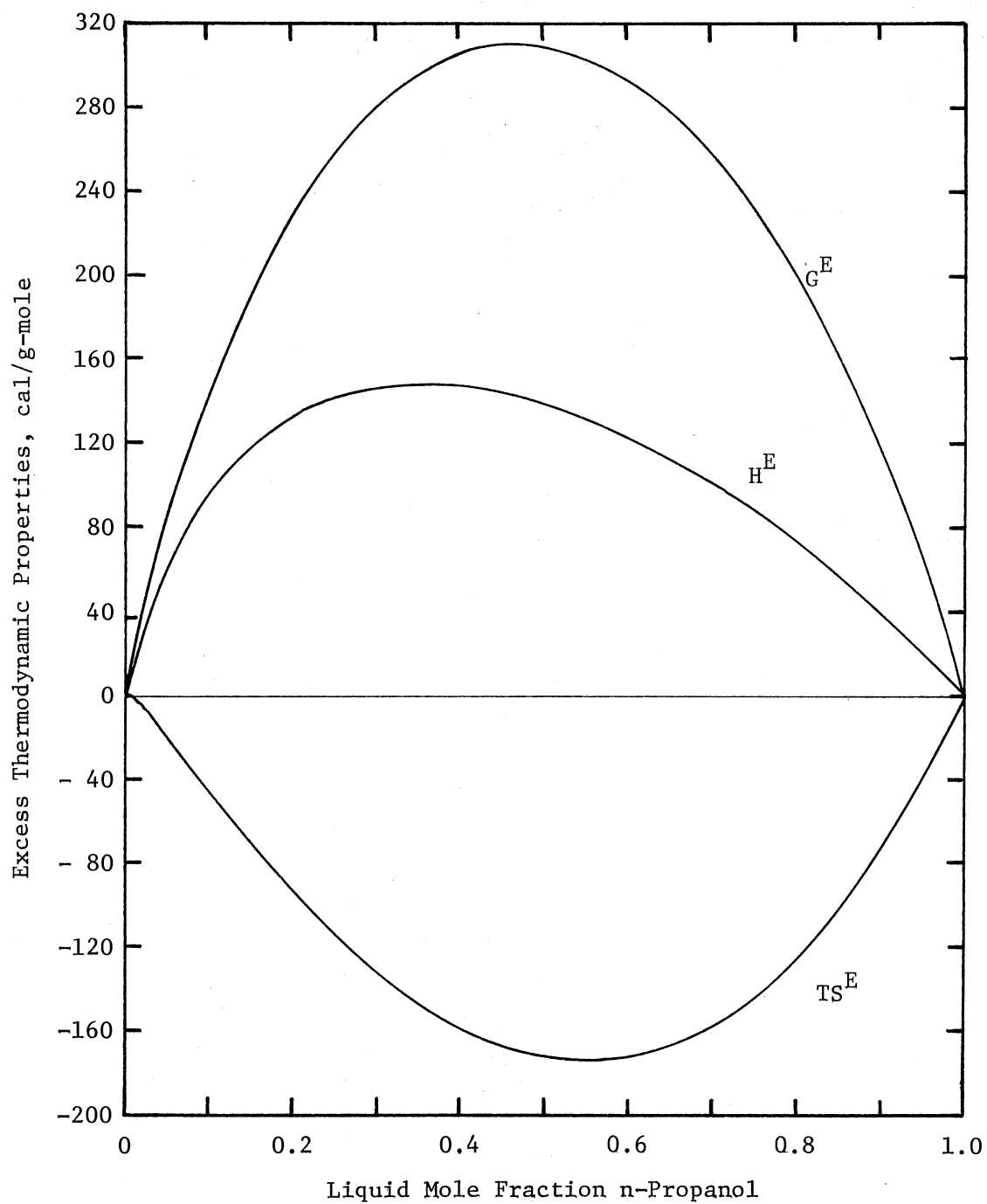
Figure 45. Excess Thermodynamic Properties at 25°C
for the System n-Propanol(1)-n-Hexane(2)

4. The temperature-excess entropy product is negative, except
    at low concentrations of alcohol, with a minimum in a mix-
    ture rich in the polar component, i.e., high concentration
    of alcohol. The positive temperature-excess entropy products
    shown at low concentration of alcohol are due to the loss
    of orientation order that must follow the breaking of the
    hydrogen bonds. Since this breaking of hydrogen bonds is
    purely due to a dilution effect, the TS^E value will become
    negative with increasing concentration of alcohol.

5. The binary systems of alcohol-benzene have higher heats of
    mixing and excess entropies and lower excess Gibbs free
    energies than those of alcohols with cyclohexane or n-hexane.
    This behavior is due to a more favorable energy interaction
    between a hydroxyl group and the more polarizable electrons
    of an aromatic molecule than with the less polarizable
    electrons of a saturated molecule. This interaction leads
    to the breaking of more hydrogen bonds and to a considerably
    larger and positive values of excess entropy of the systems
    of alcohol-benzene.

Comparison with Literature Data

Comparisons of the results from this study with those reported
in the literature are discussed in this section. The first part is a
direct comparison, i.e., the present data are compared with the avail-
able data in the literature at 25°C. The second part is an indirect
comparison in which the present data are compared for mutual

consistency with the available data in the literature at temperatures other than 25°C.

Direct Comparison

For the system methanol-benzene, only one VLE data point at 25°C is reported by Scatchard and coworkers (48). As indicated in the P-x diagram (Figure 6) and y-x diagram (Figure 19), the agreement between these two data is excellent.

The systems of ethanol-benzene and ethanol-n-hexane at 25°C have been investigated by Smith and Robinson (51). For both systems, the vapor pressures presented by this study are about 3 mmHg higher at 0.9 liquid mole fraction of ethanol. For the ethanol-benzene system at 0.5 liquid mole fraction, the vapor pressure reported by the present author is about 2 mmHg lower than that reported by Smith and Robinson.

The phase equilibrium in the system of methanol-cyclohexane has been studied by Campbell and Anand (14), and by Kurtynina, Smirnova and Andrukovich (33). However, no experimental P-x data are reported in Campbell's paper. Figure 22 shows that the y-x curve calculated from present P-x data by Mixon's method differs significantly from either set of experimental data.

The VLE data at 25°C for the system ethanol-cyclohexane are reported by Washborn and Handorf (61). Figure 10 shows considerable disagreement in the two sets of experimental P-x data between 0.6-1.0 mole fraction of ethanol. This may be caused by the large difference of pure component vapor pressure of ethanol. They indicated that the vapor pressure of pure ethanol at 25°C was about 3% low (compared with the vapor pressures from the present study and literature values).

The above error was not due to impurities in the ethanol. It may be caused by the method and apparatus used for measuring vapor pressures. The dynamic method was employed by Washborn to determine the total vapor pressures. Initially, the vapor pressures on alcohol rich mixtures and on pure ethanol were measured using a mixture of solid carbon dioxide and ether as condensing medium. Several attempts were also made to improve the vapor pressure measurement of alcohol by substituting liquid air and sulfuric acid, respectively, for the carbon dioxide-ether mixture as the condensing medium. In each case the vapor pressures of pure ethanol were practically the same and were about 3% low. However, the values obtained by the Smith-Menzies isoteniscope method agreed very well with the literature values.

Indirect Comparison

Two different approaches that can be used for indirect comparison of literature data at different temperature have been discussed by Smith (50). Only the rigorous approach will be adopted in this study.

As shown by Van Ness (55), the Gibbs-Duhem equation may be integrated at constant composition to yield

$$(G^E/T)_{T_2} = (G^E/T)_{T_1} - \int_{T_1}^{T_2} (H^M/T^2)dT + \int_{P_1}^{P_2} (V^M/T)dP \tag{VI-2}$$

For the systems studied, the last term on the right-hand side can be neglected (50). Equation VI-2 may be simplified to

$$(G^E/T)_{T_2} = (G^E/T)_{T_1} - \int_{T_1}^{T_2} (H^M/T^2)dT \tag{VI-3}$$

Equally spaced values of G^E at T_2 were evaluated by Equation VI-3 from the present 25^oC G^E data and from heat of mixing data available in the literature. The G^E-x data at T_2 were then used as input data in Mixon's method for calculation of vapor pressures and vapor mole fractions. Sufficient heat of mixing data were available for this calculation in the systems of methanol-benzene, ethanol-benzene, n-propanol-benzene, ethanol-n-hexane and n-propanol-n-hexane. (See Table I).

Instead of graphically integrating H^M/T^2 from 25^oC to a higher temperature T_2, the values of H_M/T^2 were fitted as a function of T as follows:

$$H^M/T^2 = a_o + a_1/T \qquad \text{(VI-4)}$$

where the constants a_o and a_1 are determined by statistical methods. Substituting Equation VI-4 into Equation VI-3 gives

$$(G^E/T)_{T_2} = (G^E/T)_{T_1} = 298.16k - a_o (T_2 - 298.16)$$

$$\text{(VI-5)}$$

$$- a_1 \ln (T_2/298.16)$$

VLE data for the system methanol-benzene are reported by Scatchard, Wood and Mochel (48) at 35 and 55^oC, and by Lee (34) at 40^oC. Predicted VLE data are compared with smoothed experimental data in Tables XXXVII, XXXVIII and XXXIX. Graphical comparisons are shown in Figures 46, 47 and 48 for P-x data, and in Figures 49, 50 and 51 for y-x data. Results in Tables XXXVII and XXXIX. and in Figures 46 and 48 show that, at either low or high methanol concentrations, the predicted vapor pressures are higher than Scarchard's experimental values. The

TABLE XXXVII

PREDICTED AND EXPERIMENTAL VLE DATA AT 35°C FOR THE SYSTEM METHANOL(1)-BENZENE(2)

Liquid Mole Fraction x_1	Vapor Pressure, mmHg		Vapor Mole Fraction, y_1	
	Predicted	Experimental Data*	Predicted	Experimental Data*
0.10	282.9	267.0	0.498	0.462
0.20	286.7	284.1	0.511	0.512
0.30	288.7	288.0	0.520	0.529
0.40	290.4	290.0	0.530	0.540
0.50	292.0	292.0	0.549	0.555
0.60	292.4	292.0	0.578	0.571
0.70	290.8	290.0	0.607	0.599
0.80	285.5	282.2	0.641	0.644
0.90	267.6	262.0	0.721	0.735

* Smoothed experimental data of Scatchard, Wood and Mochel (48).

TABLE XXXVIII

PREDICTED AND EXPERIMENTAL VLE DATA AT 40°C FOR THE SYSTEM METHANOL(1)-BENZENE(2)

Liquid Mole Fraction x_1	Vapor Pressure, mmHg		Vapor Mole Fraction, y_1	
	Predicted	Experimental Data*	Predicted	Experimental Data*
0.10	348.3	338.2	0.495	0.485
0.20	355.7	356.9	0.513	0.520
0.30	358.9	361.7	0.523	0.531
0.40	361.3	364.4	0.534	0.538
0.50	363.5	365.9	0.554	0.550
0.60	364.2	366.0	0.583	0.560
0.70	362.4	363.5	0.612	0.575
0.80	356.0	352.0	0.646	0.612
0.90	334.3	325.3	0.725	0.710

* Smoothed experimental data of Lee (34).

TABLE XXXIX

PREDICTED AND EXPERIMENTAL VLE DATA AT 55°C FOR THE SYSTEM METHANOL(1)-BENZENE(2)

Liquid Mole Fraction x_1	Vapor Pressure, mmHg		Vapor Mole Fraction, y_1	
	Predicted	Experimental Data*	Predicted	Experimental Data*
0.10	624.3	594.0	0.496	0.480
0.20	654.7	640.0	0.529	0.526
0.30	664.9	660.0	0.544	0.548
0.40	671.6	669.0	0.557	0.565
0.50	677.7	676.0	0.578	0.582
0.60	681.2	678.0	0.608	0.608
0.70	679.9	676.3	0.638	0.638
0.80	670.2	664.0	0.672	0.674
0.90	634.7	623.0	0.748	0.752

* Smoothed experimental data of Scatchard, Wood and Mochel (48).
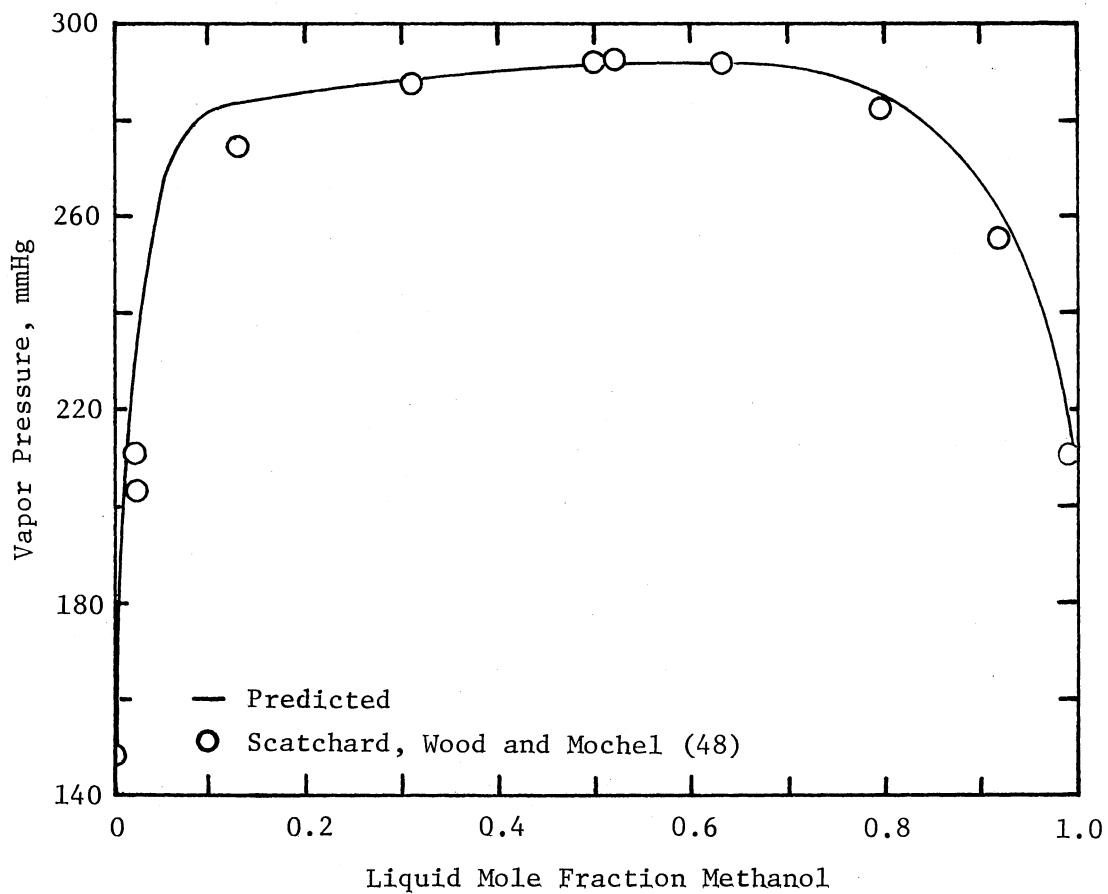
Figure 46. Vapor Pressure at 35°C for the System
Methanol(1)-Benzene(2)
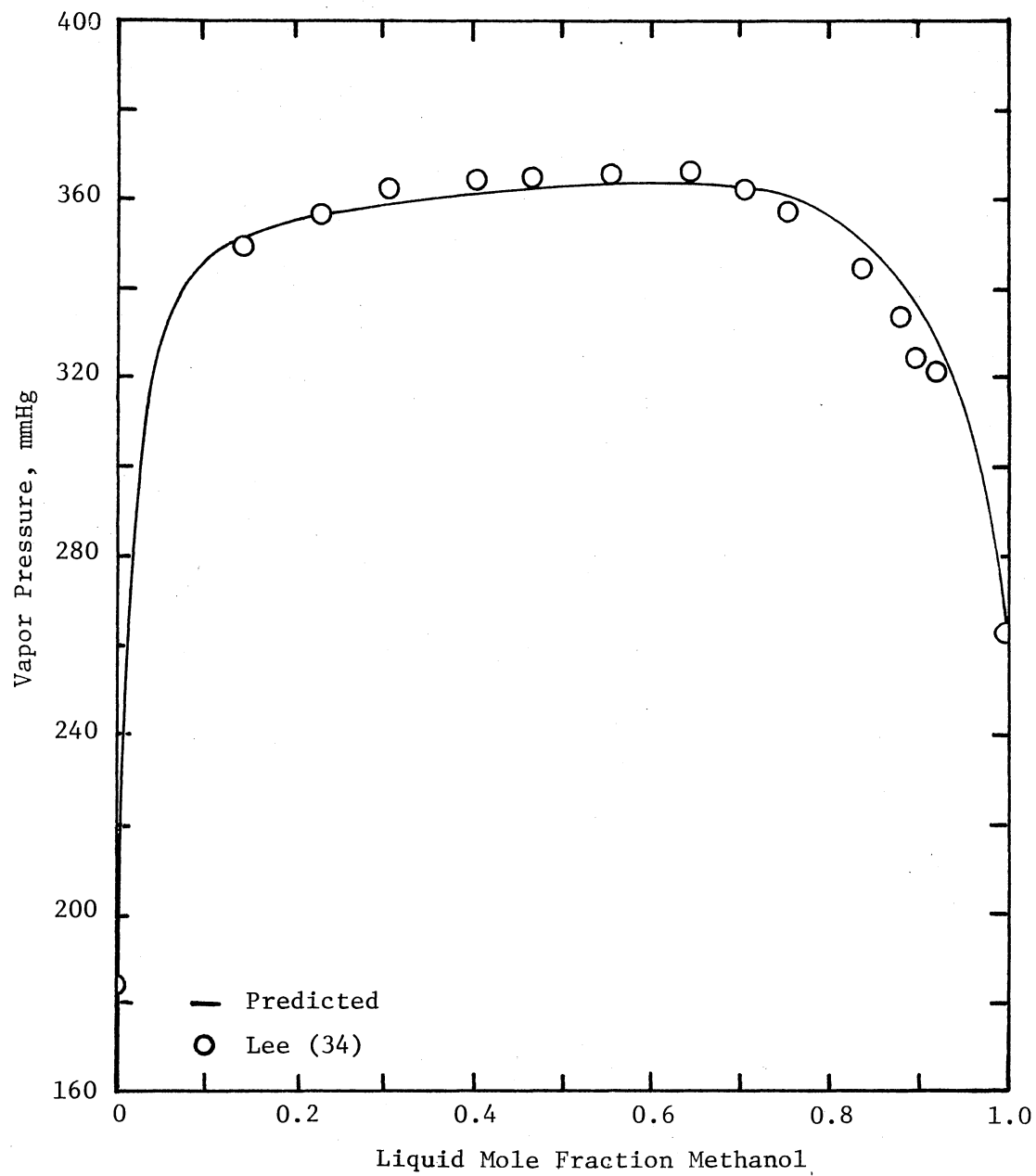
Figure 47.   Vapor Pressure at 40°C for the System
Methanol(1)-Benzene(2)

Figure 48. Vapor Pressure at 55°C for the System
Methanol(1)-Benzene(2)
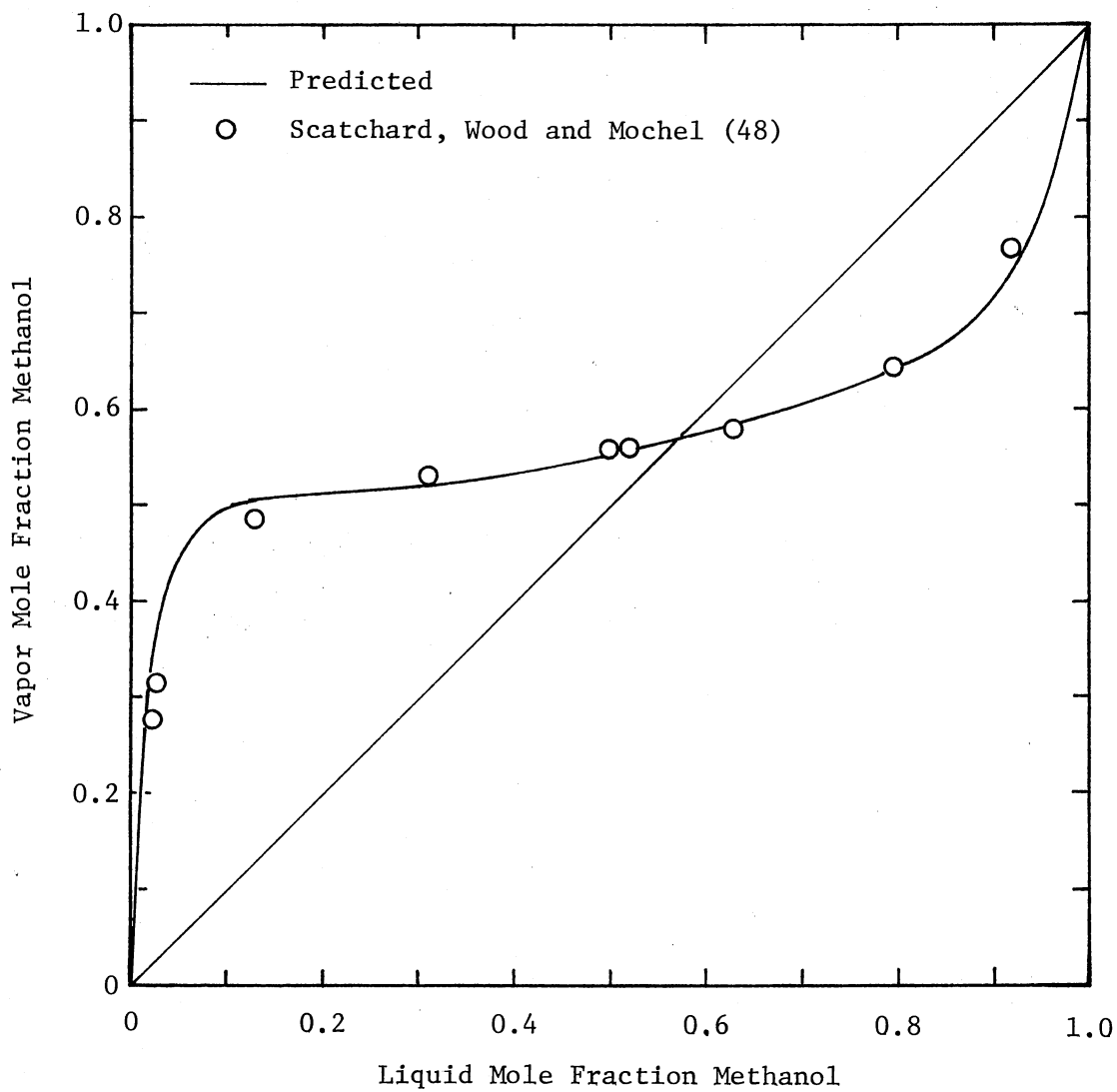
Figure 49. Vapor-Liquid Composition Data at 35°C
           for the System Methanol(1)-Benzene(2)
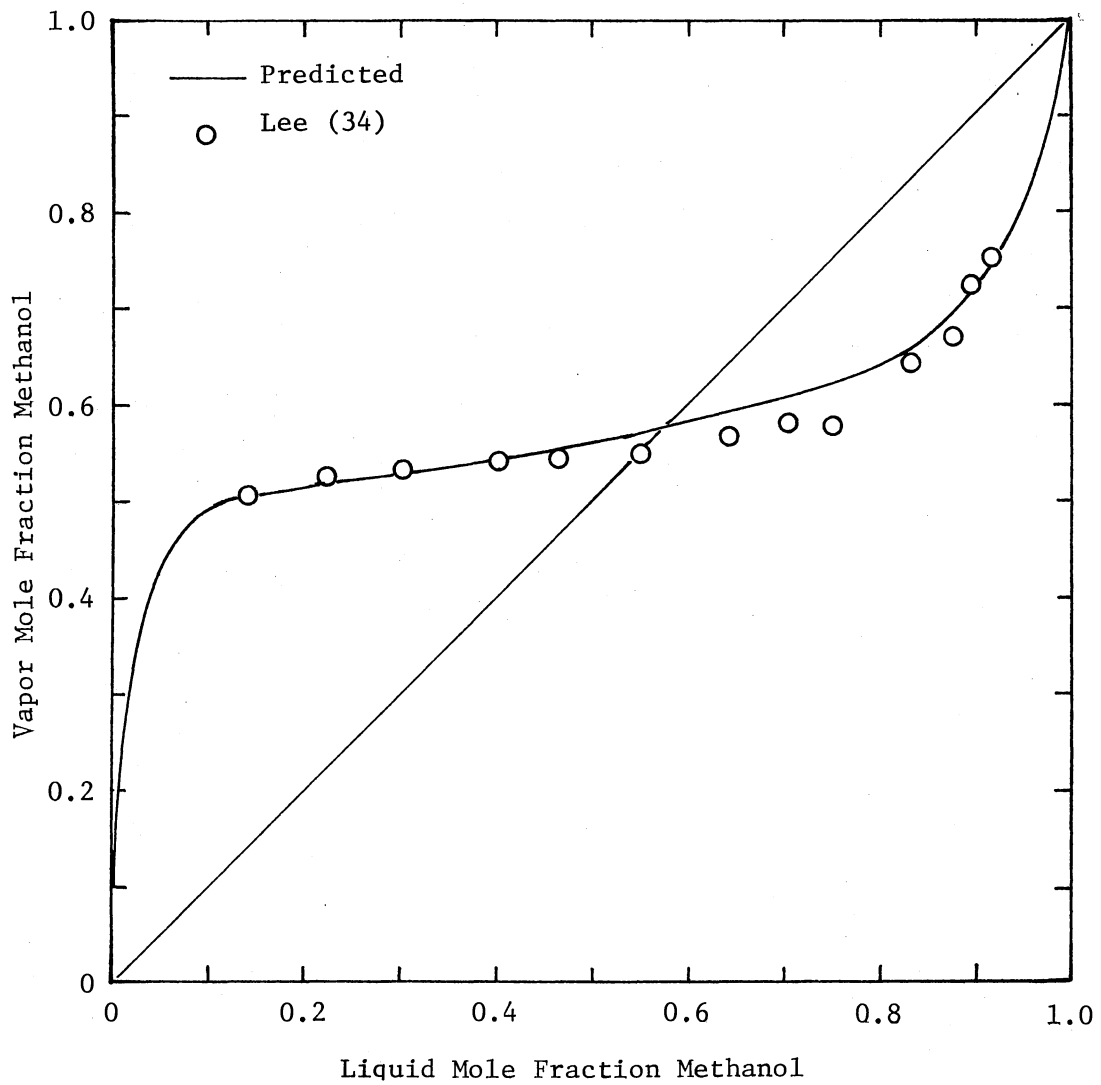
Figure 50. Vapor-Liquid Composition Data at $40^{\circ}C$
for the System Methanol(1)-Benzene(2)
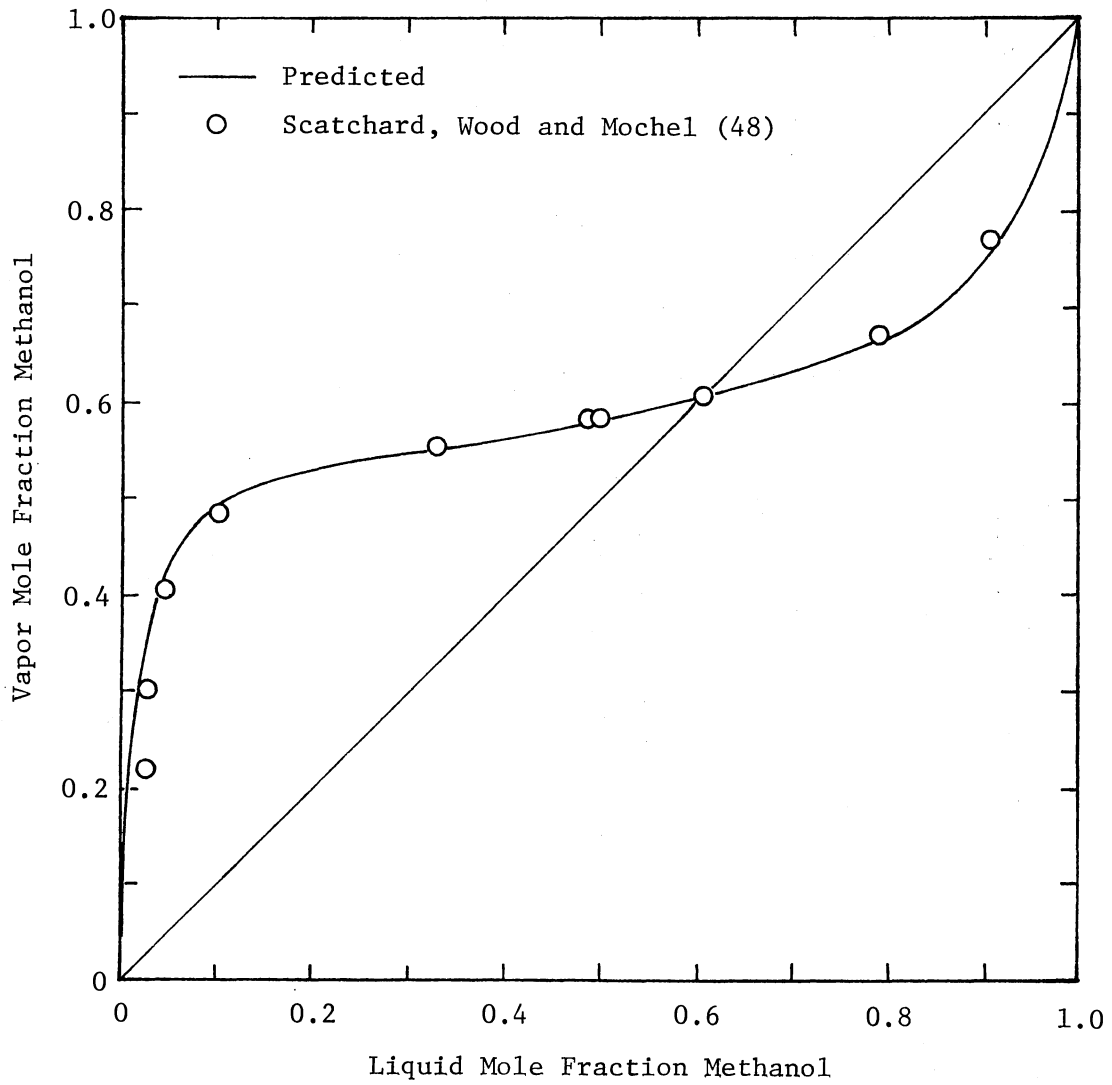
Figure 51.   Vapor-Liquid Composition Data at 55°C
              for the System Methanol(1)-Benzene(2)

average deviations in vapor mole fraction are 0.016 at 35°C and 0.007 at 55°C. Table XXXVIII and Figure 47 indicate that the predicted vapor pressures do not agree qualitatively with Lee's experimental values. The average deviation in vapor mole fraction between predicted and Lee's data is 0.016.

For the system ethanol-benzene, Brown and Smith (11) measured equilibrium data at 45°C, and Ho and Lu (29) at 55°C. Results of the predicted and smoothed experimental data are shown in Table XL and XLI, and in Figures 52 through 55. For both temperatures, the predicted vapor pressures are lower than experimental values except at high liquid mole fraction of ethanol. In general, the predicted data are in better agreement with Brown's data.

The phase equilibrium in the system n-propanol-benzene has been studied by Lee (34) at 40°C and by Brown and Smith (12) at 45°C. Predicted and smoothed experimental VLE data are listed in Tables XLII and XLIII. Graphical comparisons are shown in Figures 56 and 57 for P-x data, and in Figures 58 and 59 for y-x data. Results for these two temperatures are similar. Predicted vapor pressures are lower than experimental values at liquid mole fraction n-propanol less than 0.70, and higher otherwise. The average deviations in vapor mole fraction between predicted and smoothed experimental data are 0.013 at 40°C and 0.014 at 45°C.

VLE data at 55°C for the system ethanol-n-hexane are reported by Ho and Lu (29), and Kudryavtseva and Susarev (31). Predicted and smoothed experimental data are listed in Table XLIV. Figures 60 and 61 show the graphical comparison for P-x data and y-x data, respectively. Predicted vapor pressures are lower than both sets of experimental

TABLE XL

PREDICTED AND EXPERIMENTAL VLE DATA AT $45^{\circ}C$ FOR THE SYSTEM ETHANOL(1)-BENZENE(2)

Liquid Mole Fraction x_1	Vapor Pressure, mmHg		Vapor Mole Fraction, y_1	
	Predicted	Experimental Data*	Predicted	Experimental Data*
0.10	295.2	295.5	0.288	0.289
0.20	303.2	306.0	0.324	0.333
0.30	305.2	308.1	0.355	0.359
0.40	306.9	309.0	0.393	0.382
0.50	305.5	308.0	0.418	0.404
0.60	301.3	303.0	0.444	0.431
0.70	292.4	292.0	0.483	0.470
0.80	277.4	273.0	0.538	0.536
0.90	247.1	238.0	0.642	0.662

*   Smoothed experimental data of Brown and Smith (11).

TABLE XLI

PREDICTED AND EXPERIMENTAL VLE DATA AT 55°C FOR THE SYSTEM ETHANOL(1)-BENZENE(2)

Liquid Mole Fraction x_1	Vapor Pressure, mmHg		Vapor Mole Fraction, y_1	
	Predicted	Experimental Data*	Predicted	Experimental Data*
0.10	435.6	440.0	0.295	0.288
0.20	452.4	459.1	0.342	0.344
0.30	457.8	466.5	0.377	0.376
0.40	462.4	470.5	0.418	0.403
0.50	461.6	471.0	0.445	0.430
0.60	456.4	465.0	0.474	0.460
0.70	444.7	450.0	0.514	0.502
0.80	424.5	422.0	0.569	0.569
0.90	383.0	372.5	0.671	0.715

* Smoothed experimental data of Ho and Lu (29).
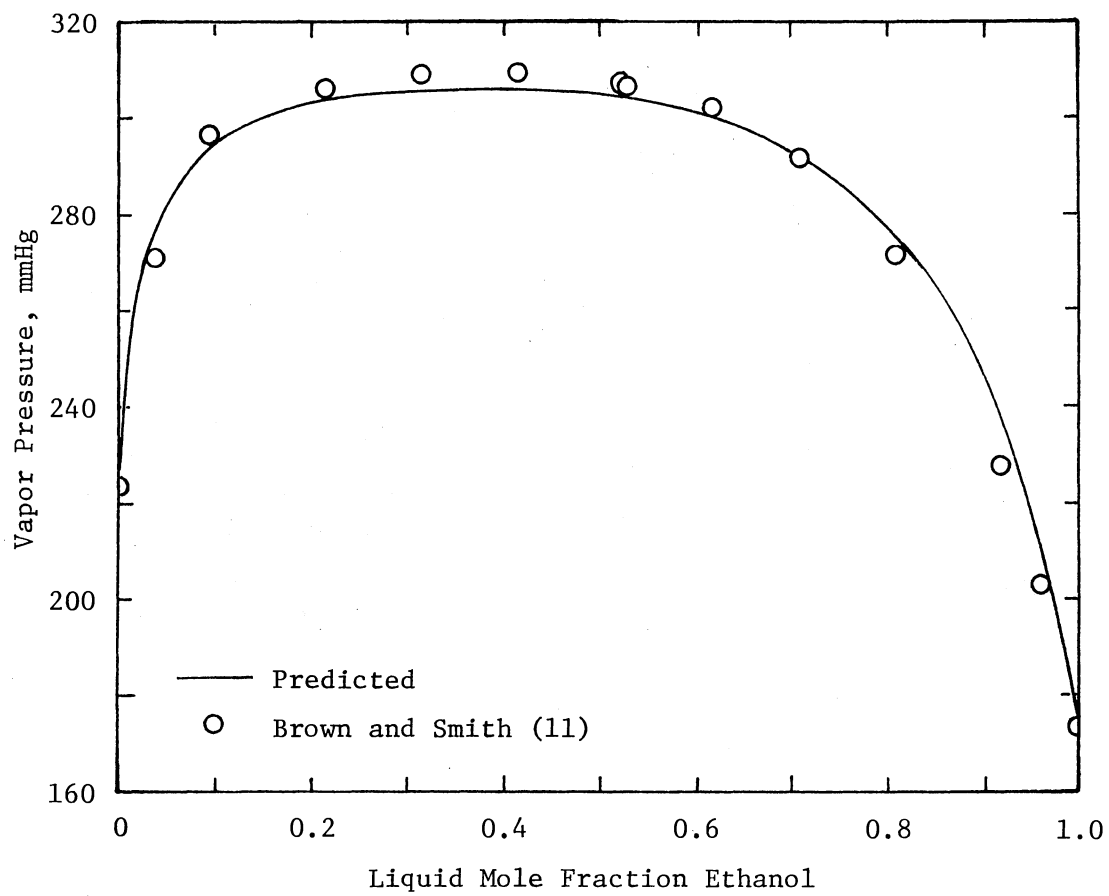
Figure 52. Vapor Pressure at 45°C for the System
Ethanol(1)-Benzene(2)

Figure 53. Vapor Pressure at 55°C for
the System Ethanol(1)-
Benzene(2)
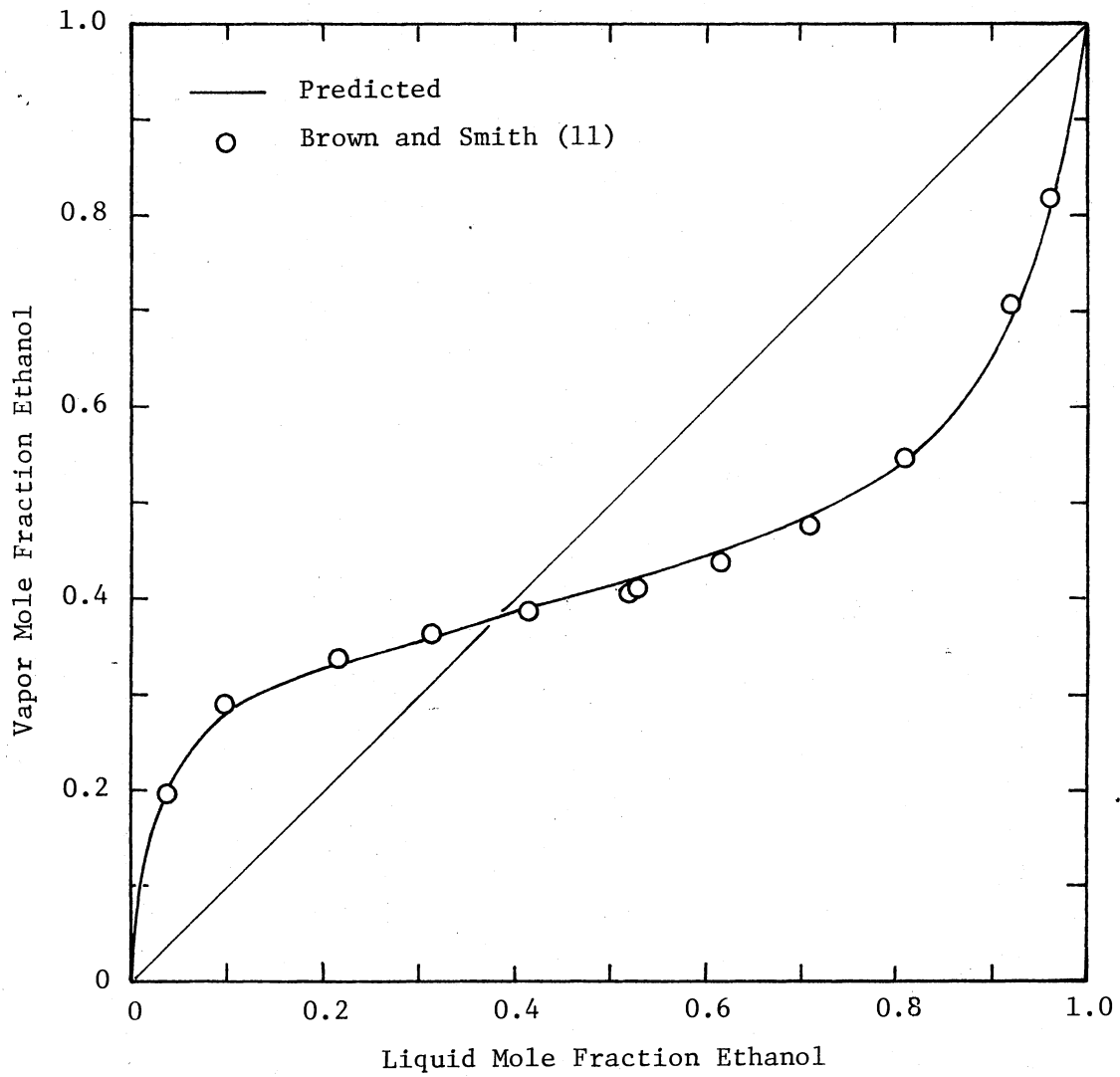
Figure 54. Vapor-Liquid Composition Data at 45°C
for the System Ethanol(1)-Benzene(2)
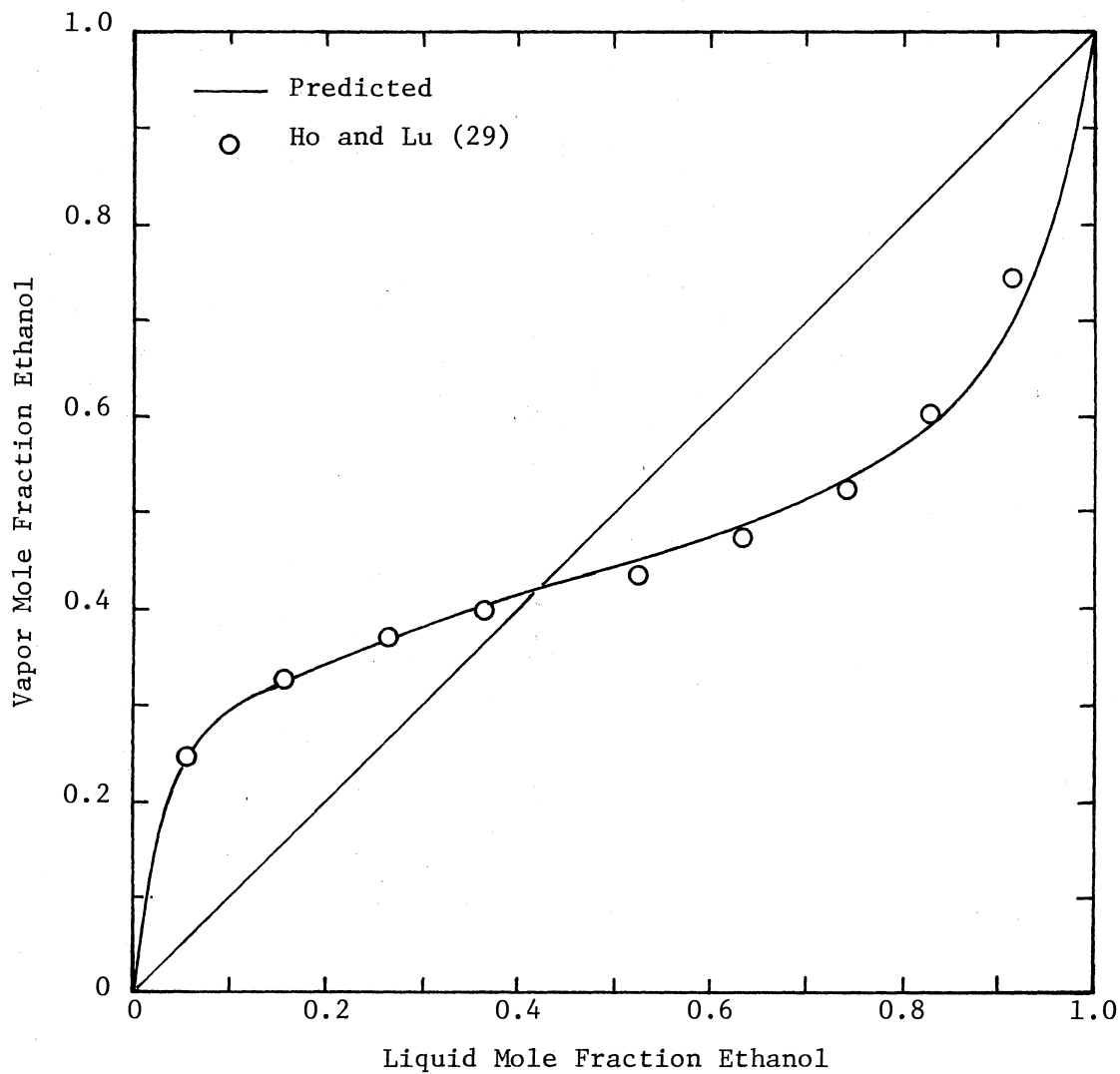
Figure 55. Vapor-Liquid Composition Data at 55°C
for the System Ethanol(1)-Benzene(2)

TABLE XLII

PREDICTED AND EXPERIMENTAL VLE DATA AT 40°C FOR THE SYSTEM N-PROPANOL(1)-BENZENE(2)

Liquid Mole Fraction x_1	Vapor Pressure, mmHg		Vapor Mole Fraction, y_1	
	Predicted	Experimental Data*	Predicted	Experimental Data*
0.10	189.3	195.0	0.106	0.116
0.20	187.9	195.2	0.144	0.144
0.30	184.6	192.9	0.167	0.166
0.40	179.8	188.5	0.189	0.178
0.50	173.9	182.2	0.210	0.186
0.60	166.0	173.1	0.234	0.204
0.70	156.0	158.4	0.262	0.236
0.80	140.9	135.2	0.306	0.292
0.90	111.2	100.9	0.414	0.414

* Smoothed experimental data of Lee (34).

TABLE XLIII

PREDICTED AND EXPERIMENTAL VLE DATA AT 45°C FOR THE SYSTEM N-PROPANOL(1)-BENZENE(2)

Liquid Mole Fraction x_1	Vapor Pressure, mmHg		Vapor Mole Fraction, y_1	
	Predicted	Experimental Data*	Predicted	Experimental Data*
0.10	232.6	238.5	0.114	0.118
0.20	232.0	238.0	0.159	0.159
0.30	228.4	234.0	0.185	0.177
0.40	222.9	229.1	0.209	0.194
0.50	215.9	222.0	0.233	0.216
0.60	206.5	211.5	0.259	0.239
0.70	194.7	195.8	0.290	0.277
0.80	176.8	170.0	0.337	0.347
0.90	141.7	130.0	0.449	0.492

*   Smoothed experimental data of Brown and Smith (12).
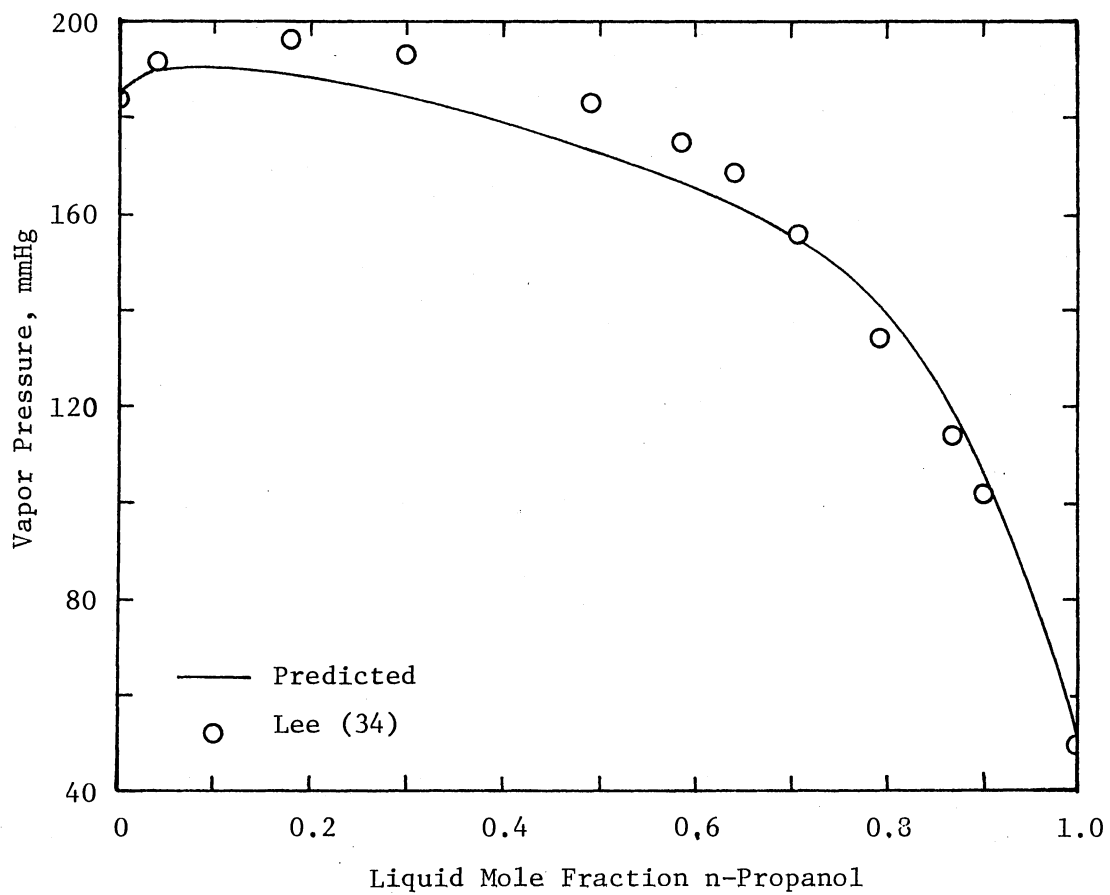
Figure 56.   Vapor Pressure at 40°C for the System
n-Propanol(1)-Benzene(2)
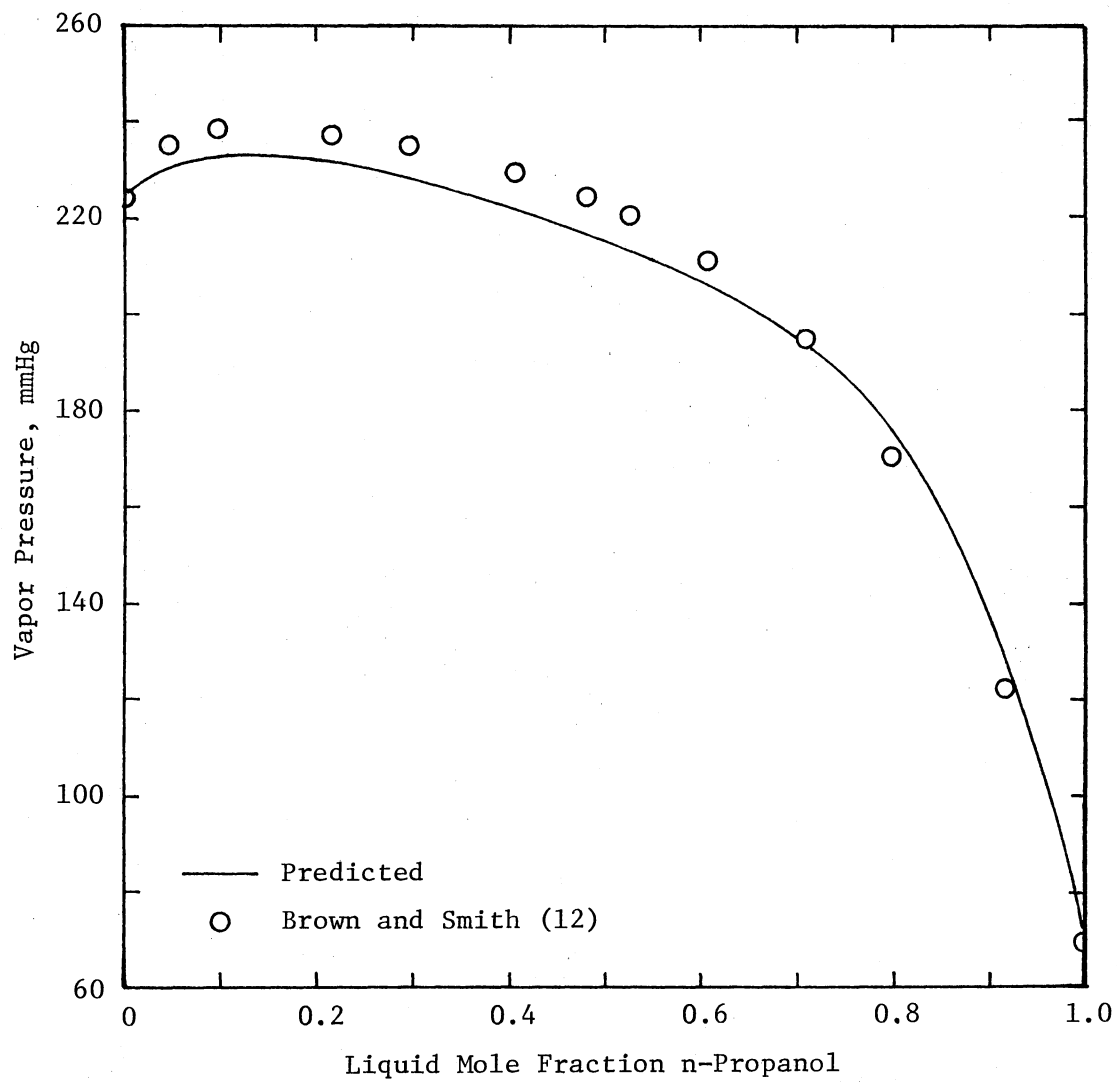
Figure 57. Vapor Pressure at 45°C for the System
n-Propanol(1)-Benzene(2)
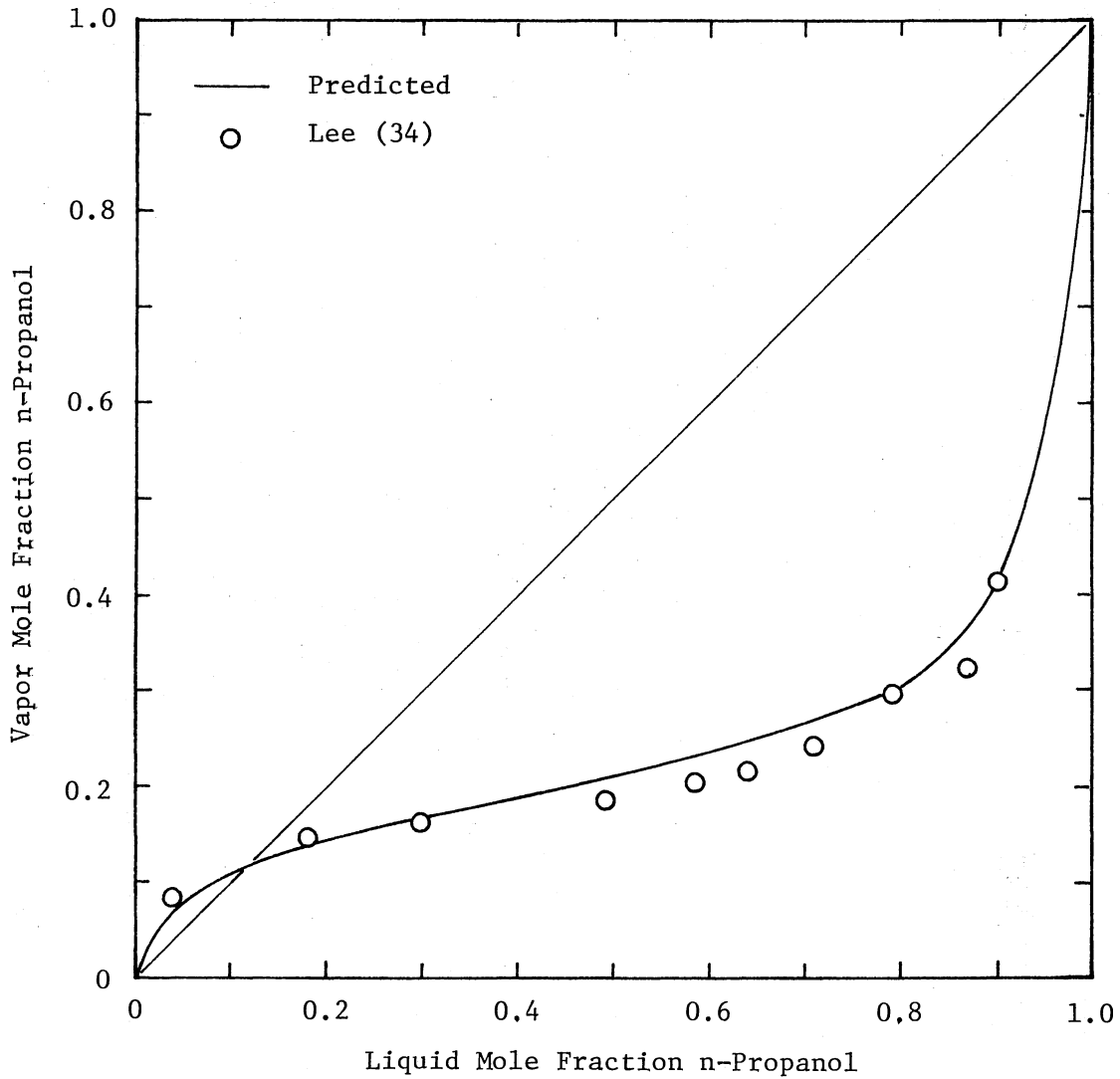
Figure 58.   Vapor-Liquid Composition Data at $40^{\circ}C$
for the System n-Propanol(1)-Benzene(2)
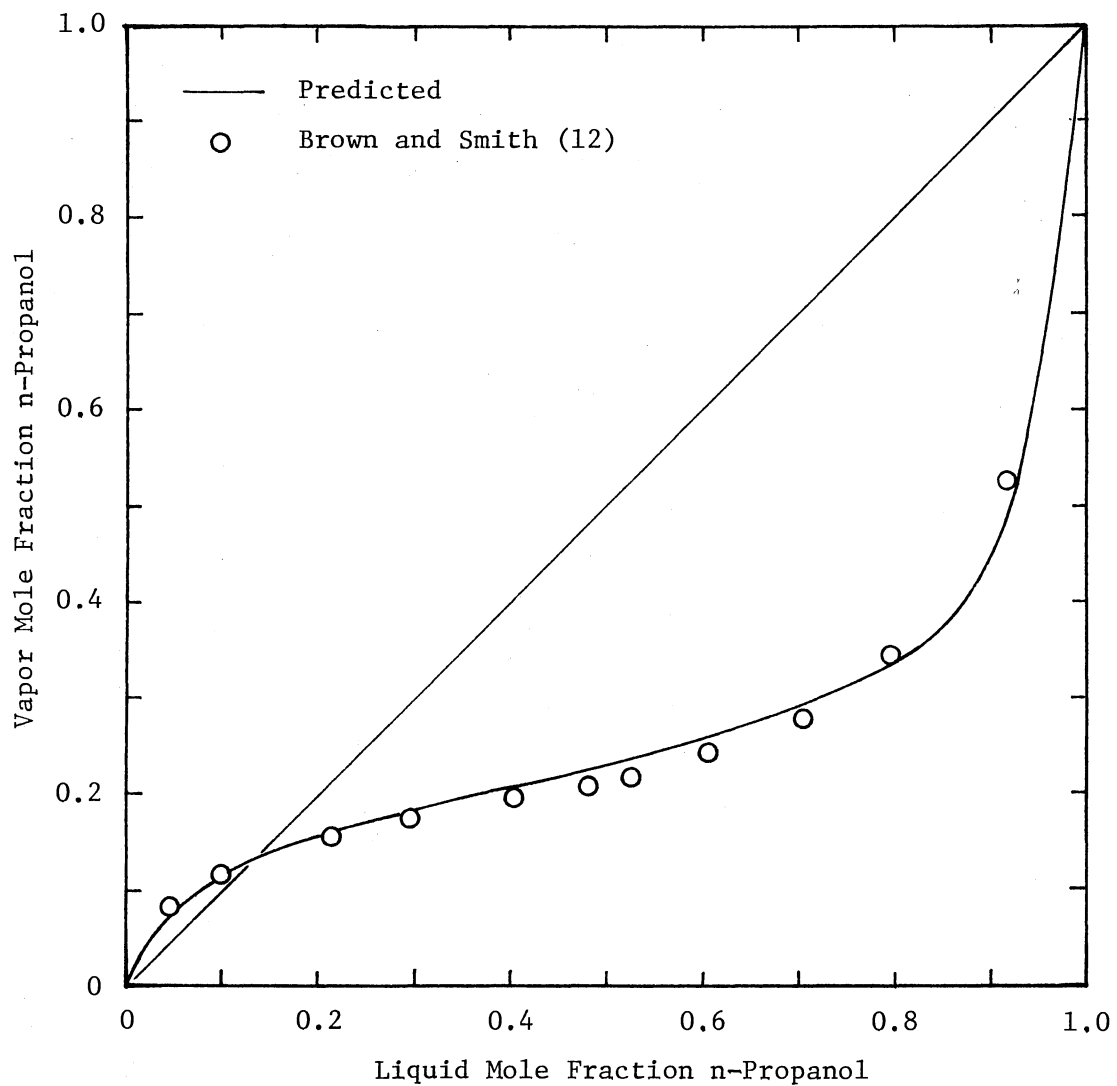
Figure 59.   Vapor-Liquid Composition Data at 45°C
for the System n-Propanol(1)-
Benzene(2)

TABLE XLIV

PREDICTED AND EXPERIMENTAL VLE DATA AT 55°C FOR THE SYSTEM ETHANOL(1)-N-HEXANE(2)

Liquid Mole Fraction x_1	Vapor Pressure, mmHg			Vapor Mole Fraction, y_1		
	Predicted	Experimental Data* I	II	Predicted	Experimental Data* I	II
0.10	653.0	654.0	652.0	0.298	0.294	0.304
0.20	663.4	672.3	668.0	0.323	0.335	0.323
0.30	665.9	679.2	669.0	0.337	0.355	0.325
0.40	665.6	679.9	669.0	0.344	0.368	0.330
0.50	663.4	678.6	668.0	0.350	0.379	0.334
0.60	658.5	671.9	665.0	0.359	0.390	0.336
0.70	647.0	654.4	651.0	0.372	0.402	0.346
0.80	618.0	623.0	615.0	0.402	0.434	0.386
0.90	541.9	538.1	528.0	0.479	0.525	0.480

* Smoothed experimental data of I: Ho and Lu (29)
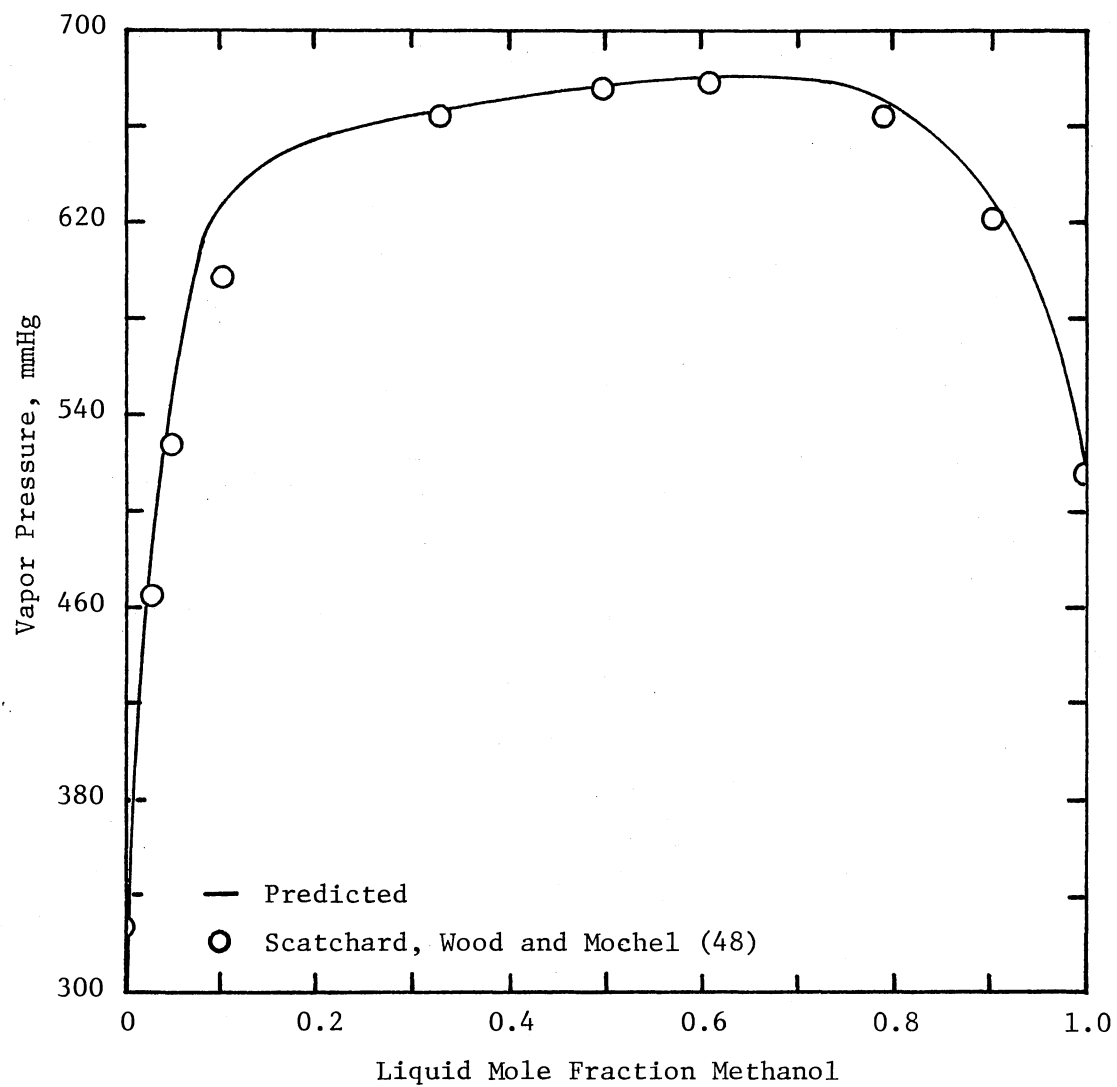   II: Kudryavtseva and Susarev (31).
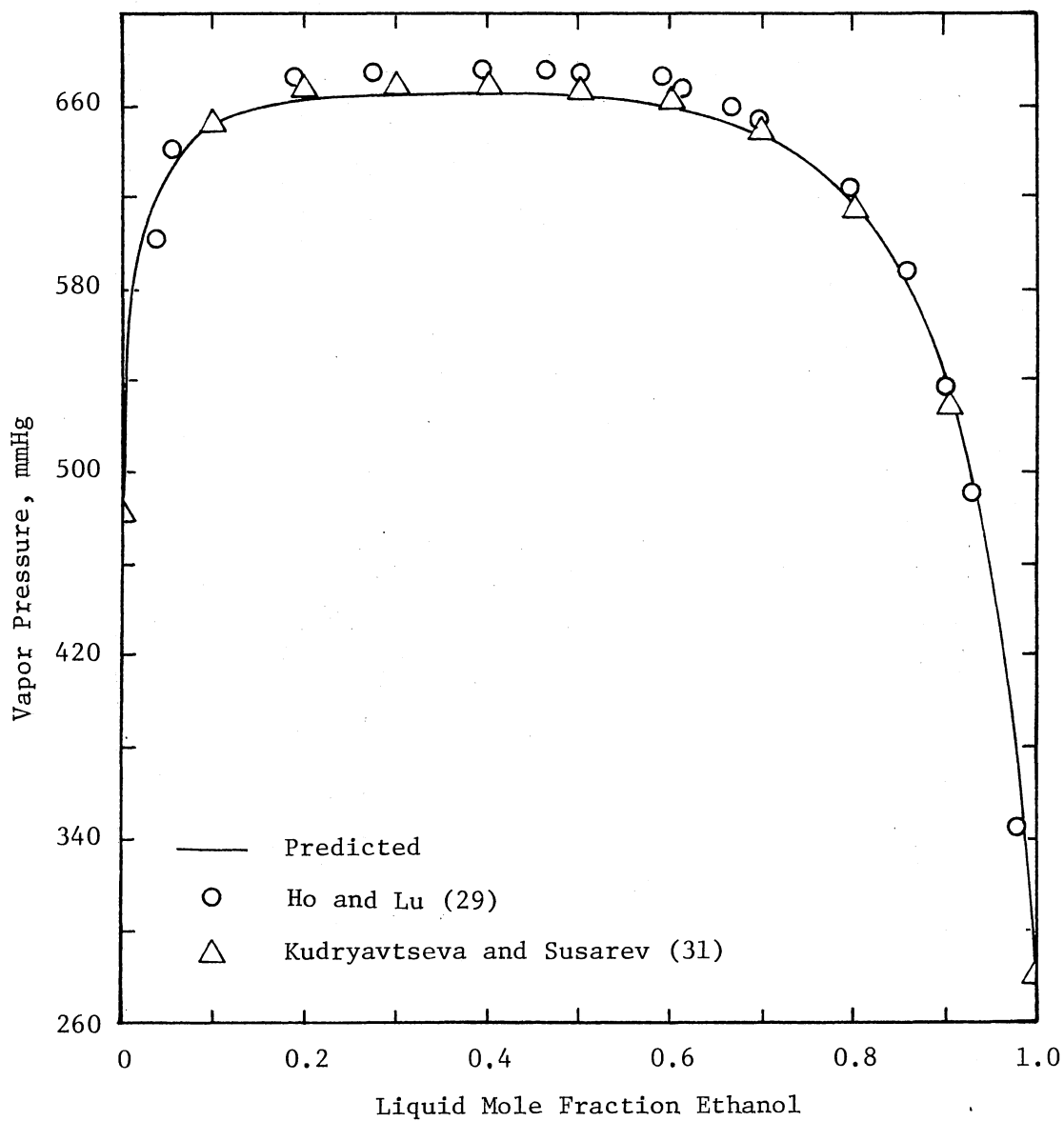
Figure 60.   Vapor Pressure at 55°C for the System
Ethanol(1)-n-Hexane(2)
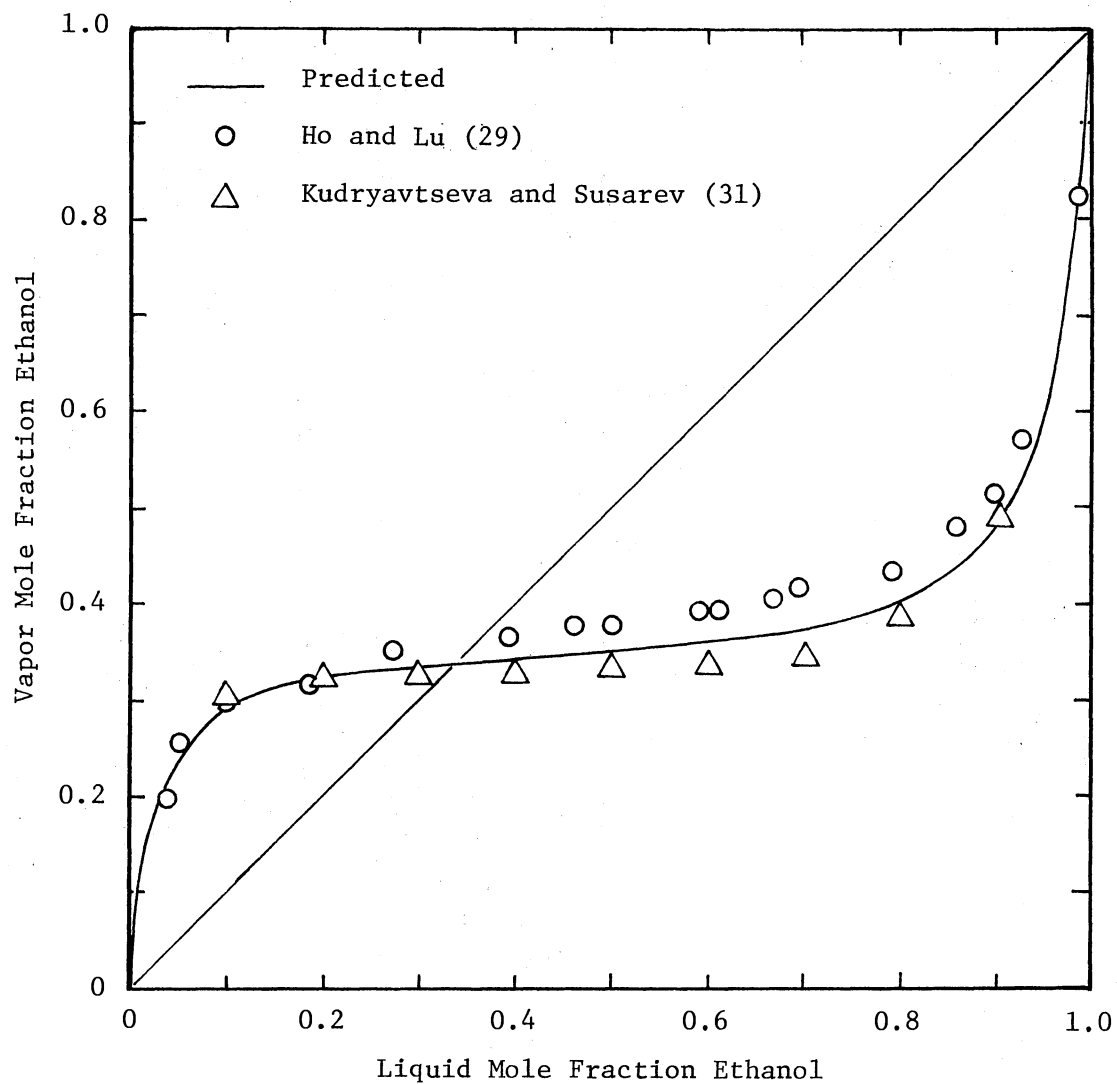
Figure 61. Vapor-Liquid Composition Data at 55°C
for the System Ethanol(1)-n-Hexane(2)

data except in the high ethanol concentration range. As pointed out

by Smith (50), the use of a circulating still with a gas cap to regu-

late pressure may cause higher experimental vapor pressures. Figure

61 shows that the predicted y-x curve lies between the two experimental

y-x curves over most of the composition range.

Brown, Fock and Smith (10) measured the VLE data for the system

n-propanol-n-hexane at $45^{\circ}C$. Predicted and experimental VLE data

are shown in Table XLV. Graphical comparisons appear in Figures 62

and 63 for P-x data and y-x data, respectively. Excluding end points,

only five experimental data points are available. It is not practical

to obtain smoothed experimental P-x and y-x curves based on these five

data points. Table XLV and Figure 62 show the predicted P-x data

to agree with Brown's data within an average of 2 mmHg. From Table

XLV and Figure 63, the predicted y-x data agree with Brown's data

within an average of 0.006 vapor mole fraction. The good agreement of

the predicted P-x data and y-x data with Brown's data indicate that

the P-x data at $25^{\circ}C$ from this study, Brown's $45^{\circ}C$ VLE data, and the

heat of mixing data by Brown, Fock and Smith (9) are mutually consis-

tent.

Since the indirect comparison involves use the G^E-x data at

$25^{\circ}C$ and experimental heat of mixing data at different temperatures to

evaluate G^E-x data at T_2, the uncertainty in experimental heat of

mixing data is expected to effect the G^E calculation and VLE prediction.

However, increase (or decrease) the heat of mixing uniformly by 2% will

only result in decrease (or increase) the G^E by 0.04% and the vapor

pressure by 0.06% (with a magnitude of 0.05 mmHg). This indicates that

TABLE XLV

PREDICTED AND EXPERIMENTAL VLE DATA AT 45°C FOR THE SYSTEM N-PROPANOL(1)-N-HEXANE(2)

Liquid Mole Fraction x_1	Vapor Pressure, mmHg		Vapor Mole Fraction, y_1	
	Predicted	Experimental Data*	Predicted	Experimental Data*
0.10	365.6	--	0.127	--
0.20	362.5	--	0.137	--
0.2847	359.0	360.85	0.145	0.1361
0.30	358.8	--	0.146	--
0.40	353.9	--	0.162	--
0.4447	350.5	349.36	0.157	0.1489
0.50	347.1	--	0.162	--
0.5289	345.3	345.24	0.163	0.1566
0.5410	344.2	344.19	0.166	0.1584
0.60	337.8	--	0.172	--
0.70	324.0	--	0.185	--
0.7440	314.0	306.79	0.192	0.1926
0.80	297.0	--	0.209	--
0.90	241.8	--	0.269	--

* Experimental data of Brown, Fock and Smith (10).

157
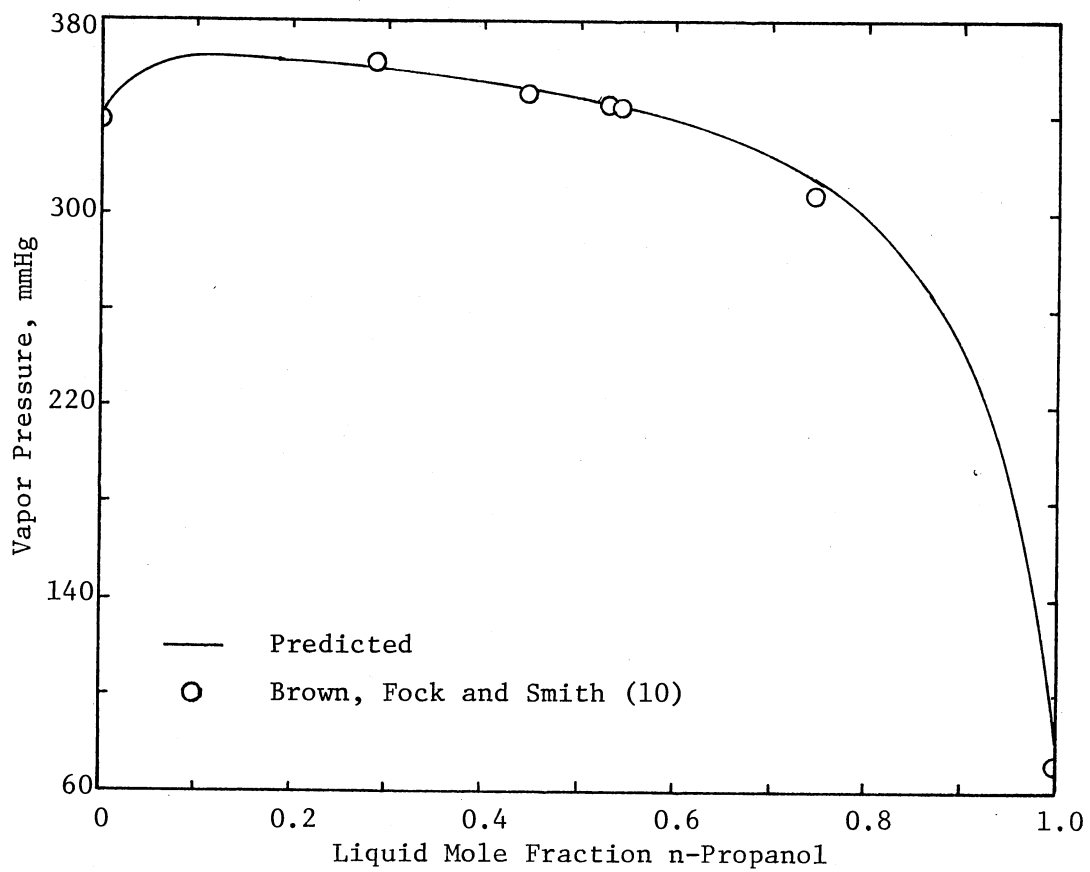
Figure 62.   Vapor Pressure at 45°C for the System
n-Propanol(1)-n-Hexane(2)
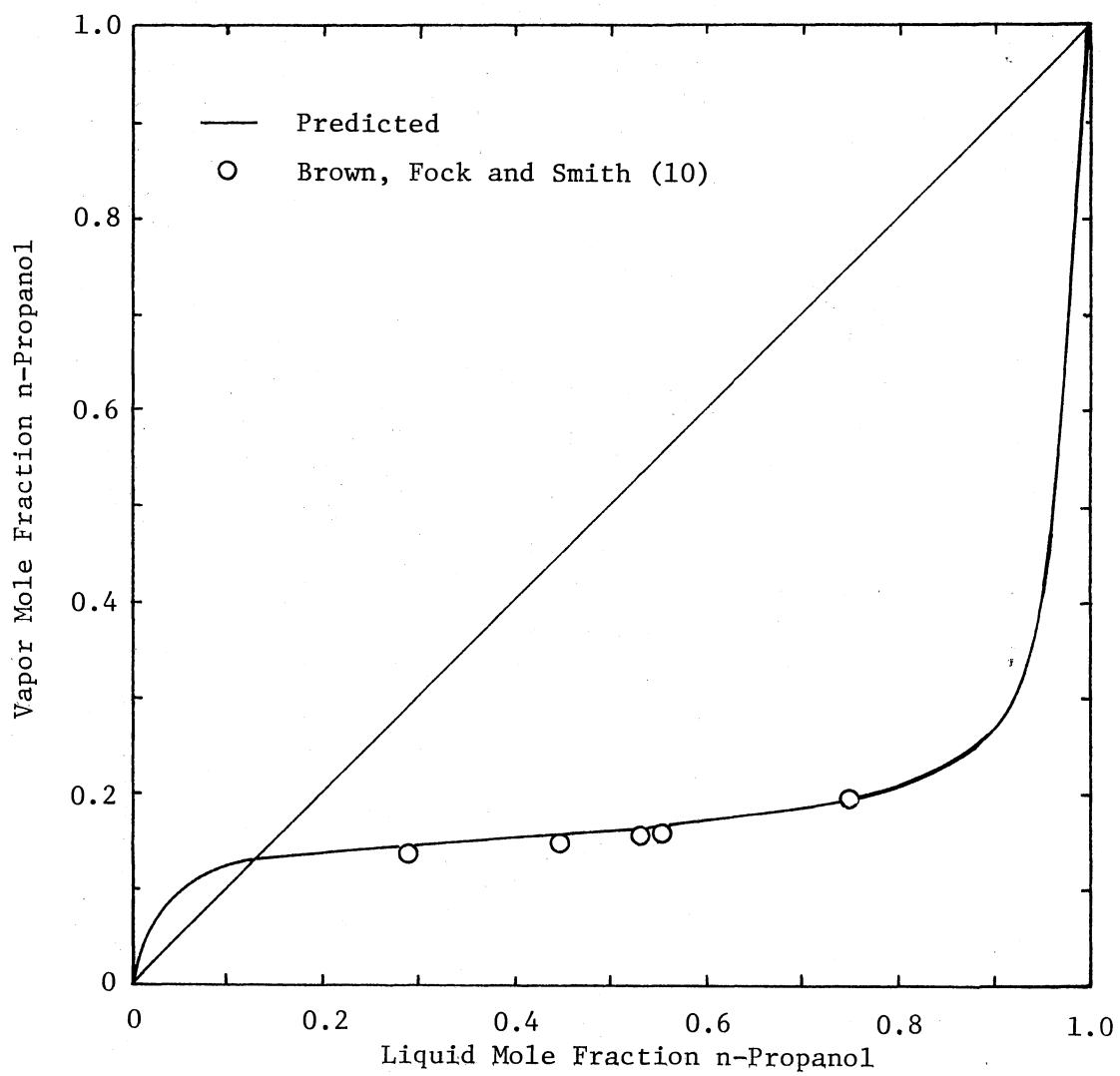
Figure 63. Vapor-Liquid Composition Data at 45°C for the System n-Propanol(1)-n-Hexane(2)

the uncertainty in heat of mixing does not have significant effect on VLE prediction.

Summary

The predicted vapor pressures are in best agreement with Brown's data (10, 11, 12) with an absolute average deviation of 3.7 mmHg. The worst case is obtained by comparison with Ho's data (29) with an absolute average deviation of 8.1 mmHg.

For vapor composition prediction, the predicted values are in best agreement with Scatchard's data (48) with an absolute average deviation of 0.008 mole fraction. The worst results in vapor composition prediction is also obtained by comparison with Ho's data (29) with an absolute average deviation of 0.016 mole fraction.

For vapor pressure prediction, the maximum deviation occurs at $55^{o}C$. This may be due to the extrapolation of heat of mixing data to $55^{o}C$ (the highest temperature at which experimental data are available is $45^{o}C$).

For vapor pressure or vapor composition prediction, there is no significant difference in deviation for individual components. This indicates that none of the chemicals used in this study has unusually high impurity.

CHAPTER VII

APPLICATIONS OF GROUP CONTRIBUTION THEORIES

The group contribution theories discussed in Chapter II were

tested for their applicability in predicting excess thermodynamic

properties and vapor-liquid equilibrium data. First, these theories

were applied to the representation of excess thermodynamic properties.

Then, the excess thermodynamic properties thus obtained were used to

predict vapor pressures and vapor compositions for the binary systems

studied. Results of the prediction were compared with experimental

data.

Excess Thermodynamic Properties

Three group contribution theories were employed in the present

study to predict excess Gibbs free energies for the binary systems.

Results were compared with the values calculated by Mixon's method

from experimental P-x data.

Quasi-Lattice Theory (QLT)

For the binary mixtures in the present study, there are ten

interactions: H-H, H-O, H-I, H-S, O-O, O-I, O-S, I-I, I-S, and

S-S. The exchange energy of interaction between like segments

(i.e., H-H, O-O, I-I and S-S) is zero by definition. Previous investi-

gators (23, 24, 32) indicate that certain exchange energies may be

neglected by reasoning that their magnitudes might be expected to be small. However, results show that the best fit to heat of mixing data can be achieved by placing no restrictions on the energy parameters and allowing all six parameters to be regressed.

With the number and type of contact points specified in Table XLVI. the exchange energies for each binary system were evaluated by fitting the quasi-lattice theory to experimental heat of mixing data at $25^{\circ}C$. The energy parameters thus evaluated are listed in Table XLVII along with values given by previous investigators.

In Table XLVII, the O-I interaction energy of the system methanol-benzene is a negative number, contrary to the sign for the other three such energies. The other unexpected feature shown in Table XLVII is that the energies of the H-S and H-I, and O-S and O-I for the alcohol-n-paraffin systems are different by more than might be expected. Results by Kuo (32) also indicate this feature. The I-S interaction energies for the alcohol-n-hexane and alcohol-cyclohexane systems are very small as expected. For the alcohol-benzene system, due to the great difference in the molecular structure between the paraffin-type and aromatic-type segments, the I-S interaction energy is expected to be significant as shown in the table.

The results of fitting the quasi-lattice theory to the experimental heat of mixing data (by non-linear regression) to evaluate the energy parameters are shown in Table XLVIII. Graphical comparisons are shown in Figures 64 through 70. These figures show that reasonable agreement between the quasi-lattice theory and the experimental heat of mixing data can be obtained for the binary systems studied.

TABLE XLVI

NUMBER AND TYPE OF CONTACT POINTS,
SITES AND COORDINATION NUMBERS
FOR EACH COMPONENT

Component	$n_H z_H$	$n_O z_O$	$n_I z_I$	$n_S z_S$	z^*	r_a	r_p
Methanol	1	2	3	–	4	2	–
Ethanol	1	2	5	–	4	3	–
n-Propanol	1	2	7	–	4	4	–
Benzene	–	–	–	12	4	–	5
Cyclohexane	–	–	–	12	4	–	5
n-Hexane	–	–	–	14	4	–	6

* The coordination number, z, is given by

$$\sum_u n_u z_u = rz - (2r - 2)$$

TABLE XLVII

INTERACTION ENERGY PARAMETERS AT 25°C

(Units: cal/g-mole)

System	Ω'_{O-H}	Ω'_{H-S}	Ω'_{H-I}	Ω'_{O-S}	Ω'_{O-I}	Ω'_{I-S}	Lit. Source
Methanol-Benzene	-3715	-650	304	-306	-86	126	
	(-3200)**	(-410)	(0)[a]	(-210)	(0)	(82)	24
Ethanol-Benzene	-4326	-1064	241	-356	72	177	
	(-3200)	(-545)	(0)	(-300)	(0)	(81)	24
Ethanol-Cyclohexane	-3805	-357	-307	-122	-438	3.9	
	(-3200)	(--)[b]	(0)	(--)	(0)	(-49)	23
Ethanol-n-Hexane	-3749	-203	-314	-211	-417	0.8	
n-Propanol-Benzene	-3403	-323	1345	-244	234	154	
	(-3200)	(-545)	(0)	(-300)	(0)	(87)	24
n-Propanol-Cyclohexane	-3992	-419	-124	-270	-524	1.0	
n-Propanol-n-Hexane	-3860	-230	-208	-264	-514	1.0	
Alcohol-Benzene*	-3556	-797	1233	-13	763	141	
Alcohol-Cyclohexane*	-3674	-60	-317	-326	-643	1.3	
Alcohol-n-Hexane*	-3827	-283	-42	-164	-388	0.8	
	(-3748)	(-251)	(-253)	(-251)	(-465)	(<1)	32#

* These parameters are employed to represent the excess thermodynamic properties.

** Literature values are given in parentheses.

\# Evaluated by fitting the quasi-lattice theory to the heat of mixing data of nine alcohol-n-paraffin systems at 30°C

a These parameters are neglected by reasoning that their magnitudes might be expected to be small.

b These values are negligible after regression.

TABLE XLVIII

HEAT OF MIXING AT $25^{\circ}C$ BY THE QUASI-LATTICE THEORY

System	Mole Fraction Alcohol	ΔH^M, cal/g-mole		Deviation	
		Expt'l*	Calc'd	cal/g-mole	%
	0.010	31.00	24.96	-6.04	-19.49
	0.020	55.00	44.56	-10.44	-18.99
	0.030	75.00	60.68	-14.32	-19.09
	0.040	90.50	74.37	-16.13	-17.82
	0.050	100.90	86.25	-14.65	-14.52
	0.075	121.00	109.99	-11.01	-9.10
	0.100	136.00	127.71	-8.29	-6.09
	0.125	148.20	141.51	-6.69	-4.51
	0.150	156.90	152.12	-4.78	-3.05
Methanol-	0.175	163.00	160.10	-2.90	-1.78
Benzene	0.200	167.00	166.26	-0.74	-0.44
	0.300	171.50	176.32	4.82	2.81
	0.400	166.10	170.76	4.66	2.80
	0.500	148.60	153.10	4.50	3.03
	0.600	126.50	127.11	0.61	0.48
	0.700	100.00	96.12	-3.88	-3.88
	0.800	69.10	60.27	-8.83	-12.78
	0.900	35.80	25.04	-10.76	-30.06
	0.010	45.20	27.10	-18.10	-40.03
	0.020	67.00	48.79	-18.21	-27.17
	0.030	83.50	66.97	-16.53	-19.79
	0.040	99.50	82.61	-16.89	-16.97
	0.050	113.70	96.35	-17.35	-15.26
	0.075	139.00	124.61	-14.39	-10.35
	0.100	161.00	146.47	-14.53	-9.03
	0.125	177.90	163.91	-13.99	-7.87
Ethanol-	0.150	188.90	178.03	-10.87	-5.76
Benzene	0.175	196.40	189.28	-7.12	-3.63
	0.200	201.20	198.05	-3.15	-1.57
	0.300	208.00	216.45	8.45	4.06
	0.400	204.00	213.74	9.74	4.77
	0.500	187.90	196.59	8.69	4.63
	0.600	153.00	167.05	14.05	9.18
	0.700	117.40	128.32	10.92	9.30
	0.800	80.00	83.91	3.91	4.89
	0.900	39.30	38.05	-1.25	-3.17

TABLE XLVIII (Continued)

System	Mole Fraction Alcohol	ΔH^M, cal/g-mole		Deviation	
		Expt'l*	Calc'd	cal/g-mole	%
n-Propanol-Benzene	0.010	27.00	29.43	2.43	9.01
	0.020	51.50	53.35	1.85	3.59
	0.030	75.00	73.67	−1.33	−1.77
	0.040	99.20	91.39	−7.81	−7.87
	0.050	123.50	107.10	−16.40	−13.28
	0.075	151.40	139.87	−11.53	−7.61
	0.100	174.00	165.87	−8.13	−4.67
	0.125	192.60	187.01	−5.59	−2.90
	0.150	206.90	204.21	−2.69	−1.30
	0.175	219.40	218.11	−1.29	−0.59
	0.200	229.80	229.59	−0.21	−0.09
	0.300	248.40	254.03	5.63	2.27
	0.400	245.90	253.37	7.47	3.04
	0.500	224.50	233.78	9.28	4.14
	0.600	193.10	199.99	6.89	3.57
	0.700	150.50	154.90	4.40	2.93
	0.800	101.00	102.88	1.88	1.86
	0.900	51.60	48.36	−3.24	−6.28
Ethanol-Cyclohexane	0.010	22.50	25.94	3.44	15.30
	0.020	39.00	42.87	3.87	9.93
	0.030	52.00	55.62	3.62	6.96
	0.040	63.20	65.98	2.78	4.40
	0.050	72.00	74.58	2.58	3.58
	0.075	91.10	91.55	0.45	0.50
	0.100	108.00	104.35	−3.65	−3.38
	0.150	129.70	122.86	−6.84	−5.27
	0.200	141.50	135.98	−5.52	−3.90
	0.300	153.20	150.73	−2.47	−1.61
	0.400	156.70	156.80	0.10	0.07
	0.500	153.30	153.05	−0.25	−0.17
	0.600	142.50	141.67	−0.83	−0.58
	0.700	125.10	122.22	−2.88	−2.30
	0.800	99.80	93.24	−6.56	−6.58
	0.850	82.90	74.79	−8.11	−9.78
	0.900	61.20	53.25	−7.95	−12.99
	0.950	34.00	30.28	−3.72	−10.93

TABLE XLVIII (Continued)

System	Mole Fraction Alcohol	ΔH^M, cal/g-mole		Deviation	
		Expt'1*	Calc'd	cal/g-mole	%
	0.010	28.00	25.56	-2.44	-8.73
	0.020	45.10	42.15	-2.95	-6.54
	0.030	56.50	54.62	-1.88	-3.33
	0.040	65.60	64.58	-1.02	-1.55
	0.050	73.00	73.02	0.02	0.02
	0.075	87.30	89.25	1.95	2.24
	0.100	97.30	101.56	4.26	4.38
	0.150	113.50	118.86	5.36	4.72
	0.200	126.00	130.03	4.03	3.20
Propanol-	0.300	140.10	142.11	2.01	1.43
Cyclohexane	0.400	141.30	144.07	2.77	1.96
	0.500	134.00	137.96	3.96	2.96
	0.600	118.70	124.71	6.01	5.06
	0.700	94.90	104.35	9.45	9.96
	0.800	69.30	78.09	8.79	12.68
	0.850	54.80	60.66	5.86	10.70
	0.900	38.00	42.29	4.29	11.29
	0.950	19.80	23.76	3.96	20.00
	0.010	25.00	26.17	1.17	4.69
	0.020	41.80	43.02	1.22	2.92
	0.030	54.30	55.62	1.32	2.44
	0.040	64.10	65.59	1.49	2.33
	0.050	72.80	73.88	1.08	1.48
	0.075	90.20	89.76	-0.44	-0.49
	0.100	101.50	101.46	-0.04	-0.04
	0.150	117.20	117.43	0.23	0.20
	0.200	126.40	127.76	1.36	1.08
Ethanol-	0.300	136.40	138.81	2.41	1.77
n-Hexane	0.400	138.00	140.71	2.71	1.96
	0.500	133.00	135.74	2.74	2.06
	0.600	122.00	127.17	5.17	4.24
	0.700	106.00	108.34	2.34	2.21
	0.800	82.00	82.74	0.74	0.90
	0.850	66.10	65.55	-0.55	-0.84
	0.900	48.00	47.13	-0.87	-1.81
	0.950	26.80	26.22	-0.58	-2.18

TABLE XLVIII (Continued)

System	Mole Fraction Alcohol	ΔH^M, cal/g-mole		Deviation	
		Expt'l*	Calc'd	cal/g-mole	%
	0.010	16.50	26.07	9.57	57.98
	0.020	32.10	42.85	10.75	33.48
	0.030	44.40	55.34	10.94	24.65
	0.040	56.80	65.29	8.49	14.95
	0.050	65.20	73.59	8.39	12.87
	0.075	83.00	89.40	6.40	7.71
	0.100	97.00	100.76	3.76	3.87
	0.150	119.60	116.41	-3.19	-2.67
	0.200	134.70	126.60	-8.10	-6.01
n-Propanol-	0.300	145.40	136.17	-9.23	-6.35
n-Hexane	0.400	146.60	137.71	-8.89	-6.07
	0.500	137.50	130.93	-6.57	-4.78
	0.600	120.60	118.70	-1.90	-1.57
	0.700	99.50	100.14	0.64	0.64
	0.800	72.80	74.59	1.79	2.46
	0.850	57.40	59.63	2.23	3.89
	0.900	40.00	41.90	1.90	4.76
	0.950	20.60	22.19	1.59	7.74

* Source of experimental data is given in Table I.
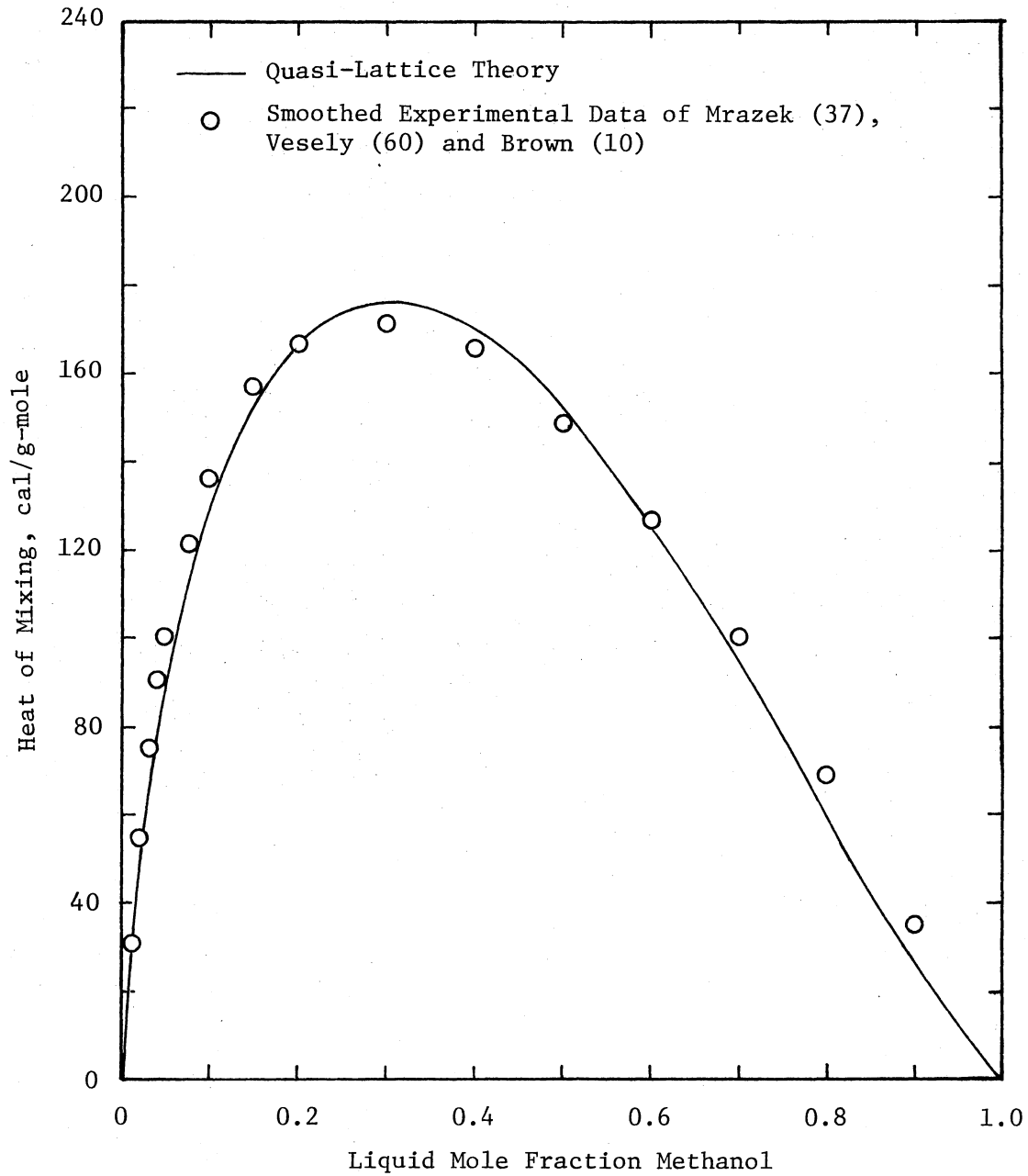
Figure 64. Heat of Mixing at 25°C for the System
Methanol(1)-Benzene(2) by the
Quasi-Lattice Theroy
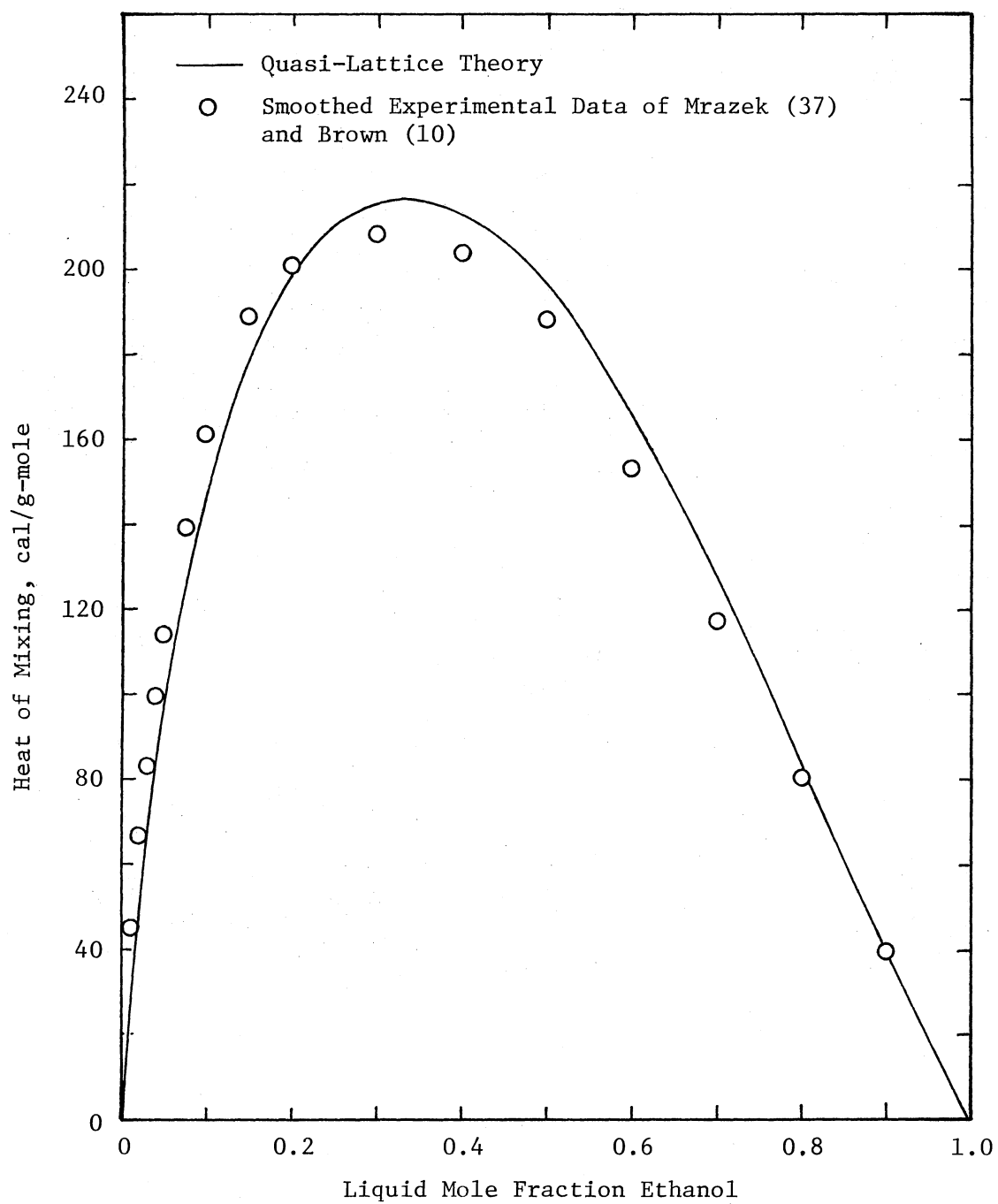
Figure 65. Heat of Mixing at 25°C for the System
Ethanol(1)-Benzene(2) by the
Quasi-Lattice Theory
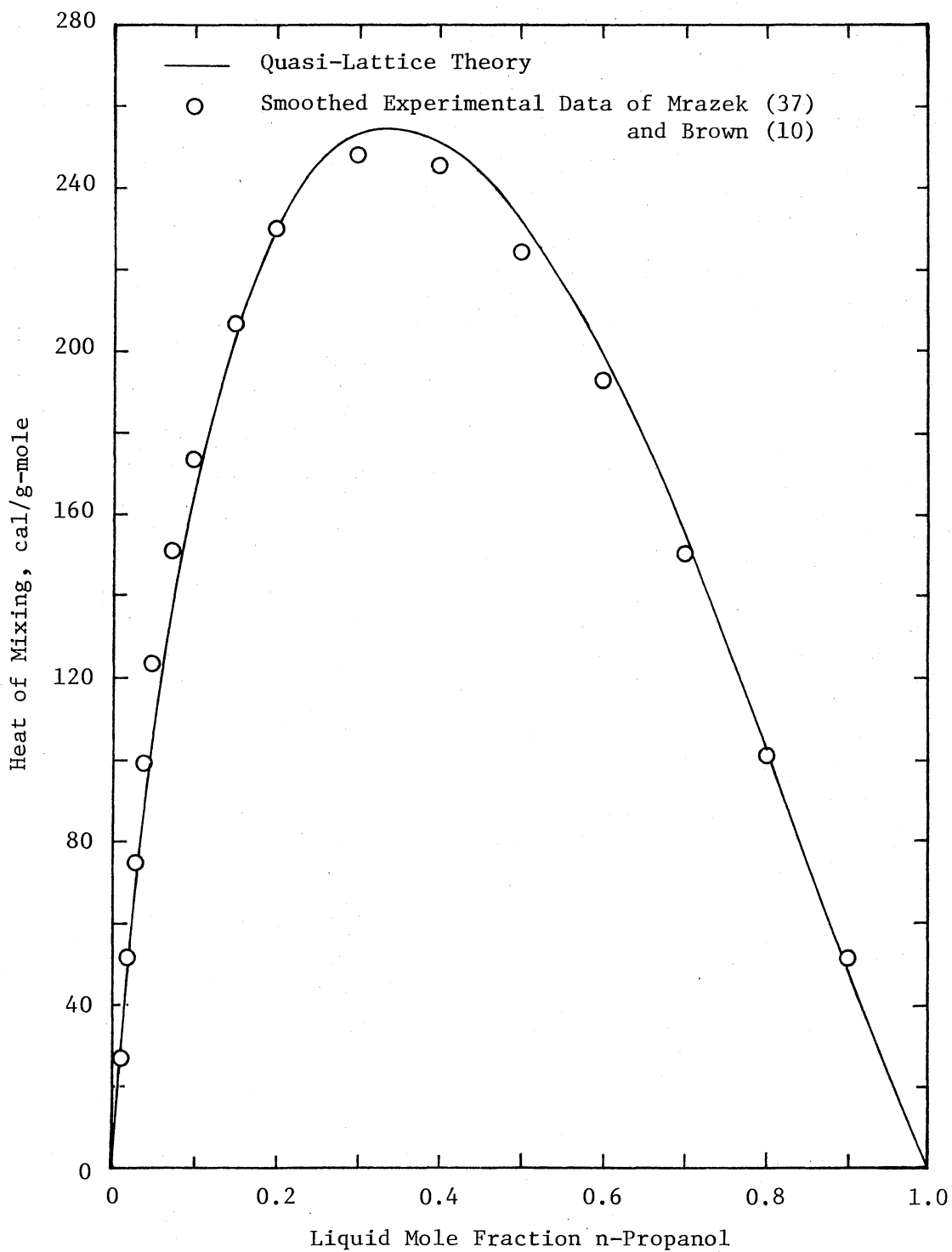
Figure 66. Heat of Mixing at 25°C for the System
n-Propanol(1)-Benzene(2) by the
Quasi-Lattice Theory
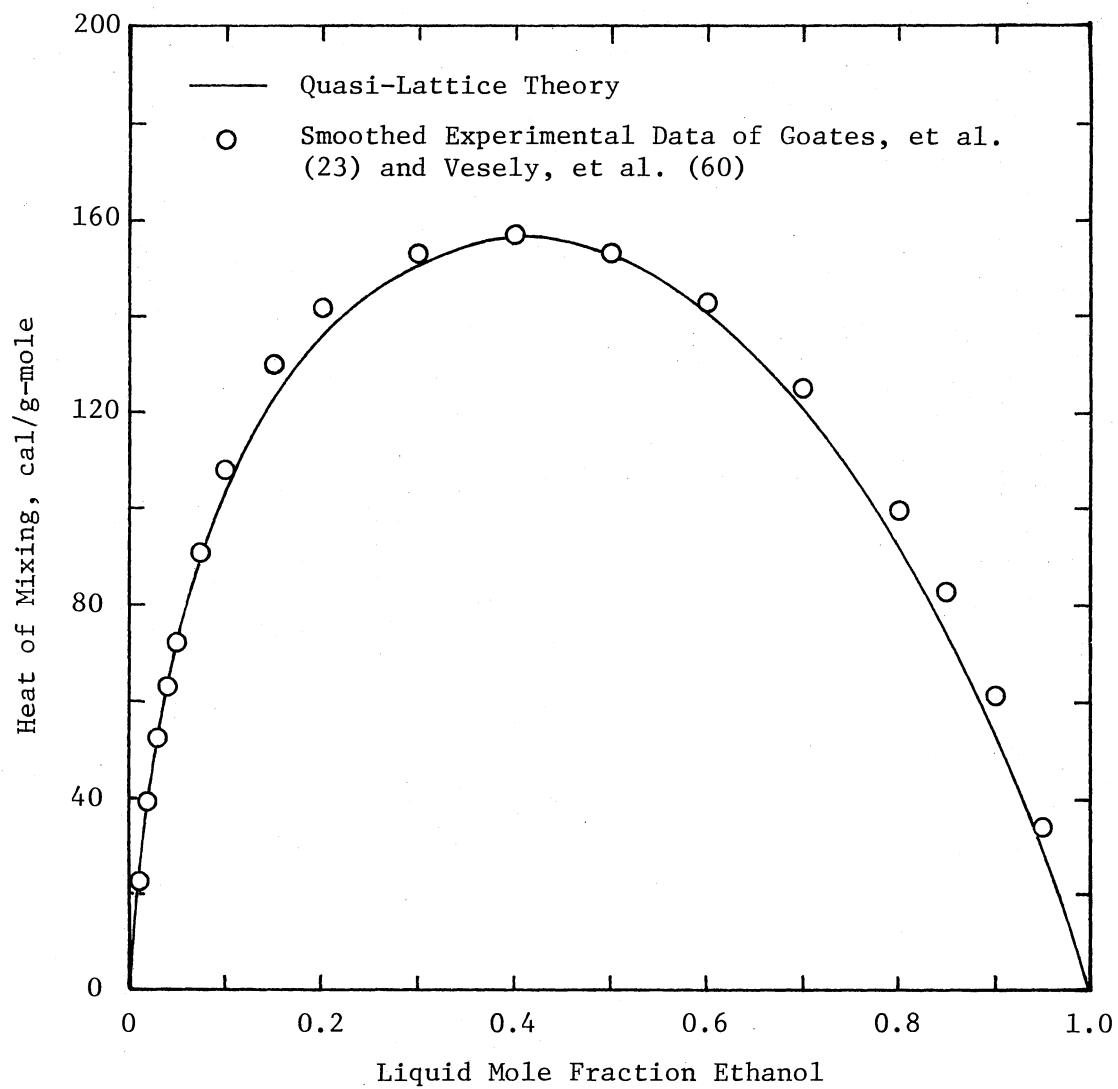
Figure 67. Heat of Mixing at $25^{\circ}C$ for the System
Ethanol(1)-Cyclohexane(2) by
the Quasi-Lattice Theory
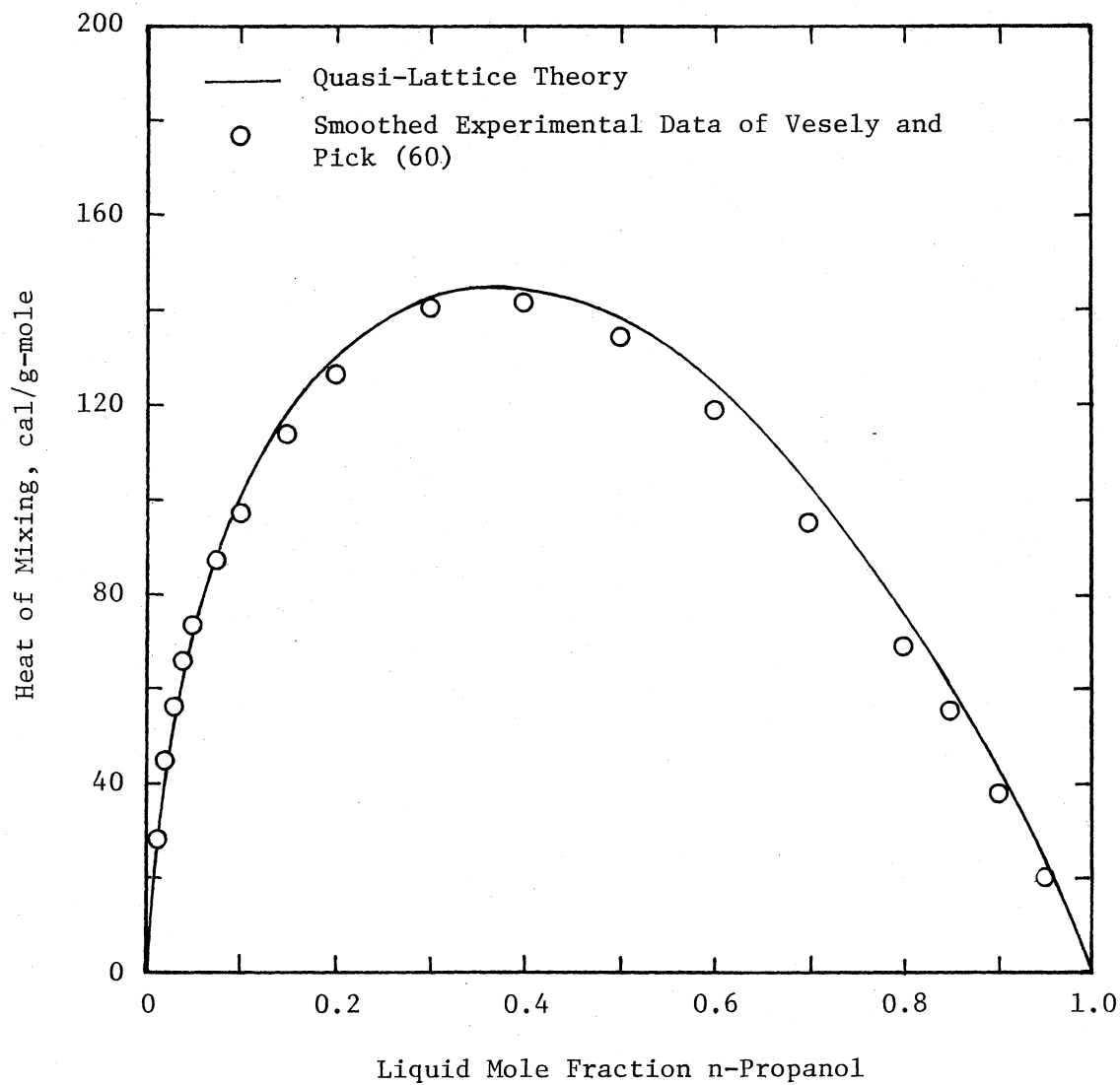
Figure 68. Heat of Mixing at $25^{\circ}C$ for the System
n-Propanol(1)-Cyclohexane(2) by
the Quasi-Lattice Theory
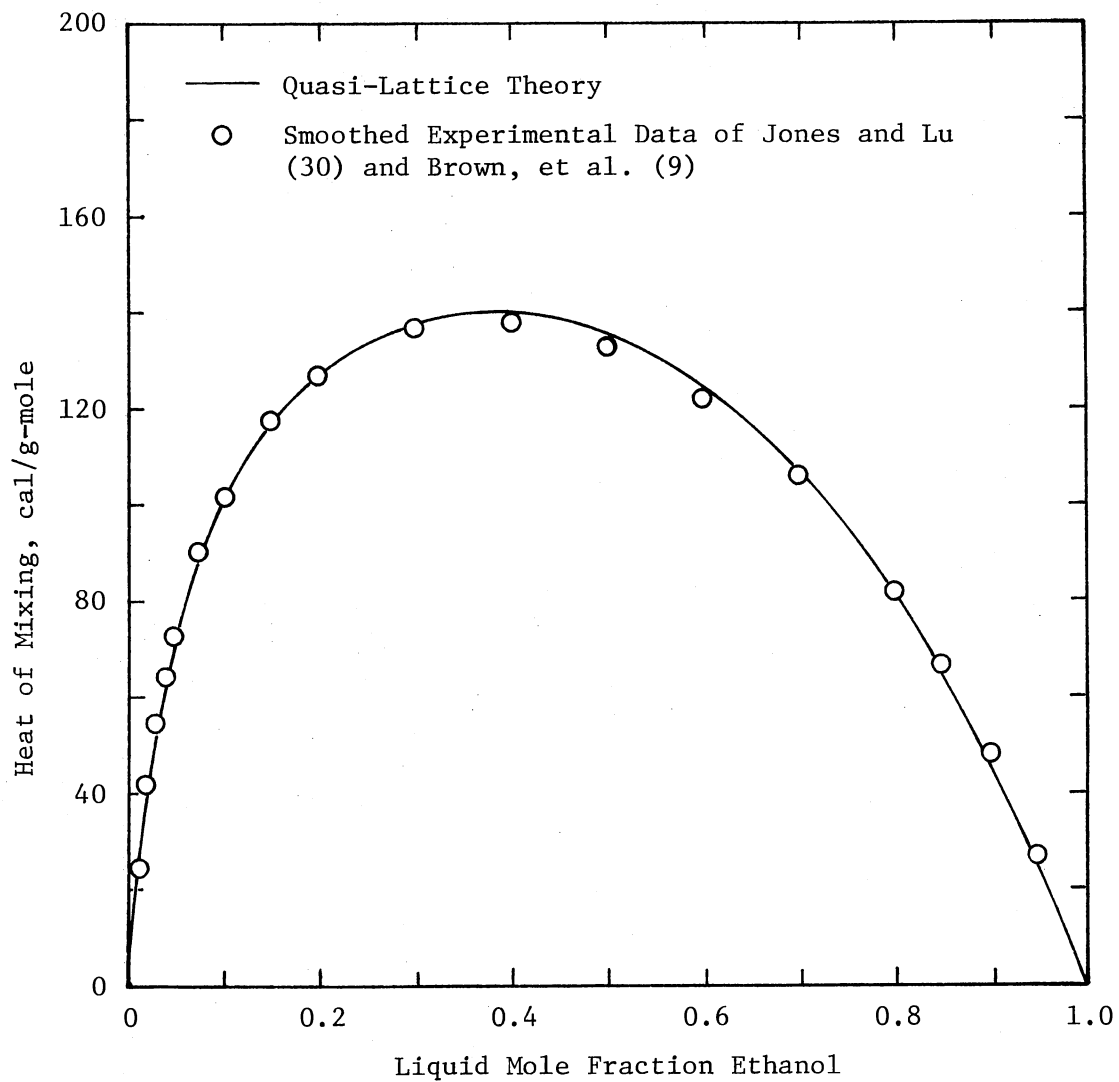
Figure 69. Heat of Mixing at 25°C for the System
Ethanol(1)-n-Hexane(2) by the
Quasi-Lattice Theory
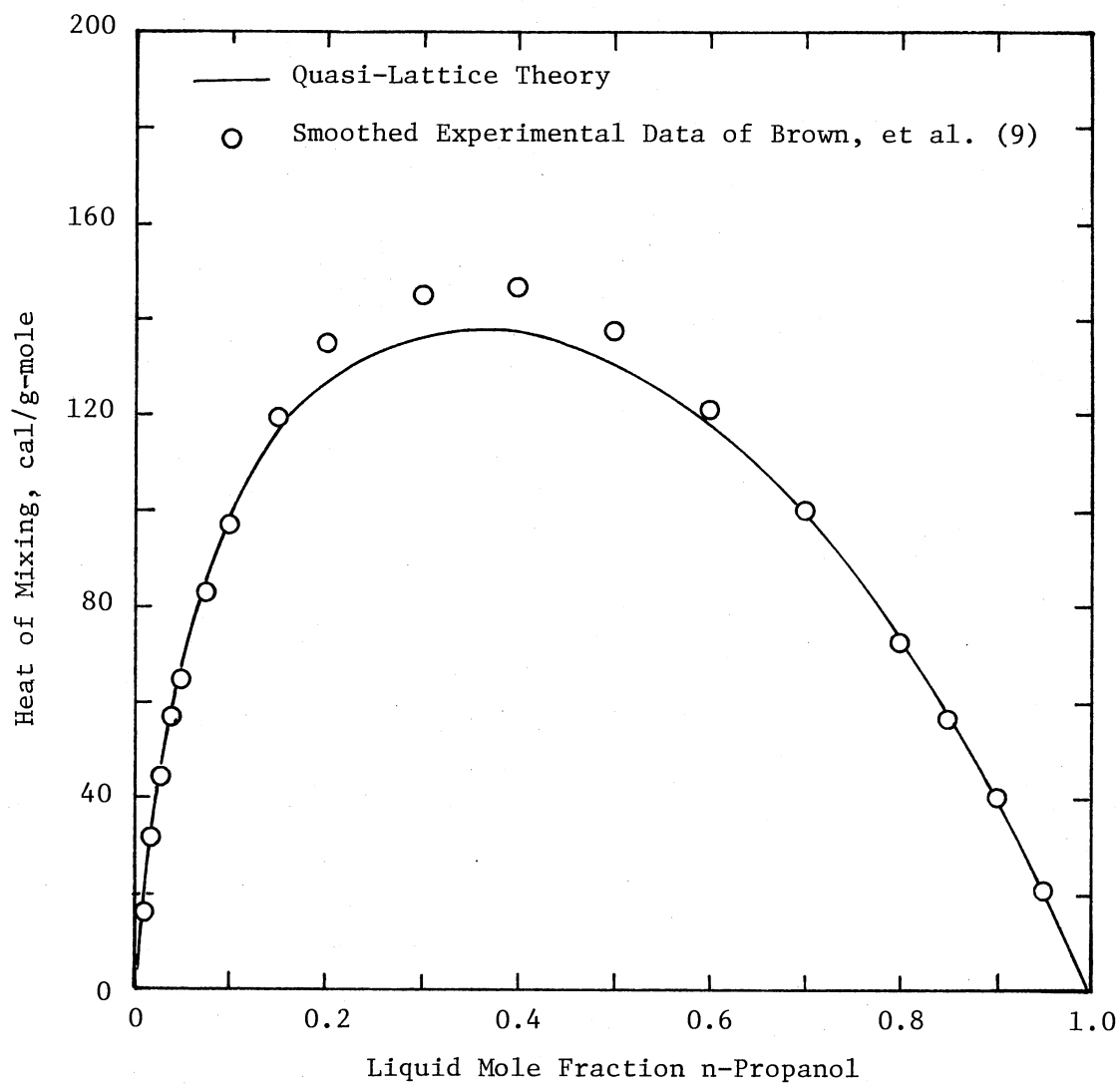
Figure 70.   Heat of Mixing at 25°C for the System
n-Propanol(1)-n-Hexane(2) by
the Quasi-Lattice Theory

The energy parameter values in Table XLVII were employed to represent the excess Gibbs free energies. Results based on the parameter set indicated by an asterisk are given in Table XLIX to compare with the values obtained by Mixon's method from experimental P-x data. Graphical comparisons are shown in Figures 71 through 77 along with results from the UNIQUAC and ASOG methods which will be discussed in next sections. These figures show that, except for the methanol-benzene system, the predicted values are higher than those obtained by Mixon's method from experimental P-x data. The predicted excess Gibbs free energies were used to calculate predicted VLE behavior by Mixon's method.

Universal Quasi-Chemical (UNIQUAC) Equation

Equations II-30 to II-32 give the excess Gibbs free energy for a binary system in terms of two adjustable binary energy parameters and two pure-component structure parameters per component, size parameter r and surface parameter q. The energy parameters and structure parameters given in Abrams' paper (3) were used to predict the excess Gibbs free energies for the systems methanol-benzene and ethanol-n-hexane. Results fo the calculation are shown in Table L and for the purpose of ease in comparison, in Figures 71 and 76. For both systems, results show that the predicted and experimental G^E-x data agree qualitatively, but that the predicted G^E values are lower than the experimental values.

TABLE XLIX

EXCESS GIBBS FREE ENERGY AT 25°C
BY THE QUASI-LATTICE THEORY

System	Mole Fraction Alcohol	G^E, cal/g-mole		Deviation	
		Expt'l	Calc'd	cal/g-mole	%
	0.010	16.00	16.34	0.34	2.10
	0.020	34.20	32.67	-1.53	-4.47
	0.030	52.10	50.67	-1.43	-2.74
	0.040	68.80	64.86	-3.94	-5.73
	0.050	81.90	75.36	-6.54	-7.98
	0.075	117.00	105.51	-11.49	-9.82
	0.100	142.80	134.70	-8.10	-5.67
	0.125	168.10	155.39	-12.71	-7.56
Methanol-	0.150	189.60	175.94	-13.66	-7.21
Benzene	0.175	210.00	196.81	-13.19	-6.28
	0.200	225.90	212.76	-13.14	-5.82
	0.300	274.30	258.28	-16.02	-5.84
	0.400	296.30	276.03	-20.27	-6.84
	0.500	296.50	275.64	-20.86	-7.04
	0.600	279.30	253.99	-25.31	-9.06
	0.700	245.20	211.52	-33.68	-13.74
	0.800	189.40	152.99	-36.41	-19.22
	0.900	108.80	79.69	-29.11	-26.75
	0.010	16.10	20.26	4.16	25.85
	0.020	31.00	34.75	3.75	12.08
	0.030	45.10	50.93	5.83	12.92
	0.040	58.30	68.91	10.61	18.20
	0.050	71.50	83.21	11.71	16.37
	0.075	100.00	112.91	12.91	12.91
	0.100	124.20	144.23	20.03	16.13
	0.125	146.00	169.53	23.53	16.12
Ethanol-	0.150	164.60	189.51	24.91	15.14
Benzene	0.175	182.10	209.47	27.37	15.03
	0.200	196.50	229.41	32.91	16.75
	0.300	238.00	277.27	39.27	16.50
	0.400	260.50	301.25	40.75	15.64
	0.500	263.00	298.25	35.25	13.40
	0.600	248.00	275.03	27.03	10.90
	0.700	215.40	230.94	15.54	7.21
	0.800	165.60	168.00	2.40	1.45
	0.900	94.70	90.52	-4.18	-4.41

TABLE XLIX (Continued)

System	Mole Fraction Alcohol	G^E, cal/g-mole		Deviation	
		Expt'l	Calc'd	cal/g-mole	%
	0.010	13.10	18.68	5.58	42.57
	0.020	24.00	40.14	16.14	67.24
	0.030	36.00	57.48	21.48	59.67
	0.040	46.10	73.83	27.73	60.16
	0.050	59.20	89.26	30.06	50.78
	0.075	82.00	124.36	42.36	51.66
	0.100	103.40	155.31	51.91	50.20
	0.125	124.00	180.19	56.19	45.31
n-Propanol-	0.150	141.30	204.72	63.42	44.88
Benzene	0.175	156.50	228.89	72.39	46.25
	0.200	171.90	245.39	73.49	42.75
	0.300	213.70	299.75	86.05	40.27
	0.400	235.90	323.22	87.32	37.02
	0.500	240.70	321.36	80.66	33.51
	0.600	229.00	294.38	65.38	28.55
	0.700	201.00	245.89	44.89	22.33
	0.800	154.20	179.10	24.90	16.15
	0.900	87.30	96.65	9.35	10.70
	0.010	18.90	22.62	3.72	19.70
	0.020	38.00	43.86	5.86	15.43
	0.030	55.10	66.01	10.91	19.80
	0.040	71.90	81.03	9.13	12.70
	0.050	87.30	100.42	13.12	15.03
	0.075	121.00	137.75	16.75	13.84
	0.100	151.80	170.20	18.40	12.12
	0.150	202.30	224.02	21.72	10.74
Ethanol-	0.200	242.30	263.72	21.42	8.84
Cyclohexane	0.300	296.60	324.47	27.87	9.40
	0.400	325.20	351.04	25.84	7.95
	0.500	331.60	354.34	22.74	6.86
	0.600	315.30	334.56	19.26	6.11
	0.700	276.60	289.51	12.91	4.67
	0.800	213.40	220.37	6.97	3.26
	0.850	171.50	176.49	4.99	2.91
	0.900	122.30	124.79	2.49	2.04
	0.950	67.30	65.14	-2.16	-3.21

TABLE XLIX (Continued)

System	Mole Fraction Alcohol	G^E, cal/g-mole		Deviation	
		Expt'l	Calc'd	cal/g-mole	%
	0.010	17.50	24.67	7.17	40.97
	0.020	35.50	42.23	6.73	18.94
	0.030	52.80	60.67	7.87	14.91
	0.040	68.00	80.46	12.46	18.33
	0.050	83.80	93.45	9.65	11.52
	0.075	115.90	131.30	15.40	13.28
	0.100	142.80	158.86	16.06	11.25
	0.150	186.30	208.56	22.26	11.95
n-Propanol-	0.200	222.20	249.17	26.97	12.14
Cyclohexane	0.300	269.30	299.08	29.78	11.06
	0.400	293.00	319.18	26.18	8.94
	0.500	295.50	318.08	22.58	7.64
	0.600	278.00	293.80	15.80	5.68
	0.700	240.50	249.79	9.29	3.86
	0.800	182.40	185.17	2.77	1.52
	0.850	145.70	146.89	1.19	0.81
	0.900	104.20	103.09	-1.11	-1.07
	0.950	55.70	52.40	-3.30	-5.92
	0.010	19.30	22.06	2.76	14.28
	0.020	36.90	45.97	9.07	24.57
	0.030	53.60	61.81	8.21	15.33
	0.040	70.00	82.30	12.30	17.57
	0.050	86.70	98.56	11.86	13.68
	0.075	121.10	134.95	13.85	11.43
	0.100	149.80	163.73	13.93	9.30
	0.150	200.00	216.49	16.49	8.24
Ethanol-	0.200	239.40	257.98	18.58	7.76
n-Hexane	0.300	295.80	315.15	19.35	6.54
	0.400	326.10	346.07	19.97	6.12
	0.500	332.40	348.97	16.57	4.99
	0.600	316.30	327.41	11.11	3.51
	0.700	277.50	286.55	9.05	3.26
	0.800	214.80	219.69	4.89	2.28
	0.850	173.70	177.47	3.77	2.17
	0.900	124.70	126.06	1.36	1.09
	0.950	67.50	67.09	-0.41	-0.60

TABLE XLIX (Continued)

System	Mole Fraction Alcohol	G^E, cal/g-mole		Deviation	
		Expt'l	Calc'd	cal/g-mole	%
	0.010	18.20	24.39	6.19	34.02
	0.020	36.00	44.39	8.39	23.31
	0.030	53.10	62.53	9.43	17.76
	0.040	69.30	79.16	9.86	14.23
	0.050	85.00	91.59	6.59	7.75
	0.075	116.00	126.12	10.12	8.72
	0.100	144.40	158.87	14.47	10.02
	0.150	190.50	207.71	17.21	9.04
n-Propanol-	0.200	227.40	242.67	15.27	6.71
n-Hexane	0.300	278.50	294.89	16.39	5.89
	0.400	204.80	315.76	10.96	3.60
	0.500	309.50	316.04	6.54	2.11
	0.600	293.90	293.03	-0.87	-0.30
	0.700	257.60	250.28	-7.32	-2.84
	0.800	199.10	187.98	-11.12	-5.58
	0.850	161.10	148.36	-12.74	-7.91
	0.900	116.30	104.61	-11.69	-10.05
	0.950	63.00	55.06	-7.94	-12.60
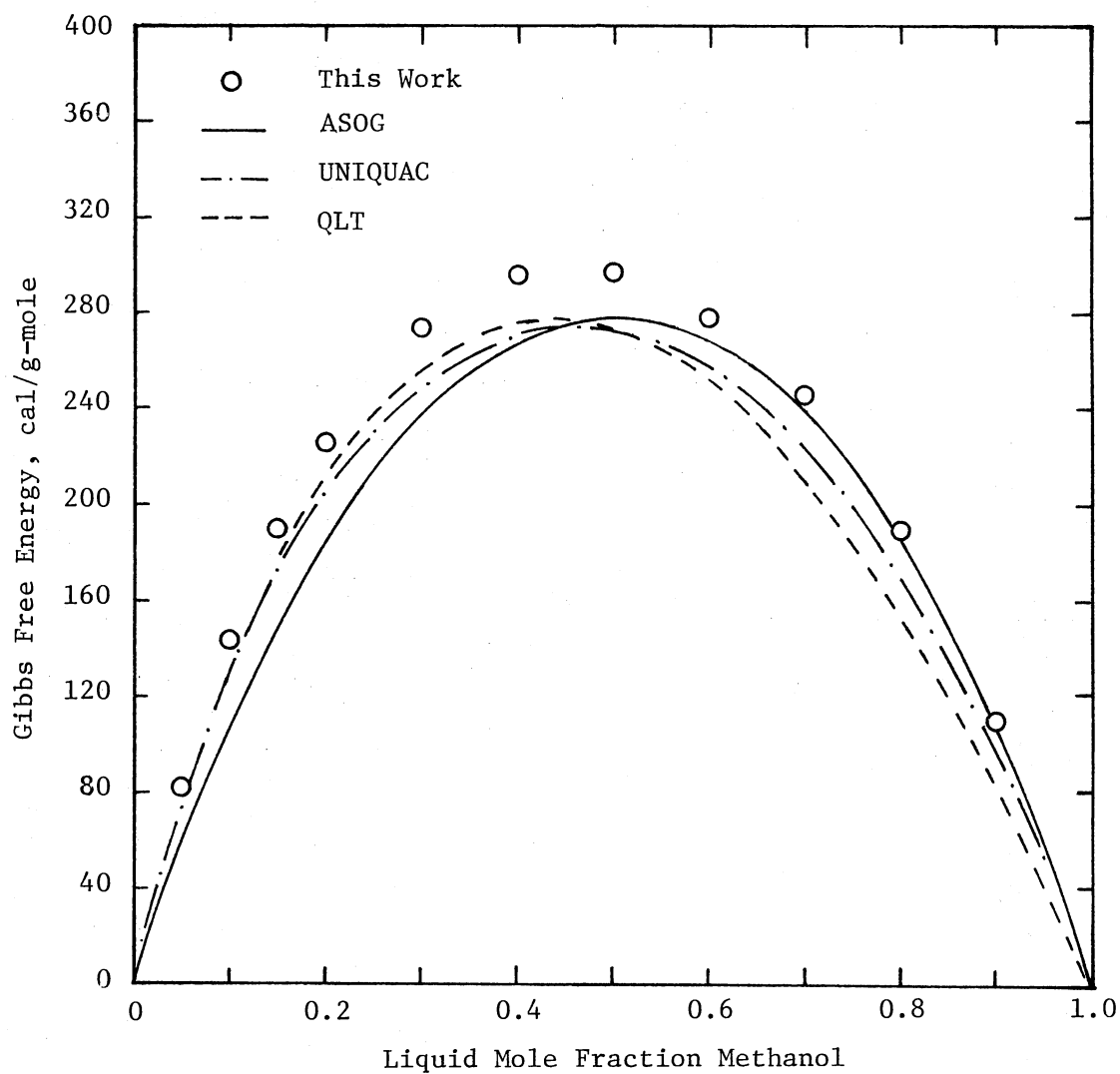
Figure 71. Excess Gibbs Free Energy at 25°C for
the System Methanol(1)-Benzene(2)
by the Group Contribution Theories
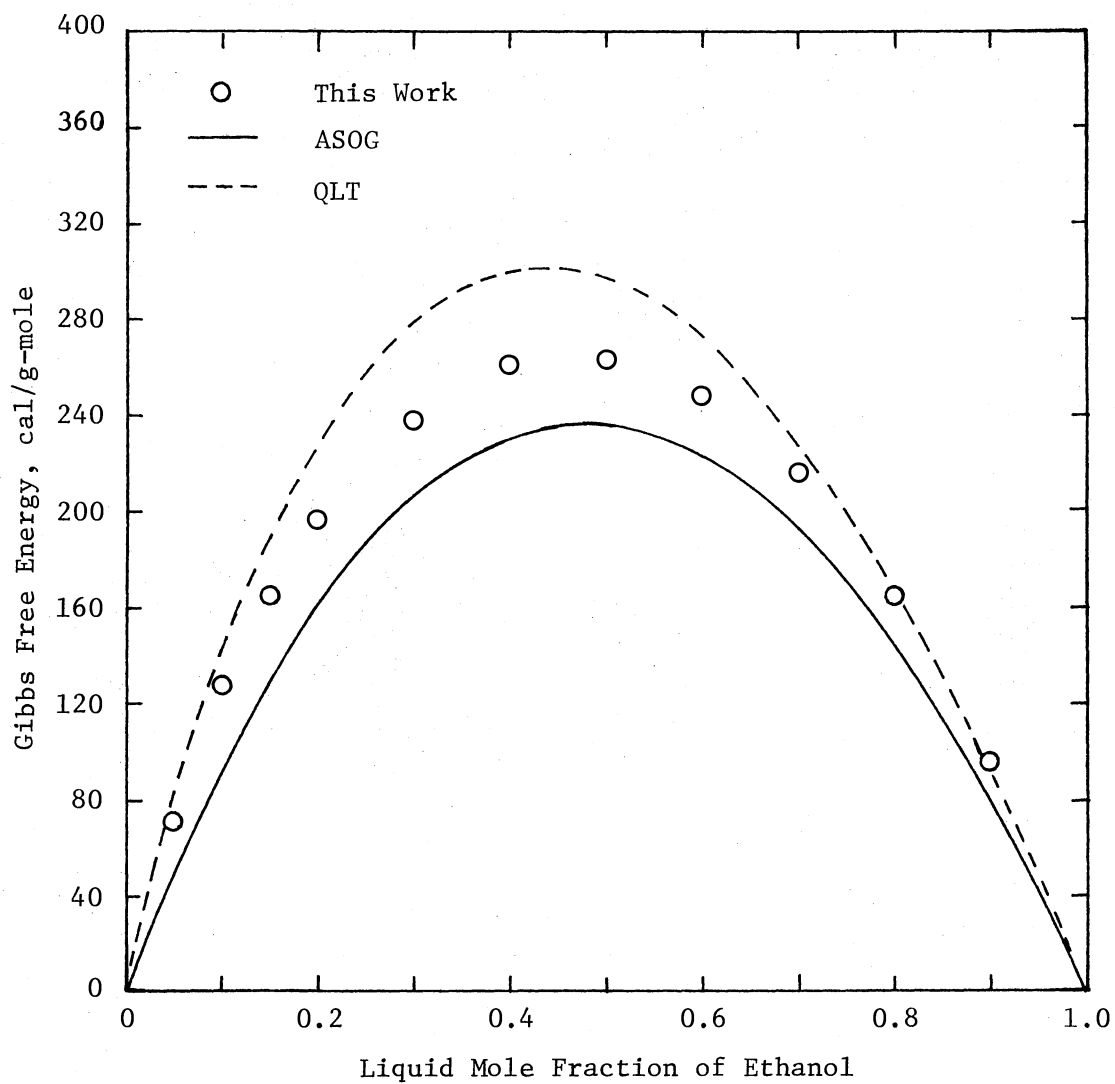
Figure 72. Excess Gibbs Free Energy at 25°C for
the System Ethanol(1)-Benzene
(2) by the Group Contribution
Theories
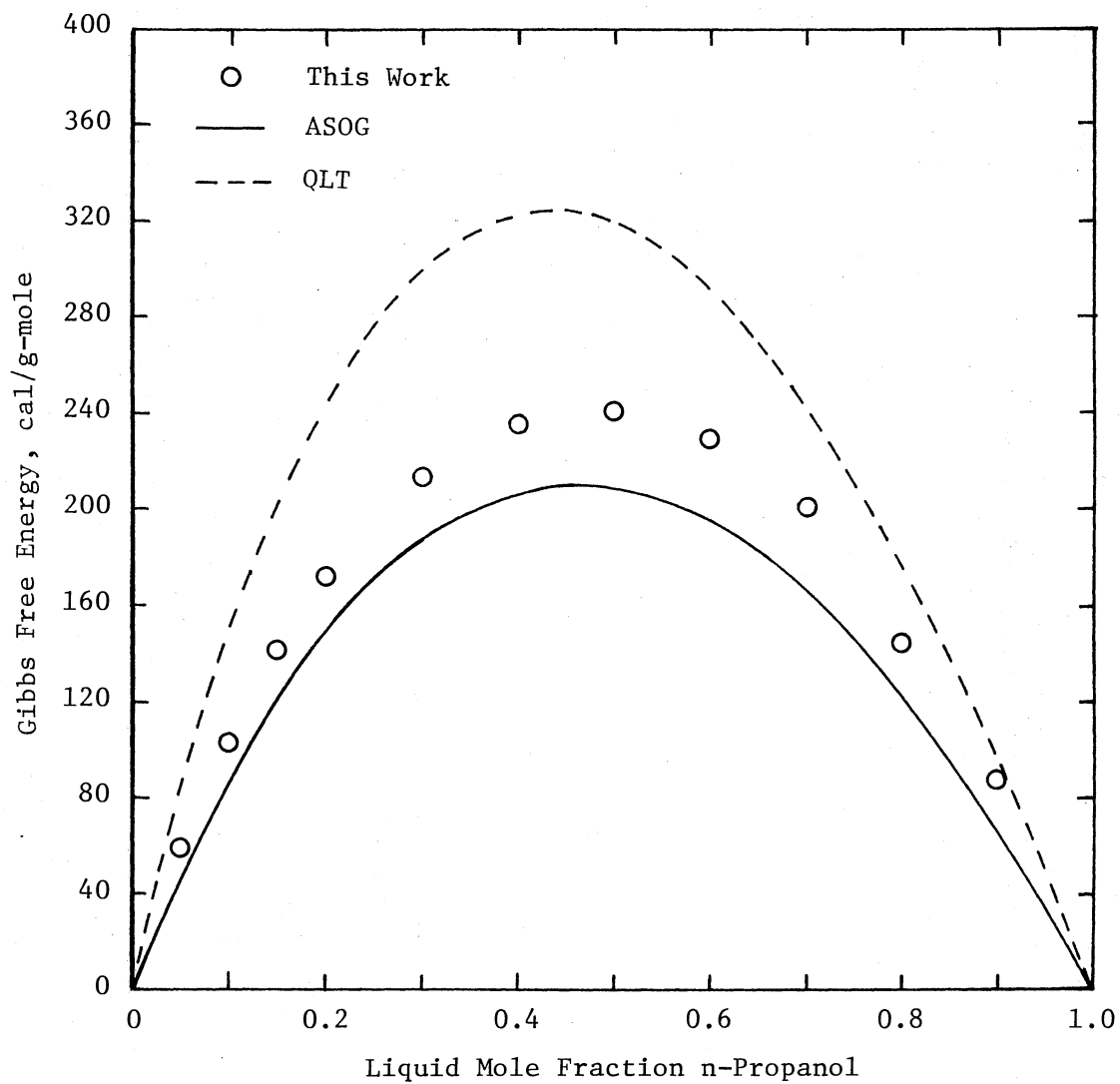
Figure 73. Excess Gibbs Free Energy at 25°C for
the System n-Propanol(1)-Benzene
(2) by the Group Contribution
Theories
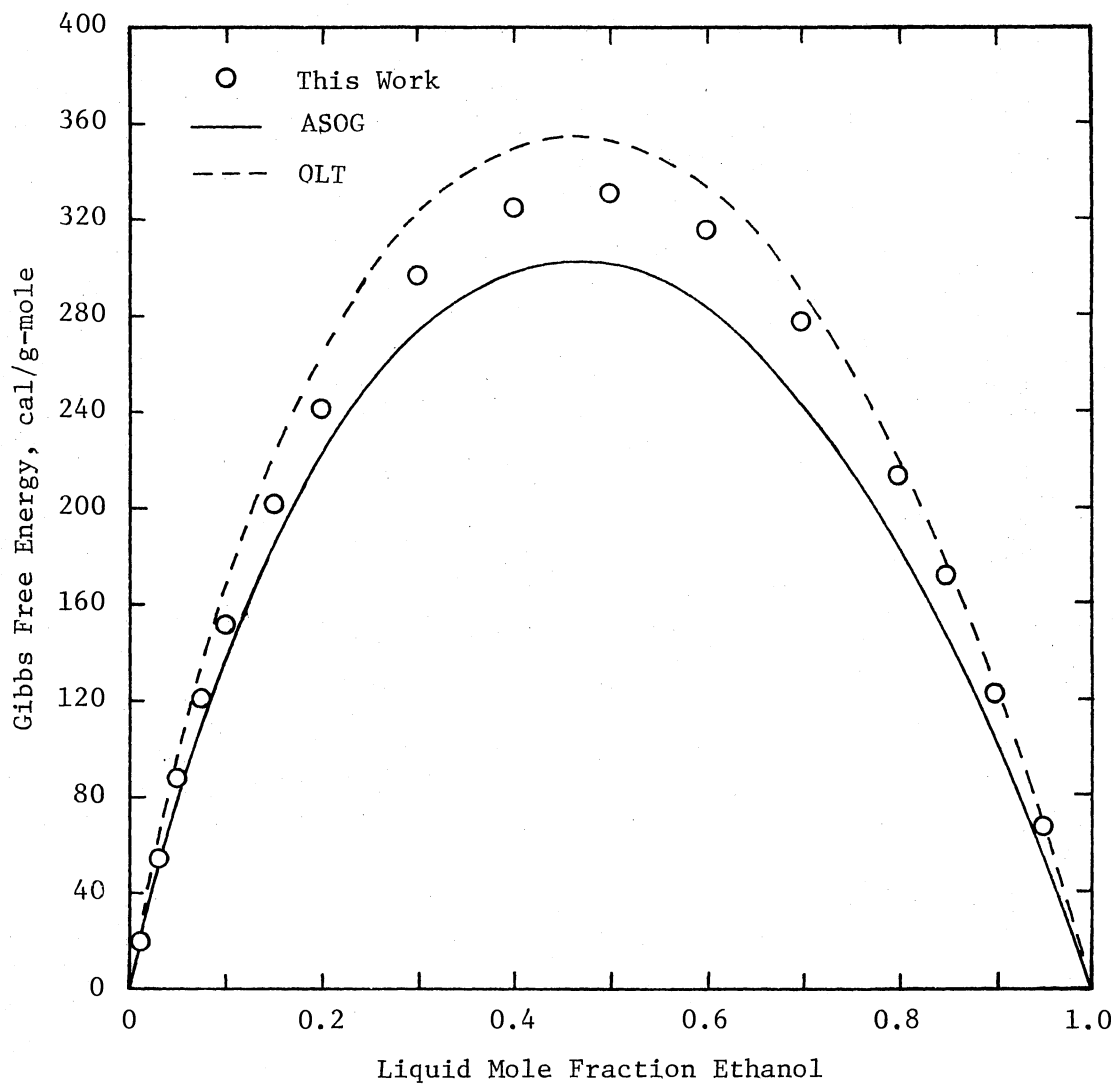
Figure 74. Excess Gibbs Free Energy at 25°C for
the System Ethanol(1)-Cyclohexane
(2) by the Group Contribution
Theories
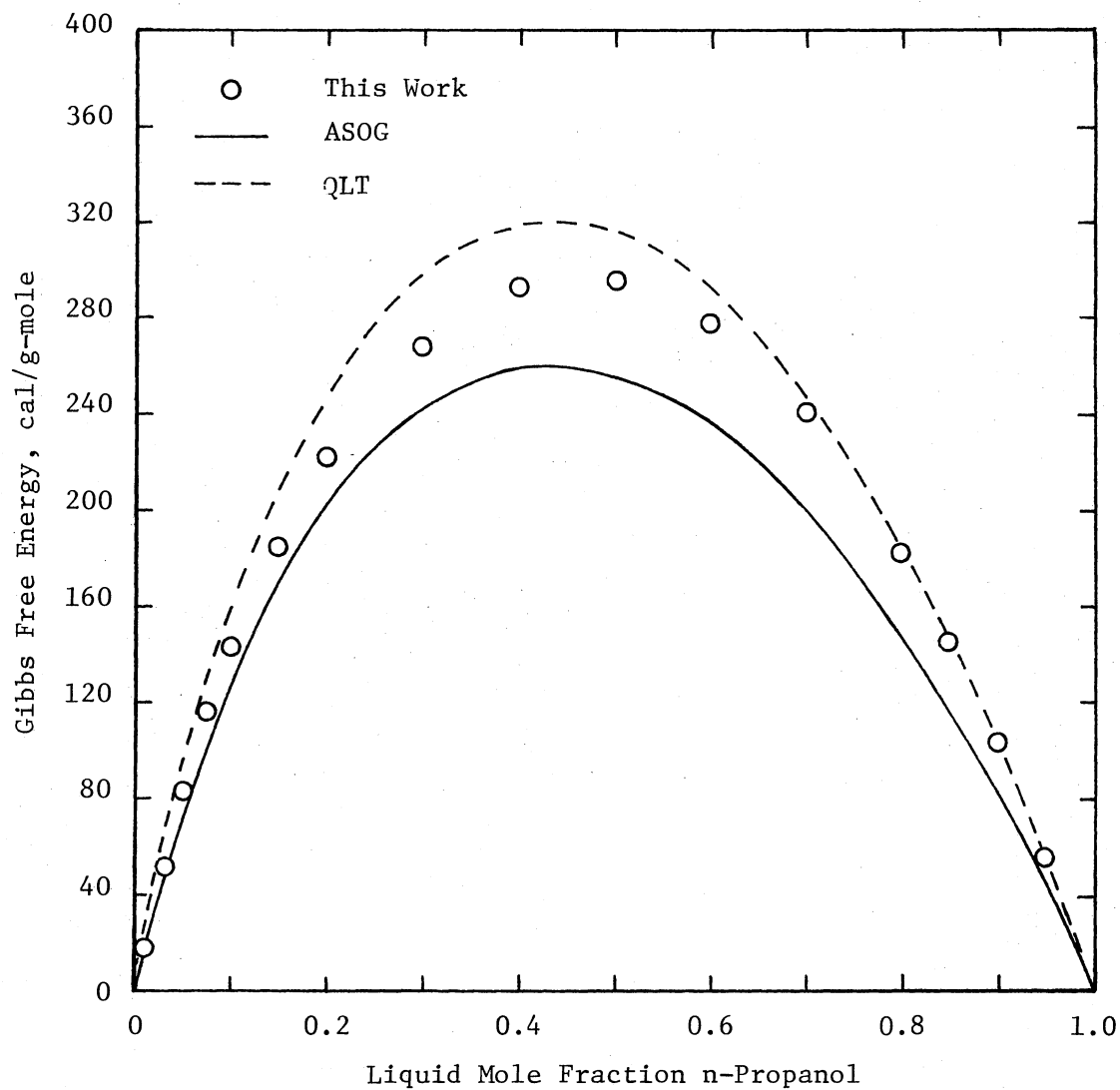
Figure 75. Excess Gibbs Free Energy at 25°C for the System n-Propanol(1)-Cyclohexane(2) by the Group Contribution Theories
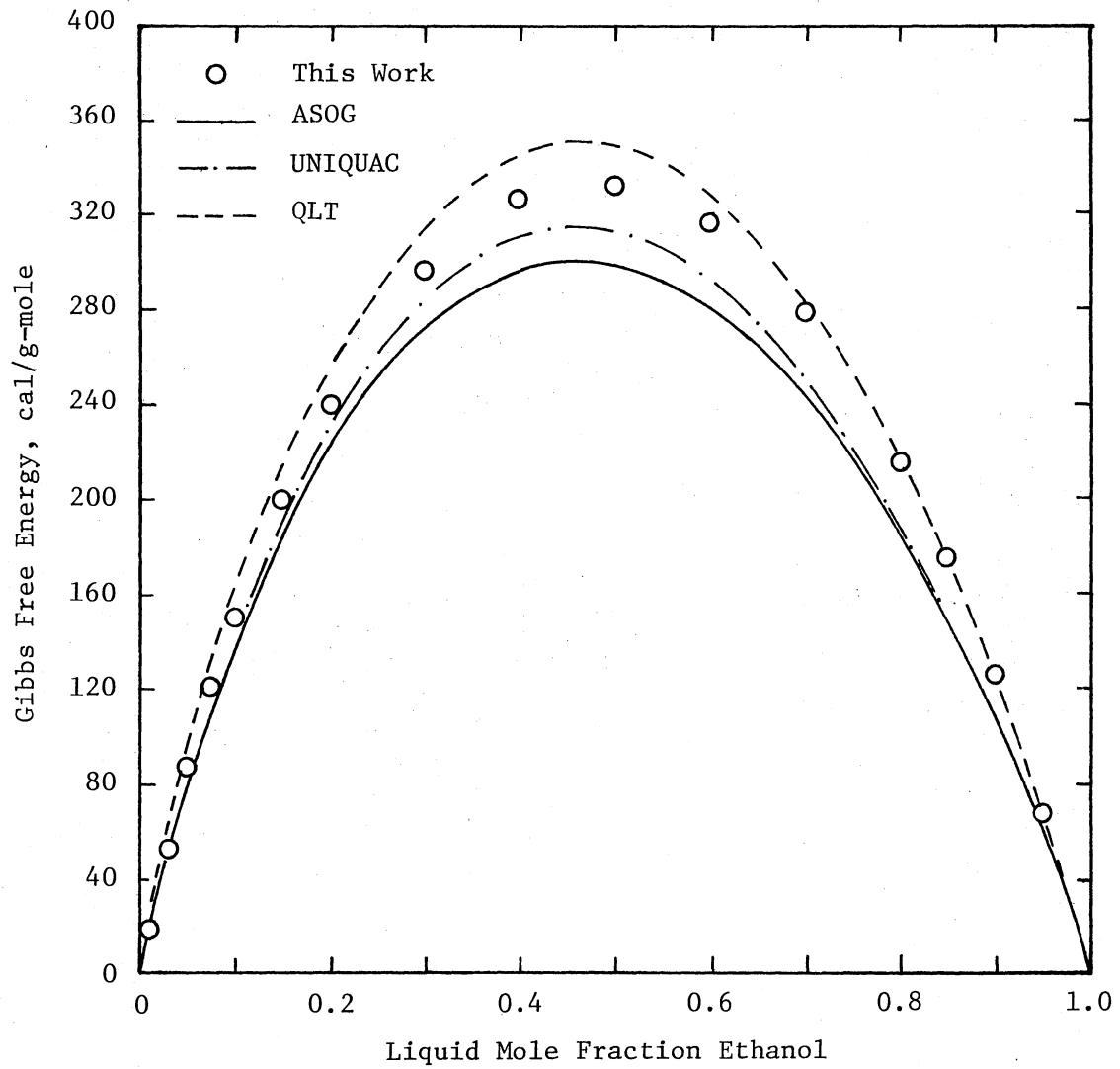
Figure 76. Excess Gibbs Free Energy at 25°C for the System Ethanol(1)-n-Hexane (2) by the Group Contribution Theories
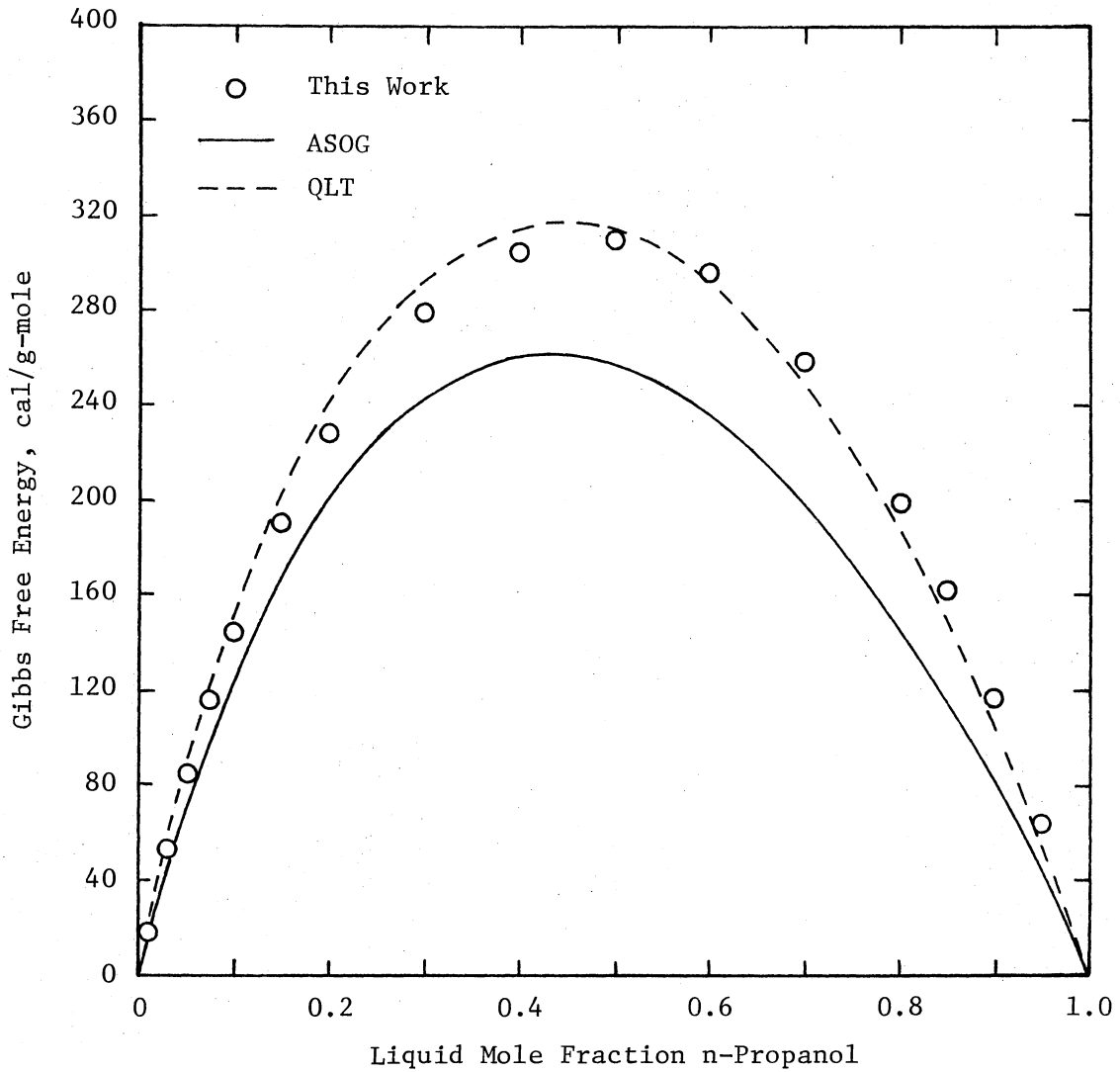
Figure 77. Excess Gibbs Free Energy at 25°C for
the System n-Propanol(1)-n-Hexane
(2) by the Group Contribution
Theories

TABLE L

EXCESS GIBBS FREE ENERGY AT 25°C
BY THE UNIQUAC EQUATION

System	Mole Fraction Alcohol	G^E, cal/g-mole		Deviation	
		Expt'l	Calc'd	cal/g-mole	%
	0.05	81.93	73.90	-8.03	-9.81
	0.10	142.84	129.73	-13.11	-9.18
	0.15	189.64	172.66	-16.98	-8.95
	0.20	225.90	205.77	-20.13	-8.91
	0.25	253.74	231.00	-22.74	-8.96
	0.30	274.30	249.67	-24.64	-8.98
	0.35	288.28	262.67	-25.61	-8.88
	0.40	296.28	270.64	-25.64	-8.65
Methanol-	0.45	299.01	274.00	-25.01	-8.36
Benzene	0.50	296.52	273.01	-23.51	-7.93
	0.55	290.12	267.80	-22.32	-7.69
	0.60	279.34	258.40	-20.93	-7.49
	0.65	264.76	244.74	-20.02	-7.56
	0.70	245.15	226.64	-18.51	-7.55
	0.75	220.33	203.82	-16.51	-7.49
	0.80	189.35	175.88	-13.47	-7.11
	0.85	152.55	142.30	-10.26	-6.72
	0.90	108.77	102.41	-6.37	-5.85
	0.95	58.71	55.34	-3.38	-5.75
	0.05	86.67	76.57	-10.11	-11.66
	0.10	149.83	139.11	-10.72	-7.15
	0.15	200.01	189.80	-10.20	-5.10
	0.20	239.41	230.29	-9.12	-3.81
	0.25	270.69	261.84	-8.85	-3.27
	0.30	295.87	285.44	-10.43	-3.52
	0.35	314.41	301.86	-12.55	-3.99
	0.40	326.20	311.73	-14.47	-4.43
	0.45	332.42	315.53	-16.89	-5.08
Ethanol-	0.50	332.42	313.62	-18.80	-5.66
n-Hexane	0.55	327.33	306.27	-21.06	-6.43
	0.60	316.31	293.66	-22.64	-7.16
	0.65	299.95	275.91	-24.04	-8.02
	0.70	277.50	253.05	-24.45	-8.81
	0.75	249.42	225.01	-24.40	-9.78
	0.80	214.82	191.69	-23.13	-10.77
	0.85	173.65	152.88	-20.76	-11.96
	0.90	124.65	108.29	-16.36	-13.12
	0.95	67.54	57.50	-10.04	-14.87

Analytical Solutions of Groups (ASOG) Method

The step-by-step calculation method outlined by Palmer (40) was applied to calculate the activity coefficients for the binary systems studied. The size groups and interaction parameters for each function group given by Derr and Deal (18) were used for calculation. The excess Gibbs free energy was then calculated by the following equation:

$$G^E = RT \sum_{i=1}^{2} x_i \ln (\gamma_i) \qquad \text{(VII-1)}$$

Results of the calculated excess Gibbs free energy are listed in Table LI. Graphical comparisons are shown in Figures 71 through 77. Qualitative agreement can be achieved between the predicted and experimental G^E-x data. However, the predicted values are lower than the experimental values.

Vapor-Liquid Equilibrium Predictions

Mixon's method, discussed in previous chapters, was employed for predicting phase equilibrium relationships for binary systems. The G^E-x data obtained from the group contribution theories together with an equation of state and vapor-nonideality corrections were used to predict the binary system vapor pressures and vapor phase compositions.

Results of calculations are shown in Tables LII through LIV. Graphical comparisons are shown in Figures 78 through 86 for P-x data and in Figures 87 through 95 for y-x data.

TABLE LI

EXCESS GIBBS FREE ENERGY AT 25^OC
BY THE ASOG METHOD

System	Mole Fraction Alcohol	G^E, cal/g-mole		Deviation	
		Expt'l	Calc'd	cal/g-mole	%
Methanol–Benzene	0.05	81.93	57.62	−24.31	−29.67
	0.10	142.84	106.99	−35.85	−25.10
	0.15	189.64	149.06	−40.58	−21.40
	0.20	225.90	184.54	−41.36	−18.31
	0.25	253.74	213.94	−39.80	−15.69
	0.30	274.30	237.65	−36.65	−13.36
	0.35	288.28	255.94	−32.34	−11.22
	0.40	296.28	269.02	−27.26	−9.20
	0.45	299.01	277.00	−22.01	−7.36
	0.50	296.52	279.95	−16.57	−5.59
	0.55	290.12	277.88	−12.24	−4.22
	0.60	279.34	270.75	−8.59	−3.08
	0.65	264.76	258.43	−6.33	−2.39
	0.70	245.15	240.76	−4.39	−1.79
	0.75	220.33	217.50	−2.83	−1.28
	0.80	189.34	188.28	−1.06	−0.56
	0.85	152.55	152.66	0.11	0.07
	0.90	108.77	110.01	1.24	1.14
	0.95	58.71	59.51	0.80	1.36
Ethanol–Benzene	0.05	71.51	52.23	−19.28	−26.96
	0.10	124.18	96.29	−27.89	−22.46
	0.15	164.64	133.22	−31.42	−19.08
	0.20	196.51	163.76	−32.75	−16.67
	0.25	220.33	188.48	−31.85	−14.46
	0.30	238.04	207.80	−30.24	−12.70
	0.35	251.79	222.06	−29.73	−11.81
	0.40	260.50	231.51	−28.99	−11.13
	0.45	263.93	236.34	−27.59	−10.45
	0.50	262.99	236.70	−26.29	−10.00
	0.55	257.65	232.69	−24.96	−9.69
	0.60	248.00	224.37	−23.63	−9.53
	0.65	233.30	211.78	−21.52	−9.22
	0.70	215.41	194.91	−20.50	−9.52
	0.75	192.31	173.74	−18.57	−9.66
	0.80	165.59	148.20	−17.39	−10.50
	0.85	132.59	118.20	−14.39	−10.85
	0.90	94.73	83.62	−11.11	−11.73
	0.95	50.89	44.29	−6.60	−12.97

TABLE LI (Continued)

System	Mole Fraction Alcohol	G^E, cal/g-mole		Deviation	
		Expt'l	Calc'd	cal/g-mole	%
	0.05	59.24	48.44	−10.80	−18.23
	0.10	103.44	88.80	−14.64	−14.15
	0.15	141.30	122.16	−19.14	−13.55
	0.20	171.93	149.33	−22.60	−13.14
	0.25	194.80	170.90	−23.90	−12.27
	0.30	213.69	187.34	−26.35	−12.33
	0.35	226.91	199.02	−27.89	−12.29
	0.40	235.85	206.25	−29.60	−12.55
n–Propanol–	0.45	240.41	209.26	−31.15	−12.96
Benzene	0.50	240.71	208.24	−32.47	−13.49
	0.55	236.74	203.36	−33.38	−14.10
	0.60	228.98	194.74	−34.24	−14.95
	0.65	216.95	182.49	−34.46	−15.88
	0.70	200.96	166.69	−34.27	−17.05
	0.75	180.04	147.41	−32.63	−18.12
	0.80	154.15	124.69	−29.46	−19.11
	0.85	122.99	98.58	−24.41	−19.85
	0.90	87.27	69.08	−18.19	−20.84
	0.95	45.62	36.23	−9.39	−20.58
	0.05	87.33	79.23	−8.10	−9.28
	0.10	151.84	139.37	−12.47	−8.21
	0.15	202.32	186.50	−15.82	−7.82
	0.20	242.25	223.60	−18.65	−7.70
	0.25	273.41	252.41	−21.00	−7.68
	0.30	296.64	274.02	−22.62	−7.63
	0.35	313.46	289.18	−24.28	−7.75
	0.40	325.19	298.43	−26.76	−8.23
Ethanol–	0.45	331.29	302.12	−29.17	−8.80
Cyclohexane	0.50	331.59	300.51	−31.08	−9.37
	0.55	326.32	293.78	−32.54	−9.97
	0.60	315.30	282.02	−33.28	−10.56
	0.65	298.83	265.28	−33.55	−11.23
	0.70	276.55	243.54	−33.01	−11.94
	0.75	248.12	216.73	−31.39	−12.65
	0.80	213.40	184.73	−28.67	−13.43
	0.85	171.51	147.34	−24.17	−14.09
	0.90	122.99	104.33	−18.66	−15.17
	0.95	67.30	55.36	−11.94	−17.74

TABLE LI (Continued)

System	Mole Fraction Alcohol	G^E, cal/g-mole		Deviation	
		Expt'l	Calc'd	cal/g-mole	%
	0.05	83.77	73.35	−10.42	−12.44
	0.10	142.78	127.78	−15.00	−10.51
	0.15	186.32	169.47	−16.85	−9.04
	0.20	222.17	201.47	−20.70	−9.32
	0.25	248.77	225.57	−23.20	−9.33
	0.30	269.27	242.91	−26.36	−9.79
	0.35	283.84	254.30	−29.54	−10.41
	0.40	292.96	260.29	−32.67	−11.15
n−Propanol−	0.45	296.64	261.33	−35.31	−11.90
Cyclohexane	0.50	295.45	257.74	−37.71	−12.76
	0.55	289.23	249.76	−39.47	−13.65
	0.60	278.03	237.59	−40.44	−14.55
	0.65	261.86	221.38	−40.48	−15.46
	0.70	240.53	201.22	−39.31	−16.34
	0.75	213.99	177.19	−36.80	−17.20
	0.80	182.35	149.35	−33.00	−18.10
	0.85	145.68	117.72	−27.96	−19.19
	0.90	104.15	82.30	−21.85	−20.98
	0.95	55.69	43.08	−12.61	−22.64
	0.05	86.67	79.23	−7.44	−8.58
	0.10	149.83	139.37	−10.46	−6.98
	0.15	200.01	186.50	−13.51	−6.75
	0.20	239.41	223.60	−15.81	−6.60
	0.25	270.69	252.41	−18.28	−6.75
	0.30	295.87	274.02	−21.85	−7.39
	0.35	314.41	289.18	−25.23	−8.02
	0.40	326.20	298.43	−27.77	−8.51
Ethanol−	0.45	332.42	302.12	−30.30	−9.11
n−Hexane	0.50	332.42	300.51	−31.91	−9.60
	0.55	327.32	293.78	−33.54	−10.25
	0.60	316.31	282.02	−34.29	−10.84
	0.65	299.95	265.28	−34.67	−11.56
	0.70	277.50	243.54	−33.96	−12.24
	0.75	249.42	216.73	−32.69	−13.11
	0.80	214.82	184.73	−30.09	−14.01
	0.85	173.65	147.34	−26.31	−15.15
	0.90	124.65	104.33	−20.32	−16.30
	0.95	67.54	55.36	−12.18	−18.03

TABLE LI (Continued)

System	Mole Fraction Alcohol	G^E, cal/g-mole		Deviation	
		Expt'l	Calc'd	cal/g-mole	%
	0.05	84.96	73.35	-11.61	-13.67
	0.10	144.44	127.78	-16.66	-11.53
	0.15	190.47	169.47	-21.00	-11.03
	0.20	227.44	201.47	-25.97	-11.42
	0.25	256.35	225.57	-30.78	-12.01
	0.30	278.45	242.91	-35.54	-12.76
	0.35	294.50	254.30	-40.20	-13.65
	0.40	304.75	260.29	-44.46	-14.59
n-Propanol-	0.45	309.73	261.33	-48.40	-15.63
n-Hexane	0.50	309.49	257.74	-51.75	-16.72
	0.55	304.34	249.76	-54.58	-17.93
	0.60	293.85	237.59	-56.26	-19.15
	0.65	278.45	221.38	-57.07	-20.50
	0.70	257.59	201.22	-56.37	-21.88
	0.75	231.35	177.19	-54.16	-23.41
	0.80	199.12	149.35	-49.77	-24.99
	0.85	161.09	117.72	-43.37	-26.92
	0.90	116.30	82.30	-34.00	-29.23
	0.95	63.04	43.08	-19.96	-31.66

TABLE LII

VAPOR-LIQUID EQUILIBRIUM DATA AT 25°C
BY THE QUASI-LATTICE THEORY

System	Liquid Mole Fraction Alcohol	Vapor Pressure (mmHg)		Vapor Mole Fraction Alcohol	
		Expt'l	Calc'd	Expt'l	Calc'd
Methanol-Benzene	0.10	174.9	171.1	0.476	0.470
	0.20	179.3	173.3	0.494	0.484
	0.30	181.0	174.4	0.504	0.492
	0.40	182.0	175.3	0.514	0.505
	0.50	182.9	176.3	0.532	0.523
	0.60	182.7	176.1	0.564	0.536
	0.70	181.3	173.4	0.593	0.568
	0.80	177.5	166.1	0.627	0.634
	0.90	165.4	150.2	0.709	0.765
Ethanol-Benzene	0.10	120.4	133.2	0.249	0.322
	0.20	123.0	132.5	0.283	0.322
	0.30	123.5	132.1	0.310	0.327
	0.40	123.2	132.3	0.336	0.329
	0.50	122.0	131.8	0.357	0.331
	0.60	119.8	130.2	0.380	0.344
	0.70	115.0	126.0	0.419	0.368
	0.80	107.4	114.7	0.474	0.430
	0.90	92.8	93.3	0.583	0.573
n-Propanol-Benzene	0.10	97.5	108.1	0.090	0.163
	0.20	96.5	107.1	0.120	0.158
	0.30	94.4	107.3	0.140	0.155
	0.40	91.9	107.7	0.156	0.150
	0.50	88.9	108.4	0.172	0.148
	0.60	84.6	107.6	0.192	0.149
	0.70	79.0	101.9	0.217	0.163
	0.80	71.2	88.0	0.252	0.201
	0.90	54.8	62.6	0.350	0.305
Ethanol-Cyclohexane	0.10	137.8	152.6	0.318	0.382
	0.20	139.4	146.7	0.333	0.356
	0.30	139.5	146.6	0.337	0.350
	0.40	139.4	146.0	0.352	0.341
	0.50	139.2	145.8	0.356	0.344
	0.60	138.5	146.0	0.362	0.343
	0.70	136.5	144.7	0.374	0.349
	0.80	131.5	138.4	0.398	0.375
	0.90	113.6	118.9	0.483	0.458

TABLE LII (Continued)

System	Liquid Mole Fraction Alcohol	Vapor Pressure (mmHg)		Vapor Mole Fraction Alcohol	
		Expt'l	Calc'd	Expt'l	Calc'd
n-Propanol-Cyclohexane	0.10	107.1	111.7	0.119	0.164
	0.20	106.6	110.7	0.134	0.149
	0.30	105.5	111.0	0.143	0.143
	0.40	104.1	110.4	0.151	0.144
	0.50	102.1	109.4	0.160	0.148
	0.60	99.4	107.3	0.169	0.154
	0.70	94.9	102.1	0.183	0.167
	0.80	85.1	89.9	0.214	0.200
	0.90	65.0	66.6	0.298	0.289
Ethanol-n-Hexane	0.10	188.8	201.1	0.226	0.275
	0.20	190.2	197.1	0.242	0.258
	0.30	190.3	196.5	0.258	0.259
	0.40	190.1	197.0	0.259	0.256
	0.50	189.4	198.2	0.262	0.249
	0.60	187.8	195.6	0.268	0.256
	0.70	184.1	191.5	0.278	0.267
	0.80	174.6	182.9	0.301	0.286
	0.90	149.0	154.5	0.368	0.354
n-Propanol-n-Hexane	0.10	159.3	163.0	0.084	0.107
	0.20	157.8	161.3	0.096	0.099
	0.30	156.0	161.3	0.102	0.100
	0.40	153.9	160.4	0.107	0.100
	0.50	150.8	158.6	0.113	0.103
	0.60	146.9	155.4	0.119	0.107
	0.70	140.4	146.3	0.128	0.118
	0.80	128.0	129.2	0.145	0.140
	0.90	100.9	94.3	0.193	0.204

TABLE LIII

VAPOR-LIQUID EQUILIBRIUM DATA AT 25°C
BY THE UNIQUAC EQUATION

System	Liquid Mole Fraction Alcohol	Vapor Pressure (mmHg)		Vapor Mole Fraction Alcohol	
		Expt'l	Calc'd	Expt'l	Calc'd
Methanol-Benzene	0.10	174.9	166.1	0.476	0.456
	0.20	179.8	169.8	0.494	0.477
	0.30	181.0	172.4	0.504	0.495
	0.40	182.0	174.6	0.514	0.518
	0.50	182.9	176.0	0.532	0.544
	0.60	182.7	176.2	0.564	0.572
	0.70	181.3	174.8	0.593	0.605
	0.80	177.5	170.9	0.627	0.649
	0.90	165.4	160.7	0.709	0.729
Ethanol-n-Hexane	0.10	188.8	186.2	0.226	0.231
	0.20	190.2	187.7	0.242	0.250
	0.30	190.3	187.4	0.258	0.248
	0.40	190.1	187.2	0.259	0.247
	0.50	189.4	186.5	0.262	0.250
	0.60	187.8	183.8	0.268	0.258
	0.70	184.1	177.3	0.278	0.276
	0.80	174.6	163.2	0.301	0.313
	0.90	149.0	132.6	0.368	0.409

TABLE LIV

VAPOR-LIQUID EQUILIBRIUM DATA AT 25°C
BY THE ASOG METHOD

System	Liquid Mole Fraction Alcohol	Vapor Pressure (mmHg)		Vapor Mole Fraction Alcohol	
		Expt'l	Calc'd	Expt'l	Calc'd
Methanol-Benzene	0.10	174.9	149.7	0.476	0.407
	0.20	179.3	167.7	0.494	0.497
	0.30	181.0	174.8	0.504	0.535
	0.40	182.0	178.0	0.514	0.557
	0.50	182.9	179.4	0.532	0.573
	0.60	182.7	179.7	0.564	0.588
	0.70	181.3	178.9	0.593	0.607
	0.80	177.5	175.6	0.627	0.639
	0.90	165.4	165.2	0.709	0.712
Ethanol-Benzene	0.10	120.4	111.8	0.249	0.212
	0.20	123.0	116.3	0.283	0.281
	0.30	123.5	117.4	0.310	0.318
	0.40	123.2	117.1	0.336	0.343
	0.50	122.0	116.0	0.357	0.367
	0.60	119.8	113.7	0.380	0.394
	0.70	115.0	109.6	0.419	0.431
	0.80	107.4	102.0	0.474	0.491
	0.90	92.8	87.5	0.583	0.615
n-Propanol-Benzene	0.10	97.5	95.3	0.090	0.078
	0.20	96.5	93.5	0.120	0.112
	0.30	94.4	91.3	0.140	0.132
	0.40	91.9	88.7	0.156	0.149
	0.50	88.9	85.2	0.172	0.167
	0.60	84.6	80.5	0.192	0.189
	0.70	79.0	73.5	0.217	0.222
	0.80	71.2	62.9	0.252	0.280
	0.90	54.8	46.6	0.350	0.410
Methanol-Cyclohexane	0.05	209.2	179.5	0.542	0.466
	0.10	213.2	197.7	0.550	0.522
	0.15	213.7	209.8	0.550	0.541
	0.20	213.7	206.5	0.550	0.549
	0.25	213.7	207.6	0.550	0.553
	0.30	213.7	208.1	0.550	0.555
	0.35	213.7	208.4	0.550	0.557
	0.40	213.7	208.5	0.550	0.557
	0.45	313.7	208.5	0.550	0.557

TABLE LIV (Continued)

System	Liquid Mole Fraction Alcohol	Vapor Pressure (mmHg)		Vapor Mole Fraction Alcohol	
		Expt'l	Calc'd	Expt'l	Calc'd
Methanol-Cyclohexane (Con't.)	0.50	213.7	208.5	0.550	0.557
	0.55	213.7	208.4	0.550	0.557
	0.60	213.7	208.4	0.550	0.557
	0.65	213.7	208.4	0.550	0.557
	0.70	213.7	208.4	0.550	0.557
	0.75	213.7	208.1	0.550	0.559
	0.80	213.7	207.2	0.550	0.564
	0.85	213.4	204.7	0.562	0.576
	0.90	210.5	198.1	0.571	0.603
	0.95	195.0	180.2	0.629	0.678
Ethanol-Cyclohexane	0.10	137.8	130.8	0.318	0.286
	0.20	139.4	133.5	0.333	0.313
	0.30	139.5	134.0	0.337	0.324
	0.40	139.4	133.9	0.352	0.333
	0.50	139.2	133.2	0.356	0.343
	0.60	138.5	131.4	0.362	0.358
	0.70	136.5	127.6	0.374	0.382
	0.80	131.5	119.4	0.398	0.428
	0.90	113.6	101.4	0.483	0.535
n-Propanol-Cyclohexane	0.10	107.1	104.3	0.119	0.106
	0.20	106.6	103.8	0.134	0.121
	0.30	105.5	102.8	0.143	0.130
	0.40	104.1	101.0	0.151	0.139
	0.50	102.1	98.2	0.160	0.150
	0.60	99.4	93.6	0.169	0.166
	0.70	94.9	86.1	0.183	0.192
	0.80	85.1	73.9	0.214	0.240
	0.90	65.0	54.0	0.298	0.354
Methanol-n-Hexane	0.05	258.2	232.5	0.424	0.359
	0.10	263.7	249.9	0.436	0.412
	0.15	265.2	255.6	0.445	0.430
	0.20	265.5	257.9	0.449	0.439
	0.25	265.9	258.8	0.449	0.443
	0.30	265.9	259.3	0.449	0.445
	0.35	265.9	259.4	0.449	0.446
	0.40	265.9	259.4	0.449	0.447
	0.45	265.9	259.4	0.449	0.447

TABLE LIV (Continued)

| System	Liquid Mole Fraction Alcohol	Vapor Pressure (mmHg)		Vapor Mole Fraction Alcohol	
		Expt'l	Calc'd	Expt'l	Calc'd
Methanol-n-Hexane (Con't.)	0.50	265.9	259.4	0.449	0.447
	0.55	265.9	259.5	0.449	0.446
	0.60	265.9	259.5	0.449	0.446
	0.65	265.9	259.5	0.449	0.446
	0.70	265.9	259.3	0.449	0.447
	0.75	265.9	258.7	0.449	0.449
	0.80	265.9	257.0	0.449	0.454
	0.85	265.3	252.6	0.456	0.465
	0.90	262.4	241.4	0.461	0.493
	0.95	245.1	212.0	0.502	0.575
Ethanol-n-Hexane	0.10	188.8	182.9	0.226	0.205
	0.20	190.2	184.7	0.242	0.226
	0.30	190.3	184.5	0.258	0.235
	0.40	190.1	183.7	0.259	0.243
	0.50	189.4	181.9	0.262	0.252
	0.60	187.8	178.4	0.268	0.264
	0.70	184.1	171.4	0.278	0.285
	0.80	174.6	157.4	0.301	0.325
	0.90	149.0	127.5	0.368	0.425
n-Propanol-n-Hexane	0.10	159.3	155.5	0.084	0.071
	0.20	157.8	154.0	0.096	0.082
	0.30	156.0	151.9	0.102	0.088
	0.40	153.9	148.9	0.107	0.094
	0.50	150.8	144.0	0.113	0.103
	0.60	146.9	136.4	0.119	0.114
	0.70	140.4	124.2	0.128	0.133
	0.80	128.0	104.7	0.145	0.169
	0.90	100.9	73.0	0.193	0.262
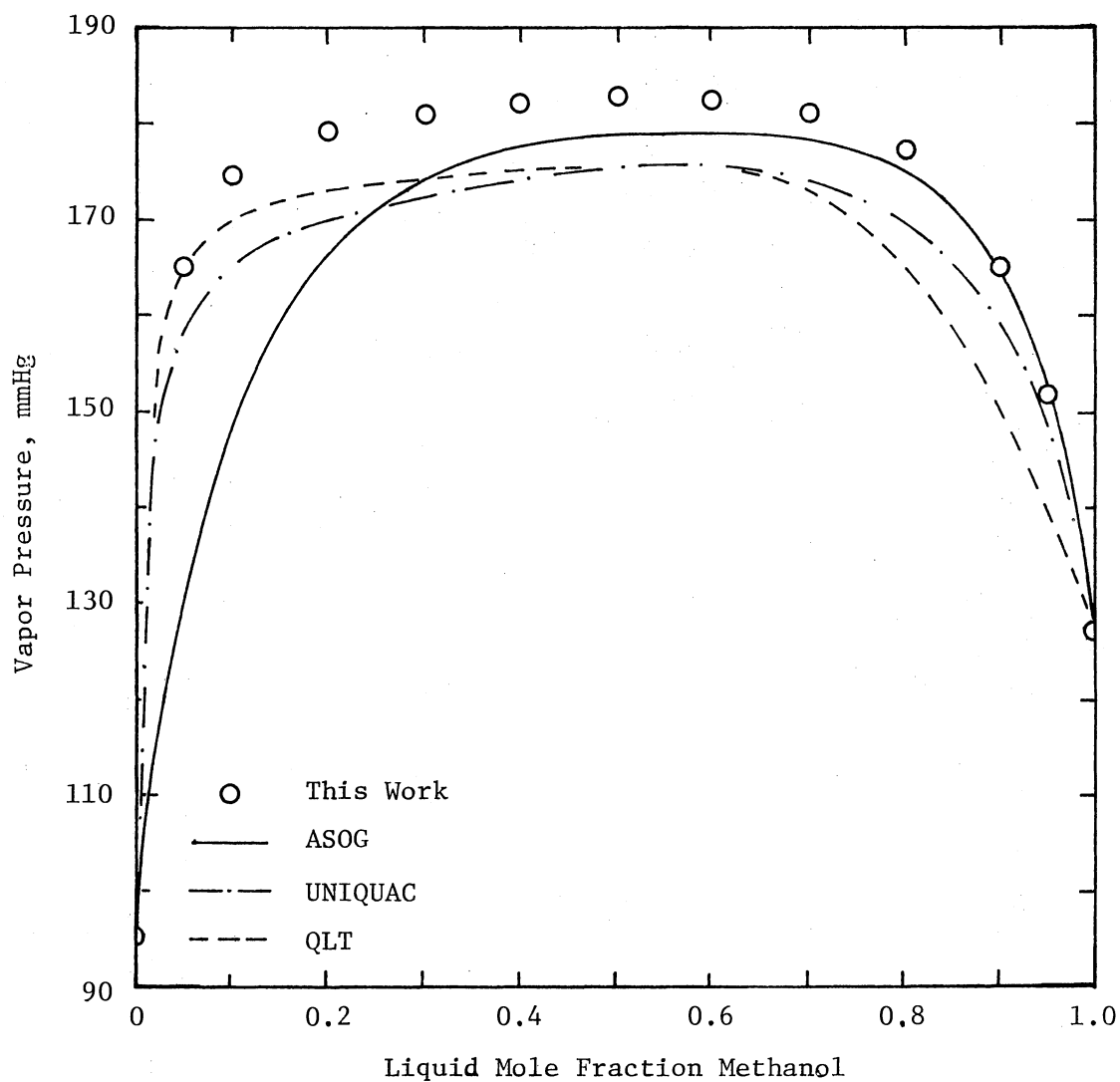
Figure 78. Vapor Pressure at 25°C for the System
Methanol(1)-Benzene(2) by the
Group Contribution Theories
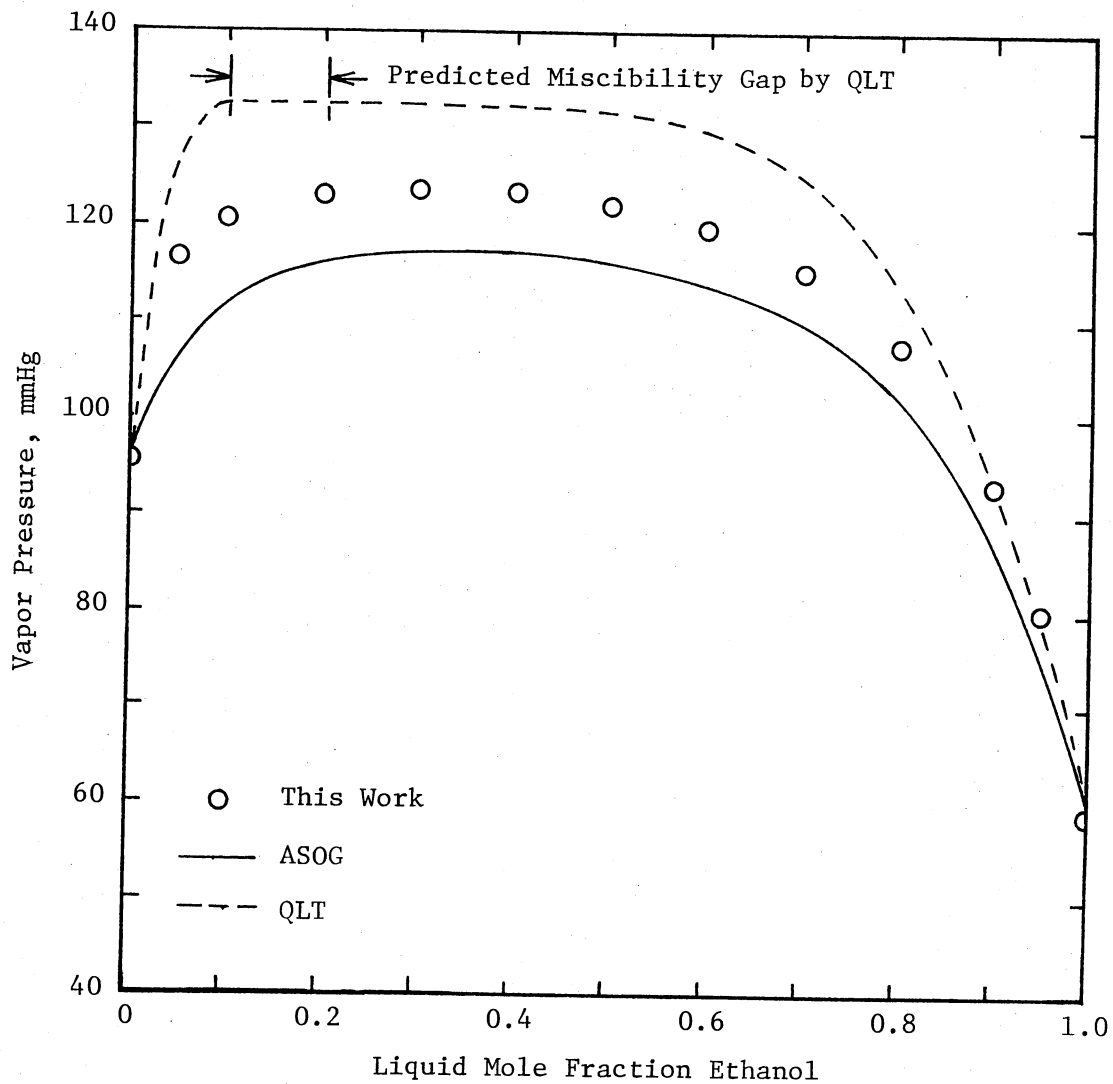
Figure 79.   Vapor Pressure at 25°C for the System
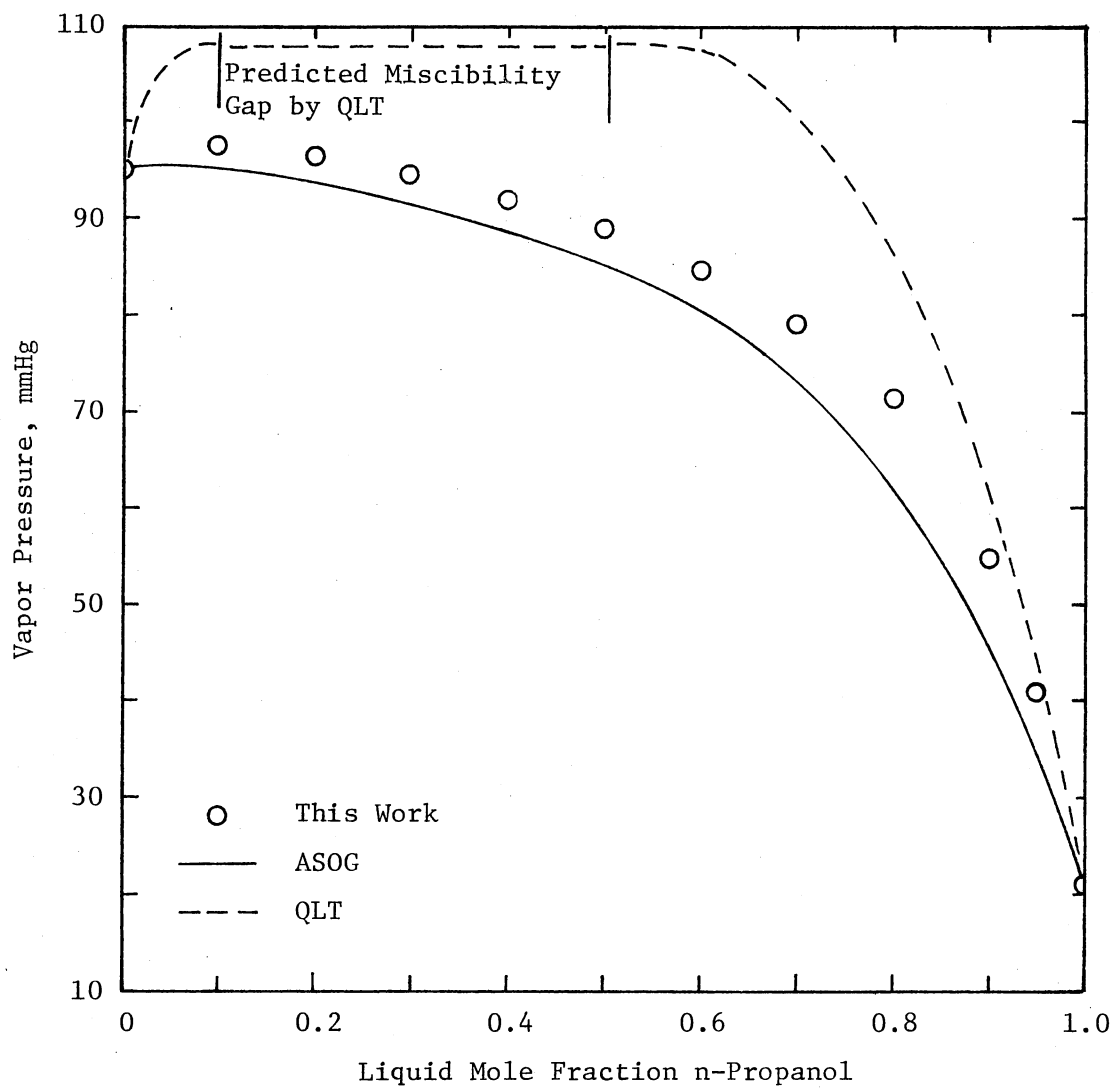Ethanol(1)-Benzene(2) by the
Group Contribution Theories

Figure 80. Vapor Pressure at $25^{\circ}C$ for the System
n-Propanol(1)-Benzene(2) by
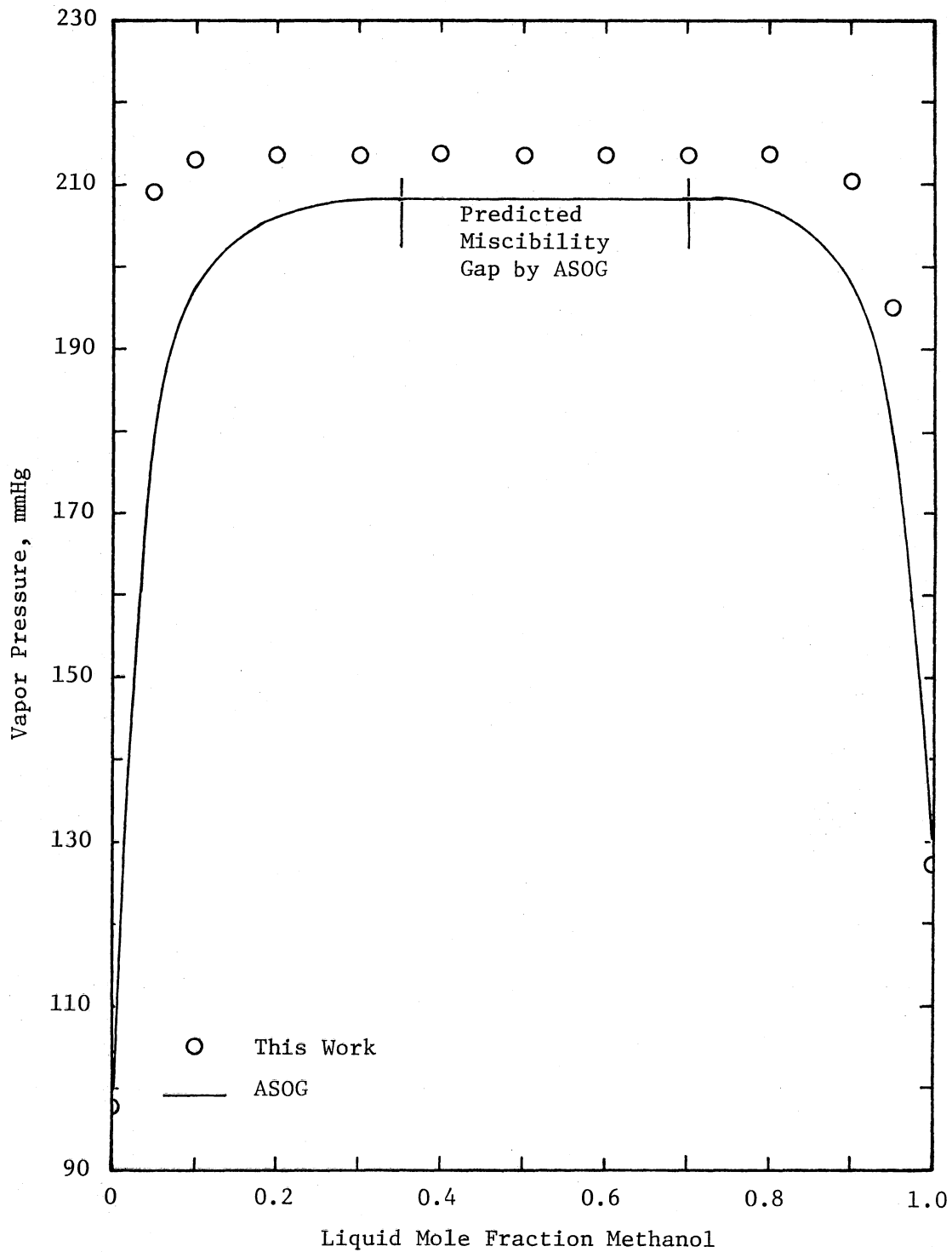the Group Contribution Theories

Figure 81. Vapor Pressure at 25°C for the System
Methanol(1)-Cyclohexane(2) by
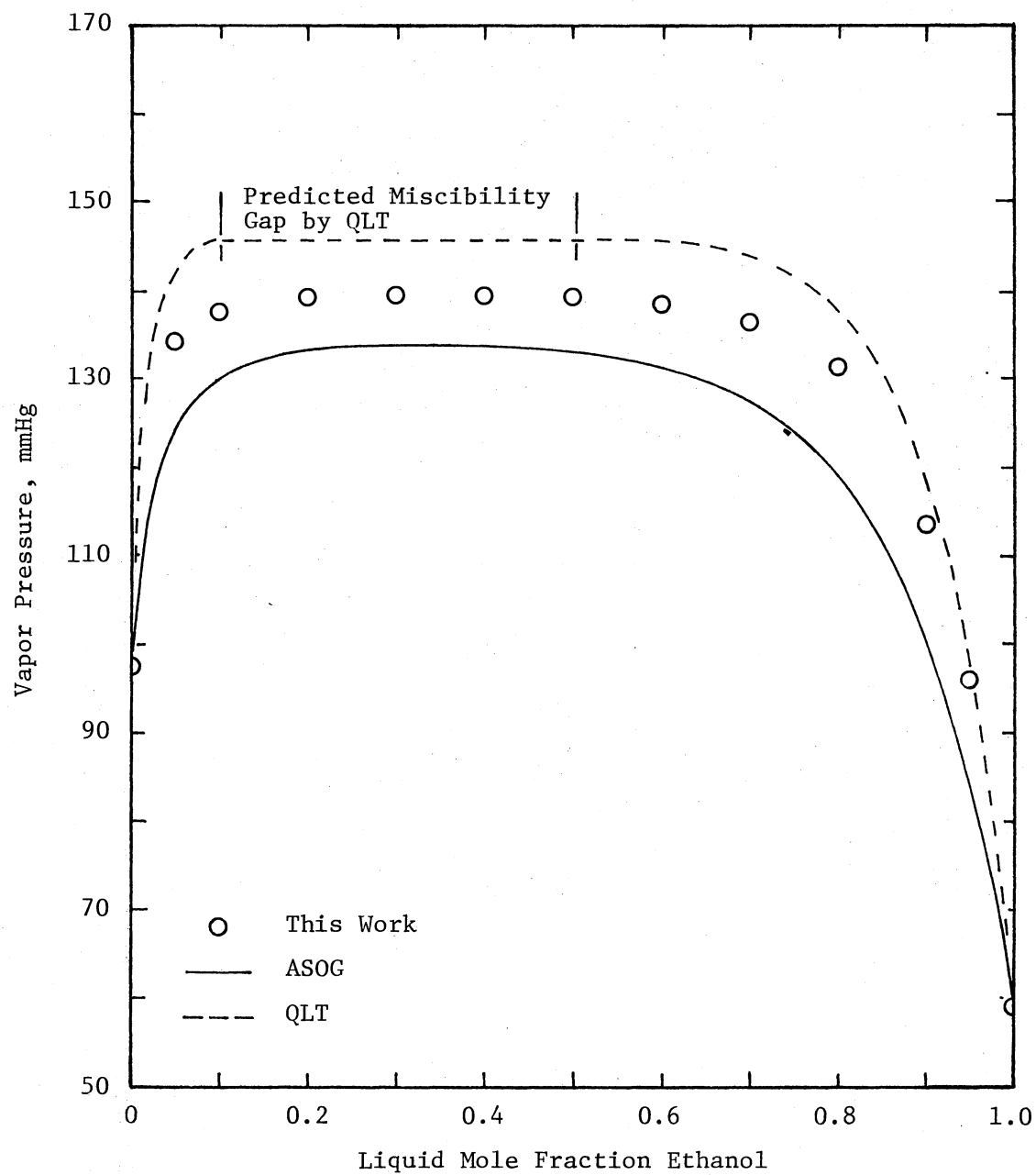the Group Contribution Theories

Figure 82. Vapor Pressure at 25°C for the System
Ethanol(1)-Cyclohexane(2) by
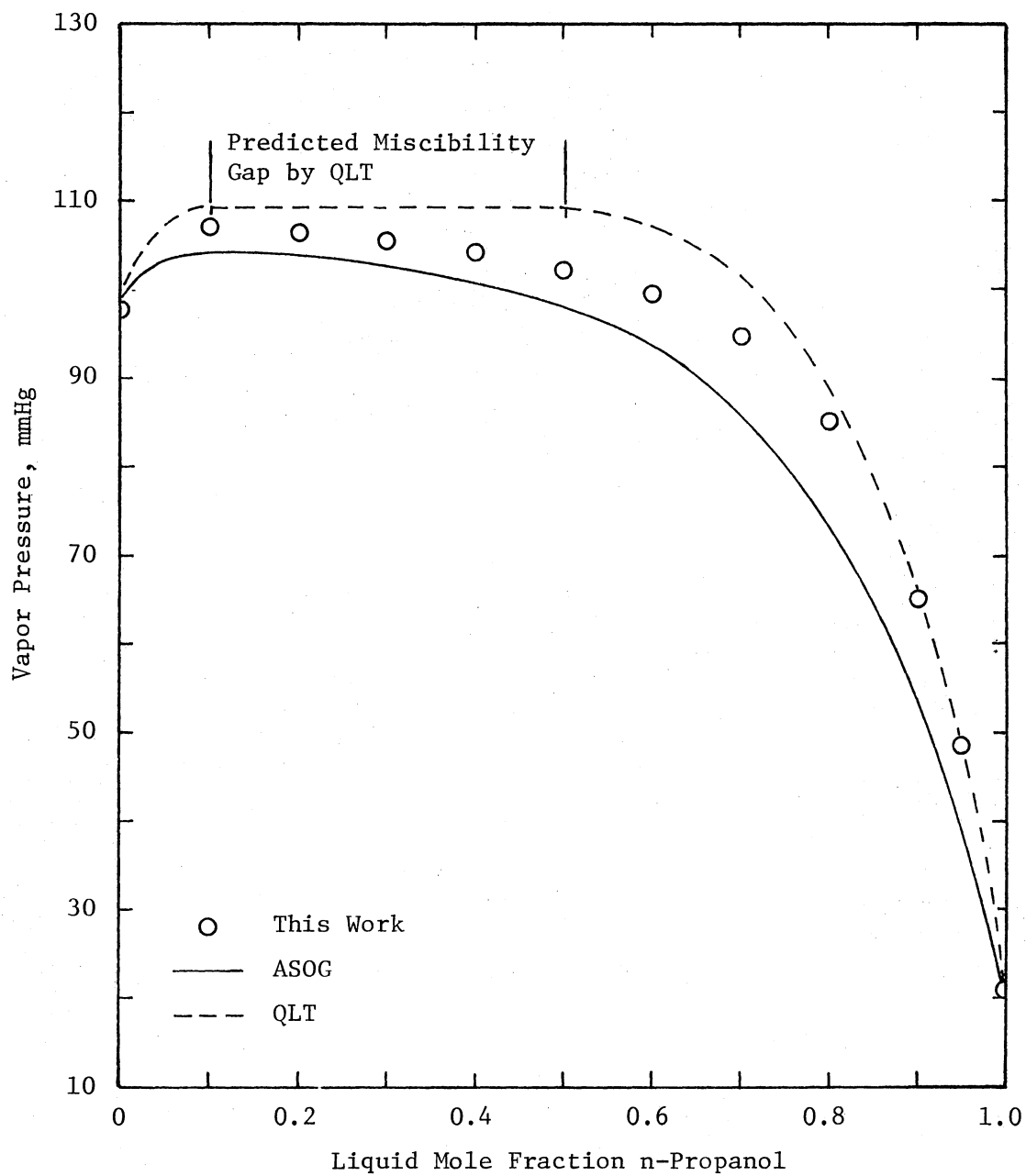the Group Contribution Theories

Figure 83. Vapor Pressure at 25°C for the System
n-Propanol(1)-Cyclohexane(2) by
the Group Contribution Theories

Figure 84. Vapor Pressure at 25°C for the System
Methanol(1)-n-Hexane(2) by the
Group Contribution Theories

Figure 85. Vapor Pressure at $25^{\circ}C$ for the System
Ethanol(1)-n-Hexane(2) by the
Group Contribution Theories

Figure 86. Vapor Pressure at 25°C for the System
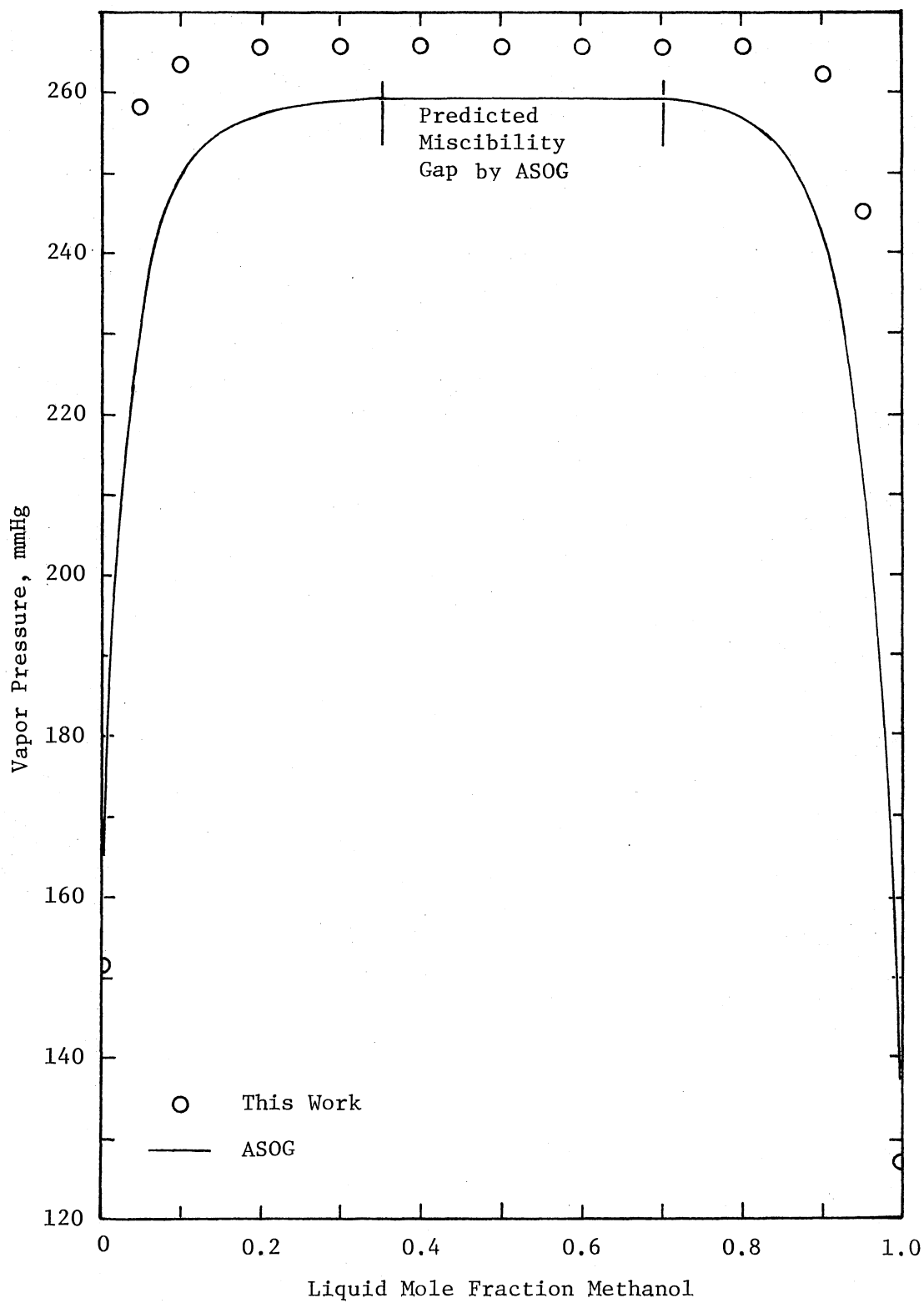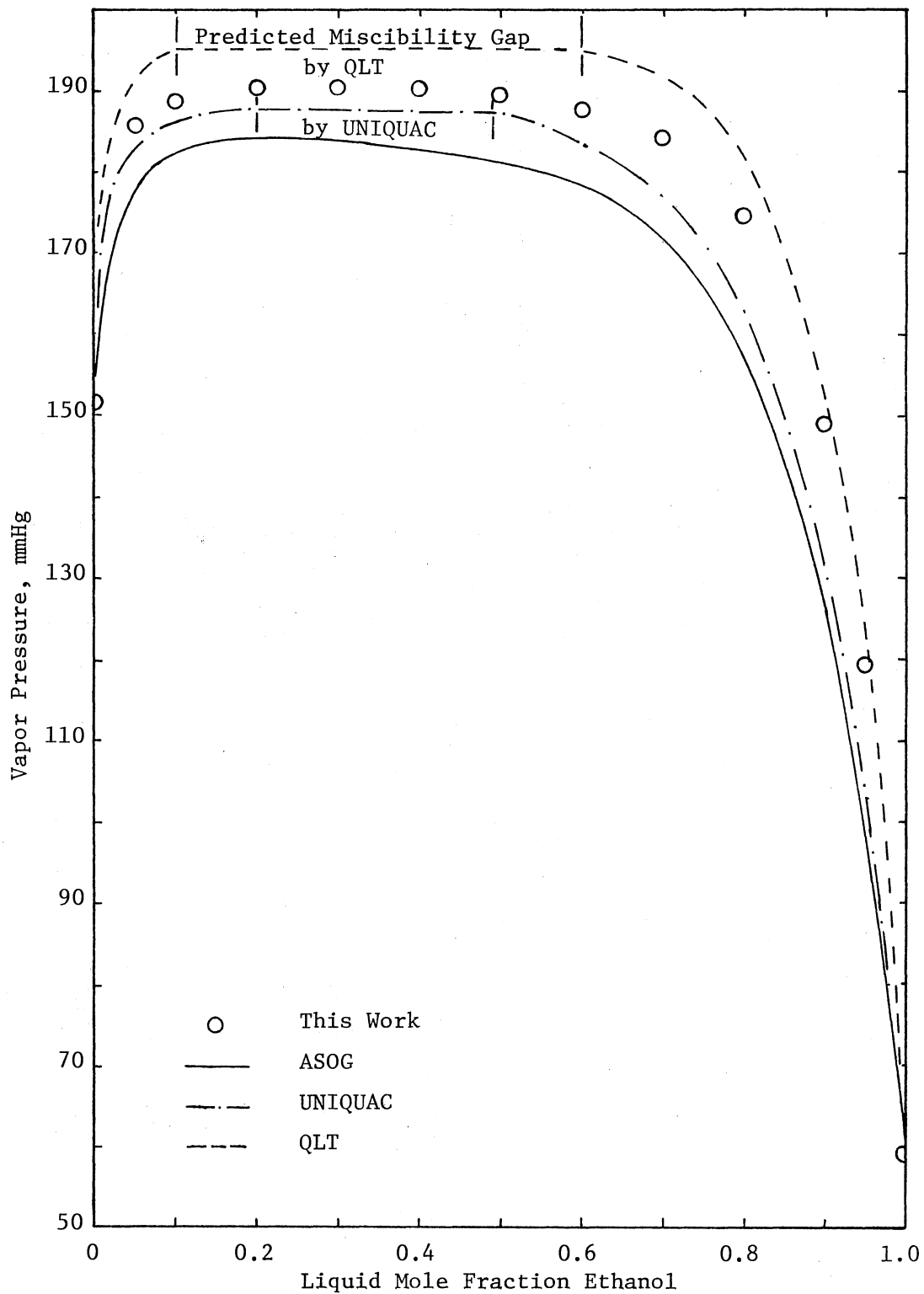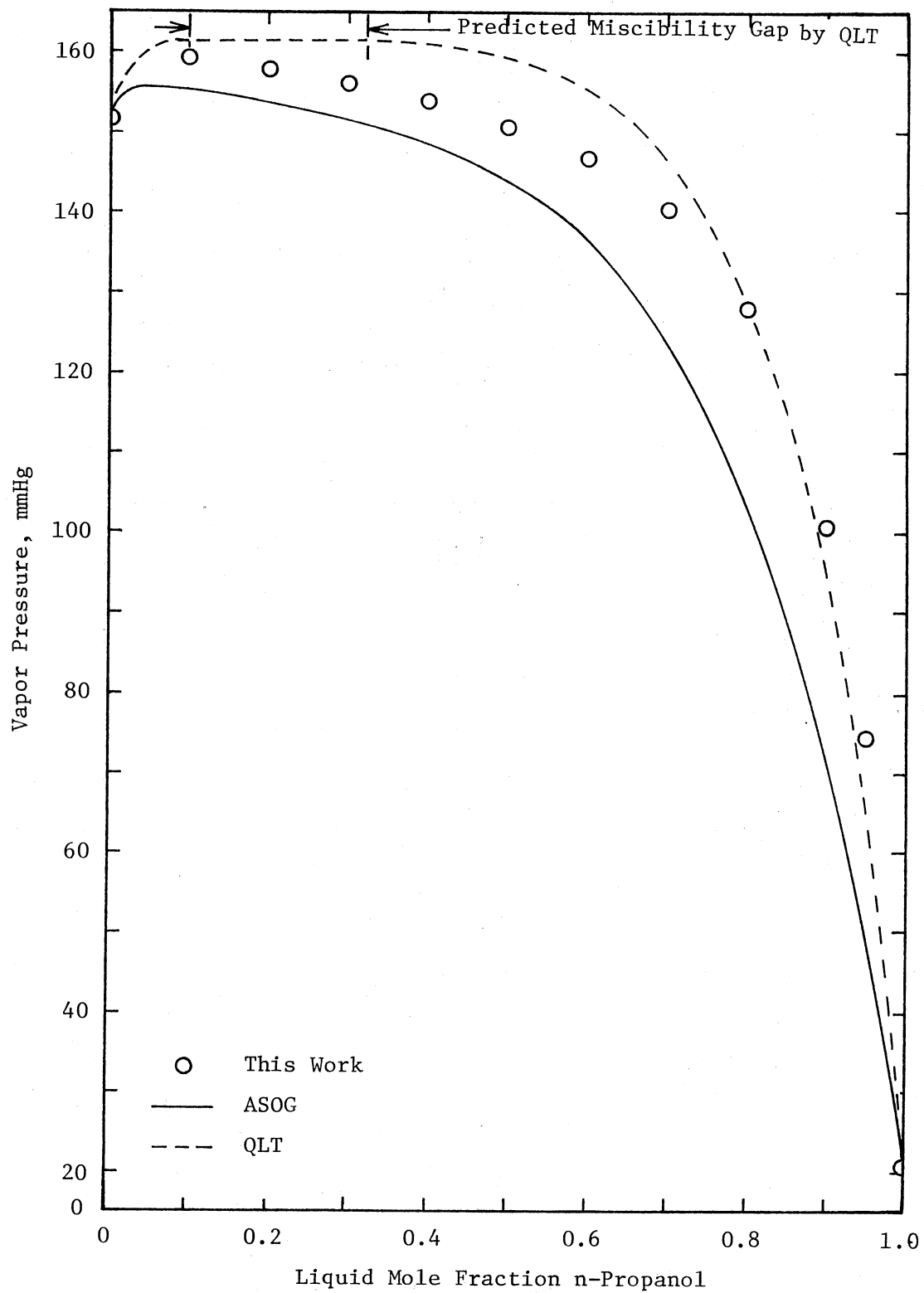n-Propanol(1)-n-Hexane(2) by the
Group Contribution Theories

Figure 87. Vapor-Liquid Composition Data at 25°C
for the System Methanol(1)-
Benzene(2) by the Group Contri-
bution Theories

Figure 88. Vapor-Liquid Composition Data at 25°C
for the System Ethanol(1)-
Benzene(2) by the Group Contri-
bution Theories

Figure 89.   Vapor-Liquid Composition Data at 25°C
for the System n-Propanol(1)-
Benzene(2) by the Group Contri-
bution Theories

Figure 90.   Vapor-Liquid Composition Data at 25°C
for the System Methanol(1)-
Cyclohexane(2) by the Group
Contribution Theories

Figure 91.   Vapor-Liquid Composition Data at 25°C
              for the System Ethanol(1)-
              Cyclohexane(2) by the Group
              Contribution Theories

Figure 92. Vapor-Liquid Composition Data at 25°C
for the System n-Propanol(1)-
Cyclohexane(2) by the Group
Contribution Theories
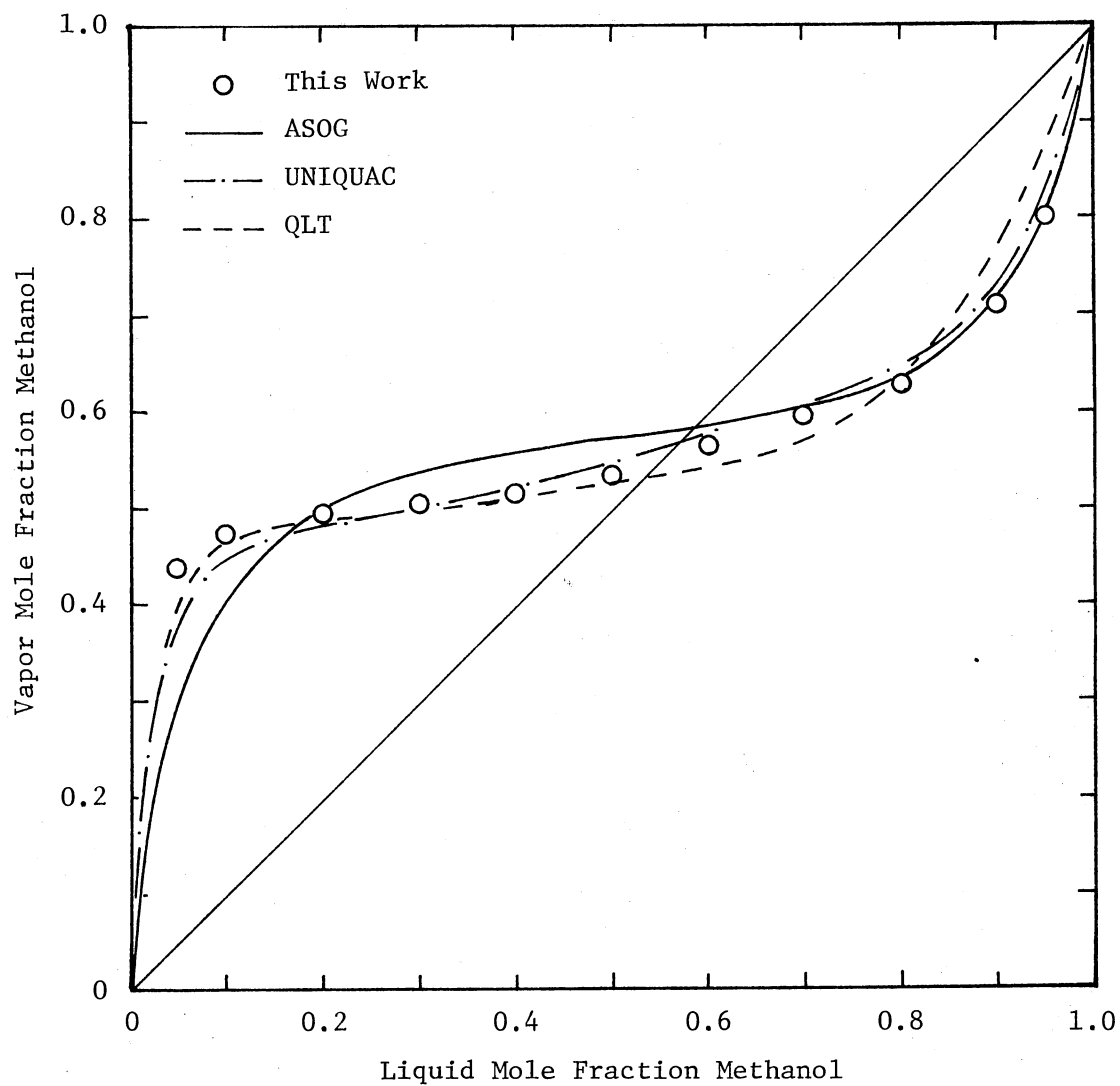
Figure 93.   Vapor-Liquid Composition Data at 25°C
             for the System Methanol(1)-
             n-Hexane(2) by the Group
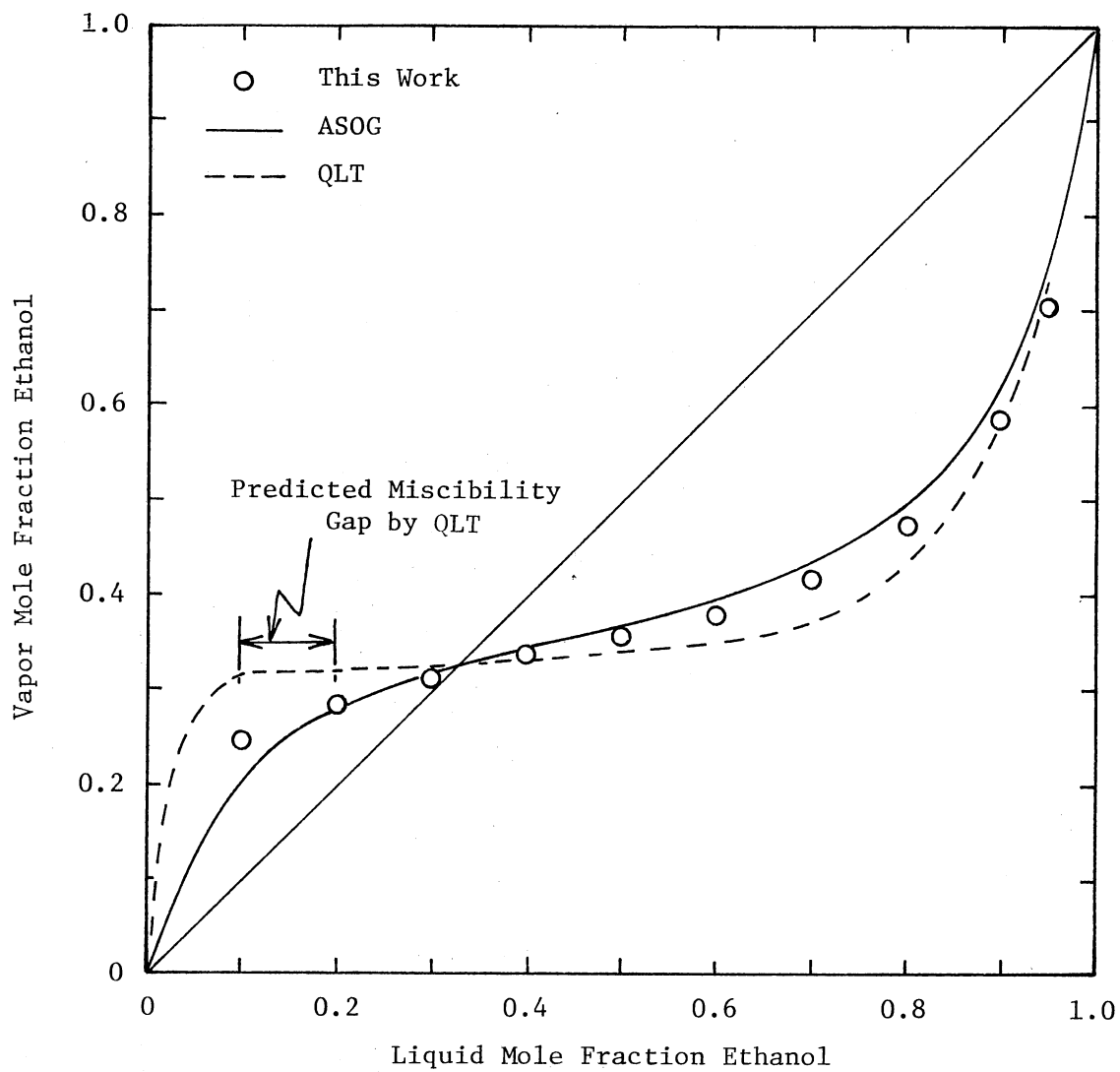   Contribution Theories

Figure 94. Vapor-Liquid Composition Data at 25°C
for the System Ethanol(1)-n-Hexane
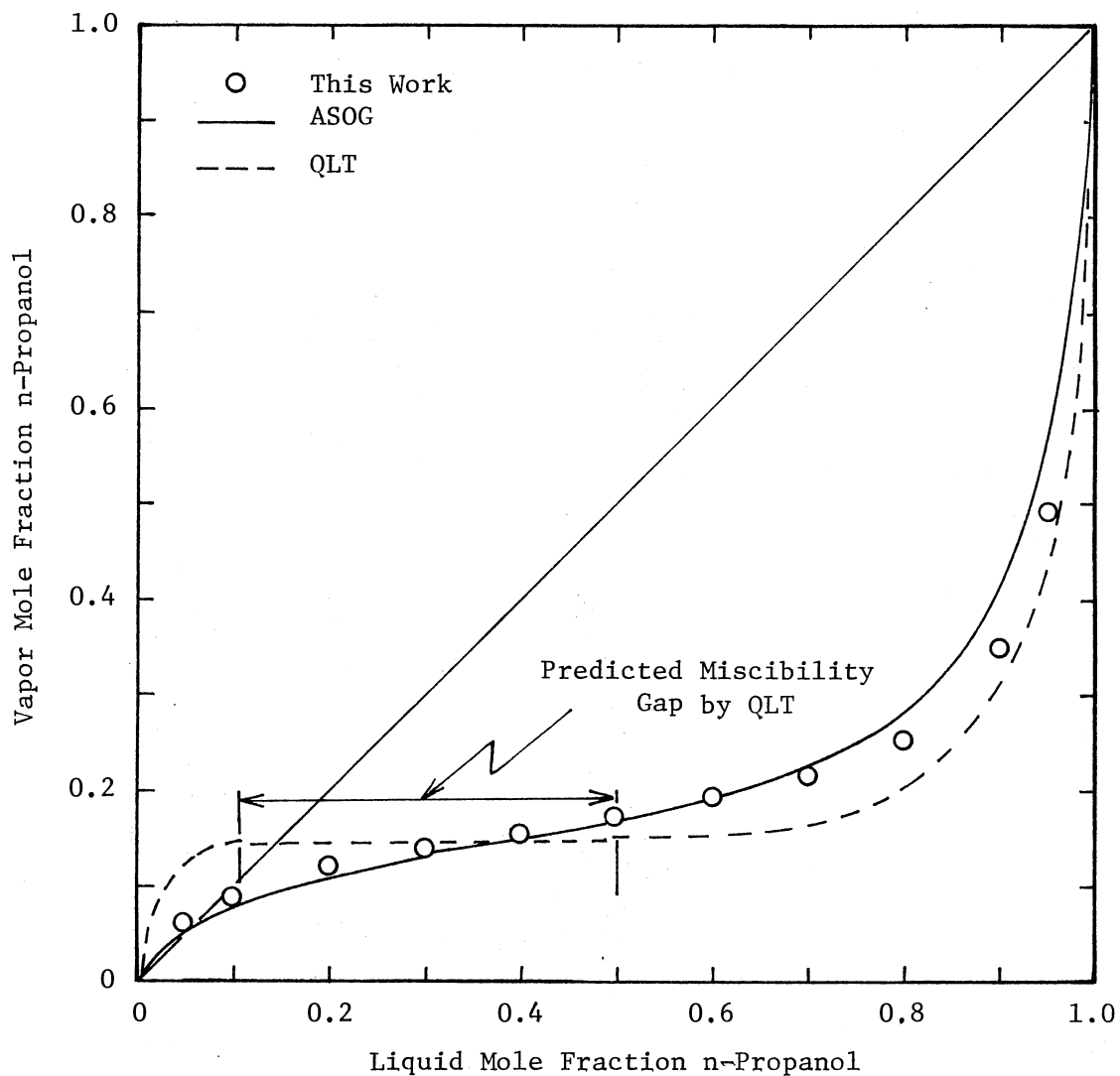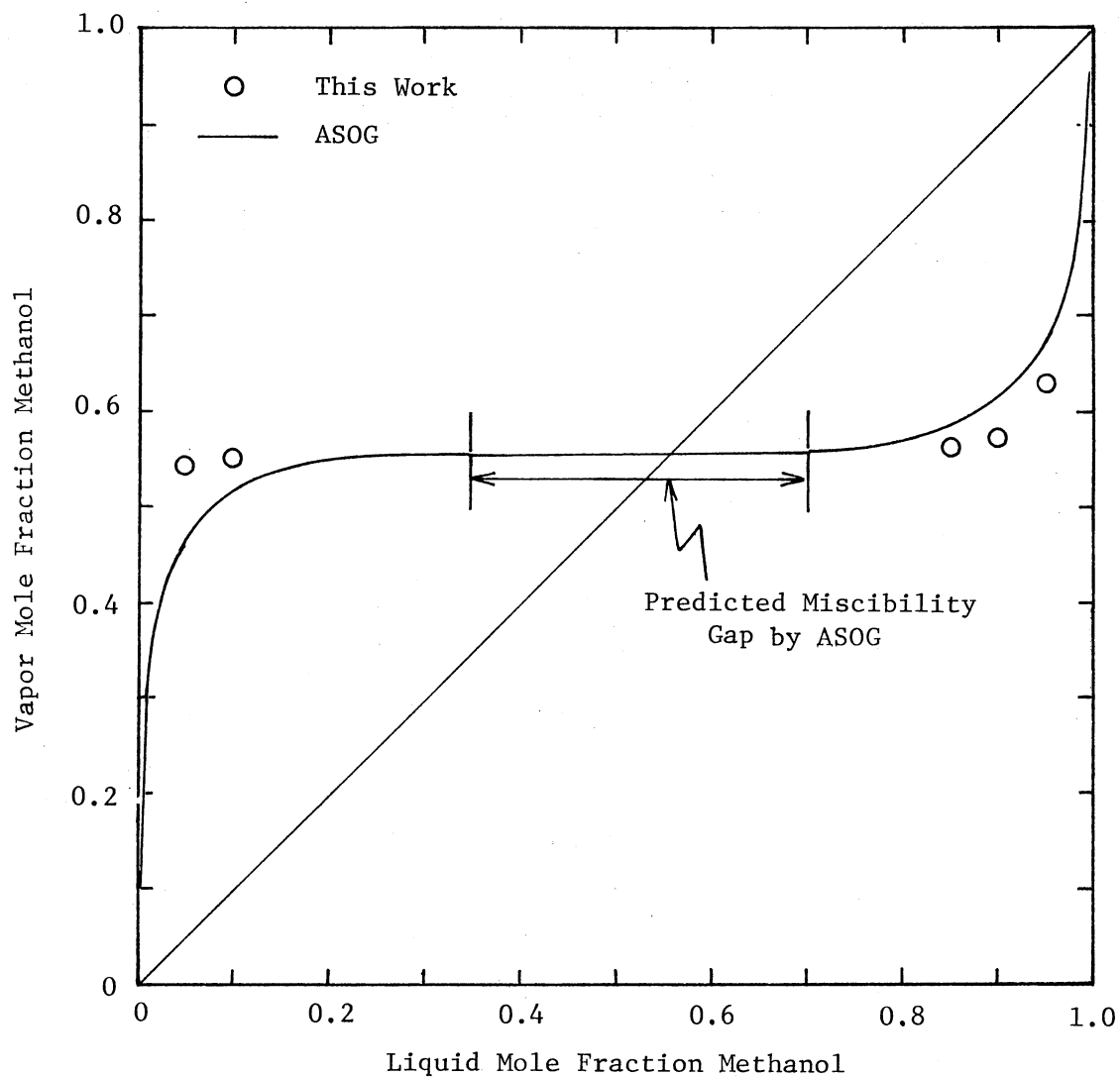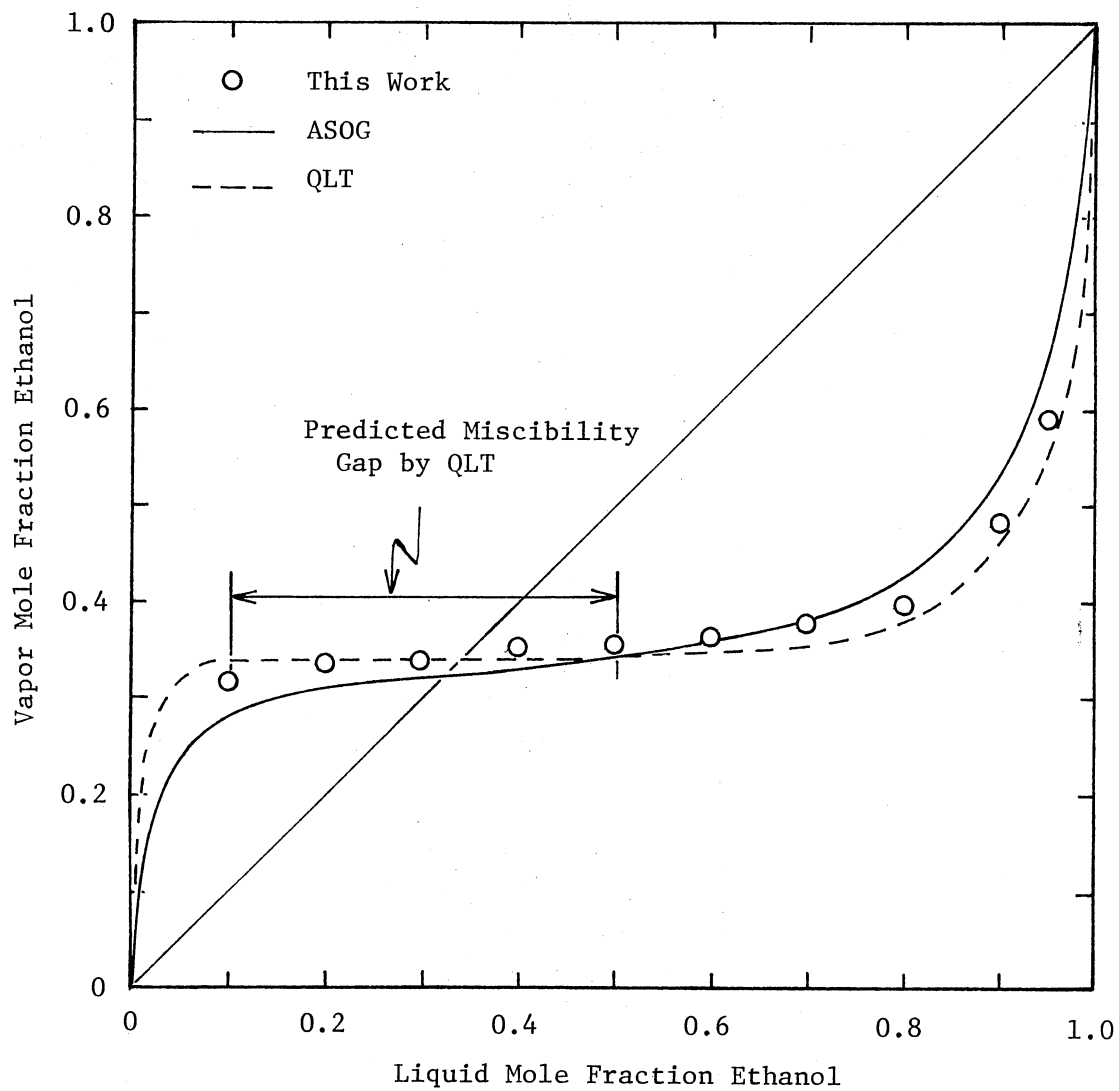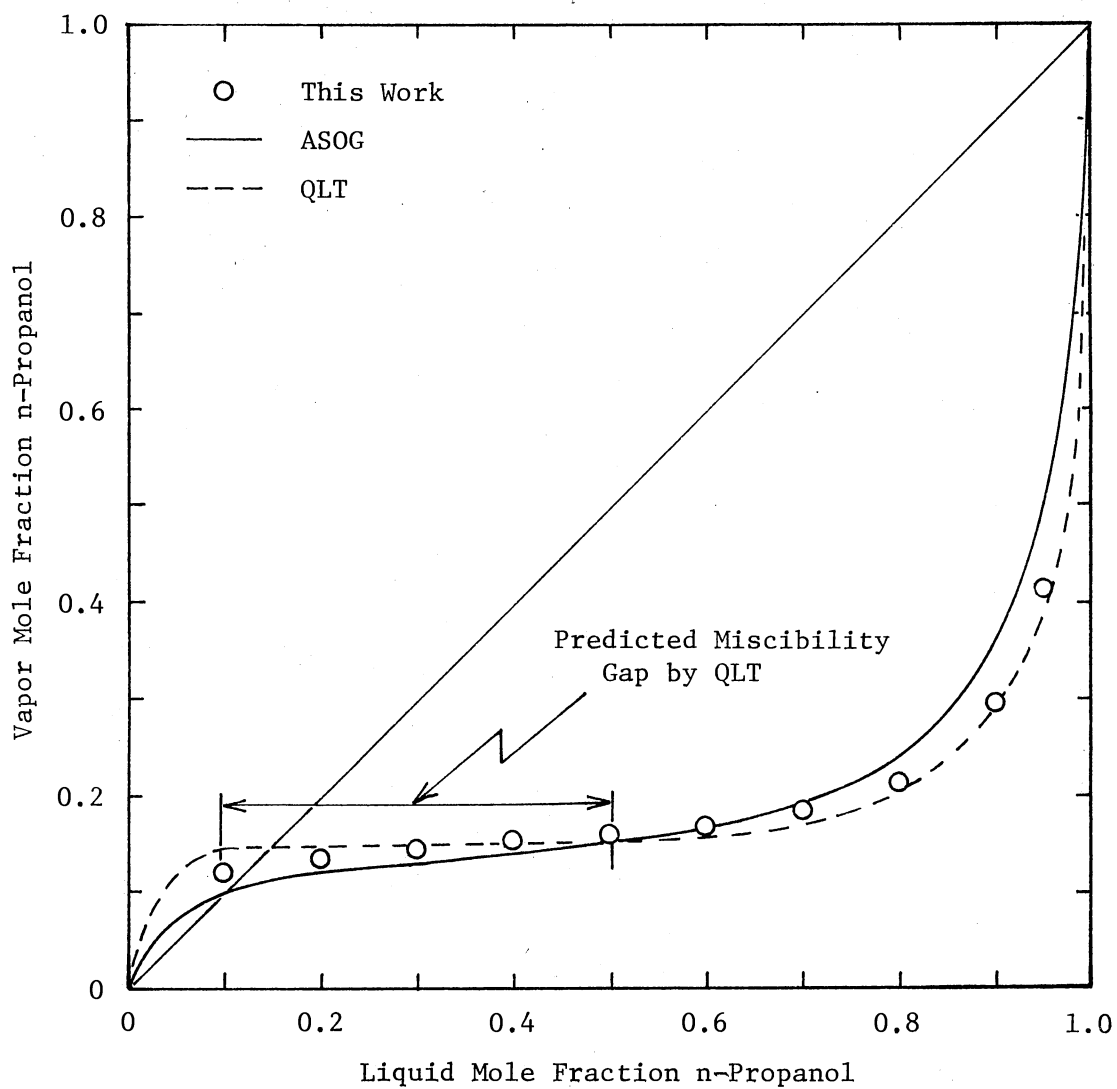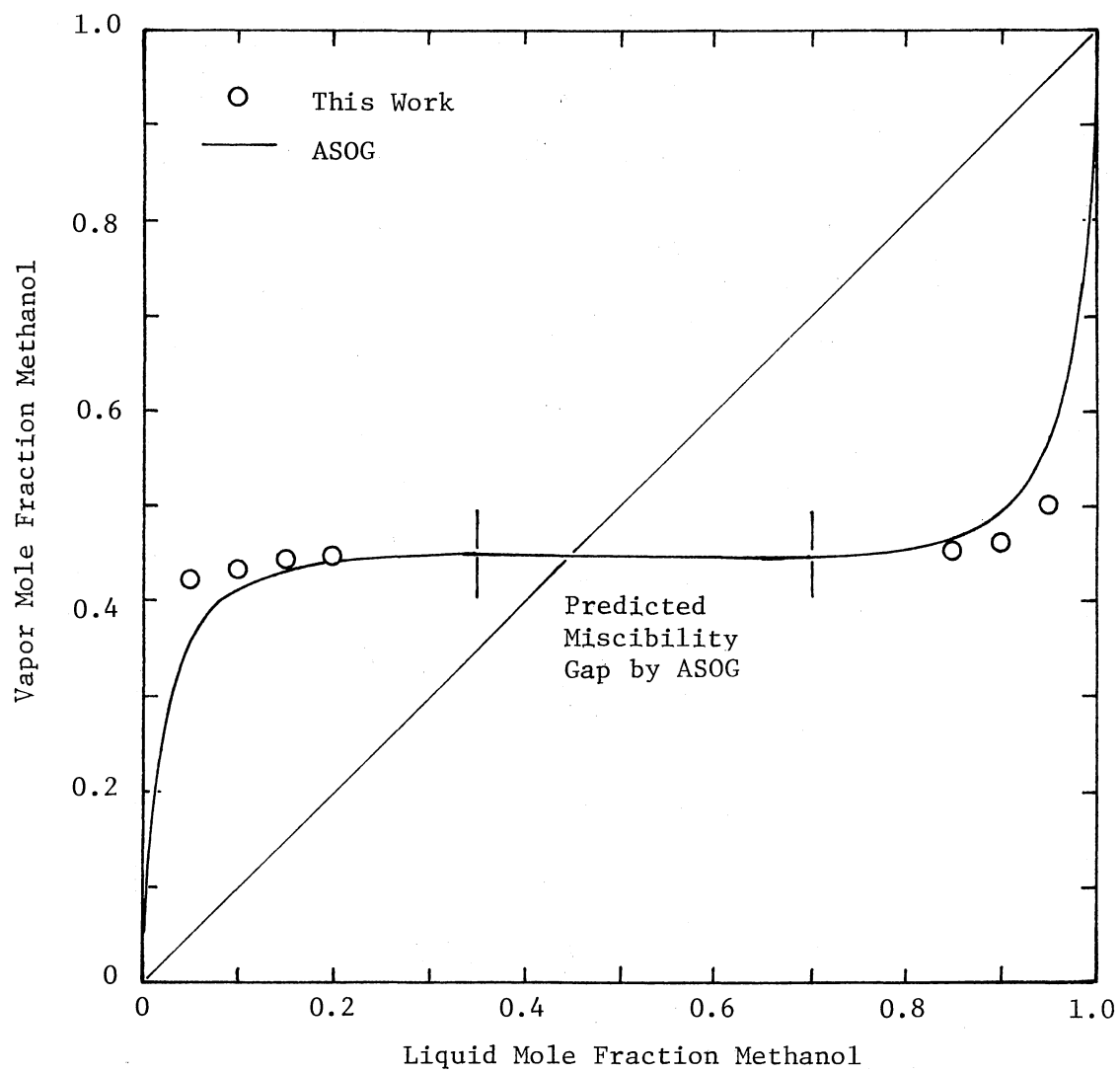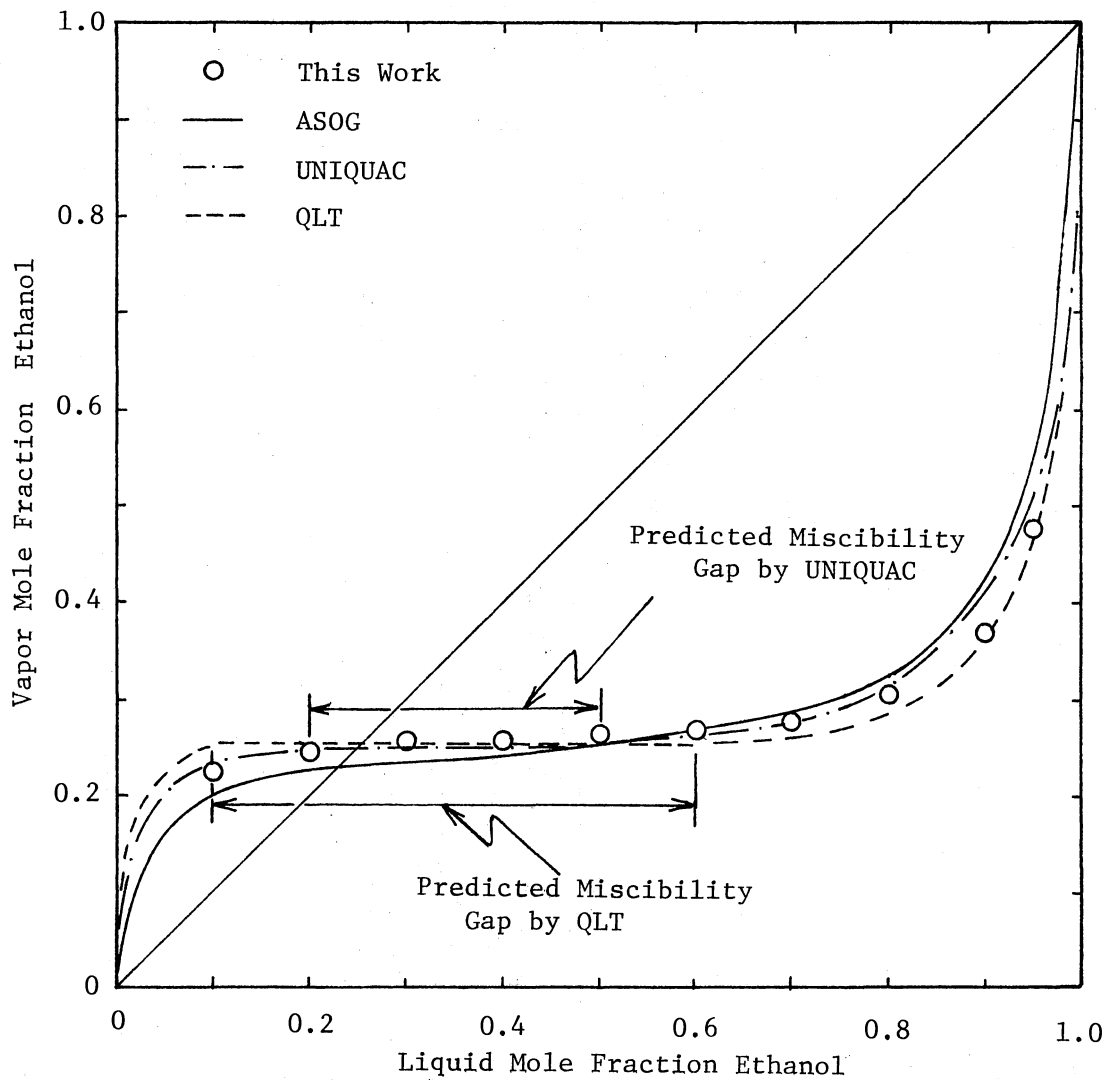(2) by the Group Contribution Theories
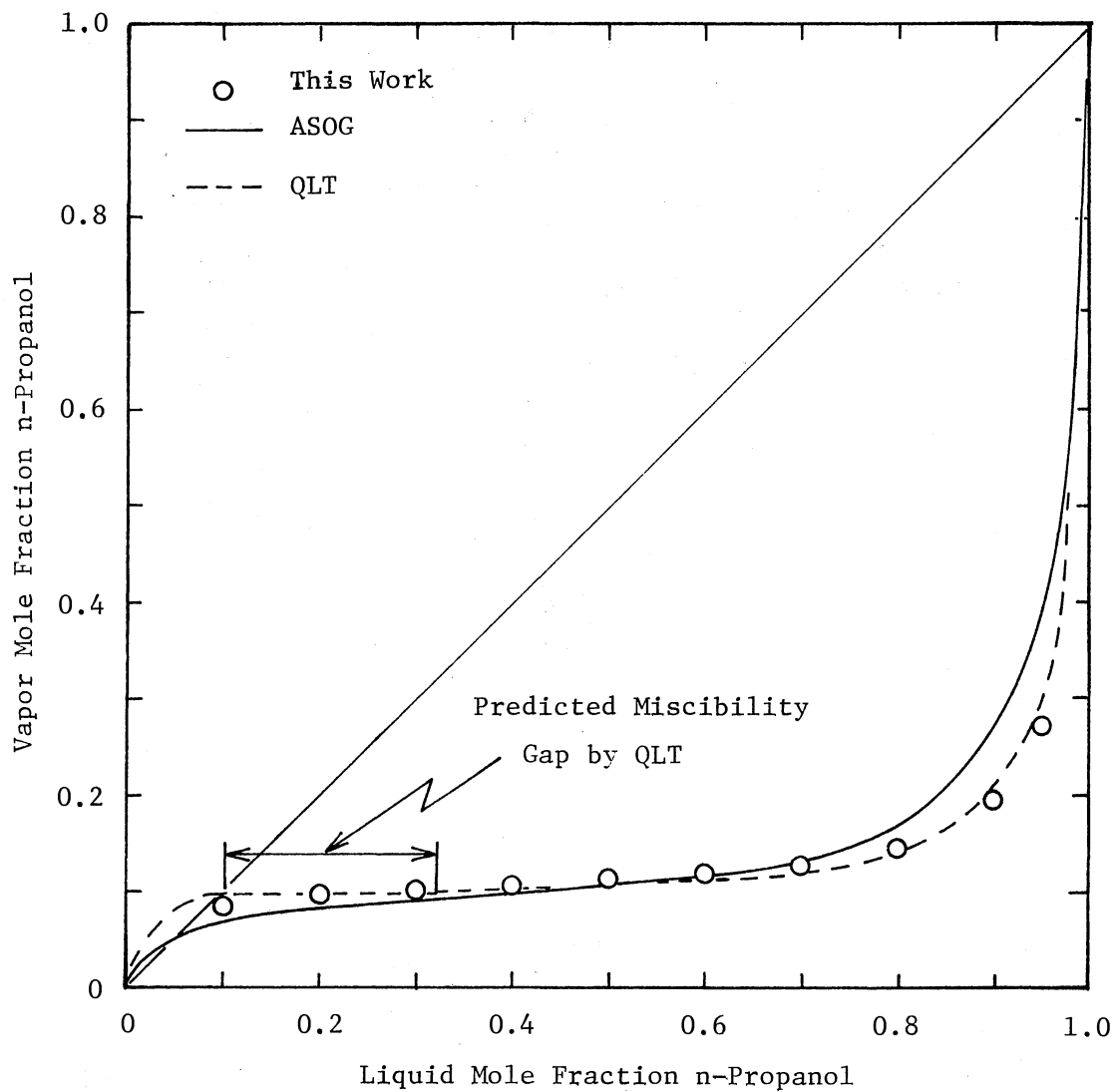
Figure 95.   Vapor-Liquid Composition Data at 25°C
              for the System n-Propanol(1)-
              n-Hexane(2) by the Group Contri-
              bution Theories

Quasi-Lattice Theory (QLT)

The excess Gibbs free energy calculated by the quasi-lattice
theory for seven miscible systems were used as input data in Mixon's
method for VLE calculation.

For the system methanol-benzene, the predicted vapor pressures
are lower than experimental values by an absolute average deviation
of 7.9 mmHg. For the other six systems, the predicted vapor pressures
are higher than experimental values by an absolute average deviation
of 5 mmHg for n-propanol-n-hexane system to 16 mmHg for n-propanol-
benzene system. The predicted vapor pressures and vapor compositions
are not smooth in the low concentration range of alcohol and, in fact,
display maximum and minimum values. These indicate that a phase
separation has occurred, contrary to the experimental results.

When a binary mixture splits into two separate liquid phases,
there exist two points with a common tangent on the plot of Gibbs free
energy of mixing as function of mole fraction if the Gibbs free energy
of mixing is treated as a continuous function. The Gibbs free energy
of mixing is calculated from the following equation:

$$\Delta G^M = G^E + RT \sum_i x_i \ln (x_i) \qquad (VII-2)$$

where G^E's are calculated from group contribution theories. A typical
plot of Gibbs free energy as function of mole fraction for the system
ethanol-n-hexane is shown in Figure 96; a common tangent for the ΔG^M-x
curve predicted by quasi-lattice theory is apparent. The predicted two
liquid phases in equilibrium have compositions of 0.28 and 0.61 mole
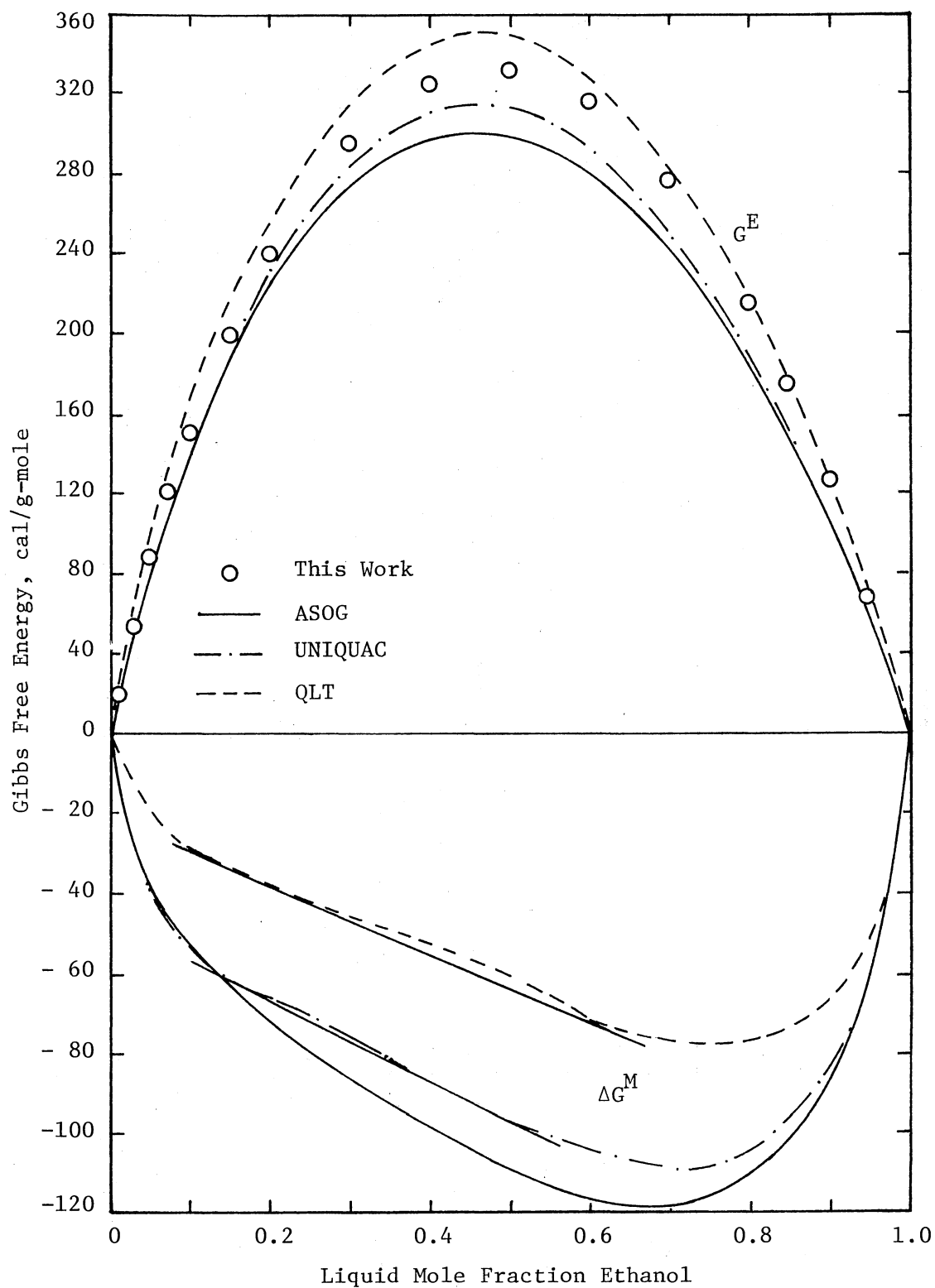
Figure 96. Gibbs Free Energy at 25°C for the System
Ethanol(1)-n-Hexane(2) by the
Group Contribution Theories

fractions of ethanol. Experimental results show that the ethanol-n-hexane system is completely miscible at 25°C.

Universal Quasi-Chemical (UNIQUAC) Equation

The VLE prediction for the binary systems methanol-benzene and ethanol-n-hexane using G^E-x data from UNIQUAC equation are shown in Table LIII. Graphical comparisons between predicted and experimental values are shown in Figures 78 and 85 for P-x data and in Figures 87 and 94 for y-x data.

For the methanol-benzene system, the predicted vapor pressures are lower than the experimental values by an absolute average deviation of 7 mmHg. The predicted vapor compositions are agree very good with values calculated from experimental P-x data.

For the ethanol-n-hexane system, the predicted vapor pressures are also lower than the experimental values by an absolute average deviation of 6 mmHg. The predicted y-x curve indicated that the ethanol-n-hexane system is partially mixcible at 25°C. The predicted two liquid phases in equilibrium have compositions of about 0.2 and 0.5 mole fractions of ethanol. This phase separation can be easily observed by a plot of Gibbs free energy of mixing as function of mole fraction, shown in Figure 96, which exhibits a common tangent. However, experimental results indicate that ethanol-n-hexane system is totally miscible at 25°C.

Analytical Solutions of Groups (ASOG) Method

Results of VLE prediction by ASOG method are listed in Table LIV and, for ease of comparison, in Figures 78 through 86 for P-x data and in Figures 87 through 95 for y-x data.

The predicted vapor pressures are lower than the experimental values for all binary systems, ranged from an absolute average deviation of 4 mmHg for n-propanol-benzene system to 11 mmHg for n-propanol-n-hexane system. However, Figures 79 through 86 show that qualitative agreement between the predicted and experimental P-x data is obtained for these binary systems.

As shown in Figures 87 through 95, the vapor compositions predicted by the ASOG method match quite well with the values calculated by Mison's method from experimental P-x data. However, for the two partially mixcible systems, methanol-cyclohexane and methanol-n-hexane, the ASOG method fails to predict correctly the phase compositions at which the system separates into two liquid phases. The ASOG method predicts that the two liquid phases in equilibrium have compositions of 0.35 and 0.70 mole fractions of methanol for both systems. The experimental phase compositions in equilibrium at 25°C are 0.12 and 0.83 mole fractions of methanol for methanol-cyclohexane system, and 0.21 and 0.81 mole fractions of methanol for methanol-n-hexane system. Therefore, the application of the ASOG method to partially miscible systems must be considered only an approximation.

Summary

Quasi-Lattice Theory

Reasonable representation of heat of mixing data of binary systems studied has been obtained by the quasi-lattice theory. However, the

asymmetry of the excess Gibbs free energy curves is not correctly

reflected by the quasi-lattice theory.

For systems containing ethanol and n-propanol, the predicted vapor

pressures and vapor compositions have maximum and minimum values at low

concentration range of alcohols. This indicates that the quasi-lattice

theory erroneously predicts immiscible regions for these systems at

25°C, contrary to experimental results. This is due to the fact that

the quasi-lattice theory does not reflect properly the asymmetry of

the excess Gibbs free energy curves.

Universal Quasi-Chemical Equation

The energy parameters and structure parameters given in Abrams'

paper (3) were used for preliminary investigation of the applicability

of the UNIQUAC equation. Energy parameters were available only for

the systems methanol-benzene and ethanol-n-hexane from the present study.

Results of the prediction show that the UNIQUAC equation only pro-

vides a qualitative representation of the excess Gibbs free energies

and vapor pressures. For the ethanol-n-hexane system, the UNIQUAC

equation also erroneously predicts immiscible regions at 25°C.

The preliminary investigation indicates that the UNIQUAC equation

does not perform suitable in the VLE prediction for the binary systems

studied. No work was attempted to optimize the energy parameters based

on the present experimental data.

Analytical Solutions of Groups Method

The interaction parameters given by Derr and Deal (18) were used

for excess Gibbs free energy and VLE prediction. Since the primary

objective was to compare the experimental data with the values predicted by the ASOG method, no attempt was made to optimize the parameters based on the experimental results from the present study.

The predicted excess Gibbs free energies are lower than the experimental values. However, the asymmetry of the excess Gibbs free energy curves is properly reflected by the ASOG method.

The ASOG method only provides a qualitative representation of the binary system vapor pressures. The predicted vapor compositions match quite well with the values calculated by the Mixon's method. Thus the ASOG method predicts VLE data with better results than the quasi-lattice theory and the UNIQUAC equation.

CHAPTER VIII

CONCLUSIONS AND RECOMMENDATIONS

The present study consisted of the investigation of isothermal vapor-liquid equilibrium for binary mixtures of alcohols with benzene, cyclohexane and n-hexane, and the application of group contribution theories to excess thermodynamic properties and vapor-liquid equilibrium predictions. The conclusions and recommendations from this study are summarized in this chapter.

Experimental Apparatus

An apparatus was constructed which can be used to measure iso-thermal solution vapor pressures for the binary mixtures over the entire liquid composition range. The following conclusions were summarized about the apparatus:

1. The apparatus employed in present study was easy to calibrate and operate.

2. Use of calibrated glass injection bulbs permits rapid and accurate measurements of liquid compositions.

Concerning the experimental apparatus, the following recommendations are offered for future study:

1. The present apparatus is limited to pressure of less than one atmosphere. This restriction could be relaxed by modi-fication of the pressure-measurement method. The use of a

224

nulling device in the constant air bath with a highly accurate

pressure gauge such as the fused quartz precision pressure

gauge would be a possible solution.

2. Addition of a third degassing assembly and a third liquid

   storage bulb would expand its capabilities to study the vapor-

   liquid equilibria for ternary systems.

3. An automatic device for dispensing liquid nitrogen from a

   storage dewer to the cold finger of degassing assembly could

   be used to maintain the level of liquid nitrogen. This will

   increase the convenience of use of the apparatus and reduce

   the amount of effort required to maintain the level of liquid

   nitrogen in the cold finger.

4. The present apparatus could be used to measure solution

   vapor pressures at a temperature other than 25°C. Extension

   to other temperatures would require a liquid bath with a

   different working fluid, such as ethanol for lower tempera-

   ture or ethylene glycol for higher temperature.

Experimental Results

The following conclusions were reached from the experimental

results:

1. The measured vapor pressures were estimated to have impre-

   cisions of no more than $\pm$ 0.2 mmHg.

2. The errors in total composition calculation due to volume

   measurement were estimated to be no more than $\pm$ 0.00064 mole

   fraction unit; while the error due to liquid compressibility

   were negligible. The liquid compositions were estimated to

have imprecision of no more than 0.0008 mole fraction

unit.

3. In general, the Van Laar model gives better results than the 2-parameter Redlich-Kister model in fitting experimental vapor pressure-liquid composition data.

4. The Redlich-Kister model will require at least three (and even up to seven) parameters in order to obtain results comparable to the Wilson model.

5. Significant improvement in fitting experimental vapor pressures can be obtained by using 3-parameter Redlich-Kister model instead of 2-parameter Redlich-Kister model.

6. The Wilson model appears to be the best 2-parameter model in representing the experimental vapor pressure data.

7. The experimental results from the present study appear to be in best agreement with experimental data by Brown, et al. and by Scatchard, et al.

Concerning the data reduction, the following recommendation is suggested for future study:

More work should be done to find a better convergence routine for Mixon's method to make convergence more rapid.

Group Contribution Theories

The conclusions drawn from the investigation of group contribution theories to excess thermodynamic properties and vapor-liquid equilibrium predictions are summarized as follows:

1. Reasonable representation of heat of mixing data of binary systems by the quasi-lattice theory was obtained.

2. The excess Gibbs free energies predicted by the quasi-lattice theory were higher than the experimental excess Gibbs free energies.

3. The excess Gibbs free energies predicted by the universal quasi-chemical equation and the analytical solutions of groups method were lower than the experimental values. However, the asymmetry of the excess Gibbs free energy curves is properly reflected by these two theories.

4. Both the quasi-lattice theory and the universal quasi-chemical equation did not perform suitably in predicting solution vapor pressures and phase equilibrium relationships for the systems studied.

5. The analytical solutions of groups method provides only a qualitative description of the binary system vapor pressures.

6. The vapor compositions predicted by the analytical solutions of groups method agreed quite well with the values calculated by the Mixon's method from the experimental vapor pressure data.

7. The analytical solutions of groups method appears to be superior to the quasi-lattice theory and the universal quasi-chemical equation in predicting vapor pressures and phase equilibrium relationships.

Concerning group contribution theories, the following recommendation is made as guideline for future study:

For better analysis of the group contribution theories, additional experimental excess thermodynamic properties and

phase equilibrium data are needed. These data should be reliable and available at a variety of temperatures and/or pressures for investigating the temperature and/or pressure effects on the group parameters.

BIBLIOGRAPHY

1. Abbott, M. M., J. K. Floess, G. E. Walsh, and H. C. Van Ness, AIChE J. _21_, 72 (1975).

2. Abbott, M. M. and H. C. Van Ness, AIChE J. _21_, 62 (1975).

3. Abrams, D. S. and J. M. Prausnitz, AIChE J. _21_, 116 (1975).

4. Barker, J. A., J. Chem. Phys. _20_, 1526 (1952).

5. Barker, J. A., Aust. J. Chem. _6_, 207 (1953).

6. Barker, J. A., J. Chem. Phys. _21_, 1391 (1953).

7. Beers, Y., "Introduction to the Theory of Error," 2nd ed., Addison-Wesley, Reading, Massachusetts (1957).

8. Bell, T. N., E. L. Cussler, K. R. Harris, C. N. Pepela, and P. J. Dunlop, J. Phys. Chem. _72_, 4693 (1968).

9. Brown, I., W. Fock, and F. Smith, Aust. J. Chem. _17_, 1106 (1964).

10. Brown, I., W. Fock, and F. Smith, J. Chem. Thermo. _1_, 273 (1969).

11. Borwn, I. and F. Smith, Aust. J. Chem. _7_, 264 (1954).

12. Brown, I. and F. Smith, Aust. J. Chem. _12_, 407 (1959).

13. Byer, S. M., R. E. Gibbs, and H. C. Van Ness, AIChE J. _19_, 245 (1973).

14. Campbell, A. N. and S. C. Anad, Can. J. Chem. _50_, 479 (1972).

15. Chu, J. C., S. L. Wang, S. L. Levy, and R. Paul, "Vapor-Liquid Equilibrium Data," J. W. Edwards, Publisher, Inc., Ann Arbor, Michigan (1956).

16. Cruickshank, A. J. B. and A. J. B. Cutler, J. Chem. Eng. Data _12_, 326 (1967).

17. Davison, R. R., W. H. Smith, and K. W. Chun, AIChE J. _13_, 590 (1967).

18. Derr, E. L. and C. H. Deal, I. Chem. E. Symposium Series 32,
    3:40 (1969) in "International Symposium on Distillation
    1969, Brighton England Proceedings," Inst. of Chem. Engrs.,
    London, England.

19. Dodge, B. F., "Chemical Engineering Thermodynamics," McGraw-
    Hill Book Co., Inc., New York, N.Y. (1944).

20. Dullien, F. A. L., Ph.D. Thesis, University of British Columbia
    (1960).

21. Ferguson, J. B., J. Phys. Chem. 36, 1123 (1932).

22. Gibbs, R. E. and H. C. Van Ness, Ind. Eng. Chem. Fund. 11, (3),
    410 (1972).

23. Goates, J. R., R. L. Snow, and M. R. James, J. Phys. Chem. 65,
    335 (1961).

24. Goates, J. R., R. L. Snow, and J. B. Ott, J. Phys. Chem. 66,
    1301 (1962).

25. Hala, E., J. Pick, V. Fried, and O. Vilim, "Vapor-Liquid Equi-
    librium," 2nd ed., Pergamon Press, New York, N.Y. (1967).

26. Harris, H. G. and J. M. Prausnitz, AIChE J. 14, 737 (1968).

27. Hermsen, R. W. and J. M. Prausnitz, Chem. Eng. Sci. 18, 485 (1963).

28. Hibben, J. H., J. Res. Natl. Bur. Std. 3, 97 (1927).

29. Ho, J. C. K. and B. C.-Y. Lu, J. Chem. Eng. Data 8, 549 (1963).

30. Jones, H. K. D. and B. C.-Y. Lu, J. Chem. Eng. Data 11, 488 (1966).

31. Kudryavtseva, L. S. and M. P. Susarev, Zh. Pvik. Khim. 36,
    1471 (1963).

32. Kuo, C. M., Ph.D. Thesis, Oklahoma State University, Stillwater,
    Oklahoma (1971).

33. Kurtynina, L. M., N. A. Smirnova, and P. F. Andrukovich, Khim.
    Termodin. Rustvorov, No. 2, 43 (1968).

34. Lee, S. C., J. Phys. Chem. 35, 3558 (1931).

35. Ljunglin, J. J. and H. C. Van Ness, Chem. Eng. Sci. 17, 531 (1962).

36. Mixon, F. O., B. Gumoski, and B. H. Carpenter, Ind. Eng. Chem.
    Fund. 4, 455 (1965).

37. Mrazek, R. V. and H. C. Van Ness, AIChE J. 7, 190 (1961).

38. O'Connell, J. P. and J. M. Prausnitz, Ind. Eng. Chem. Process Design and Development 6, 245 (1967).

39. Orye, R. V. and J. M. Prausnitz, Ind. Eng. Chem. 57,(5), 18(1965).

40. Palmer, D. A., Chem. Eng. 82, No. 12, 80 (1975).

41. Pierotti, G. J., C. H. Deal, and E. C. Derr, Ind. Eng. Chem. 51, 95 (1959).

42. Reynolds, T. J., M. S. Thesis, Washington University, St. Louis, Missouri (1974).

43. Robinson, R. L., Jr., Ph.D. Thesis, Oklahoma State University, Stillwater, Oklahoma (1964).

44. Savini, C. G., D. R. Winterhalter, and H. C. Van Ness, J. Chem. Eng. Data 10, 168 (1965).

45. Savini, C. G., D. R. Winterhalter, and H. C. Van Ness, J. Chem. Eng. Data 10, 171 (1965).

46. Scatchard, G. and F. G. Satkiewicz, J. Am. Chem. Soc. 86, 130 (1964).

47. Scatchard, G., G. M. Wilson, and F. G. Satkiewicz, J. Am. Chem. Soc. 18, 125 (1964).

48. Scatchard, G., S. E. Wood, and J. M. Mochel, J. Am. Chem. Soc. 68, 1957 (1946).

49. Schnaible, H. W., H. C. Van Ness, and J. M. Smith, AIChE J. 3, 147 (1957).

50. Smith, V. C., M.S. Thesis, Oklahoma State University, Stillwater, Oklahoma (1970).

51. Smith, V. C. and R. L. Robinson, Jr., J. Chem. Eng. Data 15, 391 (1970).

52. Strubl, K., V. Svoboda, R. Holub, and J. Pick, Collect. Czech. Chem. Commun. 35, 3004 (1970).

53. Timmermans, J., "Physico-Chemical Constants of Pure Organic Compounds," 2, Elsevier, N.Y. (1965).

54. Van Laar, J. J., Zh Physik. Chem. 72, 723 (1910).

55. Van Ness, H. C., "Classical Thermodynamics of Non-Electrolyte Solutions," MacMillan Co., N.Y. (1964).

56. Van Ness, H. C., S. M. Byer, and R. E. Gibbs, AIChE J. 19, 238 (1973).

57. Van Ness, H. C., N. K. Kochar, and C. A. Soczek, J. Chem. Eng. Data 12, 346 (1967).

58. Van Ness, H. C., C. A. Soczek, G. L. Peloquin, and R. L. Machado, J. Chem. Eng. Data 12, 217 (1967).

59. Vesely, F. and J. Pick, Collect. Czech. Chem. Commun. 32, 4134 (1967).

60. Vesely, F. and J. Pick, Collect. Czech. Chem. Commun. 34, 1854 (1969).

61. Washburn, E. R. and B. H. Handorf, J. Am. Chem. Soc. 57, 441 (1935).

62. Weast, R. C., Editor, "Handbook of Chemistry and Physics," 55th ed., Chemical Rubber Company, Cleveland, Ohio (1974).

63. Wilson, G. M., J. Am. Chem. Soc. 86, 127 (1964).

64. Wilson, G. M. and C. H. Deal, Ind. Eng. Chem. Fund. 1, 20 (1962).

APPENDIX A

CORRECTION OF LIQUID COMPOSITION

DUE TO VAPOR SPACE

The composition calculated directly from known volumes of injected pure components is the total composition. Since some of the liquid injected to the cell is vaporized, the liquid composition may be different from the total composition. When the vapor pressure is below atmospheric and vapor space in the equilibrium cell is small, the amount of liquid vaporized can be neglected because of the great difference between liquid and vapor densities. However, when a correction for the amount of components in the vapor phase is required, it can be made by a simple iterative calculation. As a first step, the liquid composition may be assumed to be equal to the total composition. Then the vapor composition is calculated by either Barker's or Mixon's method. By knowing the volume of vapor space and vapor composition, the amount of liquid vaporized can be calculated. The liquid composition is then corrected and compared with the previous value. The process may be repeated until the liquid composition iteration converges. Only one iteration was required for the data in this study. For some of the binary systems, the errors in liquid composition due to varporization are negligible (less than 0.0008 mole fraction unit). However, the corrected liquid compositions are used for the vapor-liquid equilibrium calculation.

A sample calculation for liquid composition correction is demonstrated here.

System: Methanol(1)-Benzene(2)

Temperature: 25°C.

Vapor Pressure: 158.86 mmHg.

	Methanol(1)	Benzene(2)
Injected volume, V_1 (cc)	0.7645	46.7268
Liquid density, ρ_i (gm/cc)	0.7857	0.8727
Molecular weight, MW_i	32.04	78.11
Total composition, z_i	0.0347	0.9653

Assume liquid composition equal to total composition and calculate vapor composition by Barker's method with Wilson's activity coefficient model:

	Methanol(1)	Benzene(2)
Liquid composition, x_i	0.0347	0.9653
Vapor composition, y_i	0.4137	0.5863

Total cell volume (approximate)   214 cc

Total liquid volume (approximate)   47 cc

Total vapor volume, V^V 167 cc

Calculate total moles in vapor phase by virial equation of state truncated after second virial:

$$\frac{PV^V}{n_T^V RT} = 1 + \frac{n_T^V B_{mix}}{V^V}$$

B_{11} = 981.6 cc/gm-mole

B_{22} = -1528.6 cc/gm-mole

B_{12} = -942.5 cc/gm-mole

$$B_{mix} = \sum_{i=1}^{2} \sum_{j=1}^{2} y_i y_j B_{ij} = -814.7 \text{ cc/gm-mole}$$

$$n_T^V = 0.00144 \text{ moles (total moles in vapor)}$$

$$n_1^V = y_1 n_T^V = 0.00060 \text{ moles of component 1 vaporized}$$

Total moles of pure components injected:

$$n_i = \frac{\rho_i V_i}{MW_i}$$

$$n_1 = 0.01875 \text{ moles}$$

$$n_2 = 0.52206 \text{ moles}$$

Neglect amount of liquid vaporized:

$$x_1 = \frac{n_1}{n_1 + n_2} = 0.0347 = z_1 \text{ (check)}$$

Correct for liquid composition:

$$x_1 = \frac{n_1 - n_1^V}{n_1 + n_2 - n_T^V}$$

$$= 0.0337$$

Error in liquid composition, $\Delta x_1 = 0.0010$

After first iteration:

	Methanol(1)	Benzene(2)
Liquid composition, x_i	0.0337	0.9663
Vapor composition, y_i	0.4094	0.5906

$$B_{mix} = -824.4 \text{ cc/gm-mole}$$

$$n_T^V = 0.00144 \text{ moles}$$

$$n_1^V = y_1 n_T^V = 0.00059 \text{ moles}$$

Correction for liquid composition:

$$x_1 = \frac{n_1 - n_1^V}{n_1 + n_2 - n_T^V}$$

$$= 0.0337 \text{ (check)}$$

APPENDIX B

ERRORS IN TOTAL COMPOSITION CALCULATION

Error Due to Volume Measurement

The total composition is calcualted from the injected-volume
information and molar volume of each component. Thus the error in
total composition is due to the error associated with the volume of
each measuring bulb and the molar volume of each component.

The method presented by Beers (7) is used in this study for
calculation of error. Beers describes the effects of independent and
uncorrelated errors on the dependent variable with the following
equation:

$$\sigma_y^2 = \sum_{i=1}^{m} \left(\frac{\partial y}{\partial x_i} \sigma_{x_i} \right)^2$$

where the dependent variable y is a function of uncorrected, indepen-
dent variables x_1, x_2,..., and x_m.

Let

n_i = total moles of ith component being injected into
the equilibrium cell. (gm-mole)

$\overline{V}_i$ = molar volume of ith component. (cc/gm-mole)

$= \dfrac{\text{molecular weight (gm/gm-mole)}}{\text{density (gm/cc)}}$

237

V_i = total volume of ith component being injected into the equilibrium cell. (cc)

N_{ij} = number of jth measuring bulb being used to inject i^{th} component.

v_j = volume of jth measuring bulb. (cc)

Then

$$V_i = \sum_j N_{ij} v_j \qquad (B-1)$$

$$n_i = \frac{V_i}{\bar{V}_i} \qquad (B-2)$$

and

z_k = total composition of kth component

$$= \frac{n_k}{\sum_i n_i} \qquad (B-3)$$

Using Beers' expression, the standard deviations in V_i, n_i, and z_k are

$$\sigma_{V_i}^2 = \sum_j \left(\frac{\partial V_i}{\partial v_j} \right)^2 \sigma_{v_j}^2 = \sum_j N_{ij}^2 \sigma_{v_j}^2$$

or

$$\left(\frac{\sigma_{V_i}}{V_i} \right)^2 = \sum_j N_{ij}^2 \sigma_{v_j}^2 \Big/ \left(\sum_j N_{ij} v_j \right)^2 \qquad (B-4)$$

$$\sigma_{n_i}^2 = \left(\frac{\partial n_i}{\partial \bar{V}_i} \right)^2 \sigma_{\bar{V}_i}^2 + \left(\frac{\partial n_i}{\partial V_i} \right)^2 \sigma_{V_i}^2$$

$$= \frac{V_i^2}{\bar{V}_i^4} \sigma_{\bar{V}_i}^2 + \frac{1}{\bar{V}_i^2} \sigma_{V_i}^2$$

or

$$\left(\frac{\sigma_{n_i}}{n_i} \right)^2 = \left(\frac{\sigma_{\bar{V}_i}}{\bar{V}_i} \right)^2 + \left(\frac{\sigma_{V_i}}{V_i} \right)^2 \tag{B-5}$$

and

$$\sigma_{z_k}^2 = \sum_i \left(\frac{\partial z_k}{\partial n_i} \right)^2 \sigma_{n_i}^2$$

For binary mixture

$$\sigma_{z_1}^2 = \sigma_{z_2}^2 = \frac{n_2^2}{(n_1 + n_2)^4} \sigma_{n_1}^2 + \frac{n_1^2}{(n_1 + n_2)^4} \sigma_{n_2}^2$$

or

$$\left(\frac{\sigma_{z_1}}{z_1 z_2} \right)^2 = \left(\frac{\sigma_{z_2}}{z_1 z_2} \right)^2 = \sum_{i=1}^2 \left(\frac{\sigma_{n_i}}{n_i} \right)^2 \tag{B-6}$$

Substituting Equations (B-4) and (B-5) into Equation (B-6),

$$\left(\frac{\sigma_{z_1}}{z_1 z_2} \right)^2 = \left(\frac{\sigma_{z_2}}{z_1 z_2} \right)^2$$

$$= \sum_{i=1}^{2} \left(\frac{\sigma_{\overline{V}_i}}{\overline{V}_i} \right)^2 + \sum_{i=1}^{2} \left[\frac{\sum_{j=1}^{4} N_{ij}^2 \sigma_{v_j}^2}{\left(\sum_{j=1}^{4} N_{ij} v_j \right)^2} \right] \tag{B-7}$$

The volume of each measuring bulb and its standard deviation are listed in Table V in Chapter V. The molar volume at 26°C for each component is shown in Table LV. The standard deviation of molar volume associated with density measurement is also listed in the table.

TABLE LV

PURE COMPONENT MOLAR VOLUMES AT 26°C

Compound	Molar Volume $\overline{V}_i$ (cc/gm-mole)	Standard Deviation $\sigma_{\overline{V}_i}$ (cc/gm-mole)
Methanol	40.78	0.0026
Ethanol	58.75	0.0030
N-Propanol	75.23	0.0074
Benzene	89.50	0.0096
Cyclohexane	108.89	0.0035
N-Hexane	131.83	0.0062

The error in total composition due to volume measurement is calculated at each data point by computer. A sample calculation is demonstrated here with the maximum error of $\pm$ 0.00064 mole fraction unit.

Sample Calculation

System: Ethanol(1)-Cyclohexane(2)

Temperature: 25°C.

Vapor Pressure: 139.53 mmHg

	Component 1	Component 2
N_{i1}	5	2
N_{i2}	4	2
N_{i3}	0	2
N_{i4}	0	2
Volume Injected V_i, cc	10.6979	50.0164
Moles Injected n_i, gm-mole	0.1821	0.4593
Total Composition z_i	0.2839	0.7161

From Equation (B-7), the error in total composition is

$$\left(\frac{\sigma_{z_1}}{z_1 z_2} \right)^2 = \left(\frac{\sigma_{z_2}}{z_1 z_2} \right)^2 = \sum_{i=1}^{2} \left(\frac{\sigma_{\overline{V}_i}}{\overline{V}_i} \right)^2 + \sum \left[\frac{\sum_{j=1}^{4} (N_{ij}^2 \sigma_{v_j}^2)}{\left(\sum_{j=1}^{4} N_{ij} v_j \right)^2} \right]$$

$$= (\frac{0.0030}{58.75})^2 + (\frac{0.0035}{108.89})^2 + \frac{5^2 \times 0.0040^2 + 4^2 \times 0.0066^2}{10.6979^2}$$

$$+ \frac{2^2 \times 0.0040^2 + 2^2 \times 0.0066^2 + 2^2 \times 0.0041^2 + 2^2 \times 0.0042^2}{50.0164^2}$$

$$= 9.86 \times 10^{-6}$$

or

$$\sigma_{z_1} = \sigma_{z_2} = \pm\ 0.00064$$

Error Due to Liquid Compressibility

The degassed liquids in storage bulbs are under pressure higher than atmospheric. Another possible error in total composition may result from using the density at atmospheric pressure. However, the error is small enough that it may be neglected for the following two reasons:

(1) The isothermal compressibility is very small.

(2) The pressure in the storgage bulb is less than 1.5 atm.

VITA

Shuen-cheng Hwang

Candidate for the Degree of

Doctor of Philosophy

Thesis: VAPOR-LIQUID EQUILIBRIA AND GROUP CONTRIBUTION THEORIES FOR BINARY SYSTEMS OF ALCOHOLS AND HYDROCARBONS

Major Field: Chemical Engineering

Biographical:

Personal Data: Born in Pingtung, Taiwan, March 3, 1945, the son of Chin-fu and Wang Chiu Hwang. Married to Lois L. Y. Fan, Taipei, Taiwan, August 19, 1971.

Education: Attended elementary and junior high schools in Pingtung, Taiwan; graduated from Kaohsiung High School in 1963; received the Bachelor of Science degree in Chemical Engineering from Taiwan Cheng Kung University in June, 1967; received the Master of Science degree with a major in Chemical Engineering in May, 1972; completed requirements for the Doctor of Philosophy degree in December, 1975.

Professional Experience: Employed as an engineering trainee by the Formosa Plastics Corporation, Kaohsiung, Taiwan, July to November, 1968; employed as graduate assistant, School of Chemical Engineering, Oklahoma State University, 1969 to 1975. Currently employed as a Postdoctoral Researcher at Department of Chemical Engineering, Rice University, Houston, Texas.

Membership in Scholarly or Professional Societies: Omega Chi Epsilon, American Chemical Society, affiliate member of the American Institute of Chemical Engineers, student member of the Oklahoma Society of Professional Engineers and the National Society of Professional Engineers.